ISBN 978-1-100-23499-1
$50.00
55000
9 781100 234991

Geological Survey of Canada
Bulletin 607

Tectonostratigraphy and allochthonous salt tectonics of Axel Heiberg Island, central Sverdrup Basin, Arctic Canada
J.C. Harrison and M.P.A. Jackson

Bureau of Economic Geology
Report of Investigations No. 279

Geological Survey of Canada
Bulletin 607

Bureau of Economic Geology
Report of Investigations No. 279

Tectonostratigraphy and allochthonous salt tectonics of Axel Heiberg Island, central Sverdrup Basin, Arctic Canada

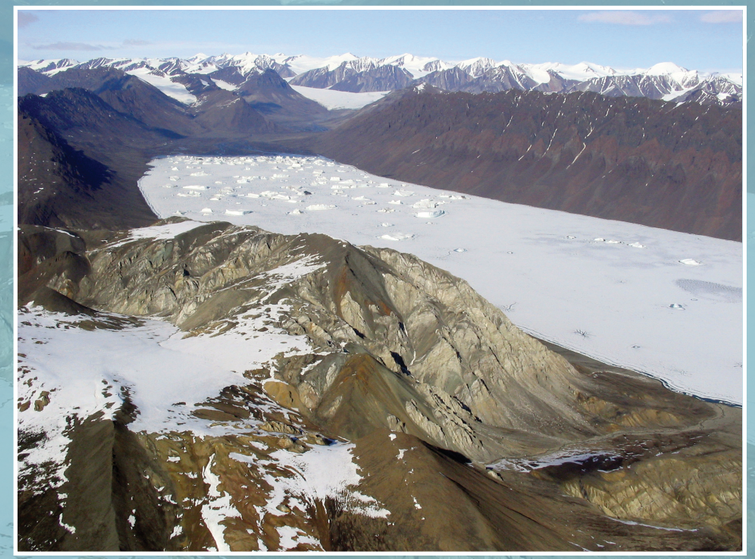

J.C. Harrison and M.P.A. Jackson

2014

Natural Resources Canada
Ressources naturelles Canada
Canada

Bureau of Economic Geology

ISSN 0068-7626
Catalogue No. M42-607E-PDF
ISBN: 978-1-100-23499-1
doi: 10.4095/293840

Cover illustration: *Agate Fiord Southeast Diapir is exposed along the west shore of Agate Fiord of western Axel Heiberg Island. Evaporites here have been thrust to the east over Upper Paleocene Iceberg Bay Formation (lower right). Dark cliffs at upper left and on the opposite side of the fiord are tholeiitic basalts of the Upper Cretaceous Strand Fiord Formation. Dark areas within the evaporites are tholeiitic gabbros of the Lower Cretaceous Queen Elizabeth swarm.*

Research was funded by the Applied Geodynamics Laboratory consortium and the Jackson School of Geosciences Foundation and Kosmos Energy (Jackson) and by the Climate Change Technology Innovation and Investment—Unconventional Gas Supply, Northern Resources Development and Geo-mapping for Energy and Minerals programs of Natural Resources Canada (Harrison).

Critical review:
Peter Eichhubl (Bureau of Economic Geology, Jackson School of Geosciences, The University of Texas at Austin)
Ashton Embry (Geological Survey of Canada)

Authors:
J.C. Harrison (Geological Survey of Canada)
M.P.A. Jackson (Bureau of Economic Geology, Jackson School of Geosciences, The University of Texas at Austin)

This publication is available for free download through GEOSCAN (http://geoscan.ess.nrcan.gc.ca)

Series Editor: Peter Eichhubl
Media Manager: Cathy J. Brown
Style Editor: Susann V. Doenges
Senior Graphics Designer: Jamie H. Coggin
Computer Illustrators: Anastasia Grebnova, Nancy Cottington
Photographic Editing: David M. Stephens
Manager, Publication Sales: Amanda R. Masterson

This publication and other Bureau publications are available from

Publication Sales
Bureau of Economic Geology
The University of Texas at Austin
University Station, Box X
Austin, Texas 78713-8924 USA
Web: http://www.beg.utexas.edu
Phone: 512-471-7144
Fax: 512-471-0140
E-mail: pubsales@beg.utexas.edu
Online Bureau Store: http://begstore.beg.utexas.edu/store/

Geological Survey of Canada
Bulletin 607

Bureau of Economic Geology
Report of Investigations No. 279

Tectonostratigraphy and allochthonous salt tectonics of Axel Heiberg Island, central Sverdrup Basin, Arctic Canada

J.C. Harrison and M.P.A. Jackson

2014

Natural Resources Canada
Ressources naturelles Canada

Bureau of Economic Geology
Scott W. Tinker, Director
Jackson School of Geosciences
The University of Texas at Austin
Austin, Texas 78713-8924 USA

Contents

Abstract

Axel Heiberg Island (northern Nunavut) contains the thickest Mesozoic section in Sverdrup Basin. The approximately 370 km long island is second only to Iran in its concentration of exposed diapirs. Forty-six diapirs of Carboniferous evaporites and associated minibasins are impressively exposed on the island. Regional anticlines, which formed during the Paleogene Eurekan Orogeny, trend roughly north on a regular approximately 20 km wavelength and probably detach on the autochthonous Carboniferous Otto Fiord Formation evaporites. These evaporites comprise halite overlain by thick anhydrite containing thin limestone beds. Unlike the rest of the island, a 60 km wide area, known as the wall-and-basin region, has bimodal fold trends and irregular (<10 km) fold wavelengths. Here, crooked, narrow walls of superficially gypsified anhydrite crop out in tight anticline cores, which are separated by wider synclinal minibasins. We interpret the wall-and-basin region to detach on a shallow, partly exposed canopy of coalesced allochthonous evaporite sheets. This inference is based on four lines of evidence: 1) a halving of fold wavelength relative to folds outside the wall-and-basin region, 2) the exposure of anomalously young strata of Paleogene and Late Cretaceous age, 3) the occurrence of clustered equant minibasins having similarities to those in the northern Gulf of Mexico, and 4) a strikingly uniform level of piercement pointing to a stratiform allochthonous source layer. A canopy would require an evaporite depocentre, which may have ponded in a sinistral pull-apart basin of Carboniferous age. Strata record a salt-tectonic history spanning the Late Triassic (Norian) epoch to the Paleogene period. Stratigraphic thinning against diapirs and angular unconformities up to 90° indicate mild regional shortening in which diapiric roof strata were bulged up and flanking strata steepened. This bulging culminated during Hauterivian times, when diapiric evaporites broke out and coalesced at the surface to form a canopy. As the canopy was buried, it yielded second-generation diapirs, which rose between minibasins subsiding into the canopy. A consistent high emplacement level indicates that all exposed diapirs inside the wall-and-basin region rose from the canopy. In contrast, diapirs along the wall-and-basin margins were sourced in autochthonous salt as first-generation diapirs. Apart from the large diapir-centred unconformities, Jurassic-Cretaceous depositional evidence of salt tectonics also includes submarine debris flows and boulder conglomerates shed from at least three emergent diapirs. The report area's geological history includes six main tectonostratigraphic phases in the wider Arctic area, beginning with Carboniferous rifting and ending with the Paleogene Eurekan Orogeny. Extreme local relief, tectonic slide blocks, steep talus fans, and subaerial debris flows suggest that many wall-and-basin diapirs continue to rise today. Freeboard calculations suggest that the rise of diapirs having surface relief of even 400 m could be driven purely by gravitational loading, but additional mild tectonic shortening cannot be ruled out.

The Axel Heiberg canopy is one of only three known exposed evaporite canopies, each revealed at a different structural level: above the canopy (Axel Heiberg), through the canopy (Great Kavir, Iran), and possibly beneath a canopy (Sivas Basin, Turkey).

Résumé

On trouve dans l'île Axel Heiberg (nord du Nunavut) la coupe du Mésozoïque la plus épaisse du bassin de Sverdrup. Seul l'Iran présente une concentration de diapirs affleurants qui dépasse celle de cette île d'une longueur d'environ 370 km. Quarante-six diapirs d'évaporites carbonifères et les mini-bassins associés sont exposés de façon impressionnante dans cette île. Des anticlinaux régionaux qui se sont formés pendant l'orogenèse eurékienne du Paléogène présentent une direction à peu près nord et une longueur d'onde régulière d'environ 20 km, et résultent probablement d'un décollement au-dessus des évaporites autochtones de la Formation d'Otto Fiord du Carbonifère. Ces évaporites sont formées d'halite surmontée d'anhydrite épaisse contenant de minces couches de calcaire. Contrairement au reste de l'île, dans une zone de 60 km de largeur connue sous le nom de « région des murs et bassins », la direction plis est bimodale et la longueur d'onde de ceux-ci est irrégulière (< 10 km). À cet endroit, des murs sinueux et étroits d'anhydrite gypsifiée en surface affleurent dans le coeur d'anticlinaux serrés, lesquels sont séparés par des mini-bassins synclinaux plus larges. D'après notre interprétation, la région des murs et bassins surmonte une surface de décollement le long d'une voûte peu profonde et partiellement exposée formée de nappes coalescentes d'évaporites allochtones. Cette déduction est basée sur quatre éléments de preuve: 1) diminution de moitié de la longueur d'onde des plis par rapport à ceux situés à l'extérieur de la région des murs et bassins; 2) affleurement de strates anormalement jeunes du Paléogène et du Crétacé tardif; 3) présence d'amas de mini-bassins équidimensionnels qui s'apparentent à ceux observés dans le nord du golfe du Mexique; et 4) niveau rigoureusement uniforme de perçage des diapirs, pointant vers une couche source stratiforme et allochtone. L'existence d'une voûte de diapirs nécessite un dépocentre d'évaporites qui pourrait avoir été confiné à un bassin de transtension senestre datant du Carbonifère. Les strates montrent des vestiges d'un passé tectonique salifère qui s'échelonne de l'époque du Trias tardif (Norien) jusqu'à la période du Paléogène. L'amincissement stratigraphique contre les diapirs et les discordances angulaires dont l'angle peut atteindre 90 degrés indiquent qu'il y a eu un léger raccourcissement régional qui a entraîné le renflement des strates du toit des diapirs et le raidissement des strates sur leurs flancs. Ce renflement a culminé pendant le Hauterivien, au moment où les évaporites diapiriques ont percé leur couverture et sont entrées en coalescence à la surface pour former une voûte. À mesure que la voûte était ensevelie, elle a généré la formation de diapirs de deuxième génération qui se sont élevés entre les mini-bassins qui s'enfonçaient dans la voûte. Dans la région des murs et bassins, le niveau de mise en place élevé et uniforme des diapirs exposés indique que ceux-ci se sont tous élevés à partir de la voûte. En revanche, les diapirs le long des marges de la région des murs et bassins proviennent du sel autochtone sous forme de diapirs de première génération. En dehors des grandes discordances centrées sur les diapirs, les indices sédimentaires d'une tectonique salifère au Jurassique-Crétacé comprennent des coulées de débris sous-marines et des conglomérats à blocs alimentés par au moins trois diapirs émergés. L'histoire géologique de la région couverte par ce rapport compte six des principales phases tectonostratigraphiques de la grande région de l'Arctique, qui débute par un rifting au Carbonifère et se termine par l'orogenèse eurékienne au Paléogène. La topographie extrême de l'endroit ainsi que la présence de blocs de glissement tectonique, de cônes alluviaux abrupts et de coulées de débris subaériennes laissent croire que de nombreux diapirs de la région des murs et bassins continuent de se soulever de nos jours. Les calculs de l'espace libre indiquent que l'ascension de diapirs d'une hauteur relative aussi élevée que 400 m peut être occasionnée par la charge gravitationnelle uniquement, mais la possibilité d'un faible raccourcissement tectonique ne peut être exclue.

La voûte de diapirs de l'île Axel Heiberg est l'une de trois voûtes d'évaporites exposées connues, chacune se situant à un niveau structural différent, soit au-dessus de la voûte (île Axel Heiberg), à travers la voûte (Grand Kavir, Iran) et, possiblement, sous la voûte (bassin de Sivas, Turquie).

Introduction

The Sverdrup Basin depocentre, which is of Carboniferous to Cenozoic age, is exposed on Axel Heiberg Island in northern Nunavut, Canada. The 370 km long island is second only to Iran in its concentration of exposed evaporite diapirs and intervening minibasins. Despite spectacular exposure in a polar desert, however, the Sverdrup Basin structure has been little studied owing to its

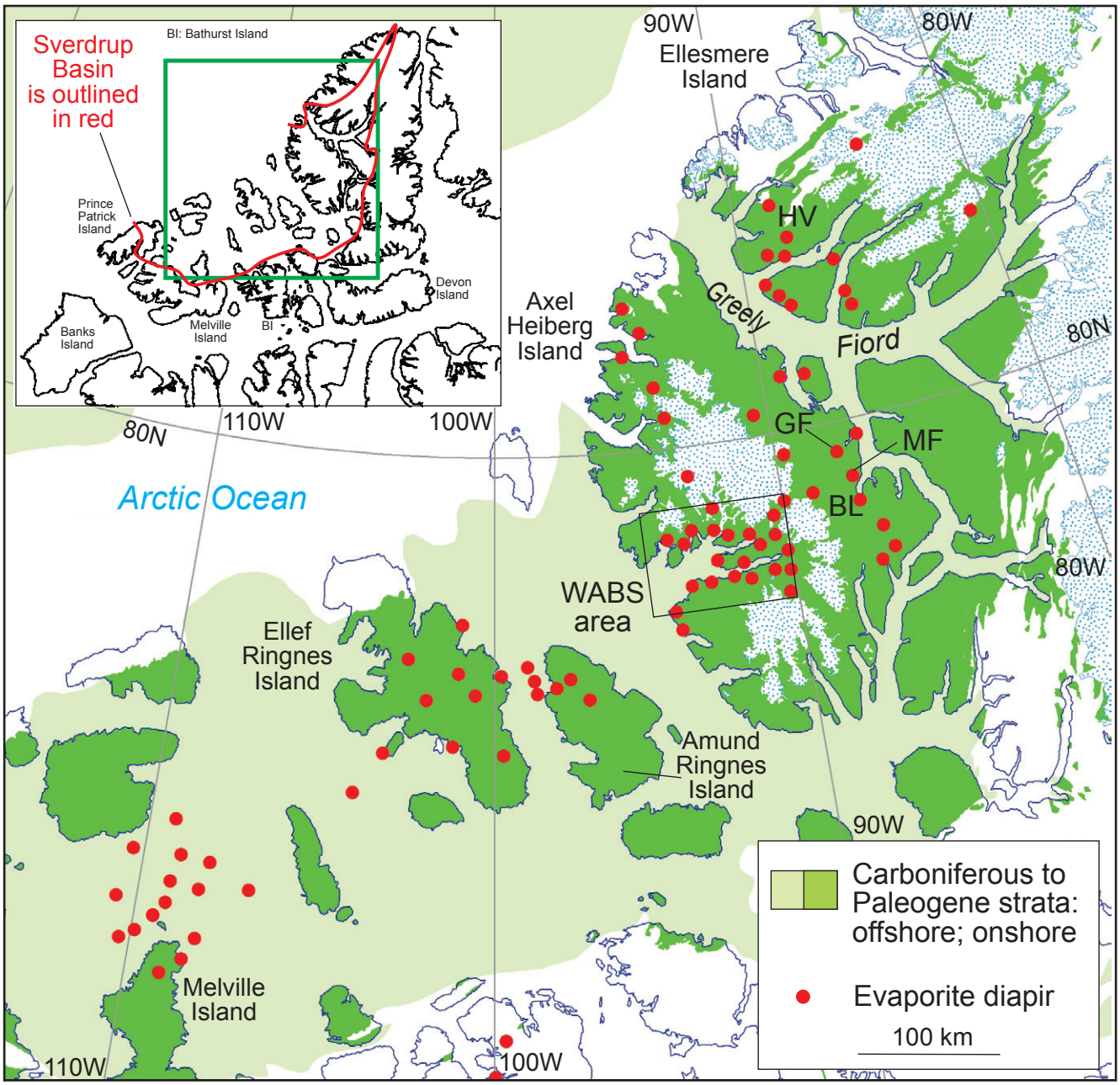

Figure 1. Location map of Sverdrup Basin showing evaporite diapirs, distribution of Carboniferous to Paleogene strata, and the area of the wall-and-basin structure (WABS). Described structures outside wall-and-basin region include Mokka Fiord (MF) and Gibs Fiord (GF) diapirs. Three Lakes diapir is near Mokka Fiord diapir. The Hvitland Peninsula area (HV) of northern Ellesmere Island features both autochthonous and para-autochthonous evaporites. Locations outside wall-and-basin region linked to measured sections of Figure 11 include Amund Ringnes Island and Buchanan Lake (BL) on eastern Axel Heiberg Island.

remote setting at 79°N, only 1200 km from the North Pole.

In examining the salt tectonics in western Axel Heiberg Island we concentrated on the peculiar geology of the so-called wall-and-basin structure (WABS) region (Fig. 1; van Berkel et al., 1984). On first view, aspects of this region were reminiscent of the combination of minibasins and salt canopies well developed in the Gulf of Mexico Basin (summarized by Diegel et al., 1995). If so, western Axel Heiberg Island suggested an opportunity to evaluate field relationships, origin, and evolution of minibasins, salt diapirs, and allochthonous salt sheets in an area of superb outcrop exposure. Our fieldwork in 2004, which resulted in a new geological map of the wall-and-basin region (Fig. 2), focused on answering questions related to mobile salt in a relatively young sedimentary basin: 1) Is the wall-and-basin region underlain by a salt canopy, and is the canopy anywhere exposed? 2) Did the ellipsoidal wall-and-basin region synclines originate as long-lived minibasins, or are they short-lived features associated with the Paleogene Eurekan Orogeny?

During and after our field activities, other distinct wall-and-basin features emerged and prompted more geological questions: 3) What influence, if any, did pre-existing structural anisotropy have on later salt-tectonic activity? 4) What is the relationship between plate tectonics and phases of diapirism and canopy emplacement? 5) What triggered emplacement of the salt canopy? and 6) How does the inferred canopy compare with other exposed salt canopies around the world?

Location and access

The study area is located in a region of hills and low mountain ranges locally covered by ice caps and glaciers. The area is centred on Expedition and Strand fiords on western Axel Heiberg Island, and in the drainage basins leading into these fiords from the southwestern, central, and northwestern parts of the island. We investigated a roughly rhombic region bounded by the exposed extent of linear salt walls and tight salt-cored anticlines separated by elliptical and kidney-shaped synclines. The area includes the southwestern quarter of Strand Fiord map sheet (NTS 59-H), the southeastern quarter of Middle Fiord map sheet (NTS 59-G), and a sliver of territory along the northwestern edge of Glacier Fiord map sheet (NTS 59-E). Access to the island is by helicopter from the weather station and airstrip at Eureka, located 130 km to the northeast on northern Ellesmere Island. Eureka is reached by fixed-wing aircraft operating out of the settlement of Resolute, situated 520 km south of the report area on southern Cornwallis Island.

Previous work

Evaporite diapirs in Canada's Arctic Islands were discovered during the Franklin search expeditions of the mid-nineteenth century. Material collected from northern Melville Island (Fig. 1) in 1855 by G.H. Richards and S. Osborn was identified as selenite by Sir Edward Belcher. This discovery was one of many scientific and geographic accomplishments incidental to the far-ranging search (1846–59) for the ill-fated crew and ships of Sir John Franklin.

About 100 years later, the characteristic circular shape of the Canadian Arctic diapirs was revealed by the first aerial photographs of the northern Arctic Islands between 1947 and 1953 (Heywood, 1955, 1957). The expectation that strata deformed by Canadian Arctic salt diapirs might have petroleum potential was a scientific motivation for Operation Franklin. This major helicopter-supported reconnaissance was conducted in 1955 by the Geological Survey of Canada over much of the central Canadian Arctic Islands. Results established the existence of both the Sverdrup Basin of Carboniferous to Paleogene age and the abundant evaporite diapirs on several large islands in the centre of the basin. The diapirs were shown on the first geology maps of the region, including those on Ellef Ringnes and Axel Heiberg islands (Geological Survey of Canada, 1959; Heywood, 1959). The final report of Operation Franklin (Fortier et al., 1963) provides a summary description of map units, measured stratigraphic sections, targeted studies of diagnostic marine fauna, and regional and locally detailed geological maps and cross-sections. This operation included, in reconnaissance fashion, all areas of our 2004 fieldwork on west-central Axel Heiberg Island.

Regional-scale geological mapping by R. Thorsteinsson, E.T. Tozer, and other officers of the Geological Survey of Canada continued on Axel Heiberg Island from 1956 to 1963. They systematically described upper Palaeozoic strata of the

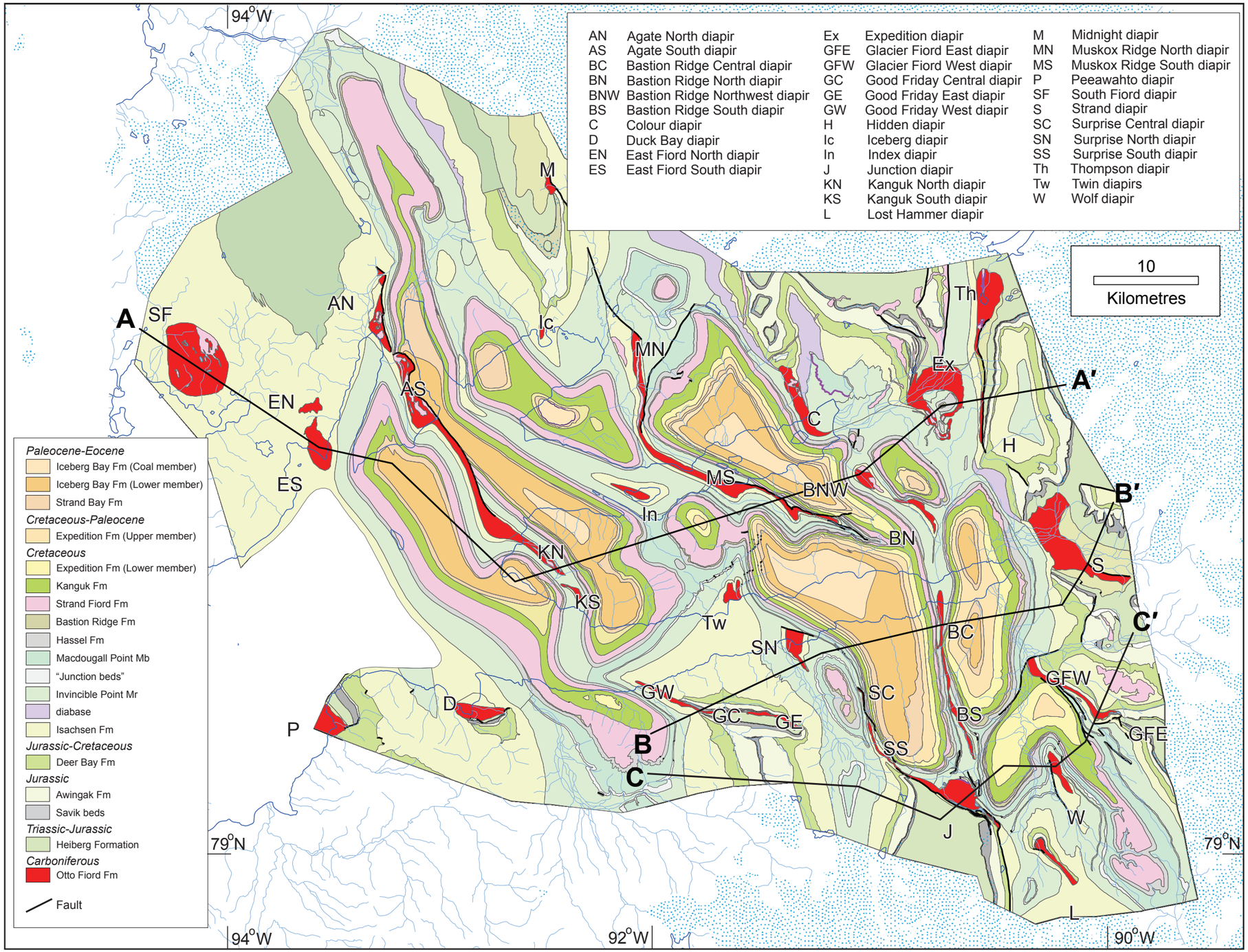

Figure 2. Geological map showing 35 named evaporite diapirs (red) in the study area of west-central Axel Heiberg Island. *See* Figure 53 for cross-sections.

Arctic Islands and produced 16 coloured geological maps (scale 1:250 000) covering all of Axel Heiberg Island and much of western Ellesmere Island (Thorsteinsson, 1974). Three of these map sheets include the wall-and-basin region (GSC A-series maps 1299A, Middle Fiord; 1301A, Strand Fiord; and 1304A, Glacier Fiord; Thorsteinsson, 1971a, b, 1972a).

The Expedition Fiord area of western Axel Heiberg Island became a focus for subsequent detailed studies of central Sverdrup Basin geology, beginning with the Jacobsen-McGill Arctic Research Expedition of 1959 to 1962 (Muller, 1963). Notable contributions relevant to the present study included a regional-scale geology map of an area north and east of the head of Expedition Fiord (scale 1:50 000) and measured sections of Mesozoic strata located north and south of the heads of Expedition and Strand fiords (Fricker, 1963). A subsequent expedition report by Hoen (1964) provided a black-and-white geological map of the entire Strand Fiord–Expedition Fiord area at a scale of 1:60 000 and a report containing locally detailed maps, structure sections, and descriptions of selected diapirs.

Western Axel Heiberg Island was again a focus for university and federal government research activities in the late 1970s and early 1980s. This research included studies of Mesozoic strata (Embry, 1991, and references contained therein), including those containing volcanic flows (Embry and Osadetz, 1988), paleomagnetic studies on Cretaceous volcanic rocks (Wynne et al., 1988), Cretaceous and Paleogene sediments, including a geological map of the Eureka Sound Group (Ricketts, 1991), macrofauna (Jeletzky, 1980, 1983; Poulton, 1984), foraminifers (Wall, 1983), and an important study of the wall-and-basin region mapped and analyzed by van Berkel et al. (1984) and van Berkel (1986). This study was part of a campaign by the University of Toronto to elucidate the internal structure of several diapirs on the island by fabric mapping and strain analysis (Schwerdtner and Clark, 1967; Hugon and Schwerdtner, 1982; Schwerdtner and Osadetz, 1983; van Berkel et al., 1983; Schwerdtner and van Kranendonk, 1984). The stratigraphic work of A.F. Embry on Axel Heiberg Island and throughout Sverdrup Basin since the 1970s has resulted in a comprehensive understanding of surface and subsurface Arctic Mesozoic stratigraphy. This regional perspective is summarized in a seminal Decade of North American Geology (DNAG) contribution to Arctic regional geology by Embry (1991) and includes an overview of stratigraphic nomenclature, regional stratigraphic sections, isopach maps, and paleogeographic maps. Regardless of this extensive research, the Strand Fiord–Expedition Fiord area does not fit readily into the regional picture of Sverdrup Basin geology summarized by Embry (1991) because intense salt-tectonic activity has greatly affected sediment accumulation. This anomaly is the impetus for our study focusing on the wall-and-basin region.

This study

Data for our study were obtained during five days of aerial reconnaissance of the diapirs and surrounding strata of central Axel Heiberg Island and 12 days of ground-based mapping of selected diapirs on central Axel Heiberg Island between July 1 and July 22, 2004. Key field localities (Fig. 2) included Junction diapir (July 2–5), Muskox Ridge South diapir (July 8–10), and Expedition diapir (July 11–13). We also conducted brief ground-based studies at Good Friday West diapir, Glacier diapir, Wolf diapir (in the west), and Three Lakes diapir (in the east) and elsewhere as described in this report. A sixth day of helicopter reconnaissance and selected ground studies in northern Ellesmere Island (July 17) provided stratigraphic and structural context for autochthonous upper Palaeozoic evaporites exposed north of Greely Fiord (Fig. 1).

Our mapping included reinterpreting approximately 75 pairs of stereoscopic air photographs of the entire wall-and-basin region of western Axel Heiberg Island; photographs were supplied by the National Air Photo Library (NAPL, Ottawa). Bedding attitudes that we measured during the 2004 field season were augmented by published bedding attitudes on the maps of Fortier et al (1963), Fricker (1963), Hoen (1964), Thorsteinsson (1974), van Berkel et al (1984), and Ricketts (1991). Made available late in our effort to compile a new geological map of the region were satellite images and two sets of detailed digital elevation models (DEMs) contoured at intervals of 25 and 50 m. These products were generated by Paul Budkewitsch and colleagues at the Canada Centre for Remote Sensing (CCRS, Ottawa). For reasons described below, these models were enormously useful for

acquiring unit thickness data and many additional bedding attitudes.

Bedding attitudes were calculated using three-point techniques applied to 1) georeferenced raster copies of the NAPL air photograph set, 2) georeferenced geological contacts mapped from the interpreted stereoimagery and by fieldwork, and 3) 25 m elevation contour files generated from georeferenced CCRS satellite images and related DEM data. The contour file was draped on the geological line work. From this it was simple to determine local bedding attitudes where geological contacts cross topographic contours. Calculated attitudes are especially reliable where dips are less than 10° and geological contacts intersect each of three or more topographic contours in at least two places. Reliability decreases as topographic contours bunch together (as a result of uncertainties in georeferencing and uncertainties in the position of geological contacts on cliff faces) and as bedding increases beyond about 45°. Nevertheless, more than 400 bedding attitudes were calculated by this method for the eastern part of the wall-and-basin region. In select circumstances it was possible to calculate the dip of bedding up to approximately 60°.

The tally of bedding attitudes from all sources for the wall-and-basin region is approximately 1000. These data provide a reasonably complete three-dimensional picture of structure and bedding-thickness variation for 17 exposed map units. Unit thicknesses calculated using bedding measurements and stereoscopic methods were checked against unit thicknesses in published measured sections. From the combined set of unit thickness, we constructed isopach maps for each of the major Upper Triassic through Eocene bedrock map units of the wall-and-basin region; many of the isopach maps are illustrated in the present publication, and all, in Harrison and Jackson (2008). Representative field photographs are presented both in the present publication and in Harrison and Jackson (2008). This latter work also includes a map of photo locations.

Geological point, line, and polygon data for the Strand Fiord–Expedition Fiord region were compiled onto a new geological map at 1:100 000 scale (Harrison and Jackson, 2011). Subsurface geology is illustrated on three regional structural cross-sections, described later in this report.

Geological setting

The report area of west-central Axel Heiberg Island is near the geographical and geological centre of the Carboniferous to Paleogene Sverdrup Basin (Fig. 1, 3). The basin is 1300 km long and 500 km wide, stretching southwest from northern Ellesmere Island. Salt diapirs are dominant in a northeasterly trending belt as much as 200 km wide along the basin axis between northern Melville Island and northern Ellesmere Island. Although the central part of the basin contains the thickest Mesozoic strata, thickness variation determined by the present study is extremely variable near the examined diapirs.

Exposed and unroofed salt diapirs in western Sverdrup Basin are associated with favourable conditions for hydrocarbon generation and preservation. Proven reserves for the western Sverdrup Basin are 17.5 Tcf gas and 1.9 Bbbl oil; total resources are estimated to be 44 to 50 Tcf gas and 3.5 to 5.5 Bbbl oil (Chen et al., 2000). The report area is along the axial diapir belt in the east-central part of Sverdrup Basin. This area has traditionally been considered less promising for hydrocarbons because of 1) a high concentration of diabase sills and dykes, 2) a deep level of erosion that has removed Jurassic and Cretaceous reservoir rocks from many areas, and 3) the increased intensity of shortening caused by the Paleogene Eurekan Orogeny.

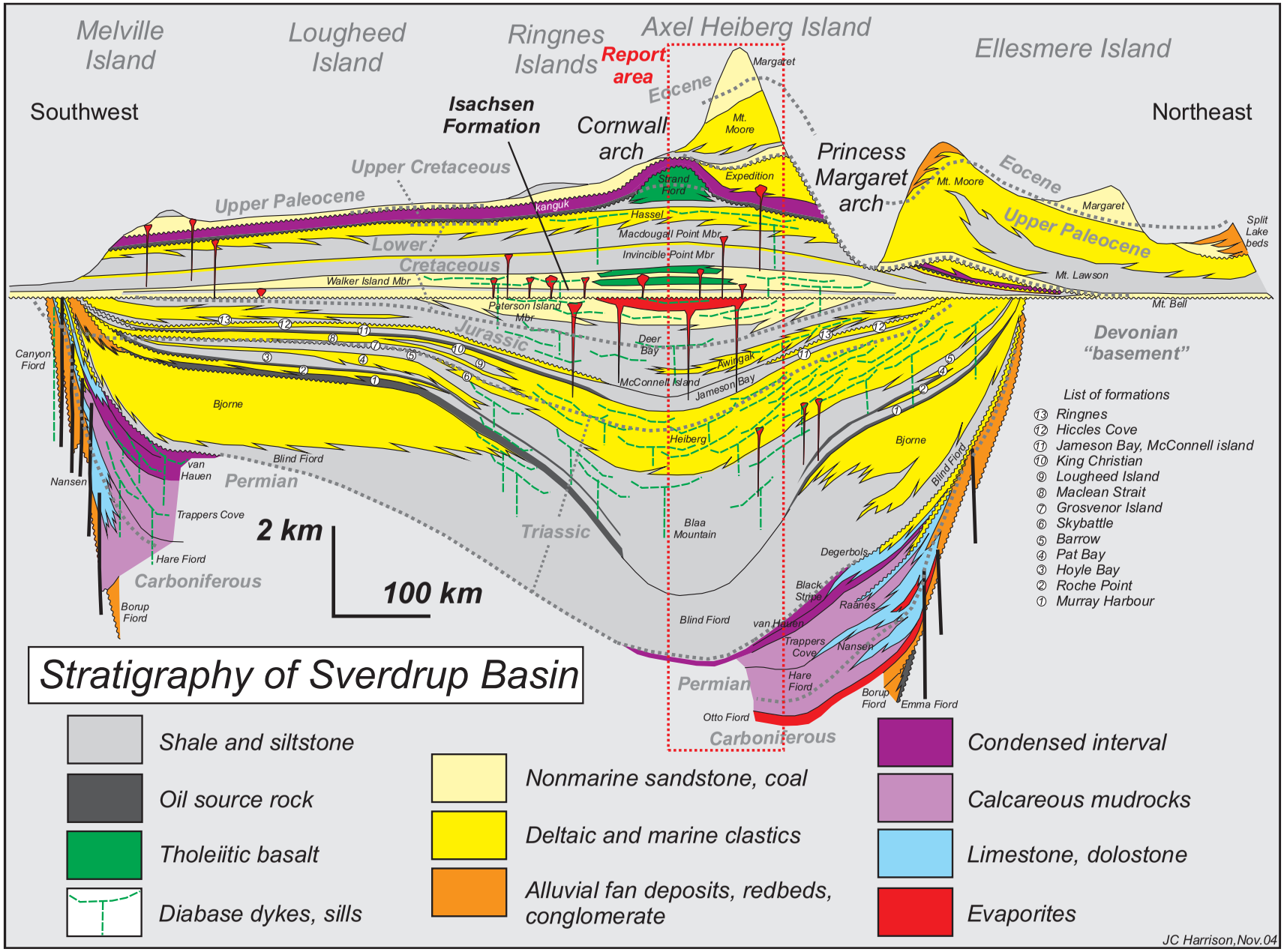

Figure 3. Simplified stratigraphy of Sverdrup Basin between Melville Island and Ellesmere Island. The report area (red rectangle) is in the basin centre. Vertical exaggeration is about 50×.

Tectonostratigraphic History

The margins of Sverdrup Basin are associated with a widespread angular unconformity between Devonian and Carboniferous rocks. In places, for example on northern Ellesmere Island, Lower Carboniferous redbeds at the base of Sverdrup Basin overlie tectonized strata of Neoproterozoic and Cambrian age (Fig. 4). The pre-Carboniferous succession represents the folded and peneplained roots of the Franklinian fold belt, which is part of a lower Palaeozoic orogen exposed south and east of Sverdrup Basin and traceable from northern Alaska and northern Yukon through Banks Island, the Parry, Devon, and Ellesmere islands, to north Greenland. The base of Sverdrup Basin across northernmost Ellesmere Island lies above Pearya Composite Terrane (Trettin, 1998). This area is a region of Mesoproterozoic and younger slivers of continental crust that were accreted to ancestral North America during the Silurian and Devonian deformation phases of the Franklinian Orogen.

Sverdrup Basin and the underlying Franklinian Basin were shortened together during the Paleogene Eurekan Orogeny—deformation caused by the independent plate motions of the ancestral Greenland plate during seafloor spreading in the Labrador Sea and the North Atlantic between approximately 62 and 33 Ma (i.e. chrons 27n to chron 13 or base late Palaeocene to end Eocene). This orogen features far-travelled thrusts between Ellesmere Island and northwest Greenland, and

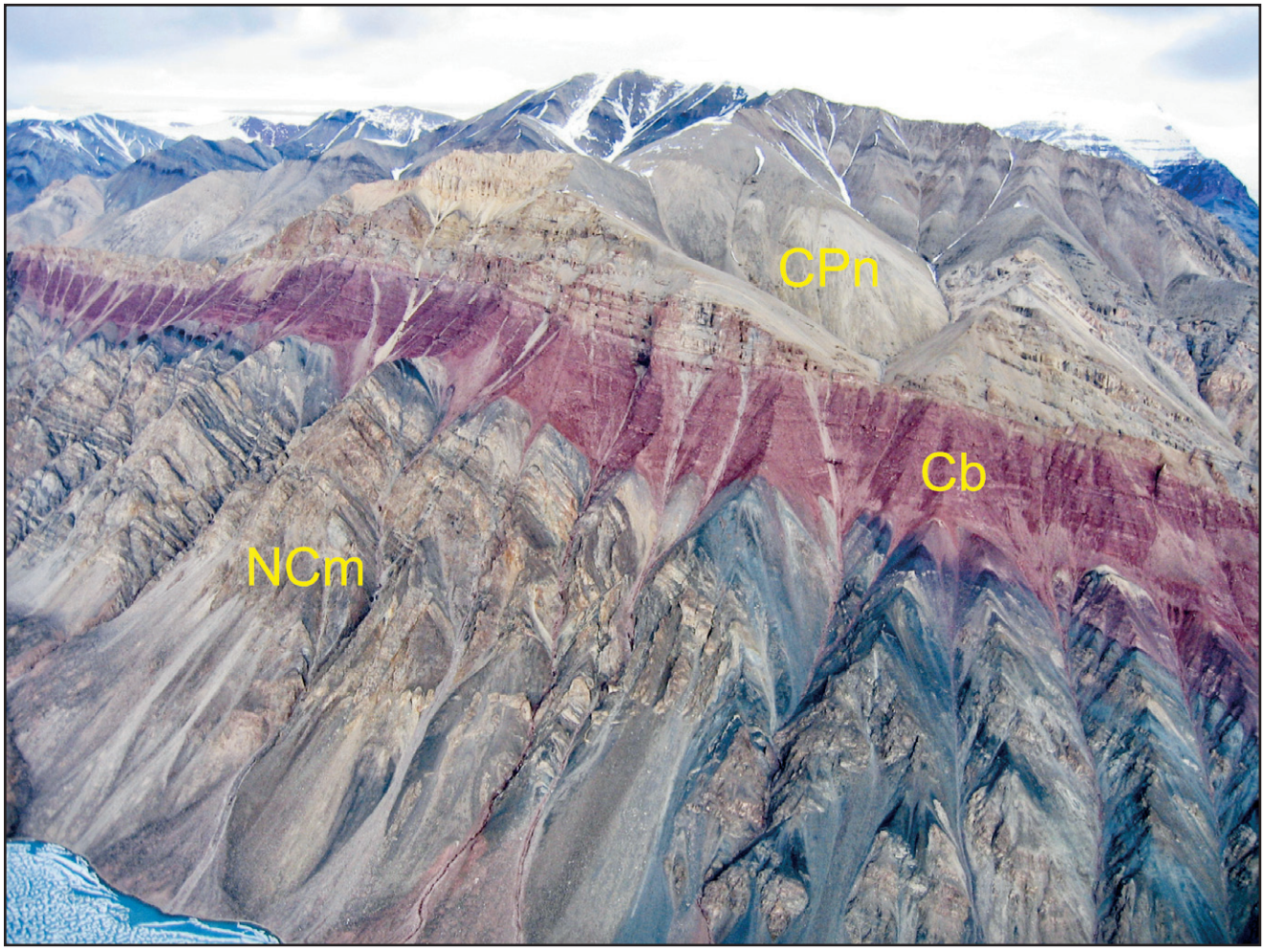

Figure 4. In view from base to top are overturned Grant Land Formation (Ediacaran and Lower Cambrian; NCm), Carboniferous redbeds of Borup Fiord Formation (Cb), and higher Carboniferous Nansen Formation (CPn). (GSC Photo No. 2013-062)

folds, thrusts, and transpressional faults at various scales within the eastern Sverdrup Basin. Eurekan deformation dies away to the west. The end of Eurekan deformation is marked by a profound regional angular unconformity that separates Paleogene and Neogene strata.

The following description of map units includes summaries of age ranges of these units as drawn from the international time scale of Gradstein et al (2012). An exception are ages of Carboniferous units which are based on North American ammonite biostratigraphy. Wherever possible terms of the the equivalent international time scale are also provided although uncertainty exists in the detailed correlation of these two schemes.

Sverdrup Basin rifting (early Carboniferous to mid-Permian)

Rift-related structures of the first tectonostratigraphic phase are exposed on the basin margins and are imaged on seismic profiles (Davies and Nassichuk, 1991). Rifting produced relatively isolated pockets of fluvial and lacustrine sediments during the late Visean age. During the Serpukhovian the rift system expanded and filled with redbeds (Borup Fiord Formation; Fig. 4) in what would become the axis of Sverdrup Basin. Hypersaline marine water flooded the rift basin during the Bashkirian. Evaporites of the Otto Fiord Formation accumulated in the rift axial region from northern Melville Island to northern Ellesmere Island. Carbonates and redbeds began to accumulate in an expanded rift complex now exposed on northern Melville, Bathurst, and Devon islands and on central Ellesmere Island (Davies and Nassichuk, 1991). Open-marine conditions during the Moscovian succeeded the axial evaporites. Discrete facies belts of shelf and slope carbonates and basinal shale were formed (Davies and Nassichuk, 1991).

Borup Fiord Formation

Definition: Known basal strata of Sverdrup Basin are represented by the Borup Fiord Formation on northern Axel Heiberg Island and across much of northern Ellesmere Island. The lower contact in most areas is a widespread angular unconformity above folded and overturned Neoproterozoic to Devonian strata (Fig. 4). The Borup Fiord Formation was first described by Thorsteinsson (1974) on the basis of a type section on Stepanow Creek and in other cliff exposures north and northeast of Hare Fiord on northern Ellesmere Island.

Composition and depositional setting: Dominant rock types include red-weathering quartz sandstone, polymict conglomerate, and minor arenaceous limestone. The conglomerates contain clasts to cobble grade of chert, sandstone, and polycrystalline quartz. Theriault et al (1993) provided a description and summary interpretation of 40 measured sections from northern Ellesmere Island. Unit thickness ranges from 40 to 1100 m. Conglomeratic mass-flow and sheetflood deposits in proximal alluvial fans grade into mixed sandstone, siltstone, and conglomerate associated with stream channel, braidplain, and overbank environments on distal alluvial fans. Locally abundant carbonate of mostly nonmarine origin forms nodular horizons and massive beds as much as 1.5 m thick. These carbonates were interpreted by Theriault et al (1993) as caliche paleosols.

Measured sections north of Otto Fiord on northern Ellesmere Island are part of a northeast-trending syndepositional rift system of grabens containing the Borup Fiord Formation alluvial facies deposits (as much as 190 m thick). These grabens are separated by horsts where younger marine Carboniferous limestone lies directly on peneplained lower Palaeozoic strata (Theriault et al., 1995).

Age: The age of the Borup Fiord Formation is based on a sparse foraminifers and by fauna in overlying strata. The maximum possible age range is early Serpukhovian to early Bashkirian based on the collections described by Groves et al. (1994). These authors inferred an age of mid-Serpukhovian, which is equivalent to the late Chesterian (Late Mississippian).

Otto Fiord Formation

Definition: The Otto Fiord Formation is the source of all the evaporitic diapirs of the central Sverdrup Basin. Its type area is a 10 km length of exposures along the steep shore of Hare Fiord between Van Hauen Pass and Stepanow Creek north of Hare Fiord on northern Ellesmere Island (Fig. 5). Here the Otto Fiord Formation, which is as much as 410 m thick, lies in the hanging wall of a thrust sheet emplaced southward over recessive Permian and Lower Triassic strata. Sections are described by Nassichuk and Davies (1980). Dominant rock types

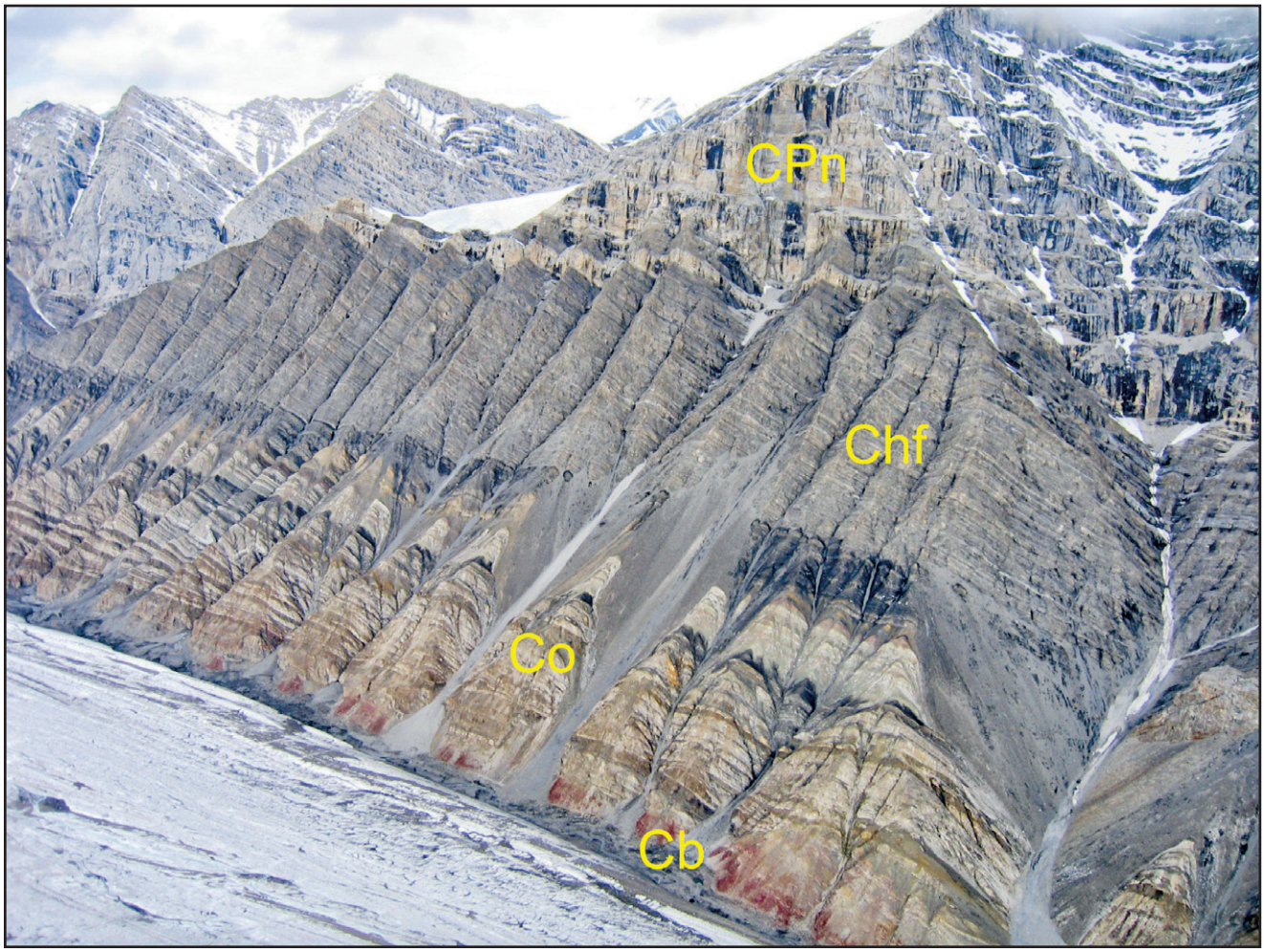

Figure 5. In view from base to top are Borup Fiord Formation redbeds (Lower Carboniferous; Cb), light grey, brown, and black layered Otto Fiord Formation (Co), dark grey and brownish-grey Hare Fiord Formation (Chf), and cliff-forming pale yellowish-grey Nansen Formation (CPn). Location: north shore of Hare Fiord, northwestern Ellesmere Island. (GSC Photo No. 2014-071)

are bedded and mosaic anhydrite with subordinate limestone, rare dolostone, and sandstone.

Composition: The limestone and anhydrite are prominently stratified and arranged in cycles, of which approximately 20 are exposed. Characteristic cycles, 8 to 50 m thick, feature laminated dark grey to black limestone grading up through increasingly bioclastic wackestone then into bedded anhydrite through a narrow interval in which limestone and anhydrite are interbedded. Typical fossils in the limestones include crinoids, bryozoans, brachiopods, trilobites, foraminifers, sponge spicules, algal material, and ammonoids. The limestones locally form mounds as much as 30 m thick (Fig. 6) in which the principal mound-forming organism is branching tubular algae resembling the dasycladacean type. Other common mound material includes skeletal fossil fragments, radial-fibrous calcite, replacive chalcedony, anhydrite, and fluorite.

Additional important stratigraphic relationships are provided by cliff exposures of the Otto Fiord Formation located east of the head of Hare Fiord. Here the Otto Fiord evaporites are built on platform-facies limestone above the Borup Fiord redbeds. Along strike are slope-facies limestones of the Nansen Formation, which grade into the base-of-slope Otto Fiord Formation anhydrite and limestone. Individual tongues of locally mounded limestone are also traceable from clinoforms of lower-slope carbonate into the evaporites. Locally significant are breccias containing angular limestone and dolostone clasts in a matrix of white dolospar and replacive dolomite. These rocks were interpreted by Nassichuk and Davies (1980) as solution-collapse breccias.

Figure 6. Limestones in Otto Fiord Formation locally form mounds as much as 30 m thick. The principal mound-forming organism is branching tubular algae resembling the dasycladacean type. Other common mound material includes skeletal fossil fragments, radial-fibrous calcite, replacive chalcedony, anhydrite, and fluorite. Location: north shore of Hare Fiord, northwestern Ellesmere Island. (GSC Photo No. 2014-072)

Rock salt: Missing from most exposures of the Otto Fiord Formation is rock salt. The Hoodoo L-41 well (Imperial Panarctic et al.), however, which tested Hoodoo diapir on south-central Ellef Ringnes Island, penetrated almost 4000 m of halite below a cap of anhydrite and limestone and overlying Lower Cretaceous sandstone (Isachsen Formation). Halite is sparingly exposed in Stolz diapir on Axel Heiberg Island (Hugon and Schwerdtner, 1982). Within the report area, signs of subsurface halite are provided by saline springs near Colour, Expedition, Junction, and Wolf diapirs (van Berkel et al., 1984; Pollard et al., 1999; Harrison and Jackson, 2008; Fig. 7).

Depositional setting: Nassichuk and Davies (1980) interpreted the Otto Fiord Formation to result from deposition of submarine evaporites. Lying along the rift axial line of the embryonic Sverdrup Basin, the Otto Fiord Formation is flanked by clinoforms of slope-facies carbonates and is succeeded by deep-water limestone and shale of the Hare Fiord Formation *(see below)*. Distinction is made between the submarine facies of the Otto Fiord Formation and the shallow-water to supratidal facies typical of sabkha evaporites.

The record of rifting in the wall-and-basin region is obscured entirely by later sedimentation. The geometry of deep faults, however, suggests that the wall-and-basin region may have been initiated by sinistral strike-slip on north-south-striking faults and by extension and pull-apart along northwesterly striking structures (Fig. 8). This inferred pull-apart basin could have accommodated anomalously thick undeformed Otto Fiord Formation evaporites in the wall-and-basin region.

Age: The age range of the Otto Fiord Formation north and east of Hare Fiord is based on conodonts, ammonites, and especially foraminifers to parallel conodonts and ammonites. This range is Serpukhovian to mid-Bashkirian (Chesterian) at the base through Moscovian to Kasimovian (Atokan to Desmoinian) in the upper part. Ammonites collected from selected diapirs confirm that evaporites correlated with the type section Otto Fiord Formation are involved in diapirism elsewhere in Sverdrup Basin. Ammonites collected and first described by Hoen (1964) from South Fiord diapir within the report area are considered late Bashkirian (early Morrowan). Other ammonite localities associated with diapiric evaporites include the Whitsunday Bay area of eastern Axel Heiberg Island (early Moscovian or early Atokan), Bunde Fiord area of northwestern Axel Heiberg Island (early early Moscovian or early Atokan), Ellef Ringnes and Amund Ringnes islands (early Moscovian or late Morrowan), and Barrow dome on northeastern Melville Island (Serpukhovian to mid-Bashkirian or Chesterian to Morrowan) (Nassichuk, 1975).

Hare Fiord and Trappers Cove formations

Definition: The Hare Fiord Formation was named and first described by Thorsteinsson (1974) for an interval of dark siltstone, shale, and limestone that conformably overlies the Otto Fiord Formation on northern Ellesmere Island (Fig. 5). The Hare Fiord Formation is exposed on northern and eastern Axel Heiberg Island and is encountered in exploratory wells of northern Melville and Prince Patrick islands farther southwest (Harrison, 1995;

Figure 7. Saline spring and mound of precipitated salt near Wolf diapir. Field photographs featured in this paper are precisely located on a map in Harrison and Jackson (2008). (GSC Photo No. 2014-073)

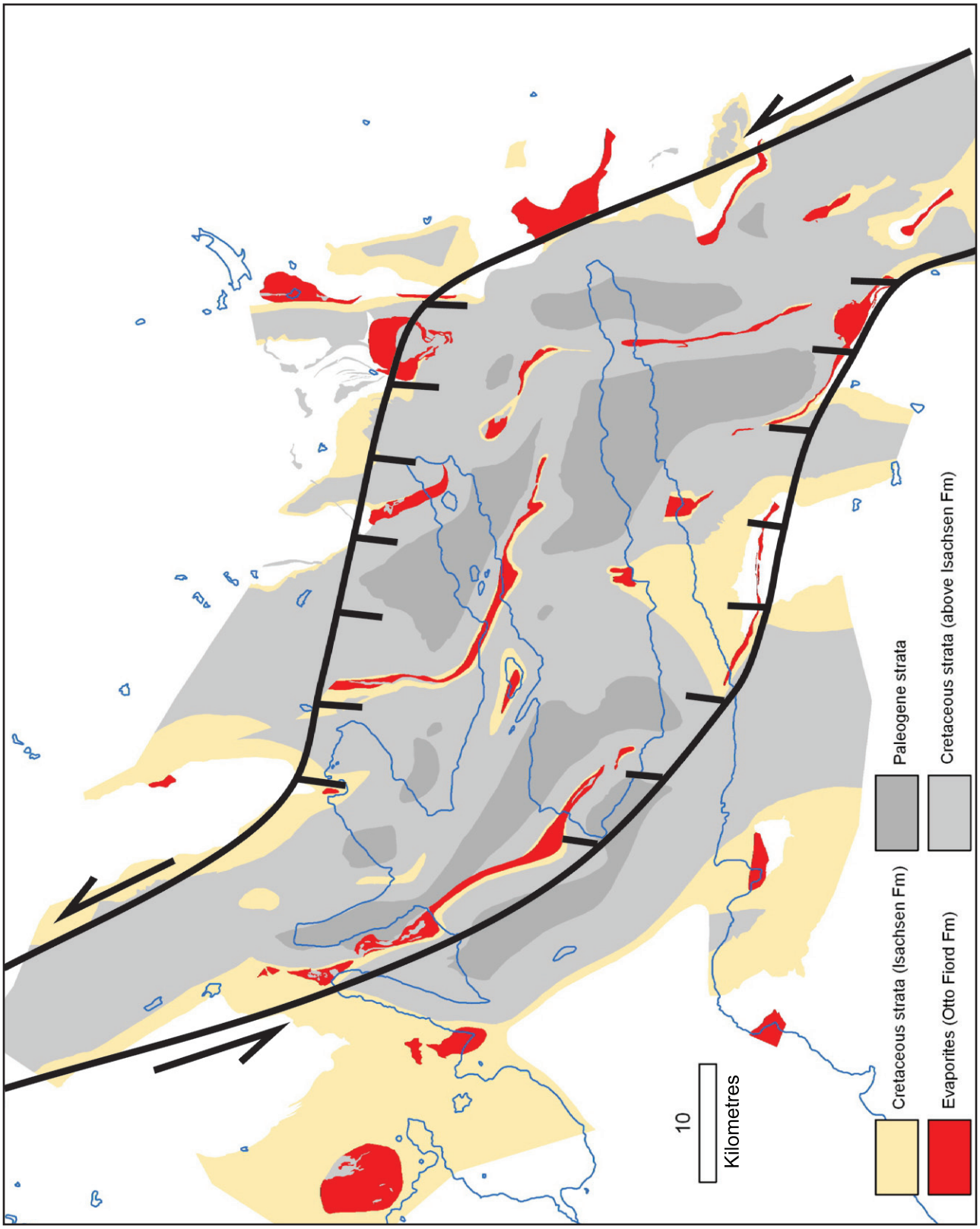

Figure 8. Hypothetical Carboniferous pull-apart structure in a sinistral releasing bend centred in the report area of western Axel Heiberg Island.

Beauchamp et al, 2001). The definition of the formation was emended by Beauchamp and Henderson (1994) to exclude beds that they assigned to a new overlying unit of Lower Permian (Artinskian) siliceous shale, chert, and minor limestone, called the Trappers Cove Formation. The paleogeographic extent and distribution of the two formations are similar. They outline a relatively deep-water realm for the central Sverdrup Basin from the Moscovian to Kasimovian (Atokan to Desmoinian) to the late Early Permian (Artinskian). Although it is likely that both units lie conformably on the autochthonous Otto Fiord Formation throughout the report area subsurface, the nearest exposures are at Buchanan Lake on eastern Axel Heiberg Island.

Composition: The type section of the Hare Fiord Formation is mostly dark siltstone, shale, and limestone (Thorsteinsson, 1974), but the emended Hare Fiord Formation is described as comprising "...greenish grey, brown and yellow shale, argillaceous limestone and chert." These strata occur as a stack of repetitive incomplete Bouma cycles (Beauchamp et al., 1995). Typical rock compositions of the Trappers Cove Formation on central Ellesmere Island are spiculitic chert and lesser shale, siltstone, and "carbonate tongues"; shale increases basinward as chert decreases (Beauchamp and Henderson, 1994).

Thickness: The combined thickness of the Hare Fiord and Trappers Cove formations is greatest at the transition from slope-facies carbonate to basin-facies strata (Fig. 9). On northern Ellesmere Island this interval is as much as 1200 m thick (Thorsteinsson, 1974). Considered separately, the emended Hare Fiord Formation ranges from 200 m to about 1000 m thick (Beauchamp et al., 1995), and the Trappers Cove Formation can locally reach 800 m (Beauchamp and Henderson, 1994). At Buchanan Lake, close to the axis of Sverdrup Basin

Figure 9. Slope-facies of Nansen Formation pass abruptly into darker basin-facies shale of Hare Fiord Formation. Location: north shore of Hare Fiord, northwestern Ellesmere Island. (GSC Photo No. 2014-074)

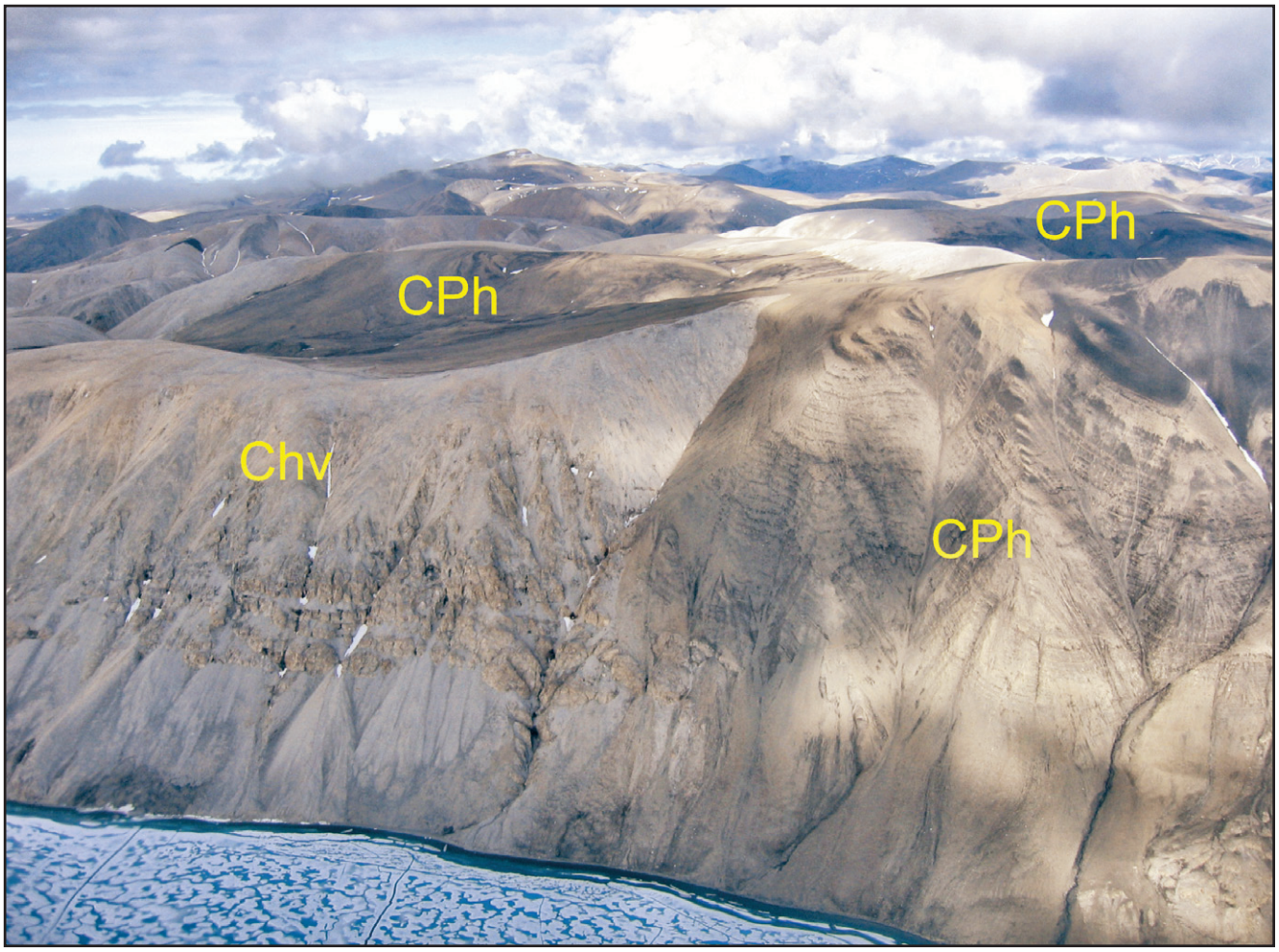

Figure 10. Hare Fiord Formation (brown shale; CPh) occupies minibasins on western Hvitland Peninsula. Each minibasin in this area is framed by dolostone of the Hvitland Formation (Chv), which is in turn underlain by Otto Fiord Formation evaporites (not in view). In the photo is one complete minibasin, the margin of a second (at right), and part of a third (at top right). (GSC Photo No. 2014-075)

during this time, the combined Hare Fiord and Trappers Cove formations are approximately 300 m thick. All the above authors noted basinward thinning of these units. Less clear is the possibility that lateral migration of Otto Fiord salt to form salt swells, pillows, and nascent diapirs may have initiated minibasins and other local thickness variations as the Hare Fiord and Trappers Cove formations accumulated (Fig. 10).

Age: The age of the basal beds of the emended Hare Fiord Formation, provided by conodont assemblages, is near the Morrowan-Atokan boundary (late Bashkirian or early Moscovian). Ammonoids collected from the lower part of the Hare Fiord Formation on eastern Axel Heiberg Island are considered early Moscovian (early Atokan) in age. The Hare Fiord Formation grades into slope-facies and shelf-facies carbonates of the Nansen Formation, which ranges into the Asselian or Sakmarian at the top. The Trappers Cove Formation is thought to be Artinskian on the basis of the presence of conodonts and ammonites but probably also includes Kungurian strata (Beauchamp and Henderson, 1994).

Sverdrup Basin passive subsidence (Late Permian to Early Jurassic)

During the Late Permian to Early Jurassic (~Pliensbachian), Sverdrup Basin evolved as a single geological entity during a postrift phase of passive subsidence (Fig. 3). Marine and nonmarine clastic wedges on the basin margins prograded episodically into deeper water muds in the basin centre.

Isopachs for this interval trend to the southwest on Ellesmere Island and to the west through the western Arctic. These directions conform to structures in the underlying Sverdrup rift system and its lower Palaeozoic basement. Shelf-margin cool-water and cold-water carbonates are found in Upper Permian to Upper Triassic stratigraphic levels. Shallow-water settings, however, are dominated by mudrocks and arenaceous sediments. The Upper Permian, widely eroded below the Triassic on the basin margins, otherwise forms a highly condensed interval of cold-water spicular glauconitic sands grading into shelf, slope, and deep-water spicular chert and mudrock (Van Hauen Formation). In contrast, sediments accumulated rapidly throughout the Triassic, especially in the Blind Fiord Formation (shale), the Blaa Mountain Group (shale), and the succeeding Heiberg Formation (deltaic sandstone) of the central Sverdrup Basin on Axel Heiberg Island. Collectively these formations can exceed 5000 m in thickness. Middle and Upper Triassic strata in Sverdrup Basin contain most of the key oil source rocks. These source rocks have been discovered by exploratory drilling in the west-central part of the basin, but they are also widely exposed in the east (Embry, 1991).

Van Hauen and Black Stripe formations

The terminal Lower Permian and the entire Upper Permian depositional record of the central Sverdrup Basin was sediment starved. This interval was assigned to the Van Hauen Formation by Thorsteinsson (1974) but now includes the Lopingian-age Black Stripe Formation of Beauchamp et al. (2009). Rock types include dark grey to black fissile nonbituminous shale, grey to black siltstone, and dark grey to black spicular chert. Rare limestone beds contain bioclasts of brachiopods and bryozoan detritus. The Van Hauen Formation conformably overlies the Trappers Cove Formation in the central areas of Sverdrup Basin on eastern and northern Axel Heiberg Island and lies on Permian limestone toward the basin margins. Their combined thicknesses in basinal areas of Axel Heiberg Island range from 180 to 360 m (Fig. 11).

Blind Fiord Formation

Definition: Succeeding the Black Stripe Formation is the Blind Fiord Formation of Lopingian to Spathian age (Beauchamp et al., 2009). The Blind Fiord Formation was named and first described by Tozer (1963b) for a 1128 m thick section of siltstone and shale near Blind Fiord on central Ellesmere Island.

Composition: The closest complete section to the report area is at Buchanan Lake. Here Souther (1963) measured a 1310 m interval, including 100 m of Cretaceous gabbro sills, that conformably overlies the Van Hauen Formation (Fig. 11). He described the Buchanan Lake section as consisting of interbedded "light-to-dark grey, buff and red weathering siltstone and dark grey, fissile shale...." Sedimentary structures include casts of annelid worm tracks, graded beds, and "turbulent" cross-beds, presumably showing soft-sediment deformation structures. Within the report area the Blind Fiord Formation is limited to an incomplete section exposed in the hanging wall of a west-dipping reverse fault between Hidden and Thompson diapirs. Fricker (1963) provided a summary description of these unfossiliferous strata and an estimate of thickness (~600 m). The lower part is interbedded dark grey shale, siltstone, and fine-grained calcareous quartz sandstone, the latter in beds as much as 0.5 m thick. Sandstone increases upsection (presumably to the west) with beds locally exceeding 1 m in the upper part of the formation. Assignment to the Blind Fiord Formation was based on the assumption that the upper contact is conformable with the Blaa Mountain Formation. However, Thorsteinsson (1974) indicated on his geology map of the Strand Fiord area that the Blind Fiord Formation at Hidden diapir is fault bounded on all sides. Because these outcrops have so far failed to yield diagnostic fossils, and the structural setting remains uncertain, identification of this belt of rocks as the Blind Fiord Formation must be considered unproven.

Isopachs for the Lower Triassic, prepared by Embry (1991), indicate that the thickness of the Blind Fiord Formation throughout the central Sverdrup Basin, including the report area, might be about 1000 to 1500 m.

Depositional environments of Blind Fiord Formation were described by Embry (1991) as offshore shelf, slope, and basin. Slope facies is most likely dominant in the central part of Sverdrup Basin on western Axel Heiberg Island.

Age: Blind Fiord Formation has been dated regionally using ammonites and bivalves, and

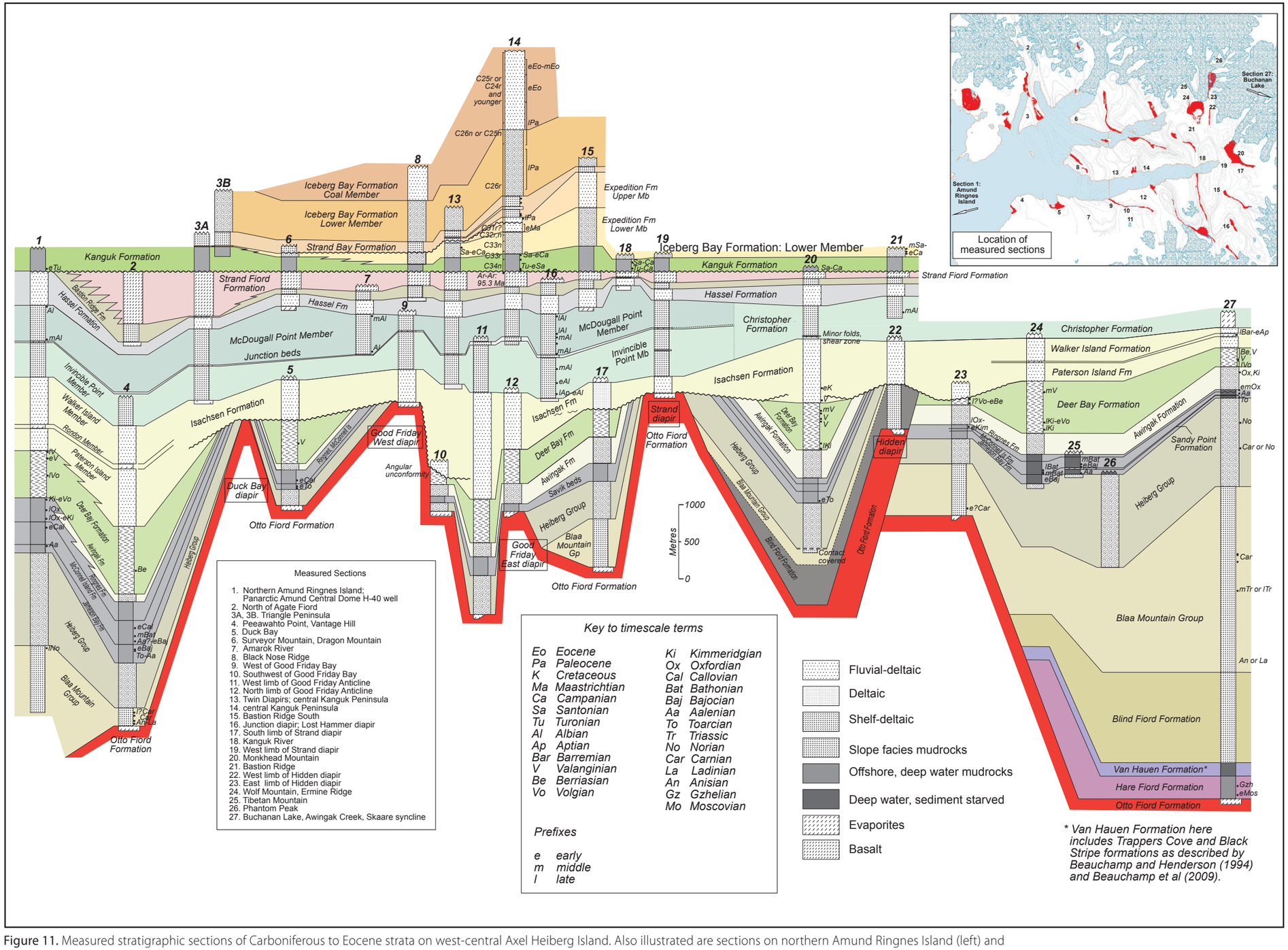

Figure 11. Measured stratigraphic sections of Carboniferous to Eocene strata on west-central Axel Heiberg Island. Also illustrated are sections on northern Amund Ringnes Island (left) and Buchanan Lake on eastern Axel Heiberg Island (right) (Fig. 1).

from this evidence it is mostly Lower Triassic (Thorsteinsson and Tozer, 1970). Charles Henderson (*in* Beauchamp et al., 2009), however, inferred from conodont biozones that the Permian-Triassic boundary lies in the lowermost strata of this formation.

Blaa Mountain Group

Definition: The Blaa Mountain Formation was named by Troelsen (1950) but was first formally defined and described by Tozer (1963b). The Buchanan Lake reference section is closest to the report area (2516 m thick). In addition, numerous diabase sills having a collective thickness of 572 m make up 18.5% of the section. The measured and illustrated section was presented by Souther (1963). The Blaa Mountain was raised to group status by Embry (1984), who recognized three formations in the basin centre: the Murray Harbour Formation at the base (outer-shelf facies to slope facies dark grey to black shale with grey shale and silty limestone increasing into the upper part of the formation; approximately 1400 m at Buchanan Lake); the Hoyle Bay Formation (outer-shelf facies to slope facies medium to dark grey shale with ironstone concretions, calcareous siltstone, and silty limestone; ~600 m); and the Barrow Formation (prodeltaic-facies and shelf-facies shale and siltstone with minor sandstone; ~300 m).

Composition: Within the report area (Fig. 11, 12), the Blaa Mountain Group is exposed 1) east of Hidden diapir, east of the head of Expedition Fiord (dark grey to greyish-black shale, grey siltstone weathering yellowish brown, and common clay ironstone concretions; 700+ m thick; Fricker, 1963), 2) on the west limb of Strand diapir east of Strand Fiord (~645 m), and 3) on the northeast side of Peeawahto diapir (black, dark grey and greenish-grey shale, minor silty shale, sandy siltstone, and sandstone; 245 m; Tozer, 1963a). A thin interval is exposed adjacent to Junction diapir (Fig. 13).

Age: The Blaa Mountain Group ranges from Anisian to Norian in age based in part on ammonite and bivalve assemblages from correlative shallow-marine shelf strata of Sverdrup Basin margin (Thorsteinsson and Tozer, 1970). Diagnostic fauna have been collected from the Buchanan Lake and Peeawahto diapir sections (Tozer, 1963a, b). Early Ladinian fauna (*Daonella frami*) occur at 38 m above the base of section at Peeawahto diapir. Middle Triassic fauna have not been found in the Buchanan Lake section. However, early Ladinian bivalves (*Daonella frami*) occur 122 m above the base of formation north of Whitsunday Bay on southeastern Axel Heiberg Island (Tozer, 1963b). Ashton Embry (pers. comm., 2006) suggested that approximately 300 m of beds is assignable to the Middle Triassic in the Buchanan Lake section. In contrast the maximum thickness of Middle Triassic Blaa Mountain in the Peeawahto section is not more than 70 m based on the lowest occurrence of Late Triassic (Carnian) fauna. This is compelling evidence of marked thinning of Middle Triassic strata between eastern Axel Heiberg Island and the Peeawahto area of western Axel Heiberg. As will be shown, Carnian and younger Mesozoic units also thin toward the Peeawahto structure. This collective evidence indicates that this locality has been a long-lived high, presumably as a consequence of salt diapirism.

Carnian faunas have been collected from both the Buchanan Lake and the Peeawahto sections. From the lowest occurrence of Carnian fauna (at 945 m above base) to the top of the Blaa Mountain Group, the Buchanan Lake Carnian interval is inferred to be at least 1571 m thick (Souther, 1963). In contrast, the Carnian interval in the Peeawahto section, which contains diagnostic macrofauna at 38 and 183 m above the base of the Blaa Mountain Group, is not less than 172 m and not more than 206 m thick. Here, again, is strong evidence of dramatic thinning toward the Peeawahto structure presumably as a consequence of local syndepositional diapirism.

Heiberg Formation

Definition: The Heiberg Formation was named and first described by Souther (1963) on the basis of a type section at Buchanan Lake on eastern Axel Heiberg Island. The unit has three members, introduced in the re-evaluation of the Heiberg Formation by Embry (1983) who correlated surface sections to exploratory wells across the central and eastern Sverdrup Basin. We have not attempted to map out the divisions of the Heiberg Formation. Stratigraphic complications in the formation near the head of Expedition Fiord, however, may be linked to syndepositional salt tectonics (*see* Structure section).

Composition: The three fold subdivision of the Heiberg Formation comprises 1) a lower member (Romulus Member) of interbedded pale grey to

white sandstone, siltstone, and shale in coarsening-upward cycles 5 to 50 m thick, the depositional settings of which were considered to be delta-front-nearshore shelf by Embry (1991), 2) a middle member (Fosheim Member) of mostly fluvial–delta plain light grey sandstone, and lesser siltstone, carbonaceous shale, and coal interbeds, and 3) a relatively thin upper member (Remus Member) of delta-front-nearshore shelf deposits dominated by resistant light brown, pale grey, and white sandstone cemented by quartz, siderite, and clay. The Heiberg Formation near the diapirs within the report area weathers to a distinctive bright hematitic red, most likely derived from ironstone beds in the Fosheim Member (Fig. 14).

Thickness: The Heiberg Formation is 1422 m thick in the Buchanan Lake type section, excluding 194 m of gabbro sills that represent about 12% of the section (Souther, 1963). The Heiberg Formation is more than 1250 m thick north of Phantom Lake (Fig. 14) near Eureka Pass but only 331 m thick on the east side of Hidden diapir (Fricker, 1963) and either 460 or 610 m thick at Peeawahto diapir (Fig. 15). In all these localities the Heiberg Formation overlies the Blaa Mountain Group. Likewise, preliminary graphic estimates indicate that at all other localities within the report area the Heiberg Formation is not more than 600 m thick where it lies on either diapiric evaporites or Blaa Mountain Group strata. Embry (1991) indicated that the thin Heiberg Formation interval east of Thompson diapir (and east of Hidden diapir) places the Fosheim Member in angular unconformable contact with the lower(?) Norian part of the Blaa Mountain Group, and that tilting and overstep of the Romulus Member are evidence of a Late Triassic to Early Jurassic phase of salt diapirism.

Age: Diagnostic fauna are scarce in the Heiberg Formation of the report area. *Meleagrinella antiqua* collected by Tozer (1963a) at 518 m above the base of the formation in the Romulus Member, *Himavaities* sp. at approximately 800 m, and *Monotis ochotica* (Keyerserling) at 853 m, also in the Buchanan Lake section, were considered early(?) Norian, middle Norian, and late Norian, respectively, by Thorsteinsson and Tozer (1970). Plant debris is common in the upper part of the formation but is nondiagnostically Triassic or Jurassic in character (W.L. Fry *in* Souther, 1963). Regional correlation of exploratory well logs, mostly through the western Sverdrup Basin by Embry (1991), indicates that the Fosheim and Remus members most likely range from Rhaetian to earliest Toarcian. This age is based on dinoflagellate assemblages as described by Davies (1984), on a Pliensbachian ammonite from the top of the formation on southern Axel Heiberg Island, and on early Toarcian and younger ammonite macrofauna in overlying strata.

Canada Basin rifting phase (~Toarcian to Valanginian)

From the Toarcian (Early Jurassic) onward, shale again accumulated slowly in the basin's centre. Sandstone intervals in the western Sverdrup Basin include important hydrocarbon reservoirs. In the report area, however, the entire Lower Jurassic (Toarcian) to Upper Jurassic (Oxfordian) interval is dominated by shale (Savik beds). In the early Middle Jurassic, locally north-trending extensional structures began to form in the southwestern Sverdrup Basin (Harrison and Brent, 2005). These new trends cut across the regional west-northwesterly trending elements that had dominated the southwestern Sverdrup Basin since the Carboniferous. The new northerly trends are locally parallel to what would become in the Cretaceous the continental margin of the Arctic Ocean. This margin is now located farther to the northwest. There is no firm indication that this extension affected Axel Heiberg Island or the adjacent islands. Also uncertain is whether extension in the report area during this interval occurred along north-south trends or along trends parallel to the regional shelf margin (east-northeast). As discussed in a later section, however, deformation could have initiated the north-trending evaporite walls common in the report area as reactive diapirs.

Above the Savik beds is the Awingak Formation (Oxfordian and Kimmeridgian), an important quartz sandstone hydrocarbon reservoir. This formation is succeeded by the Deer Bay Formation (Kimmeridgian to Valanginian), a potential aquitard of shale, siltstone, and minor marine sandstone.

Savik beds

Definition: The Savik Formation was erected for a type section of recessive black pyritic shales of Jurassic age exposed near the west end of Buchanan Lake (Souther, 1963). Savik members, formal and

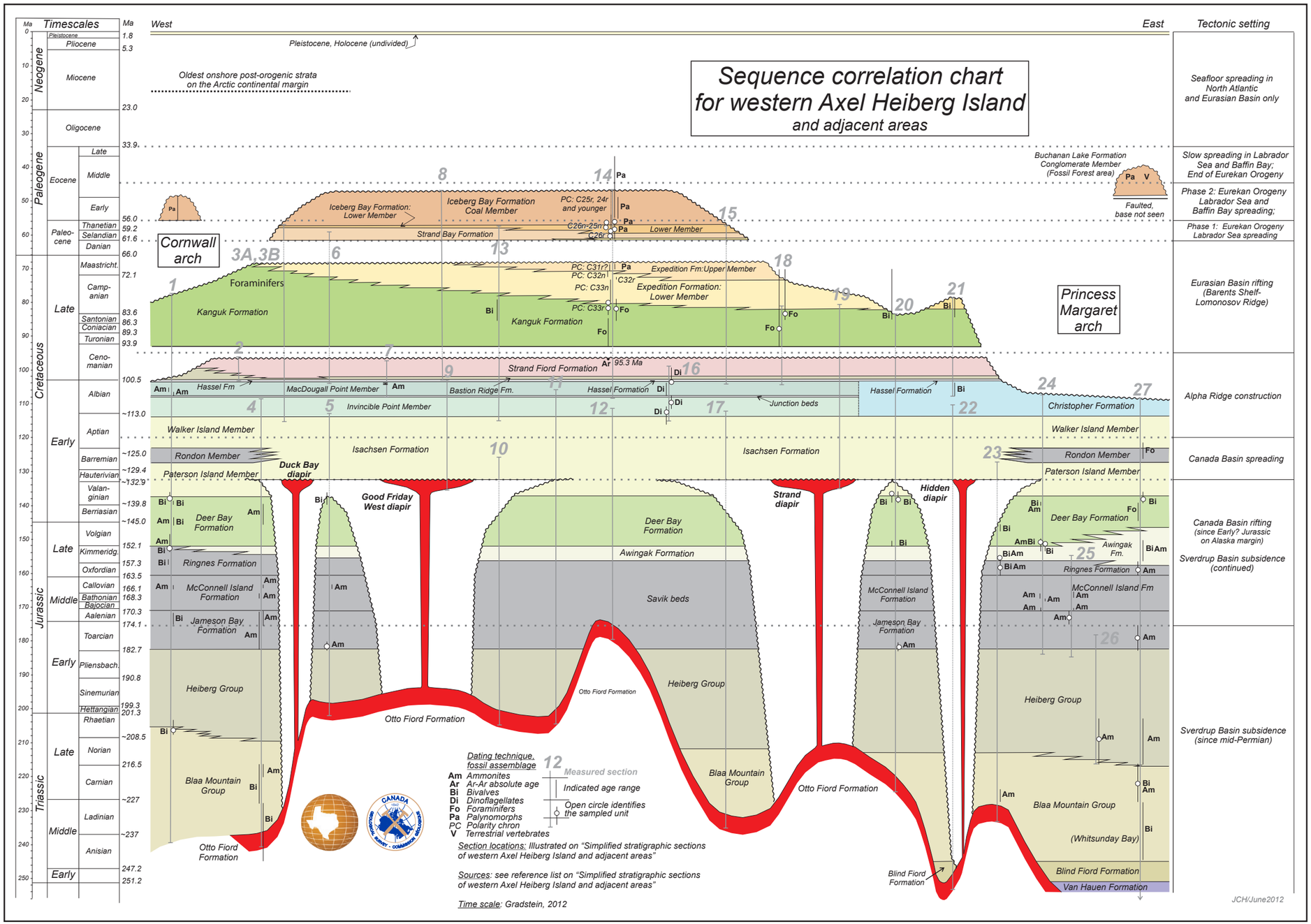

Figure 12. Chronostratigraphic correlation chart for Carboniferous to Eocene strata of west-central Axel Heiberg Island. Also illustrated are sections on northern Amund Ringnes Island, section 1 (left) and Buchanan Lake, section 27, on eastern Axel Heiberg Island (right).

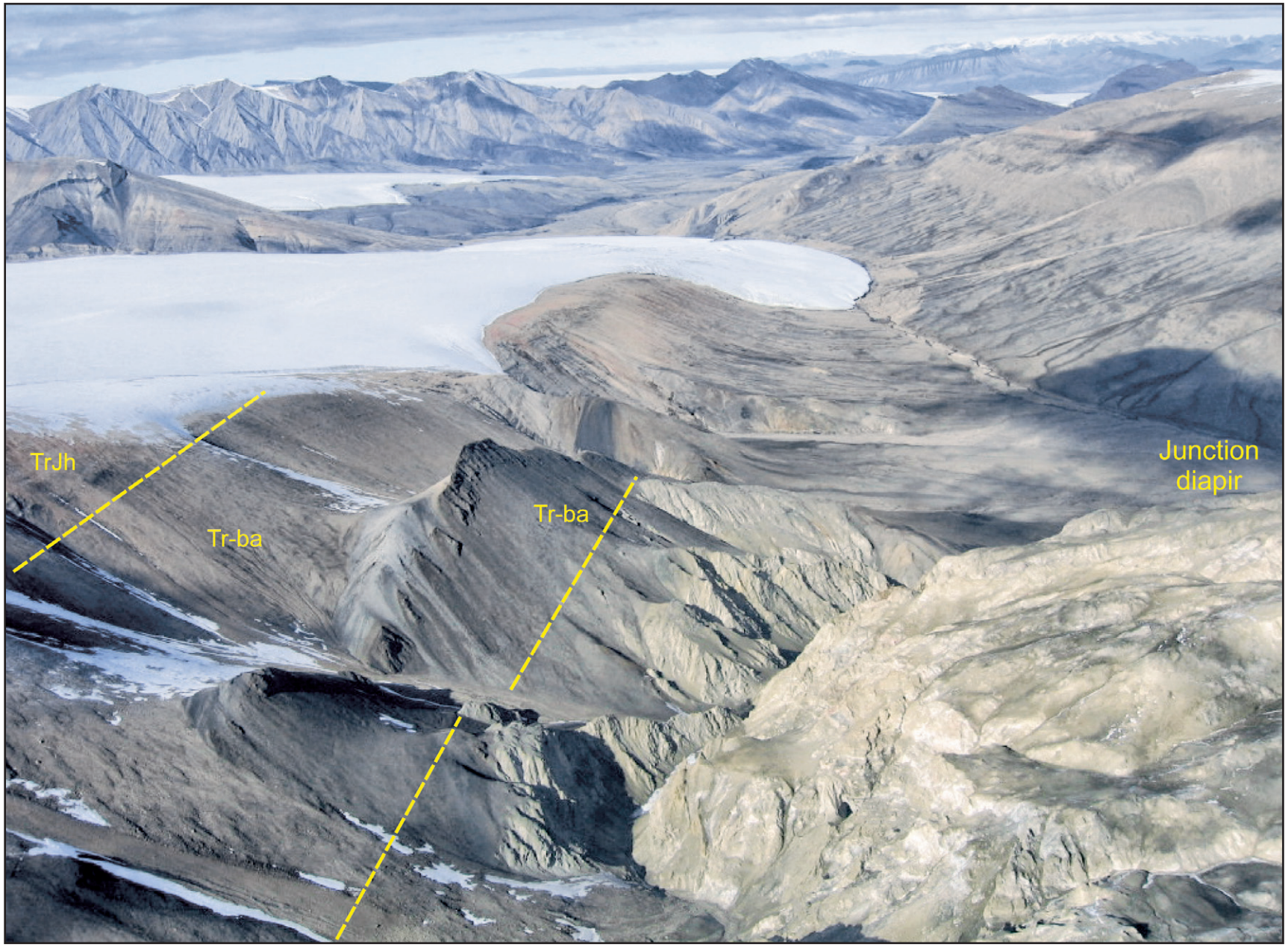

Figure 13. Exposure of dark grey Blaa Mountain Formation (Tr-ba) along the southern margin of Junction diapir, viewed to the northwest. Red-weathering beds to the south (left) are Heiberg Formation (TrJh). A sill of Cretaceous gabbro is emplaced into the medial Blaa Mountain Formation. (GSC Photo No. 2014-076)

Figure 14. Cliff section of Heiberg Formation exposed at Phantom Lake in the northeast corner of the report area. Three sills of Cretaceous gabbro cut the middle and top of section. (GSC Photo No. 2014-077)

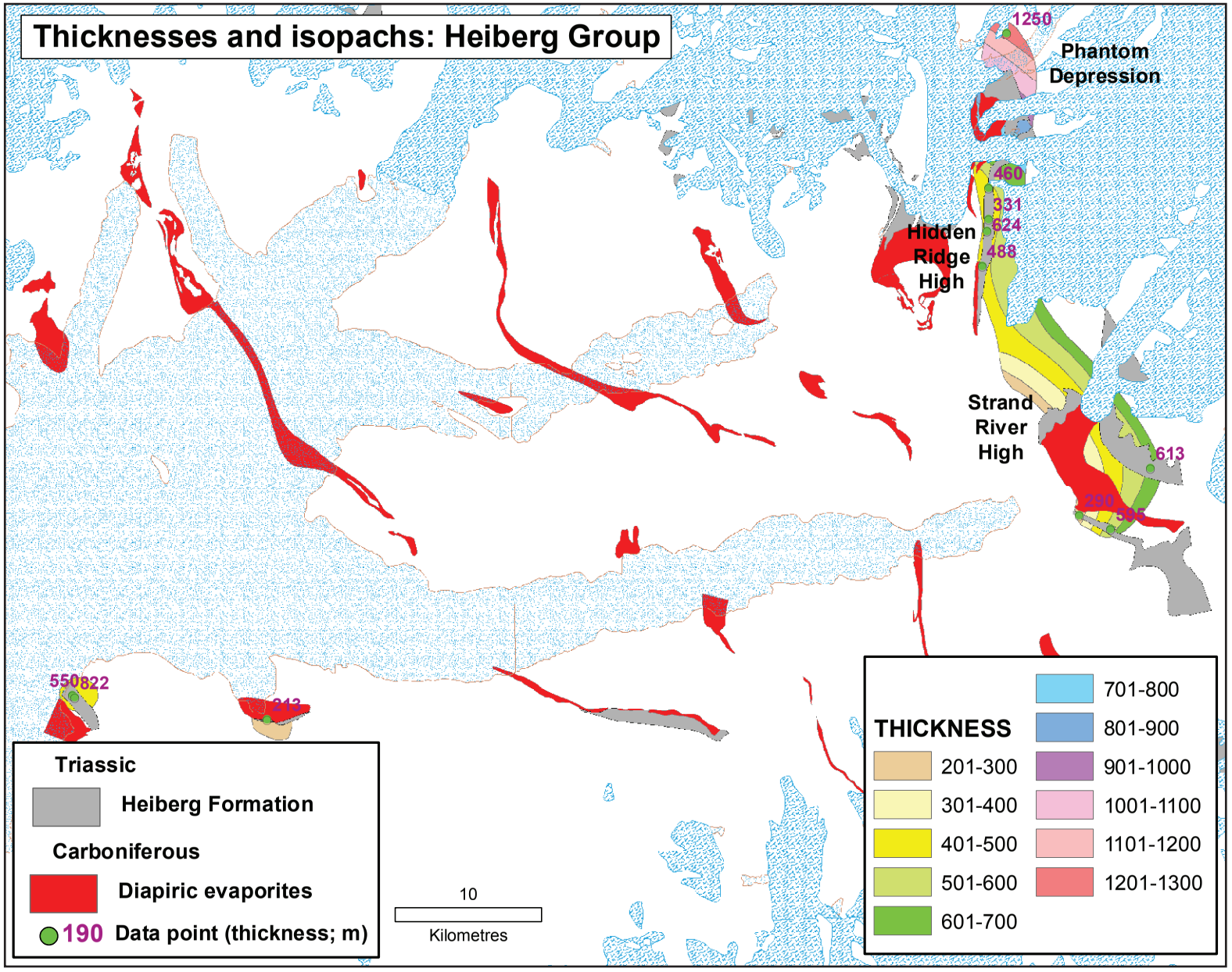

Figure 15. Isopachs and spot thicknesses for Heiberg Formation. Range of thickness is 290 to 1250 m.

informal, were subsequently identified on western Ellesmere and western Axel Heiberg islands (Fig. 10) and throughout the western Sverdrup Basin (Thorsteinsson and Tozer, 1970). Problems with stratigraphic nomenclature were recognized by Embry (1984). He abandoned the term 'Savik Formation' in favour of a new series of shale and sandstone formations assigned to the Wilkie Point Group and Ringnes Formation in western Sverdrup Basin. Embry's (1984) stratigraphic units within the report area include the the Jameson Bay, the Sandy Point, the McConnell Island, and the Ringnes formations. Except for the Sandy Point Formation, which is a discontinuous marker sandstone bed not more than 5 m thick, all these formations are dominated by dark grey to black shale with differences that are impractical to distinguish on air photographs or by distant observation (Fig. 16). For this reason we refer to the entire interval as 'Savik beds'. This term is considered synonymous with the Wilkie Point Group plus the Ringnes Formation, or the Jameson Bay through the Ringnes formations, undivided.

Composition: The original description of the Savik Formation, based on the Buchanan Lake type section and others at Strand Fiord (Souther, 1963), identified a lower part of soft, dark grey shale containing pyrite and ironstone concretionary layers and an upper part having a higher proportion of silt. The high iron sulphide and oxide content of the overall unit was also noted.

Fricker (1963) recognized three informal members of the Savik Formation on the basis of measured sections west and south of Thompson Glacier. These include

Member 3: dark grey to greyish-black shale with sideritic ironstone concretions in the lower part; siltstone and argillaceous limestone interbeds in the upper part.

Member 2: dark grey shale with silty sandstone interbeds and a sandstone marker.

Member 1: dark grey to greyish-black shale with sideritic ironstone concretions.

Embry (1984) summarized formations of the Wilkie Point Group of the central Sverdrup Basin, but in detail this description may not apply to local depositional facies on western Axel Heiberg Island. The description of the Ringnes Formation is provided by Balkwill et al. (1977) and is based on the type section on Amund Ringnes Island. The Wilkie Point Group encompasses, from top to bottom.

Ringnes Formation: dark grey to black silty shale, slightly sandy with huge yellow-buff calcareous and sideritic mudstone concretions as much as 5 m in diameter.

McConnell Island Formation: medium to dark grey glauconitic shale with pale to medium grey siltstone increasing upsection; common ironstone interbeds.

Sandy Point Formation: burrowed glauconitic sandstone, siltstone, and shale arranged in coarsening-upward cycles.

Jameson Bay Formation: medium to dark green-grey shale with siltstone laminae and interbeds; common calcareous, dolomitic, and sideritic concretions.

The Jameson Bay and Sandy Point formations may be equivalent to members 1 and 2, respectively, of Fricker (1963), and the concretionary shale facies of the Ringnes Formation is also reported from the upper Savik beds of western Axel Heiberg Island (Ashton Embry, pers. comm., 2013).

Six measured sections through the Savik beds in the report area, most notably south and west of Thompson Glacier (Fricker, 1963), and at Duck Bay and Peeawahto diapirs (Tozer, 1963a; Thorsteinsson and Tozer, 1970), have been published, in addition to sections at Buchanan Lake (Frebold, 1961; Tozer, 1963a; Thorsteinsson and Tozer, 1970; Wall, 1983) and in the Panarctic Amund Central Dome H-40 well of Amund Ringnes Island (Balkwill, 1983). Sections studied for the present report with only graphic estimates of unit thickness are near Strand and Good Friday diapirs.

Thickness: Thickness of the Savik beds ranges from less than 85 m (at Good Friday Bay) to 819 m (at Peeawahto diapir) (Fig. 17). Local thickness variation is also evident. For example, the unit thins over a distance of 25 km from 385 m at Monkhead Mountain to 108 m on the west limb of Hidden diapir. At Good Friday diapir the unit thins from 250 m to less than 85 m over a distance of 2 km. Shale components also vary in thickness: 30 to 254 m for the Jameson Bay Formation, 32 to 319 m for the McConnell Island Formation, and 30 to 245 m for the nonconcretionary facies of the Ringnes Formation.

Significant thickness variations of the Savik beds (Figure 17) display a prominent northwesterly trend. Noteworthy are minibasins and depressions

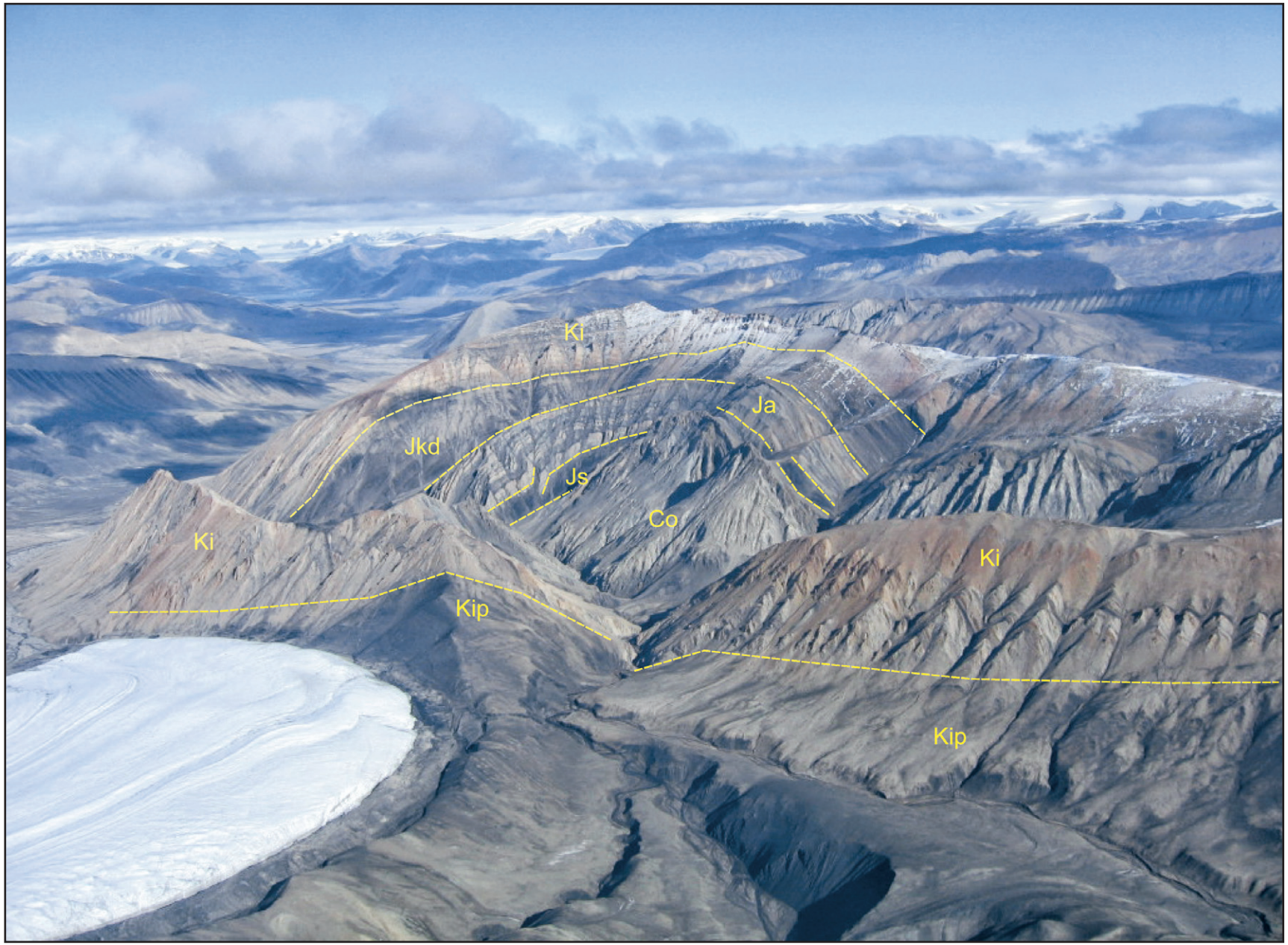

Figure 16. Map units above the evaporites (Co) at Lost Hammer diapir include the Savik beds (thin black band; Js), Awingak Formation (black and yellowish-brown striped beds; Ja), Deer Bay Formation (wide black band; JKd), and Isachsen Formation (rusty coloured resistant beds; Ki) on the skyline ridge crest and at near right. Dark foreground beds are Invincible Point Member (Kip). View is northward. (GSC Photo No. 2014-078)

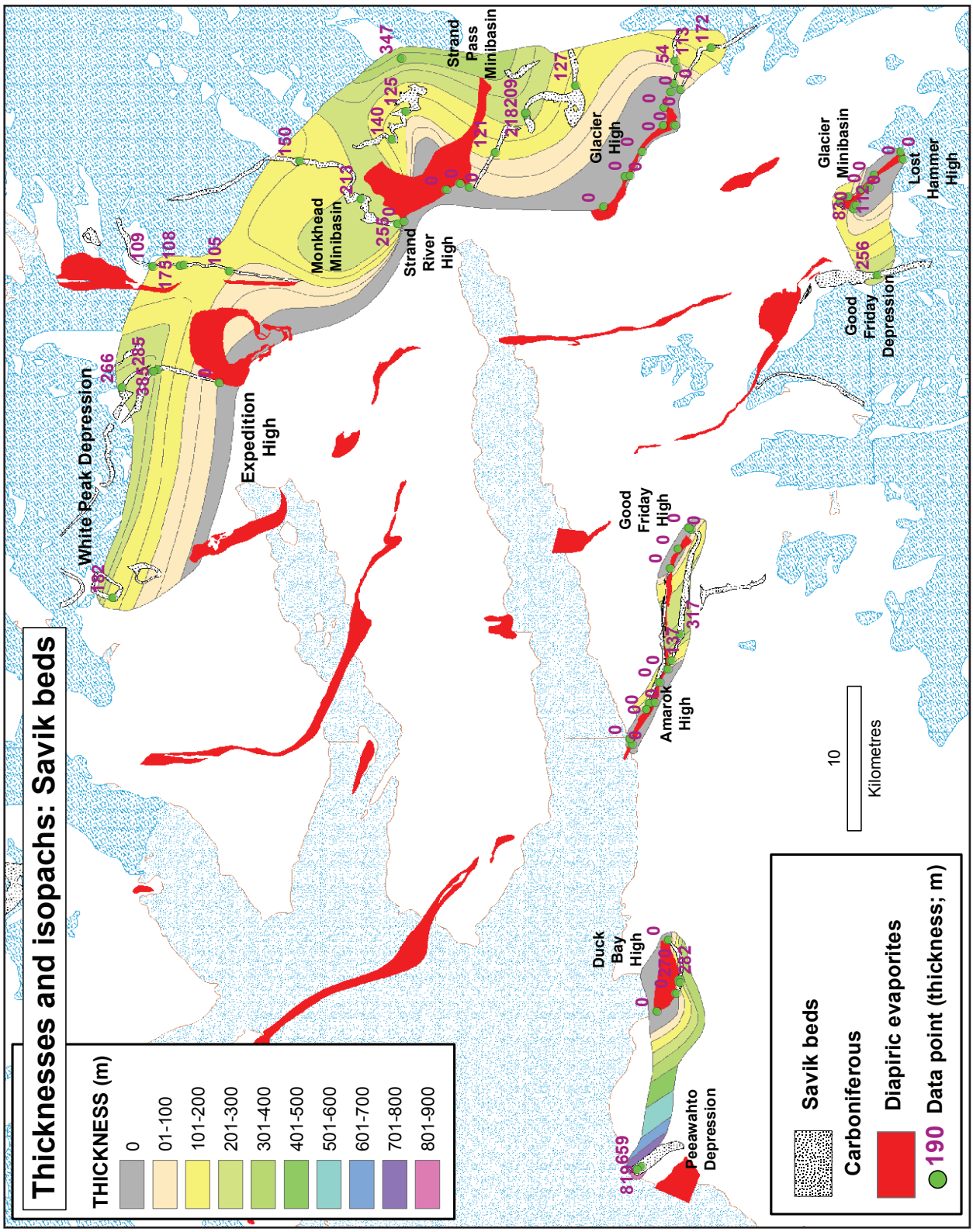

Figure 17. Isopachs and spot thicknesses for Savik beds. Range of thickness is 54 to 819 m.

east and northwest of Strand diapir and north of Expedition and Colour diapirs. The largest local thickness variation is between Duck Bay diapir (270 m) and Peeawahto diapir (819 m). In the north is White Peak depression, which trends westerly and is limited to the southwest by Colour diapir and to the southeast by Expedition diapir.

Age: Savik beds in the report area range from early Toarcian to late Oxfordian–early Kimmeridgian, on the basis of ammonites, bivalves, and foraminifers. The Jameson Bay Formation contains early Toarcian fauna (*Harpoceras* sp.) at 21 to 43 m above the base of the formation at Monkhead Mountain (Poulton, 1984) and at 18 and 46 m above the base of the formation at Duck Bay (*Harpoceras* sp., *Catacoeloceras spinatum*, Tozer, 1963a). Toarcian foraminifers of the *Flabellamina* sp. 1 assemblage occur in the Jameson Bay Formation at Buchanan Lake (Wall, 1983). Early Aalenian fauna occur at Tibetan Mountain (*Oxytoma jacksoni, Leioceras*? sp., Fricker, 1963), Peeawahto diapir, and Buchanan Lake (*Oxytoma jacksoni, Pseudoleioceras M'Clintocki*; Thorsteinsson and Tozer, 1970 and on Amund Ringnes Island (*Oxytoma jacksoni*; J.A. Jeletzky, p. 69, *in* Balkwill, 1983).

The McConnell Island Formation has fauna ranging from early Bajocian (*Arkelloceras* sp., *Stephanoceras* or *Cadomites* sp.) to mid-Bathonian (*Arctocephalites greenlandicus, Arctocephalites arcticus, Arcticoceras ishmae, Arcticoceras* sp.) and early Callovian (*Cardioceras* sp.; *Cardioceras septentrionale* zone) at Ermine Ridge and Tibetan Mountain, both near Wolf Mountain (Fricker, 1963; Poulton, 1984), at Duck Bay (Tozer, 1963a), at Peeawahto diapir (Frebold, 1964; Poulton, 1984), and on Amund Ringnes Island (J.A. Jeletzky *in* Balkwill, 1983). Aalenian to early Bajocian foraminifers of the *Ammodiscus* cf. *asper* assemblage occur at Buchanan Lake (Wall, 1983).

Strata equivalent to the Ringnes Formation contain early to middle Oxfordian fauna at Buchanan Lake (*Cardioceras* sp.; Frebold, 1961, Thorsteinsson and Tozer, 1970) and late Oxfordian to early Kimmeridgian fauna east of Hidden diapir and on Amund Ringnes Island (*Buchia concentrica* zone; J.A. Jeletzky, p. 69–70, *in* Balkwill, 1983). The Buchanan Lake section also contains Oxfordian foraminifers of the *Ammodiscus thomsi* assemblage (Wall, 1983). The Ringnes Formation thickens to the west and is younger in that direction at the expense of the overlying Awingak Formation sandstone. In the absence of the Awingak Formation, the Ringnes Formation is as young as late Kimmeridgian to early Volgian (*Buchia mosquensis* zone; J.A. Jeletzky, p. 70, *in* Balkwill, 1983) on Amund Ringnes Island.

Awingak Formation

Definition: The Awingak Formation is a resistant unit of mixed marine and nonmarine sandstone and marine shale. Its type section is near Awingak Creek south of Buchanan Lake on eastern Axel Heiberg Island (Tozer, 1963b; Thorsteinsson, 1974). The Awingak Formation was first recognized only on Axel Heiberg and Cornwall islands but has since been mapped on Ellesmere Island (Thorsteinsson and Tozer, 1970), on southern Amund Ringnes Island (Balkwill, 1983), and throughout the western Sverdrup Basin (Embry, 1991).

Composition: In the type section the formation was originally recorded as approximately 305 m thick (Souther, 1963), but it has been revised to 345 m (Wall, 1983). The original description features five sandstone members and three intervening shale members. The quartzose sandstones are loosely cemented and fine and medium grained. They are arranged in repetitive cleaning- and coarsening-upward cycles, each 9 to 15 m thick. The sandstones contain coalified plant debris and evidence of fossil roots. Weathering colours range from white and yellow in the lower part of the formation to yellow, yellow-red, and reddish orange in the upper part. The lowest of the three shale intervals (22 m) is black and pyritic and contains chert pebbles near the base. The upper two shale intervals (26 m, 34 m) are dark grey and contain red-brown mudstone concretions and thin beds.

Five published measured sections in the report area are those at Monkhead Mountain (Souther, 1963), Ermine Ridge near White Glacier and east of Thompson Glacier (Fricker, 1963), Duck Bay (Tozer, 1963a), and Peeawahto diapir (Thorsteinsson and Tozer, 1970). Souther (1963) distinguished a western facies at Monkhead Mountain (~305 m thick) from a type-section eastern facies by the greater predominance of sandstone relative to shale in the west. Repetitive coarsening-upward cycles are 10 to 30 m thick and pass from black shale intervals at the base, not more than 1.5 m thick, through fine-grained sandstone and silty sandstone with coalified plant debris, to medium-grained sandstone in the

upper part (Souther, 1963). At Thompson Glacier the section (237 m thick) is more finely divided (18 shale intervals, each 1 to 8 m thick; Fricker, 1963). In contrast, at the neighbouring White Glacier, the Awingak Formation is dominated by sandstone (only two shales of 18 m and 0.5 m in a section 283 m thick; Fricker, 1963). At Duck Bay, the section is considerably attenuated (76 m) and is dominated by carbonaceous quartz sandstone without shale mentioned (Tozer, 1963a).

Thickness: Preliminary evaluation of regional thickness variations of the Awingak Formation within the report area has been augmented by graphic estimates of formation thickness at Strand diapir and at Good Friday Bay (Fig. 17). In general, the Awingak Formation thins to the northwest through facies change to Ringnes Formation shale. The lower contact is interpreted as a downlap surface. The formation is thickest at Monkhead Mountain (383 m; Ashton Embry, pers. comm., 2005) and ranges to minima of 76 m and 105 m at Duck Bay (Tozer, 1963a) and Peeawahto diapirs (Thorsteinsson and Tozer, 1970), respectively. The formation thins markedly westward into the Ringnes Formation north of Iceberg Bay. The Awingak Formation is unrecognizable on air photographs in the mountain range west of Agate Fiord, where the exposed interval most likely includes beds correlated with the Heiberg through Deer Bay formations. This view suggests a westward facies change from pale quartz-sandstone to darker silty sandstones and siltstone.

Northwesterly trends (Fig. 18) again appear in late Oxfordian to Kimmeridgian isopachs (Awingak Formation). However, westerly trends are also evident. The northwesterly trend is especially true for the Good Friday minibasin between Good Friday East and Good Friday Central diapirs. Bounding highs on this minibasin coincide with Junction diapir to the southeast and Good Friday West diapir to the northwest. Evident for the first time is the northwest-trending Glacier minibasin on the flank of Lost Hammer diapir. This interval reaches a thickness of 360 m. A longer-lived structure in this time interval is Strand diapir, which is bounded by local depocentres to the north (Monkhead minibasin) and to the south (Strand Pass minibasin). In the north, White Peak depression remained active between and north of Colour and Expedition diapirs. This depression is not proven to be a minibasin because the associated isopachs are undefined at the lateral limit of mapping.

Stratigraphy varies adjacent to selected diapirs. The Awingak Formation thins by more than 50% to the east and to the west at Good Friday Bay. Close to the diapirs in this area the Awingak oversteps the Savik beds, in places lying directly on the Heiberg Formation or even on Otto Fiord evaporites. Similar stratigraphic relationships are noted east of Glacier diapir, and the Awingak Formation thins locally westward onto Strand diapir and southward toward Expedition diapir.

Debris flows: The relationship between diapirism and the deposition of the Awingak Formation is highlighted on the southeastern margin of Junction diapir south of Strand Fiord. Here the main body of the diapir terminates in slivers of anhydrite and diapir-associated dolomite. An eastern sliver lies between the Awingak Formation on the west and the Lower Cretaceous Isachsen Formation to the east. The western sliver of diapiric evaporite lies along the contact between the Heiberg Formation and the Savik beds to the west and the Awingak Formation to the east. These two slivers of evaporite and carbonate are separated by a complex southeasterly plunging syncline cored by recessive Deer Bay Formation. The southern limit of Otto Fiord anhydrite and dolomite occurs in hillside outcrops, which are obscured to the south by colluvium. Streambank exposures, approximately 250 m to the southeast and along strike from the southeastern end of the western evaporite sheet, reveal a distinctive diapir-marginal facies interpreted to have accumulated adjacent to the evaporite sheet and immediately prior to deposition of the typical Awingak Formation sandstone.

This facies is approximately 90 m thick and features a 20 m thick lower stratigraphic interval, probably overturned to the west. This interval comprises dark grey to black hornfelsed and pyritized matrix-supported sedimentary breccia. Angular breccia clasts of hornfelsed grey mudrock lie in a matrix of quartz sand, pyrite, and dark comminuted rock fines. This area is interpreted as the lower part of the section and is separated from an upper part by a covered interval of perhaps 10 m. The higher stratigraphic section (60 m thick), also most likely overturned, consists of dark grey to black sedimentary breccia containing angular clasts of white, sucrosic gypsum and dark

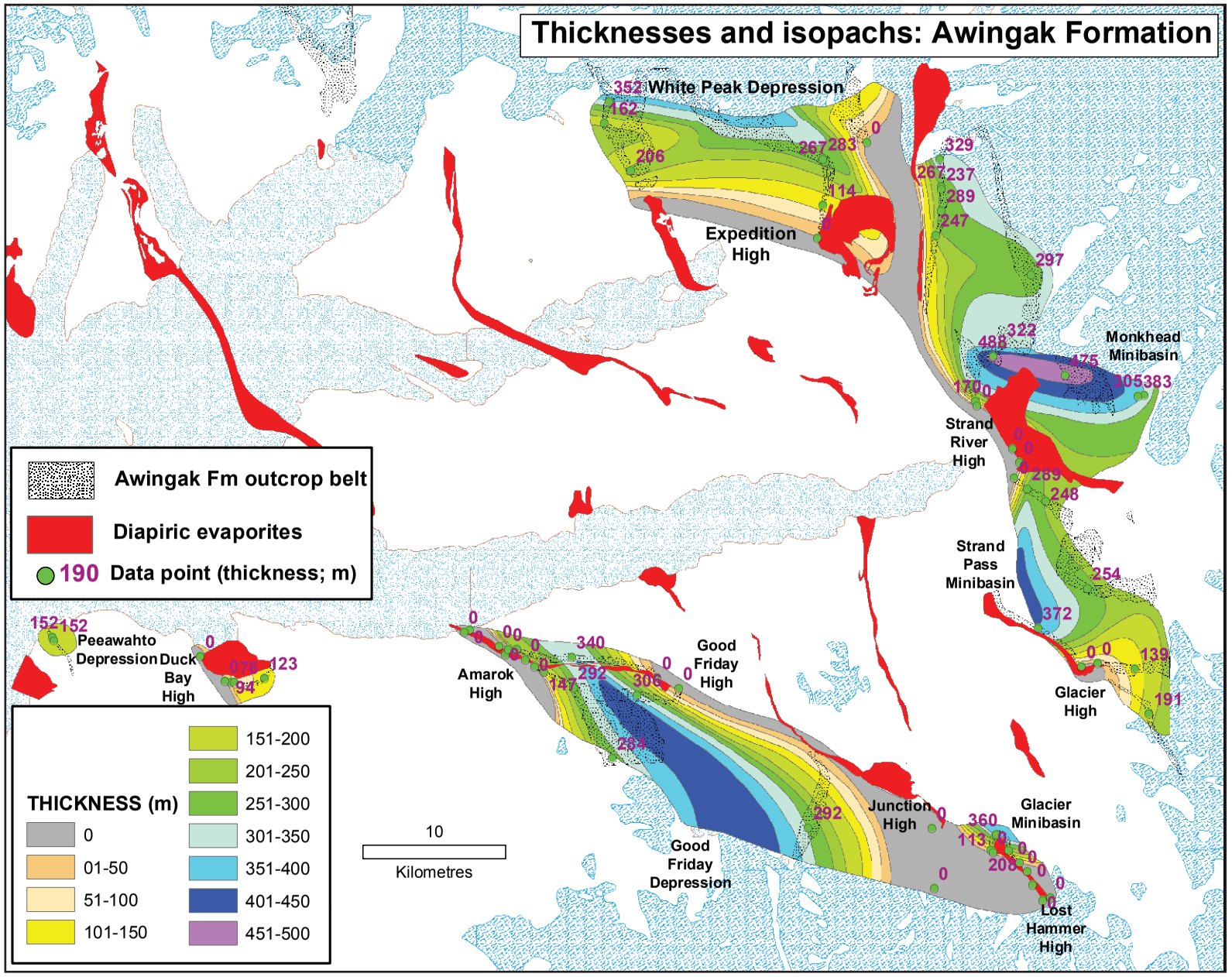

Figure 18. Isopachs and spot thicknesses for Awingak Formation. Range of thickness is 76 to 488 m.

grey-black carbonate supported by a matrix of gypsum, carbonate, and other dark rock fines (Fig. 19). Maximum clast dimensions are 20 by 80 cm. The stratigraphic top of the section is covered to the east.

Stratigraphic relationships are clearly laid out in a large and impressive outcrop, again located along strike to the southeast beyond a covered interval of approximately 100 m from the aforementioned streambank section. In these southern outcrops the breccia facies is exposed for at least 870 m between a glacier tongue and cliffs of the Awingak Formation to the east. Observations are derived from the northernmost part of this outcrop belt. The nearest underlying exposure is of the upper Savik beds (Ringnes Formation) located 150 m to the west on the opposite side of a glacier tongue and braidplain. Otherwise, the base of the section is covered by glacier ice and outwash gravel. Above this cover is 145 m of resistant-weathering sedimentary breccia with minor interbeds of cross-stratified quartz sandstone (Fig. 20). Indicated tops are to the east.

Three breccia units are obvious: a lower massive, unstructured, breccia flow at least 80 m thick (Ja-bx1), a 50 m thick breccia flow (Ja-bx2), and a 15 m thick interval of pyritized, rippled and cross-stratified quartz sandstone grading up into breccia (Ja-bx3). Breccias are matrix supported and contain angular clasts of grey shale, rounded ferruginous mudstone, rare coalified wood, and grey carbonate (Fig. 21, 22). The carbonate clasts were only seen in the top two flows at the north end of the outcrop belt. This breccia sequence is overlain to the east by yellowish-weathering quartz-sandstone containing coalified wood fragments and lesser interbeds of shale and siltstone. The contact is a recessive interval about 2 m wide. A panoramic

Figure 19. An Upper Jurassic submarine debris flow in lower Awingak Formation just southeast of Junction diapir. Matrix-supported large clasts are mostly gypsum, which was eroded from the diapir. (GSC Photo No. 2014-079)

Figure 20. Three nested submarine breccia flows (Ja-bx) in lower Awingak Formation (Ja), southeast of Junction diapir. View to the south. (GSC Photo No. 2014-080)

Figure 21. Matrix-supported debris flow of lower Awingak Formation southeast of Junction diapir. Shale clasts are derived from Savik beds. (GSC Photo No. 2014-081)

view of these exposures indicates that the top of the breccia sequence is a transgressive surface where Awingak sandstone onlaps the breccia flow top from southeast to northwest, toward Junction diapir.

These breccia units are interpreted as stacked submarine debris flows. The stratigraphic correlation to a sheet of Otto Fiord evaporite and the occurrence of gypsum and carbonate clasts in the most proximal exposures of breccia indicate that the adjacent evaporite sheet to the northwest provided this material. The southwestward disappearance of gypsum clasts at a distance of not more than 200 m from the southern preserved limit of evaporites, followed southwestward by the disappearance of carbonate clasts from the upper debris flows, indicates the extremely limited transport distance for these mechanically and chemically unstable rocks. Most clasts in the southern debris flow resemble the shale and ferruginous mudstone concretions common in the upper Savik beds. This composition suggests that uplift, erosion, and shedding of Savik and Otto Fiord evaporite-carbonate debris coincided with the extrusion of an evaporite sheet onto a basal Awingak unconformity surface. The distance of transport of these sub-Awingak debris flows has not been measured. However, aerial photographic evidence indicates a strike length of not less than 1800 m. The subsequent onlap of Awingak sandstone marks waning diapirism or increasing aggradation rate.

Age: The age of the Awingak Formation within the report area, which is mostly constrained by diagnostic marine fauna in underlying and overlying formations, ranges from late Oxfordian to late Kimmeridgian. The ammonite *Amoeboceras* sp., of late Oxfordian to early Kimmeridgian age, has been recorded at Ermine Ridge in the marine part of the Awingak Formation at 25 m above base. In the type section near Buchanan Lake,

Figure 22. Awingak Formation debris flow with rounded clast of ironstone. Ironstone concretions are a typical feature of the upper Savik beds and the Ringnes Formation, which are likely to have contributed to the debris flow. (GSC Photo No. 2014-082)

Awingak Formation contains *Aucella* (= *Buchia*) *bronni*(?) in the middle of the three shale intervals and *Buchia*? sp. with *Amoeboceras*? in the upper shale (Tozer, 1963b). The type-section Awingak Formation contains two foraminiferal assemblages (Wall, 1983). The lower of these includes arenaceous species of the *Ammodiscus thomsi* assemblage (Oxfordian and Kimmeridgian) to 230 m above the base of the formation. The entry occurrence of *Verneuilinoides graciosus* at 147 m above base is diagnostic of the early Kimmeridgian and marks the boundary between the Oxfordian and Kimmeridgian (Wall, 1983). In the upper 115 m of the formation near Buchanan Lake are occurrences of the *Glomospirella* sp. 174 assemblage (early Volgian). However, biostratigraphic evidence from the overlying Deer Bay Formation (*see below*) indicates that the top of the Awingak Formation within the report area to the west probably lies within the late Kimmeridgian.

Deer Bay Formation

Definition: The Deer Bay Formation was named for an interval of marine shales exposed on Ellef Ringnes Island (Heywood, 1955). It has been widely reported on western Ellesmere, Axel Heiberg, and Amund Ringnes islands, and throughout the western Sverdrup Basin (Tozer, 1963b; Thorsteinsson and Tozer, 1970; Balkwill, 1983; Embry, 1991), where it typically comprises marine shale, siltstone, and minor sandstone. Sections within the report area have been described at Wolf Mountain, Ermine Ridge (in the same area), Monkhead Mountain, Hidden diapir, Duck Bay, and Peeawahto diapir. Other sections have been measured graphically from air photos at Good Friday Bay and at Strand diapir. Also relevant are sections southwest of Buchanan Lake (Souther, 1963) and on Amund Ringnes Island (Balkwill, 1983).

Composition: Dark grey to greyish-black shale dominates the sections measured by Fricker (1963) at Wolf Mountain, Hidden diapir, and Monkhead Mountain (Fig. 23). The lower contact with the Awingak Formation is described as gradational. A lower member consists of dark grey to black, hard, silty shale with clay ironstone interbeds; and an upper member comprises dark grey to black silty shale, in part calcareous, with sandy siltstone interbeds. This distinction was not mentioned in the Operation Franklin reports of the formation at Duck Bay and Good Friday Bay (Glenister, 1963; Souther, 1963), where the interval is generally described as dark grey shale containing concretions or thin beds of ironstone, and ferruginous or calcareous mudstone (Fig. 24).

Glendonites: Characteristic of the upper Deer Bay Formation are layers of sideritic nodules, fist-sized clay-ironstone 'cannonball' concretions and regionally correlated horizons of glendonite 'hedgehogs' (Kemper and Schmitz, 1975). Glendonites are stellate aggregates of euhedral calcite pseudomorphous after ikaite (Swainson and Hammond, 2001). Ikaite is a hexahedral hydrous calcium carbonate ($CaCO_3.6H_2O$). In some modern marine settings it is associated with freezing sea water (Rysgaard et al., 2013) and marine cold seeps (Greinert and Derkachev, 2004). Glendonite has also been used as a paleoenvironmental indicator of cold climates in the Mesozoic (Price, 1999). The occurrence of glendonites in the upper Deer Bay Formation, and in the Aptian-Albian Christopher Formation (*see below*), is supportive evidence of cold climates in the Valanginian (Price, 1999).

Thickness: Tozer (1963b) summarized the thickness of measured sections of the Deer Bay Formation on Axel Heiberg Island. The formation is wedge shaped, with sand and silt decreasing westward in the upper part of the formation. The formation is thinnest southwest of Buchanan Lake (259 m), thickest near Monkhead Mountain (868 m; A.F. Embry, 2012 cited 853 m for a section here), and again thinner at Good Friday Bay (341 m; our graphic estimate of maximum thickness here is 590 m). Thicknesses reported by Fricker (1963) include those for Ermine Ridge (700+ m), Wolf Mountain (624.6 m), Monkhead Mountain (693.3 m), and Hidden diapir (68 m.; Embry , 2012 cited 111 m for a section here). The variation in thickness of measured sections at Monkhead Mountain can be attributed to a gradational contact with the Awingak Formation and to contrasting definitions of the lower boundary of the formation. The formation thins markedly adjacent to some diapirs, such as along the west side of Hidden diapir (68–111 m), compared with sections 10 km to the west at Wolf Mountain (624 m) and Ermine Ridge (700+ m) and 10.5 km to the south at Monkhead Mountain (693–868 m) (Fig. 25). Similarly, the maximum thicknesses of sections at Good Friday Bay (590 m) and Duck Bay (580 m) are considerably less than that measured at Peeawahto diapir (915 m). These data indicate that the Hidden, Good Friday, and Duck Bay diapirs locally controlled the thickness of the Deer Bay Formation. Evidence below indicates that thickness variation is the combined result of local facies change to the Valanginian part of the lower Isachsen Formation and a sub-Isachsen angular unconformity that cuts out the upper Deer Bay Formation next to some diapirs.

Isopach trends that appeared in Toarcian to Kimmeridgian intervals (Savik beds and Awingak Formation) continue in the Deer Bay Formation (late Kimmeridgian to middle Valanginian; Fig. 25). In particular, White Peak depression appears north of Colour and Expedition diapirs; Monkhead and Strand Pass minibasins, north and south of Strand diapir; Glacier minibasin, north of Lost Hammer diapir; and Good Friday minibasin, mostly south of Good Friday Central diapir.

Unconformities: The base of the Deer Bay Formation grades into the Awingak Formation, particularly in the east (Monkhead Mountain). This base is interpreted as a marine flooding surface. Our geological mapping and airphoto interpretation indicate that the Deer Bay Formation also oversteps the Awingak Formation and lies directly on diapiric evaporites at Lost Hammer, Glacier Fiord East, and Colour diapirs, and on the north limb of Good Friday East diapir. The Deer Bay Formation also oversteps the Awingak and Savik beds and on the south limb of Good Friday East diapir appears to lie directly on the Heiberg Formation. Truncated bedding in the upper Awingak Formation indicates that the sub–Deer Bay contact is a local angular unconformity that cuts downsection southwestward toward Glacier Fiord East diapir and northward toward Good Friday East diapir.

Age: The age of the Deer Bay Formation is provided by ammonites, bivalves, and foraminifers.

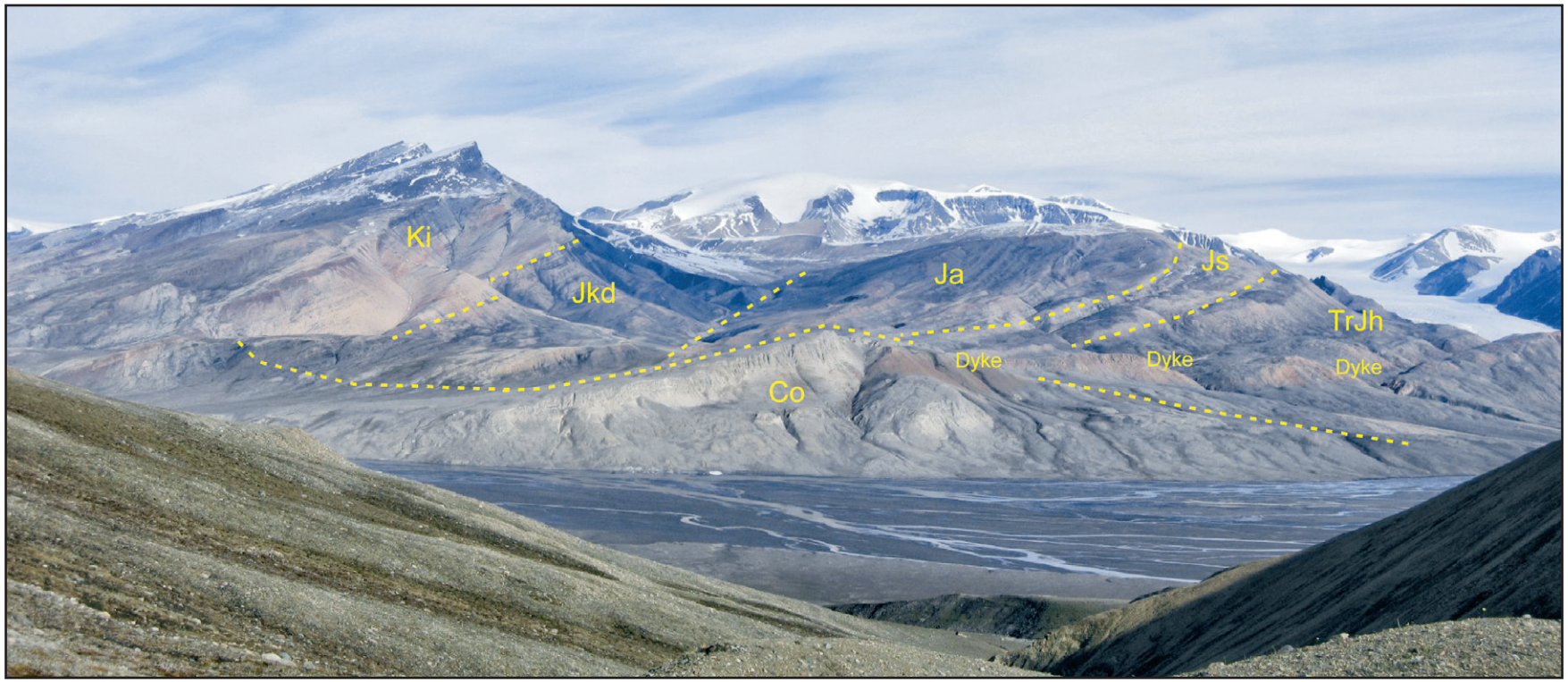

Figure 23. A minibasin at and to the east of Wolf Mountain contains strata ranging from Upper Triassic to Lower Cretaceous. The minibasin strata thin out to the south against Expedition diapir (Co). Units in view include Heiberg Formation (TrJh), Savik beds (Js), Awingak Formation (Ja), Deer Bay Formation (JKd), and Isachsen Formation (Ki). View northward across Expedition River from near the summit of Expedition diapir. (GSC Photo No. 2014-083)

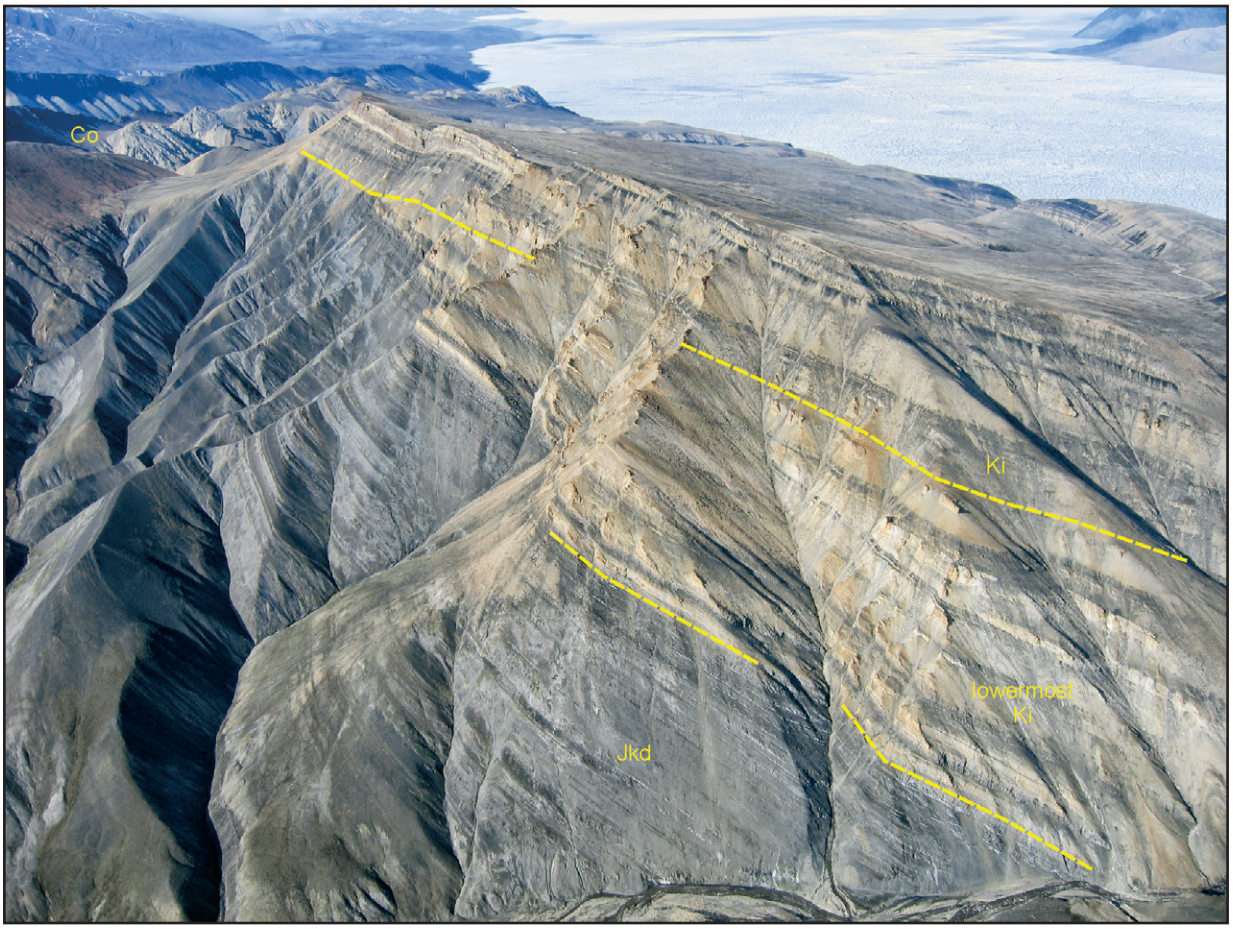

Figure 24. Medial Isachsen Formation (Ki) cuts out lower Isachsen and to the west rests on black Deer Bay Formation (JKd) in these well-exposed cliffs on the north side of Good Friday Central diapir (Co). View westward with ice-covered Strand Fiord in background. (GSC Photo No. 2014-084)

Maximum age range within the report area is late Kimmeridgian to mid-Valanginian. The oldest fauna fall in the middle Kimmeridgian to early Tithonian (Fricker, 1963; H. Frebold *in* Davies, 1984). These fauna include *Dorsoplanites*(?) sp., *Buchia* sp., and *B. rugosa*, collected from the lower part of the formation at Wolf Mountain, Hidden diapir, and Monkhead Mountain (Fricker, 1963). Later Volgian (~late early Tithonian) bivalves occur at Monkhead Mountain (*Buchia richardsonensis* n. sp.), in the lower part of the Hidden icecap section (*Buchia* cf. *richardsonensis*; *B.* cf. *russiensis*; Jeletzky, 1983), and latest Tithonian bivalves occur at 274 m above the base of the formation at Duck Bay (*B. unschensis*; Jeletzky, 1966). Diagnostic foraminifers in the lower 90 m of the formation south of Buchanan Lake are assigned to the *Arenoturrispirillina jeletzkyi* assemblage (late Volgian; Wall, 1983). Early Berriasian fauna (*Subcraspedites* cf. *suprasubdites*) have also been identified at Buchanan Lake (at 90–95 m) and Peeawahto diapir (at 315 m; Thorsteinsson and Tozer, 1970). Upper Berriasian strata are absent, which suggests a depositional break or disconformity in Deer Bay Formation that places lower (not lowest) Valanginian on lower Berriasian south of Buchanan Lake (Kemper, 1975).

The Valanginian part of the Deer Bay Formation is represented by three macrofaunal assemblages south of Buchanan Lake and on central Amund Ringnes Island (Kemper, 1975, 1977). These assemblages include *Tollia* and *Temnoptychtes* (early Valanginian), *Polyptychites* (middle Valanginian), and, on Amund Ringnes Island, *Prodichotomites* (early late Valanginian). Correlation of the early late Valanginian from Amund Ringnes Island to Buchanan Lake area is based on sedimentological arguments and the highest occurrence of regionally correlated glendonite beds that also contain the *Prodichotomites* assemblage (Kemper, 1975). Foraminifers south of Buchanan Lake are assigned

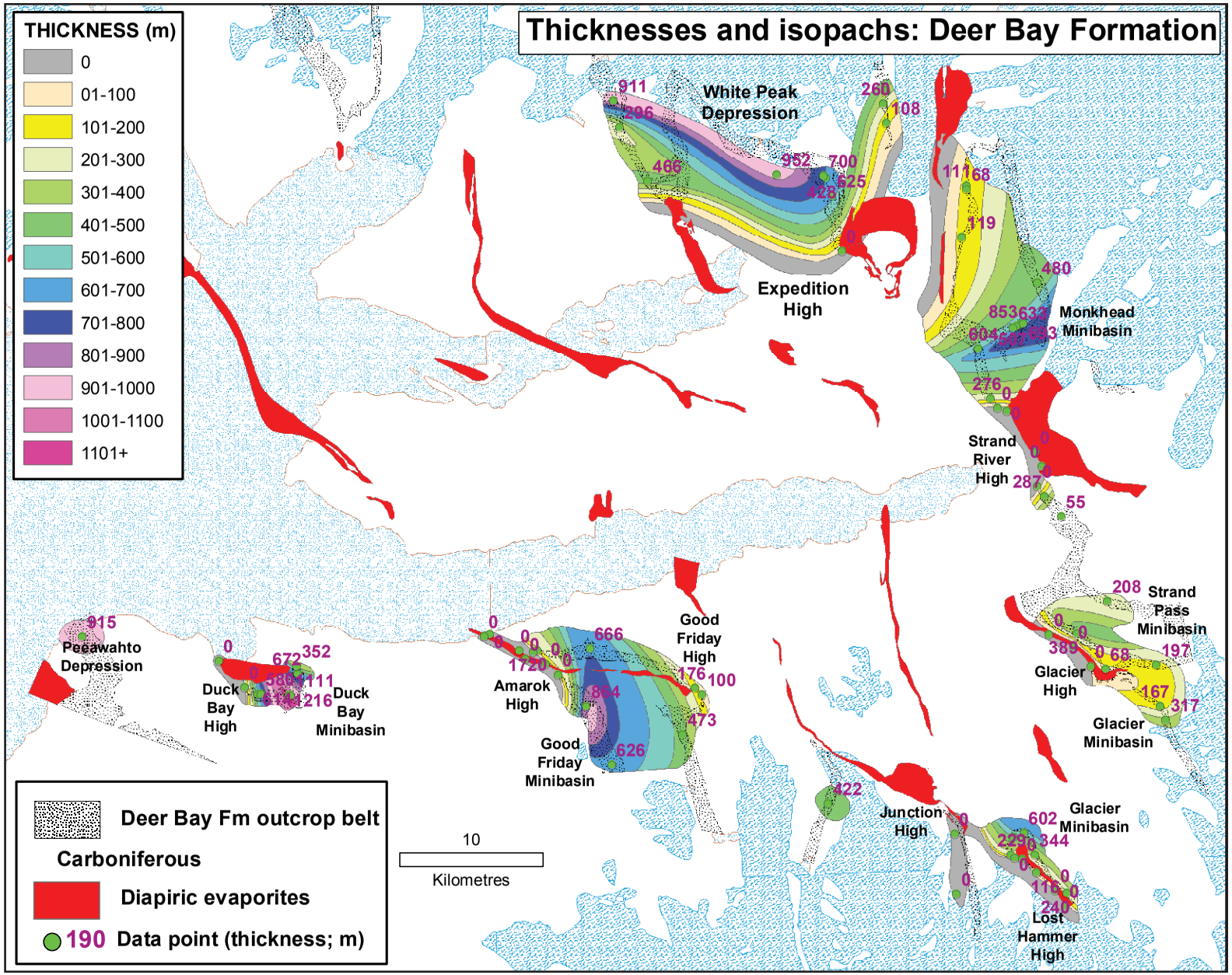

Figure 25. Isopachs and spot thicknesses for Deer Bay Formation. Range of thickness is 68 to 1216 m.

to the *Uvigerinammina* sp. 1 assemblage (Berriasian and Valanginian; Wall, 1983). Within the report area generalized early Valanginian to early late Valanginian fauna in the Deer Bay Formation include *Buchia* aff. *A. B. keyserlingi*, *B. terebratuloides*, and *Camptonectes* cf. *C. praecinctus* at Monkhead Mountain (Souther, 1963) and *B. terebratuloides* at Duck Bay (Tozer, 1963a). *Buchia keyserlingi* (early to early late Valanginian; Kemper, 1977) and *Polyptychites* (middle Valanginian; Kemper, 1977) occur in the upper Wolf Mountain and upper Monkhead Mountain sections (Fricker, 1963).

Valanginian strata are missing in the Hidden icecap section. Here the overlying Isachsen Formation has cut down to lower Berriasian or upper Volgian strata. The upper Deer Bay Formation is younger to the west and basinward. The youngest Deer Bay strata on Amund Ringnes Island contain middle late Valanginian bivalves (*Buchia inflata* and *Buchia* n. sp. aff. *B. inflata*, which appear above the highest *B. keyserlingi*; Kemper, 1977) and the middle late Valanginian ammonites *Ringnesiceras amundense*, *R. tozeri*, and *Homolsomites* cf. *H. quatsinoensis* (Kemper and Jeletzky, 1979).

Spreading phase of Canada Basin

The next major events of Sverdrup Basin accompanied seafloor spreading in the incipient Canada Basin in the Arctic Ocean. Data from exploratory drilling in northern Alaska and from seismic profiles from the southern Canada Basin have been interpreted to indicate that seafloor spreading began in the Hauterivian (Grantz et al., 2011). Seafloor spreading was most likely continuous as the Alpha-Mendeleev Ridge formed. This major submarine mountain range of the central Arctic Ocean extends 2000 km across the abyssal plain between Arctic Canada and the Arctic Russian shelf. In places the ridge is more than 400 km wide and has been interpreted as an oceanic volcanic edifice of an Icelandic hotspot type (Bruvoli et al., 2012).

Response to these events in Sverdrup Basin includes a major unconformity in quartz sandstone of the lower Isachsen Formation, the emplacement of sills and two diabase dyke swarms (Queen Elizabeth and Surprise swarms of Buchan and Ernst, 2003), and related volcanic units in shale and sandstone of Early through Late Cretaceous age.

Isachsen Formation

Definition: The history of research, general description, and widespread extent of the Isachsen Formation across the Arctic Islands (from northern Ellesmere Island to Banks Island) were provided by Embry (1985). The Isachsen Formation is a resistant-weathering unit dominated by quartz sandstone with lesser shale and siltstone. Measured thickness across the report area ranges from 230 to 1372 m (Fig. 11). A threefold subdivision is recognized in many sections, comprising lower and upper sandstone members of roughly equal thickness (Paterson Island and Walker Island members, respectively) and a thin intervening shale (Rondon Member).

Composition: The *Paterson Island Member* ranges from less than 20 m on the margins of Sverdrup Basin to a maximum of 880 m in the basin centre. The unit consists of pale grey to white quartz sandstone with lesser carbonaceous siltstone, grey shale, and coal (Embry, 1985). The sandstones range to coarse grained in the lower part and contain chert pebbles. Basal strata are arranged in coarsening-upward cycles and are interpreted to have been deposited in marginal-marine and delta-front settings. The bulk of the member has fining-upward cycles attributed to fluvial overbank and delta-plain settings (Embry, 1985). The age range is late Valanginian to Barremian (Fricker, 1963; Wall, 1983; Embry, 1985).

The *Rondon Member* (Barremian) is a recessive unit, as much as 70 m thick in the centre of the basin. It consists of dark grey shale and siltstone and lesser burrowed and bioturbated sandstone. Strata are arranged in coarsening-upward cycles, and the depositional environment is interpreted to be offshore marine (Embry, 1985).

The *Walker Island Member* (20–500 m thick and Barremian to early Aptian) consists of white to pale grey and fine- to coarse-grained sandstone interbedded with grey carbonaceous siltstone and grey shale. Coarsening-upward cycles occur in the lower and upper parts of the member, and fining-upward cycles in the middle part. This change is interpreted as a regressive transition from offshore in the Rondon Member to delta front and delta plain in the lower and middle Walker Island Member and a transgressive return to delta-front and marginal-marine settings in the upper part of the member (Embry, 1985).

The above general description of the Isachsen Formation does not apply in detail within the report area. For this we draw on the accounts of Fricker (1963) for Expedition area, sections measured during Operation Franklin by Souther (1963) and Tozer (1963a), and our own fieldwork and aerial reconnaissance.

Sections have been measured at Wolf Mountain, at Hidden Icefield, and east of the head of Strand Fiord. The Wolf Mountain section of the Isachsen Formation (~680 m thick) overlies the Deer Bay Formation and consists of medium to pale grey and yellowish-brown-weathering sandstone, in part conglomeratic, with interbedded dark grey to black shale. Twenty shale intervals are each mostly less than 10 m thick. The thickest is 17 m (at 261.5–278.5 m above base; Fricker, 1963) and is the only likely correlate of the Rondon Member. However, there is no biostratigraphic evidence to support this interpretation.

The Isachsen Formation at Hidden Icefield is a similar interbedded succession (20 shale intervals mostly 0.3–15 m thick). The top of the section, above 204.2 m from the base, is masked by ice. There are two thick shale intervals—one of 15 m (86.8–101.8 m) and one of 25 m (132.7–157.7 m).

East of Strand Fiord, the Isachsen Formation is significantly thinner (230 m) below conformable Christopher Formation shale. At the base, the Isachsen lies directly on evaporites of Strand diapir. The base of the section is marked by cataclastic breccia. The Isachsen Formation is predominantly grey and brownish-grey sandstone alternating with seven intervals of shale ranging from 4 to 18 m thick. The latter unit occurs at 72.2 to 90 m above base. A 40 m thick interval of interbedded shale and sandstone occurs from 175.2 to 210.2 m above base (Fricker, 1963). Rondon Member might correlate with any or none of these shale intervals.

Also described from the upper Isachsen Formation east of the head of Strand Fiord by Souther (1963, p. 439) is a 60+ m unit of dark green volcanic breccia and minor tuff. The volume of volcanic rock in the upper Isachsen Formation of the report area is uncertain. This uncertainty is partly due to the common occurrence of diabase sills and dykes that feed mafic igneous layers at this level. These igneous sheets, whether of intrusive or extrusive origin, are prominent in the upper Isachsen Formation across the eastern and northern part of the report area. Noteworthy are the upper Isachsen exposures that contain mafic sills and/or flows northeast of the head of Strand Fiord, at Wolf Mountain, and north and northwest of Colour diapir. Vesicular and amygdaloidal basaltic flows and diabase sills are also common in the upper Isachsen Formation on northwestern Axel Heiberg Island (Mayr et al., 2002).

One of the thickest sections of Isachsen Formation (1372 m) is exposed on the northeast flank of Peeawahto diapir (section 61 of Tozer, 1963a). The section contains Embry's (1985) three members: a 60 m thick shale (Rondon Member) between lower and upper intervals dominated by sandstone (Paterson Island Member, 775 m; Walker Island Member, 525 m, respectively). Noteworthy is a 10 m thick, unsorted breccia at 229 m above the base of the formation that contains angular clasts of green volcanic material, chert, and quartz. Evidence of volcanism is otherwise unknown at this stratigraphic level. Elsewhere in the report area, however, volcanic flows occur in the Paterson Island Member on Bjarnason Island and in the Geodetic Hills of northwestern and east-central Axel Heiberg Island, respectively (Embry and Osadetz, 1988).

Thickness: Published descriptions of the Isachsen Formation within the report area show the formation ranging up to thicknesses observed elsewhere in the central Sverdrup Basin. Anomalously thin sections of the Isachsen Formation, however, also occur—near Strand diapir, for example. The Rondon Member is locally obvious, for example, northeast of Peeawahto diapir. In most areas, however, Embry's (1985) threefold subdivision of the formation is not obvious on air photographs. Published sections have interbeds of shale but are not individually thick enough to be correlated with the regional Rondon Member. Also different from the described Isachsen Formation of Embry (1985) are volcanic breccia and tuff in some upper parts of the formation and the common interlayering of igneous sheets of intrusive or extrusive origin throughout the eastern and northern parts of the report area. Such features have also been reported from northern Axel Heiberg Island. Examples of the stratigraphically lowest evidence of volcanic activity in Isachsen time are conglomerate beds containing volcanic clasts above the lower third

(229 m above base) of the Paterson Island Member east of Peeawahto diapir and, beyond the report area, volcanic flows in these strata on eastern and northwestern Axel Heiberg Island.

Many of the minibasins and depressions evident on the Triassic and Jurassic isopach maps continued to evolve in the late Valanginian to late Aptian time slice (Fig. 26). Good Friday depocentre is still present but has migrated to the west. Glacier minibasin is still present north of Lost Hammer diapir but is now apparently linked in the north to Strand Pass minibasin. Monkhead minibasin has shifted to the west. Behind it is a paleohigh where the Isachsen Formation thins to 92 m. More stable is White Peak depression and Expedition high, which remain spatially linked to Colour diapir in the west and Expedition diapir in the east. Other paleohighs first appearing on this time slice are 1) Colour Ridge between Colour diapir and the east end of Muskox Ridge South diapir and 2) Twin Ridge between Twin diapirs and a more westerly part of Muskox Ridge South diapir. This time slice presents a mix of both westerly and northerly trending isopachs.

Hauterivian unconformity: Reconnaissance and ground-based fieldwork in 2004 led to the discovery of two important observations about the Isachsen Formation. First, an angular unconformity is located at the base of or low in Isachsen Formation near at least five diapirs (Duck Bay, Good Friday West, Good Friday East, Glacier, and Strand diapirs). An angular unconformity is also inferred under the Isachsen Formation adjacent to Lost Hammer and Expedition diapirs. The angular unconformity places the Isachsen Formation on previously deformed and eroded strata as low as Heiberg Formation at Strand, Duck Bay, and Good Friday Bay diapirs. The unconformity cuts downsection toward these diapirs and, in the opposite direction, passes into lower Isachsen Formation 230 to 250 m above a gradational lower contact with Deer Bay Formation (Fig. 24, 27, 28). This important stratigraphic relationship was previously interpreted by Thorsteinsson (1971a, b) as the result of faulting between all these units near Duck Bay, Good Friday, and Glacier diapirs. In the other areas, the angular relationship is partly obscured by colluvium and recent valley bottom gravels (Thorsteinsson, 1974). However, these discordances are clearly not faults at Duck Bay (Fig. 29) and Good Friday West diapirs. The surface is locally associated with channel-fill deposits above the unconformity. The unconformity has major implications for the salt-tectonic history, as described below.

Diapir-related conglomerates: The second important set of observations is that the base of the Isachsen Formation is interpreted as an erosion surface where it overlies the Otto Fiord Formation evaporites at Bastion Ridge South and Muskox Ridge South diapirs. Basal strata at Bastion Ridge South diapir are exposed in a stream section cutting through the eastern lower contact of the Isachsen Formation at the extreme south end of the diapir. The Isachsen Formation here is approximately 167 m thick and comprises ledge-forming quartz sandstone with recessive dark grey siltstone and shale interbeds. The lower 15 to 20 m of the formation above exposed Otto Fiord gypsum and anhydrite is matrix-supported sedimentary breccia. Angular clasts of dark grey carbonate occur in a cemented matrix of grey silt and quartz sand. This matrix is interpreted as a subaqueous debris-flow deposit with carbonate clasts derived from the subaerial erosion of the adjacent diapiric sheet in Isachsen time.

Similar depositional relationships between evaporites and Isachsen Formation are found at Muskox South diapir. Here, clasts of dark grey to black limestone, dolostone, and probable detrital gypsum in an arenaceous matrix are preserved in lenticular channel fills and thin beds where the Isachsen Formation lies on Otto Fiord anhydrite or carbonate. The contact breccia facies, here and elsewhere, is commonly pyritized. Weakly cemented sediments have also been found at Muskox South diapir. In one place, coarse-grained Isachsen quartz sandstone, containing pea-sized angular grey limestone fragments, occupies cavernous fissures on the eroded upper surface of the evaporites.

The most convincing evidence of erosional unroofing of Muskox South diapir in early Isachsen time is an anhydrite boulder conglomerate (Fig. 30). These distinctive strata are not located on the basal contact but instead are separated from the top of the diapir by 10 m of fissile black shale and approximately 6 m of mature quartz-sandstone. The anhydrite conglomerate is a towering but unstructured bed 25 to 30 m thick that consists of subrounded pale grey and pinkish-weathering anhydrite in a sparse clast-supported matrix of quartz sand (Fig. 31). Anhydrite clasts range from 20 cm to

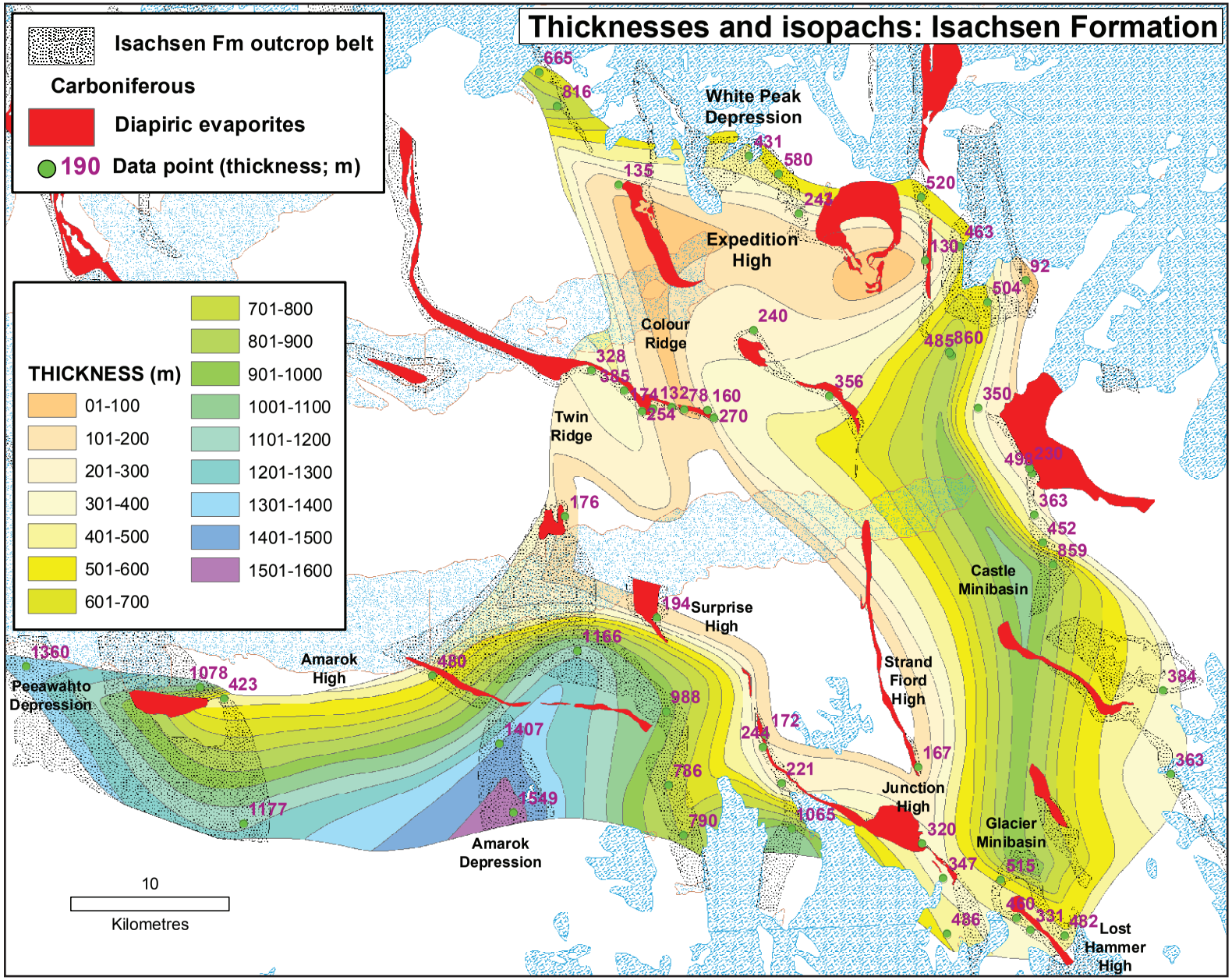

Figure 26. Isopachs and spot thicknesses for Isachsen Formation. Range of thickness is 78 to 1549 m.

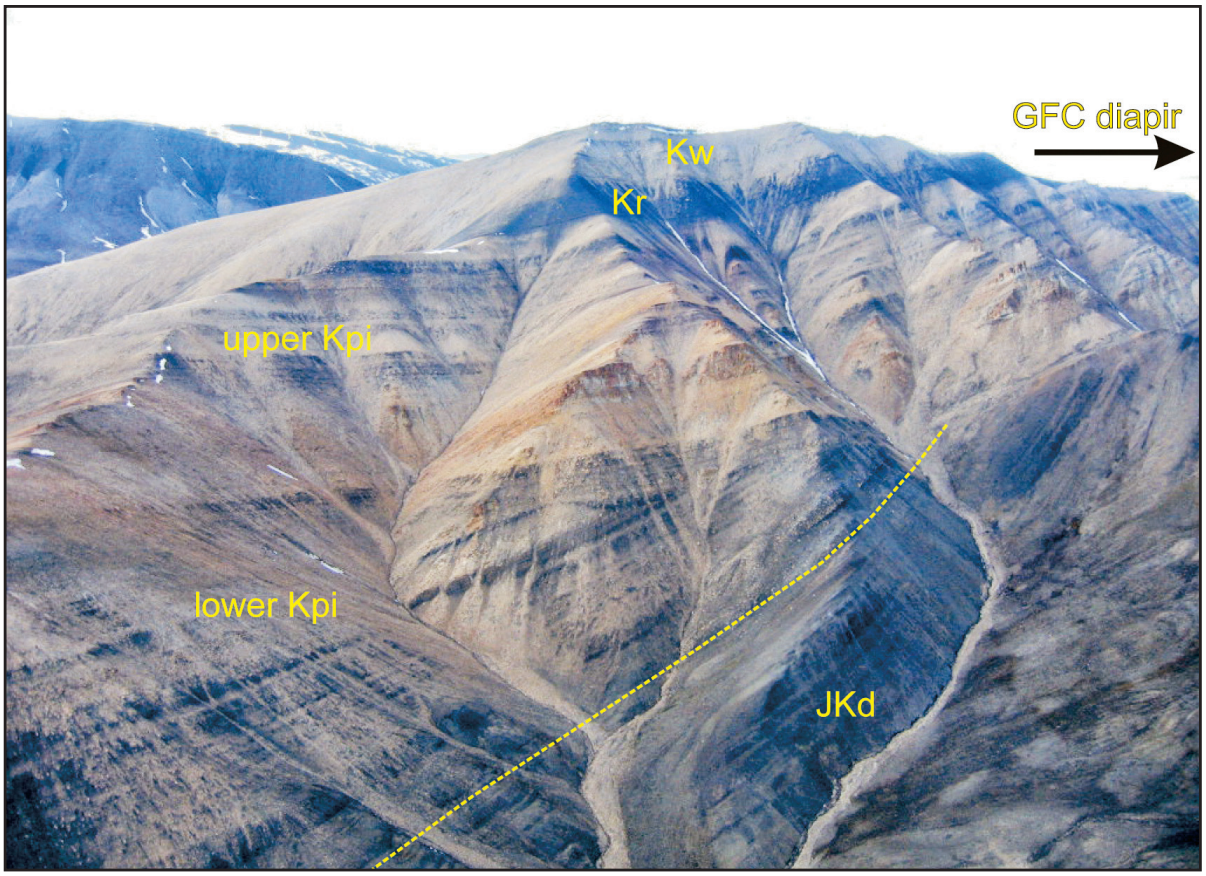

Figure 27. Angular unconformity, centred on Good Friday Central diapir (GFC), in Paterson Island Member (Kpi) of Isachsen Formation. The medial Isachsen Formation (below Rondon Member shale, Kr) cuts out the lowest Isachsen in this photograph and to the north cuts out Deer Bay Formation (JKd) and older strata in the direction of the diapir. View is to the southwest. (GSC Photo No. 2014-085)

1.5 m wide but reach a diameter of 2 m near the top. Clast rounding is attributed to mechanical abrasion during downslope transport and perhaps partial dissolution during lithification rather than to channelized currents. Starting with a marginal-marine onlap surface above the diapir, the upward progression from shale to sandstone to conglomerate is interpreted as a coarsening-upward cycle near the head of a steep, subaqueous fan.

Age: The age of the Isachsen Formation ranges from late Valanginian to Aptian. Marine bivalves of the *Buchia* ex gr. *inflata-sublaevis* assemblage, notably *B. bulloides*, have been collected from the lowest beds of the Isachsen Formation above a gradational contact with Deer Bay Formation at Monkhead Mountain (Fricker, 1963) and on Ellef Ringnes Island (Jeletzky, 1973). *Buchia* fragments of uncertain identification also occur in basal Isachsen Formation at Wolf Mountain and east of Thompson Glacier (Fricker, 1963), above the evaporites at the east end of Duck Bay diapir (Tozer, 1963a), and on the southwest coast of Axel Heiberg Island (Glenister, 1963). The *inflata-sublaevis* fauna indicate a middle to late Valanginian age. The presence of *Polyptychites* (middle Valanginian) in the upper Deer Bay Formation at Wolf Mountain and Monkhead Mountain (*see above*), however, suggests that the marine basal Isachsen Formation in these areas is probably upper Valanginian. Furthermore, the base of the formation is not older than middle upper Valanginian at Buchanan Lake and on Amund Ringnes Island based on ammonites from the highest Deer Bay Formation.

Plant fossils from the Isachsen Formation of the report area (Fricker, 1963; Tozer, 1963b) have a general Early Cretaceous aspect but are not useful for more exact dating. Marine macrofauna are not

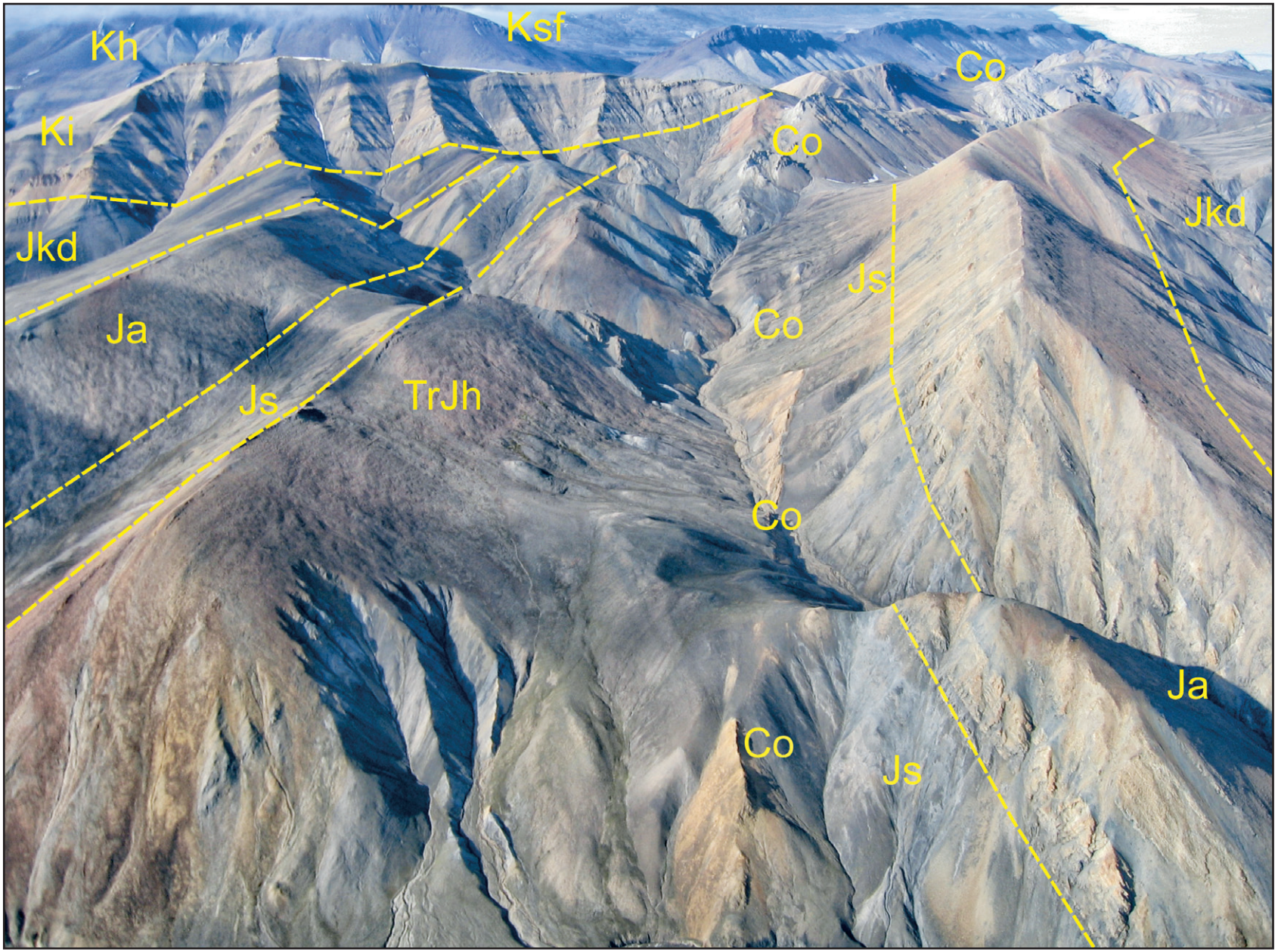

Figure 28. Angular unconformity centred on Good Friday Central diapir (Co). White cliff exposures on the right are part of the diapir. Isachsen Formation (Ki) cuts out Deer Bay Formation (highest black shales, JKd), Awingak Formation (ridge-forming grey beds, Ja), Savik beds (recessive black shales, Js), and Heiberg Formation redbeds (TrJh). Younger strata include Hassel Formation (Kh) and Strand Fiord Formation (Ksf).View is to the west. (GSC Photo No. 2014-086)

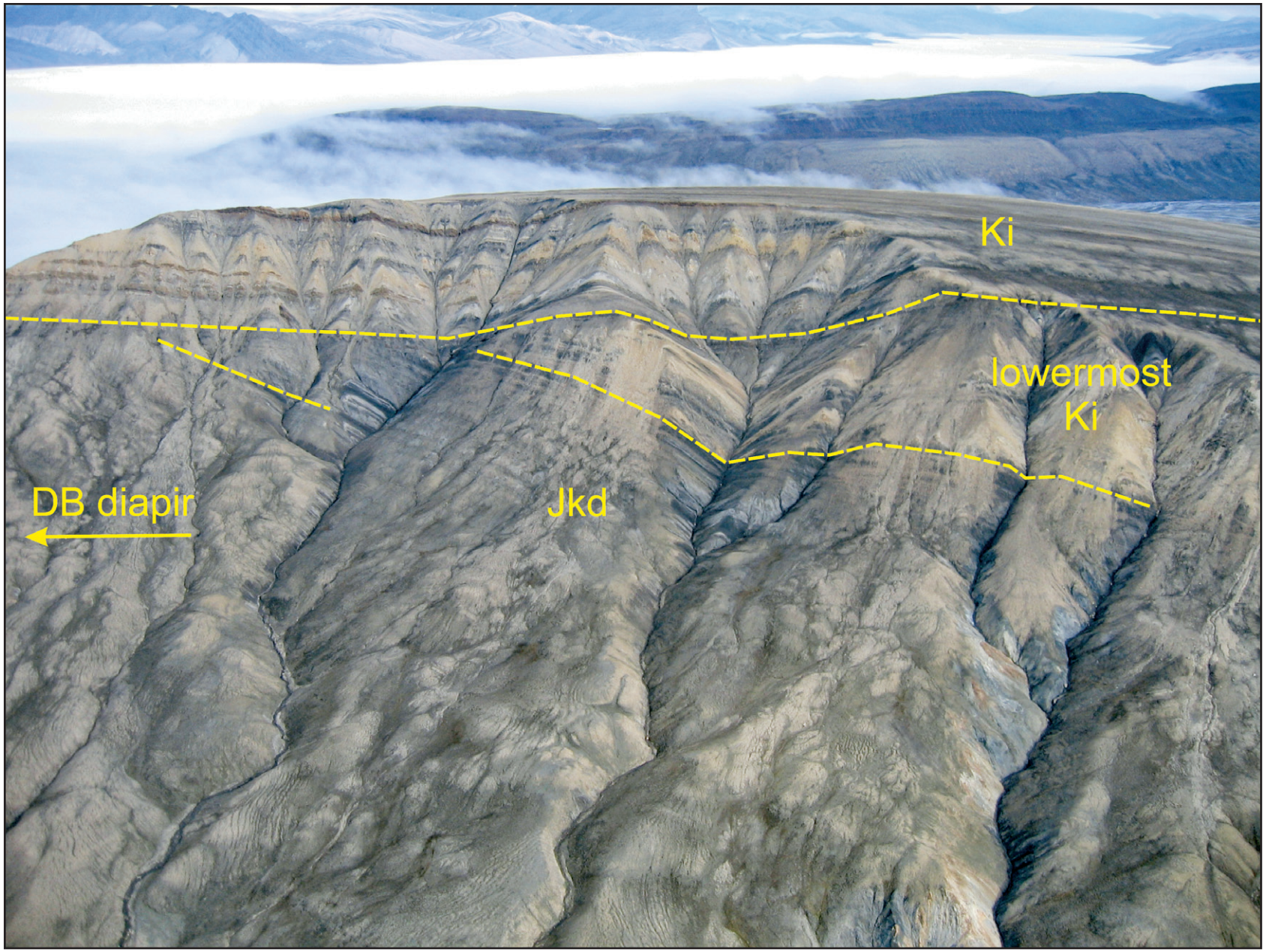

Figure 29. Angular unconformity centred on Duck Bay diapir (DB). The unconformity in lower Isachsen Formation (Ki); Deer Bay Formation (JKd) is present downsection. View is to the east. (GSC Photo No. 2014-087)

Figure 30. The south flank of Muskox Ridge South diapir (Co) is an unconformable surface below Isachsen Formation (Ki). Anhydrite boulder conglomerate beds are exposed in the diapir's roof at the location marked 'Ki-cgl'. Strata above Isachsen Formation are assigned to Invincible Point Member (Kip). View is northwest toward ice-covered Expedition Fiord. (GSC Photo No. 2014-088)

Figure 31. Anhydrite boulder conglomerate in lower Isachsen Formation, near southwest contact of Muskox Ridge South diapir. View southeast. (GSC Photo No. 2014-089)

found in the Rondon Member, and foraminifera of the *Verneuilinoides neocomiensis* assemblage from this shale unit southwest of Buchanan Lake are long ranging (Berriasian to Aptian; Wall, 1983).

A late Barremian age range is provided by plant microfossils studied by Nohr-Hansen and McIntryre (1998). Dinoflagellates of Barremian age are reported from the Isachsen Formation, including the Rondon Member, on southern Axel Heiberg Island (McIntyre *in* Embry, 1985). On the basis of the above observations, we think the Paterson Island Member below the mapped unconformity is mostly late Valanginian but may contain Hauterivian strata. The Paterson Island Member above the unconformity, most likely including the conglomerate beds with volcanic clasts east of Peeawahto diapir, is Hauterivian and perhaps also Barremian. The Rondon Member is late Barremian. The Walker Island Member, constrained in age by early Aptian dinoflagellates in the overlying lower Christopher Formation (Invincible Point Member), probably ranges to the end of the Barremian.

Christopher Formation

Definition: The Christopher Formation is a recessive unit of dark grey to black shale and silty shale with minor siltstone and very fine grained sandstone exposed throughout the report area. The lower contact with the Isachsen Formation is a well-defined topographic break drawn at a level above which shale is dominant. As described above, this contact is locally gradational. At Muskox Ridge South diapir, for example, the upper beds of the Isachsen Formation are traceable laterally into the lower Christopher Formation.

Composition: Measured thickness of the Christopher Formation ranges from 442 to approximately 1100 m. Age range is early Aptian to early late Albian. Embry (1985) recognized two distinct shale members of approximately equal

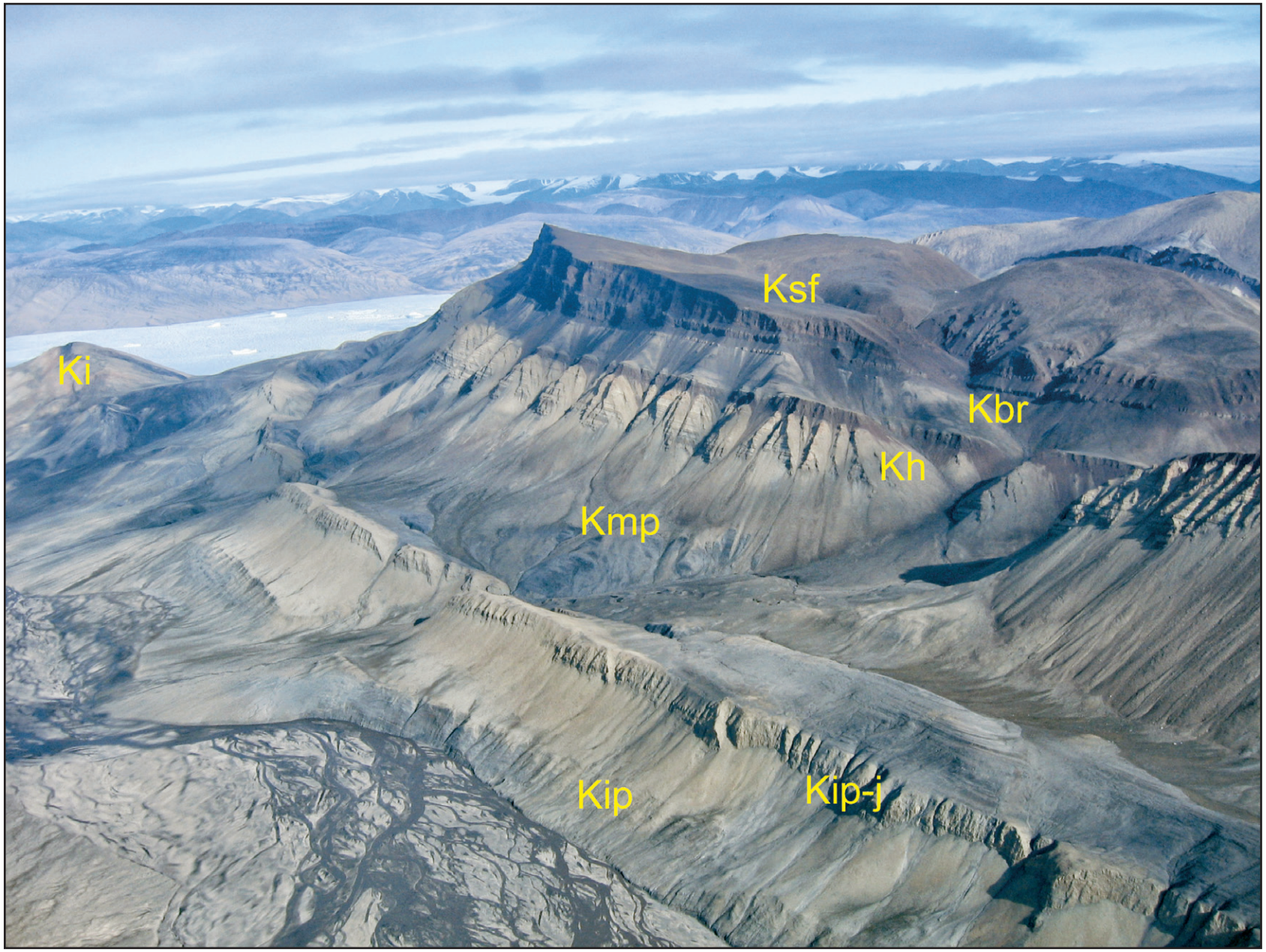

Figure 32. Stratigraphic units in view east of Surprise North diapir,: Isachsen Fornmation (Ki), recessive grey Invincible Point Member (Kip), ridge-forming Junction beds (Kip-j), valley of Macdougall Point Member (Kmp), pale cliffs of Hassel Formation (Kh) topped by a gabbro sill, dark grey recessive Bastion Ridge Formation (Kbr), and reddish–dark brown cliff-forming Strand Fiord Formation (Ksf). View north toward Strand Fiord. (GSC Photo No. 2014-090)

thickness (Fig. 32). In general, the lower unit (*Invincible Point Member*) consists of dark grey to black silty shale with minor sandstone-siltstone intervals, as much as 15 m thick, common in the lower and upper parts of the member. The sandstones are hummocky cross-stratified, rippled, and burrowed—characteristics that, together with foraminifera, dinoflagellates, bivalves, and rare ammonites, indicate a marine-shelf setting. The upper unit of Christopher Formation, the *Macdougall Point Member*, is mostly dark grey marine shale and siltstone with minor fine to very fine grained sandstone (Embry, 1985). These members of Christopher Formation are known throughout the southeastern half of the report area. The discrimination of separate members of Christopher Formation breaks down along a line joining Strand diapir in the east to Muskox South and Kanguk South diapirs in the west. Northwest of this line of facies change no obvious sandstone interval in mid-formation otherwise serves to separate the two members.

Although isopach maps are available for both members, we comment here on the combined isopachs for the entire Christopher Formation (Fig. 33). Dominant features include Glacier minibasin and Amarok depression in the southwest. In both places the Christopher Formation attains a thickness of more than 2100 m. Another depocentre is along the southern edge of Expedition diapir where the Christopher Formation exceeds 1600 m. At the other extreme is Strand Fiord high, linked in the north to Colour Ridge, where the preserved thickness of the Christopher Formation is apparently only a few hundred metres. Similar thinning is indicated on Bastion high (east of Bastion Ridge diapirs) where the preserved Christopher Formation is only 343 m thick.

Invincible Point Member

Composition: Measured sections of the Invincible Point Member are located northwest of the head of Strand Fiord (Fricker, 1963), east of Junction diapir (Nohr-Hansen and McIntyre, 1998), east of Duck Bay (Tozer, 1963a), and west of Twin diapirs on the north shore of Strand Fiord (Souther, 1963). The Invincible Point Member includes the lower 645 m of the Christopher Formation described by Fricker (1963) northwest of Strand Fiord. Dark grey to greyish-black silty shale is dominant. Subordinate are reddish-brown-weathering ironstone and calcareous mudstone concretions (some perfectly spherical and as much as 60 cm in diameter), rosettiform glendonite ('hedgehog') beds, minor calcareous cone-in-cone structures, and petrified wood. Interbeds include fine-grained sandstone, siltstone, and minor medium- to coarse-grained lithic tuff. Similar features occur in strata here considered to be Invincible Point Member along Amarok River east of Duck Bay diapir (Tozer, 1963a) and west of Twin diapirs (Souther, 1963). Anomalously thin intervals of the Invincible Point Member and of the Christopher Formation, in general, may be due to faulting and omission of section, as indicated on sections 50 and 54 of Souther (1963), located, respectively, above Strand diapir northeast of the head of Strand Fiord and on the east limb of Twin diapirs.

Two sandstone-dominated intervals can be mapped in the Invincible Point Member: the 'Junction beds' as much as 60 m thick (Fig. 4, 13) at the top of the member, and the 'Wolf tongue' of more restricted area in the middle (Fig. 4). The Wolf tongue is a fine-grained sandstone-siltstone marker located above the lower half of the Invincible Point Member. This resistant ledge is mapped on air photos from southeast of Lost Hammer diapir to west of Strand diapir in the north. It is inferred to correlate with an 8 m thick sandstone-siltstone interval at 342 to 350 m above base of formation in the section of Fricker (1963) east of the head of Strand Fiord.

The higher of the two obvious sandstone intervals in the Invincible Point Member, referred to informally as Junction beds, serves to readily locate the upper contact with the Macdougall Point Member at a distance and on air photographs. Thickest sections of the Junction beds are mapped throughout the region bounded by Junction and Glacier diapirs in the southeast and by Twin and Duck Bay diapirs in the west. A complete section is exposed on an eastward-flowing stream 975 m north of Junction diapir. The Junction beds here consist of two coarsening- and thickening-upward cycles of silty shale, siltstone, and fine-grained feldspathic quartz-sandstone, in part calcite cemented. The sandstones are grey to greenish-grey-weathering, micaceous, cross-bedded, burrowed, and bioturbated. The lower contact is gradational, and the upper contact with the Macdougall Point Member is abrupt, although it appears conformable. Junction beds are correlated with a 15 m thick sandstone-siltstone interval located at 630 to 645 m above base of formation in the section of Fricker

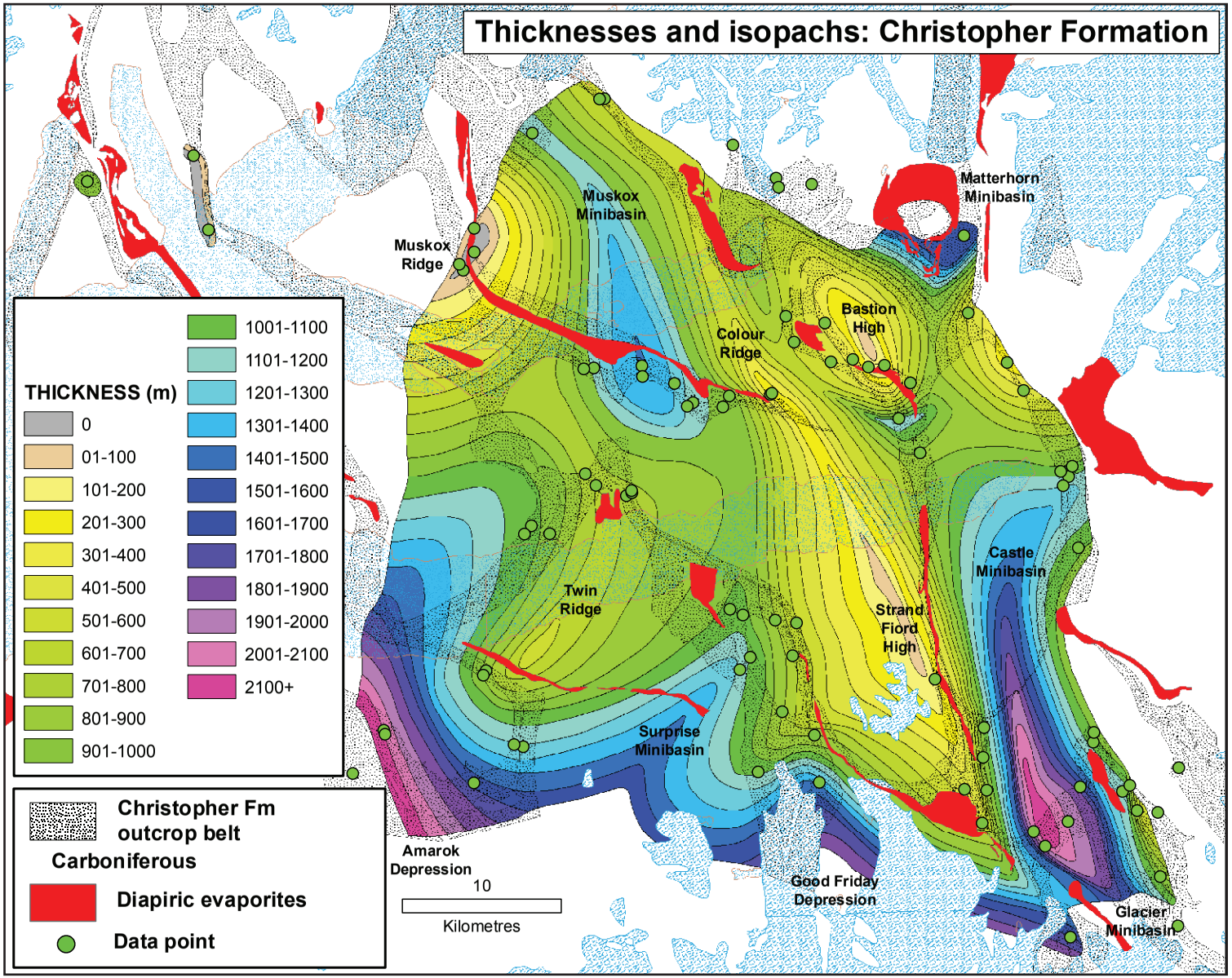

Figure 33. Isopachs for Christopher Formation. Range of thickness is up to 2100 m.

(1963) northeast of Strand Fiord. The Junction beds, approximately 60 m thick, are also described along the east side of Amarok River (Tozer 1963a), west of Twin diapirs (Souther 1963), and in the middle of a Christopher Formation section east of Junction diapir (Nohr-Hansen and McIntyre, 1998).

Stratified anhydrite: Unusual local features of the Invincible Point Member are occurrences of stratified anhydrite. One of these is a bed of pale grey anhydrite several metres thick located 150 m north of Junction diapir. Hillside outcrops of anhydrite are traceable over a distance of 340 m and form a stratigraphic marker in overturned strata between black shale and overlying thin interbeds of shale, mafic tuff, and agglomerate. A second occurrence of anhydrite is in an isolated streambank cliff section 1030 m northeast of Junction diapir (Fig. 34). Here eight compositionally layered anhydrite beds compose a 12 m section. This section includes 1) a 4 m interval above the covered base (to east) containing five anhydrite beds of approximately 10 cm each interbedded with black shale and volcaniclastic sandstone, 2) 6 m of black fissile shale, and 3) at the top, 2 m of shale and volcaniclastic sandstone containing three beds of anhydrite (80, 40, and 75 cm thick). Another potential occurrence of anhydrite in Christopher Formation near Muskox Ridge North diapir needs to be examined on the ground.

Age: Diagnostic macrofauna are rare in Invincible Point Member and equivalent strata of the lower Christopher Formation. In the Slidre Fiord map area of western Ellesmere Island, J.A. Jeletzky (*in* Sliter, 1981) reported *Cleoniceras* aff. *subbaylei* and *Archopiltes belli* (late early Albian) from immediately below sandstones potentially equivalent to Junction beds. Early Albian ammonites also occur in methogenic carbonate mounds in the lower Christopher Formation of Ellef Ringnes

Figure 34. Anhydrite layers in Invincible Point Member (Christopher Formation), 1030 m north of Junction diapir. Eight anhydrite layers compose this section of black shale, each ranging from 10 to 80 cm in thickness. View south. (GSC Photo No. 2014-091)

(Jeletzky *in* Sliter, 1981). Late Aptian *Tropeaum* and *Inoceramus* cf. *labiatiformis* occur in the lower part of the formation on Mackenzie King Island (Tozer, 1960; Jeletzky, 1970). Foraminifera, studied by Wall (1983) on western Ellesmere Island, include the *Quadrimorphina albertensis* (early Albian) and *Verneuilinoides borealis* (middle to late Albian) assemblages. Dinoflagellates have been compared and found to be similar to those occurring in West Greenland (Nohr-Hansen and McIntyre, 1998). East of Junction diapir the Invincible Point Member beds contain dinoflagellates of the *Vesperopsis mayi* Subzone (?early to late Aptian), *Senoniasphaera microreticulata* Subzone (?late Aptian to early Albian), *Lepitiodinium*? *hyalodermopse* Subzone (early Albian), and *Rhombodella paucispina* Zone (middle Albian). Supplementary dinoflagellate collections from Ellesmere and northern Melville islands indicate that the lowest part of the Christopher Formation lies within the early Aptian (Nohr-Hansen and McIntyre, 1998). In summary, the Invincible Point Member ranges from the lower(?) Aptian to the top of the lower Albian and perhaps includes some lowest middle Albian strata.

Macdougall Point Member

Composition: Like the Invincible Point Member, the Macdougall Point Member is predominantly dark grey to black silty shale. Siltstone and fine sandstone interbeds as much as about 10 cm thick contain bivalves and gastropods. These beds are too thin, however, to serve as mappable markers. Minor components of Macdougall Point Member are dusky-red-weathering ironstone and calcareous mudstone concretions, petrified wood, and thin interbeds of green lithic tuff. Glendonites are not generally found in the Macdougall Point Member. However, glendonite beds were described by Fricker (1963) from the potentially correlative upper part of the Christopher Formation at Bastion Ridge.

The lower contact of the Macdougall Point Member is drawn above the highest sandstone of the Junction beds at a level above which shale is dominant. This contact is interpreted to be a marine flooding surface. Measured thickness of the Macdougall Point Member ranges from 210 to 550 m.

Age: Diagnostic macrofauna are rare in the Macdougall Point Member. Within the report area is *Beudanticeras* sp. (early and middle Albian) from 183 m below the top of the member approximately 5 km west of Twin diapirs (H. Frebold *in* Souther, 1963) and, east of Amarok River, the ammonite *Angostropilites tozeri* within 30.5 m below the top (latest middle Albian; Jeletzky, 1980). In Expedition area are *Gastroplites* cf. *G. canadiensis* (middle Albian; Jeletzky, 1970) at 80 m below the overlying Hassel Formation near Castle Mountain and a *Gastropolites*(?) fragment at 220 m below the top (Fricker, 1963). An ammonite assemblage containing *Beaudanticeras (Grantziceras) affine* and *B. glabrum* (probably early middle Albian) occurs in the upper part of the Christopher Formation east of Junction diapir (biostratigraphic report of Jeletzky, 1983).

In general, the lower McDougall Point Member–equivalent beds on Amund Ringnes, Axel Heiberg, and Ellesmere islands contain *Cleoniceras canadense* sp. nov. and *Beudanticeras glabrum-affine* (earliest middle Albian; Jeletzky, 1970, 1980; Thorsteinsson and Tozer, 1970). A younger age for the basal beds is provided by a locality near Dragon Mountain where ammonites (*Pseudogastropolites*), inoceramids, fish remains, and palynomorphs provide a late middle Albian age (Hall et al., 2005). The youngest ammonite fauna from close to the top of the member include *Angostropilites tozeri* from the Amarok River locality and, from Ellef Ringnes Island, a related fauna including *Pseudopulchella* aff. *P. pattoni,* which correlate with the latest middle Albian *Stelckiceras liardensis* Zone of the western Canadian interior (Jeletzky, 1980). Foraminifera, studied by Wall (1983) on western Ellesmere Island, are assigned to the *Verneuilinoides borealis* assemblage (middle to late Albian). Dinoflagellate collections from a section of the Macdougall Point Member east of Junction diapir are assigned to the West Greenland middle Albian *Rhombodella paucispina* Zone and early late Albian *Wigginsiella grandstandica* Subzone (Nohr-Hansen and McIntyre, 1998). In conclusion, the indicated stratigraphic range of the Macdougall Point Member is middle Albian to lowest upper Albian.

Hassel Formation

Definition: The Hassel Formation, first described for a sandstone-dominated interval on Ellef Ringnes Island (Heywood, 1955, 1957), has since been mapped across the Arctic Islands from northern Banks Island to northern Ellesmere Island (Embry, 1991). Sections in the report area were measured and described by Fricker (1963), Souther (1963), Tozer (1963a), and MacRae (1996). Earlier

reports consider the Hassel Formation to consist of a lower sandstone and an upper shale (Tozer, 1963a). The shale unit, however, is now assigned to the Bastion Ridge Formation.

Thickness: Measured outcrop thickness of the Hassel Formation (*sensu lato*) ranges from 105 to 282 m, but isopachs of the Hassel Formation locally exceed 500 m (Fig. 35). The lower contact is gradational with the Macdougall Point Member and the upper Christopher Formation. This pale unit is generally more resistant than the bounding shale (Fig. 36), but because it also underlies cliff-forming volcanic rocks of the Strand Fiord Formation, it is commonly covered by talus of basalt and associated mafic intrusive rocks.

Composition: The Hassel Formation at the head of Expedition Fiord is described as roughly 80% sandstone and 20% shale interbeds arranged in coarsening- and cleaning-upward cycles, 5 to 20 m thick each (Fricker, 1963). Dark grey and dark brownish-grey shale is succeeded in each cycle by fine-grained and fissile sandstones that grade upward to medium and thick bedded. These sandstones are calcareous and dolomitic arkoses and subarkoses (Fricker, 1963). The feldspars are mostly sodic plagioclase, but about 20% are microcline (Fricker, 1963). Sandstone-weathering colours range from grey and olive-grey to pale yellowish brown. Additional depositional features include carbonaceous plant debris, bioturbated sediments, and occasional bivalves.

The Hassel Formation of Strand Peninsula, described by Souther (1963), consists of stacked massive beds of weakly indurated sandstone 3.5 to 12 m thick each. The lower parts of these massive beds are carbonaceous and dark grey. In contrast, the upper parts are progressively cleaner and paler sands weathering to shades of pale grey and pale greenish-grey. The sandstones contain carbonized plant debris and show evidence of burrowing (Souther, 1963). The Hassel Formation south and west of Strand Fiord is medium and thin bedded with interbeds of brown-weathering calcite-cemented sandstone and soft, unconsolidated, carbonaceous-quartz-sandstone (Tozer, 1963a). A gabbro sill is prominent in the Hassel Formation south of Strand Fiord.

MacRae (1996) measured the Hassel Formation north of East Fiord and provided an overview of the formation for much of Axel Heiberg Island. Depositional cycles in the Hassel Formation are interpreted as repetitive progradational features deposited in settings ranging from distal shoreface-offshore transition to shoreface and subaerial foreshore. Well-oxygenated conditions are indicated by common bioturbation. Foreshore deposits and probable subaerial exposure features are indicated at the top of the formation (MacRae, 1996).

Age: Dinoflagellates from the Hassel Formation of Axel Heiberg Island, including the report area, have been assigned to the *Wigginsiella grandstandica* Subzone of early late Albian age (MacRae, 1996). This age is consistent with that of *W. grandstandica* Subzone dinoflagellates and latest middle Albian ammonites in the highest beds of the underlying Macdougall Point Member (Jeletzky, 1980; Nohr-Hansen and McIntyre, 1998).

Bastion Ridge Formation

Definition: The Bastion Ridge Formation is a relatively thin and recessive shale unit above Hassel Formation sandstone and below mafic volcanic flows of the Strand Fiord Formation (Fig. 32, 36). Although these beds were originally included in the Hassel Formation by Tozer (1963a), they were separated by Fricker (1963), who erected a type section at Bastion Ridge near the head of Expedition Fiord. A detailed study of the Bastion Ridge Formation by MacRae (1996) includes 11 measured sections in the report area. Thickness ranges from 5 m in the southeast near the head of Strand Fiord to a maximum of 242 m in the northwest, north of Agate Fiord. Indicated age is late Albian (MacRae, 1996). Mapping of the Bastion Ridge Formation by airphoto interpretation without detailed fieldwork is fraught with difficulties—a problem also noted by Souther (1963). First, because the formation is recessive, it is commonly covered by blocky talus shed from the overlying Strand Fiord Formation. Second, where these beds are sunlit on aerial photographs, the contact with the Hassel Formation is marked by an upsection break in slope to darker and more recessive strata. However, these features are difficult to detect on steep slopes in shadow. Third, diabase sills and volcanic flows are common in these strata and not only shed blocky talus like the Strand Fiord Formation but also are indistinguishable from volcanic flows of the higher formation. In such places there is a tendency to interpret the base of the Strand

Fiord Formation at too low a stratigraphic level, thereby underestimating the thickness of shale. The geological map (Fig. 2 illustrates the Bastion Ridge Formation where it is readily observed on air photographs. Its apparent absence on the map above the Hassel Formation does not imply its absence in these places. However, according to Souther (1963), in some places "basalt sills" have been injected along the contact between Hassel sandstone and the overlying Strand Fiord volcanic rocks "where the shale is absent."

Composition: Fricker (1963) described the type section Bastion Ridge Formation as a fairly homogeneous unit of interbedded dark grey to greyish-black shale, brownish-grey-weathering siltstone, and minor thin beds (to 10 cm) of medium-grained sandstone that weather brownish grey and yellowish brown. Also noted are dusky-red-weathering sideritic ironstone beds, rare bivalves, and glendonites.

The Bastion Ridge Formation within the report area contains parts of two depositional sequences (MacRae, 1996). The base is commonly marked by a disconformity and transgressive flooding surface. Thin marine sandstone tongues above the base contain bivalves in some northwestern sections, which grade upsection and southeastward to marine shale. In mid-section is an important interval of bioturbated, progradational, hummocky cross-stratified marine sandstone with trace fossils. This interval thins and disappears from northwest to southeast and contains the base of the higher Bastion Ridge sequence.

Offshore marine shales of the upper Bastion Ridge sequence are overlain by mafic volcanic flows of the basal Strand Fiord Formation. Near the type section, however, volcanic flows end laterally in shale. The contact between the Bastion Ridge and Strand Fiord formations is evidently gradational and diachronous. Shale sections also contain invasive volcanic flows and diabase sills; the invasive structures are interpreted to be emplaced under a thin mud carapace (MacRae, 1996).

Age: Dinoflagellate collections from the report area indicate that the Bastion Ridge Formation lies entirely within the late Albian (MacRae, 1996). Given the fact that the Bastion Ridge Formation interfingers with the Strand Fiord Formation, however, a Cenomanian age would appear to be more likely.

Strand Fiord Formation

Definition: The Strand Fiord Formation was named by Souther (1963) for a succession of basalt flows, agglomerate, and minor pyroclastic deposits exposed throughout western and northwestern Axel Heiberg Island. Thickness at the type section on western Kanguk Peninsula is 182 m. However, subsequent studies indicate a thickness ranging from 40 m near the head of Strand Fiord to 701 m north of Agate Fiord (Fig. 37, 38) and reaching a maximum of 1033 m at Bunde Fiord on northwestern Axel Heiberg Island (Ricketts et al., 1985; MacRae, 1996). The Strand Fiord Formation is absent on Amund Ringnes Island. In this area the Bastion Ridge Formation is also missing, and the Hassel Formation is overlain directly by the Upper Cretaceous Kanguk Formation.

Composition: Typical rock types from the type section include flows (each 15–60 m thick) and sills of dark grey to black, aphanitic to very finely crystalline basalt (Souther, 1963). Flow tops, 1.5 to 10 m thick, are vesicular and amygdaloidal with amygdales filled by calcite, zeolites, chalcedony, and malachite. Other facies in the Strand Fiord area include pyroclastic breccia (agglomerate) containing ejecta fragments of basalt, Hassel sandstone (clasts to ~7 m), and Christopher shale (blocks to 3.5 m). The sections of Ricketts et al. (1985) indicate an interfingering of columnar-jointed lava flows (60 m thick each), with monomict basaltic agglomerate, polymict 'laharic' breccia, volcaniclastic sediments, and shale, particularly in sections around the head of Strand Fiord. The basalts are tholeiitic and illustrate a range of origins and implied viscosities, including pahoehoe, aa, and blocky agglomerate (Ricketts et al., 1985). Interbedded marine siltstones indicate subaqueous volcanism, but pillows have not been observed. Polymict breccias of the Strand Fiord Formation are interpreted as lahars, although an intrusive origin is also possible. Entrained wood fragments indicate subaerial explosive volcanism. Clast-supported conglomerate and cross-stratified sandstones indicate fluvial reworking, and shale containing fresh-water bivalves, coal, and plant remains (including *Metasequoia* and broad-leafed flora) represents overbank floodplain and lacustrine settings.

Extrusive Setting: The study of MacRae (1996) provides additional detail concerning the settings of volcanic activity in the Strand Fiord Formation. Flow

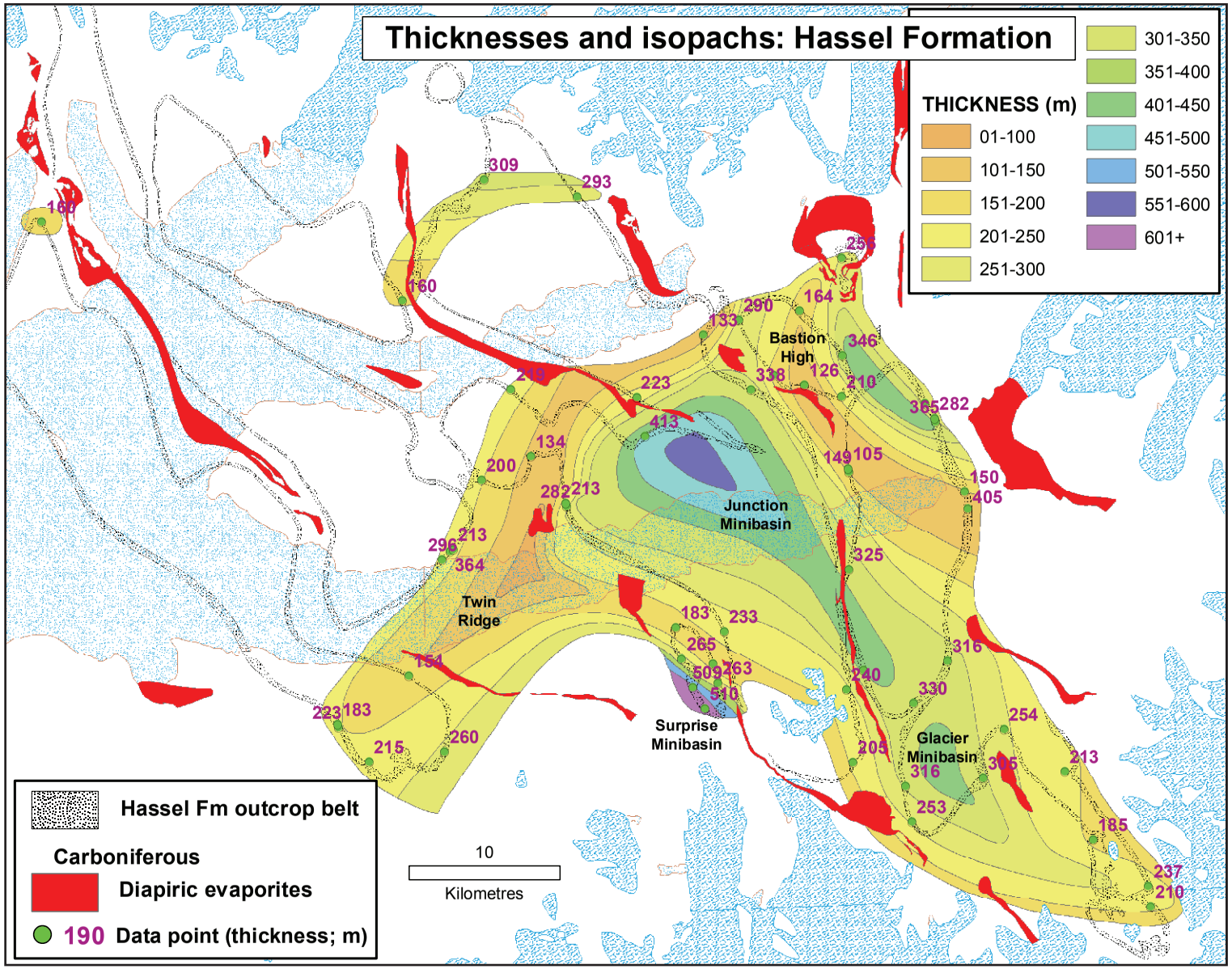

Figure 35. Isopachs and spot thicknesses for Hassel Formation. Range of thickness is 105 to 510 m.

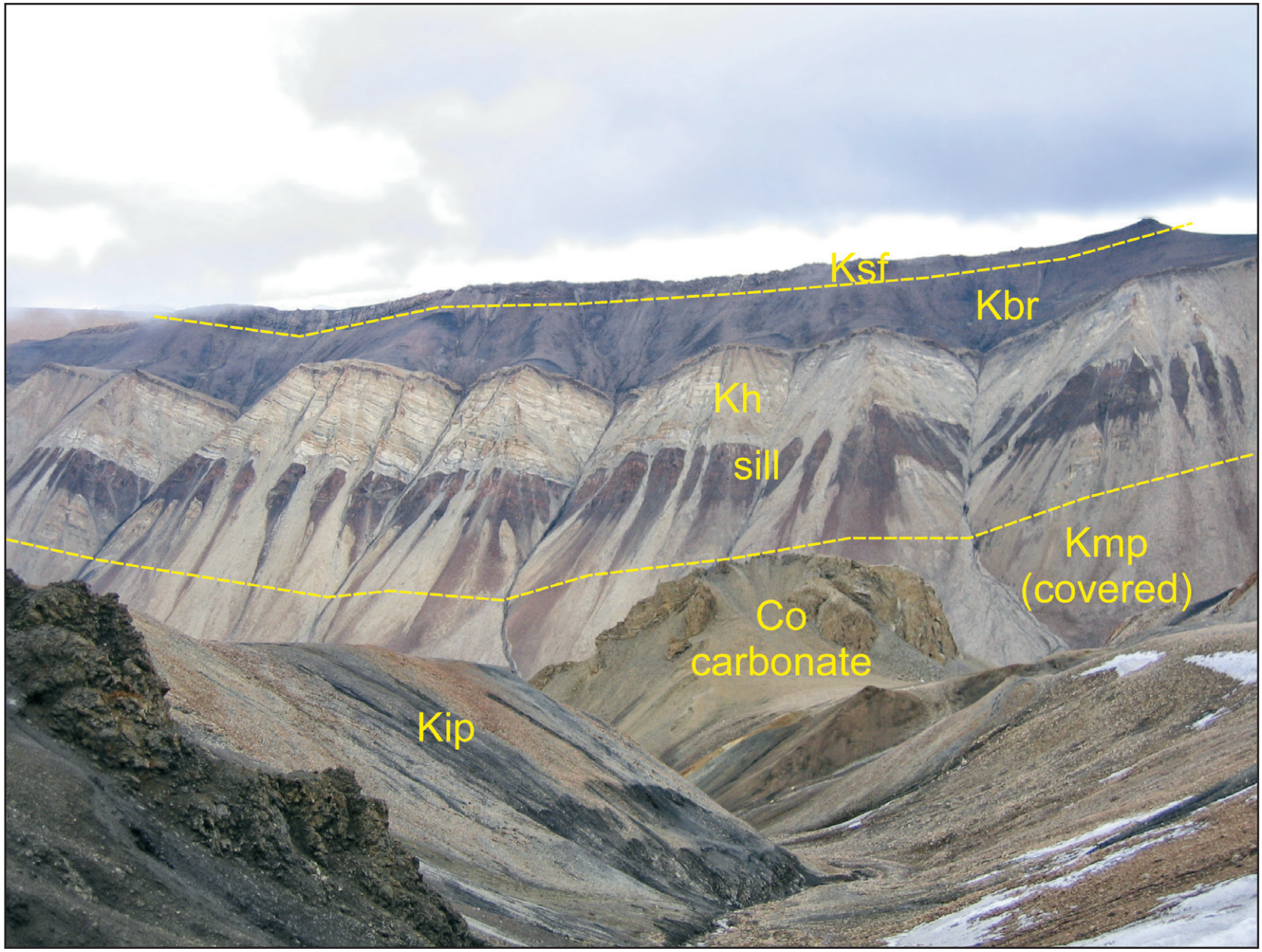

Figure 36. In this prominent section of Junction minibasin east of Junction diapir, Hassel Formation (Kh) is intruded by a sill of dark reddish-brown gabbro. Hassel strata above a break in slope are overlain by recessive Bastion Ridge Formation (Kbr) and above this by Strand Fiord Formation (Ksf). Older units in view include: Otto Fiord Formation (Co), Invincible Point Member (Kip), Macdougall Point Member (Kmp) View east. (GSC Photo No. 2014-092)

tops in the west of the report area (East Fiord) and on northwestern Axel Heiberg Island are oxidized and stained with hematite, suggesting episodic subaerial exposure. At Bastion Ridge the lower parts of some flows include pillow breccia, and soft-sediment deformation structures (flames) occur in underlying shales, indicating subaqueous extrusion. Invasive flows have been interpreted in a section at East Fiord. These flows are near-surface sills injected into soft sediments that produce pillow-like structures, chaotic breccias, and lobate sill tops. They are interpreted as a result of rapid quenching and steam explosions. Facies grade from true sills, as seen in Bastion Ridge Formation, to invasive flows and true extrusive flows typical of the Strand Fiord Formation. This variation also probably occurs along strike within individual igneous sheets. Other volcanic facies of Strand Fiord Formation include subaqueous hyaloclastite flows, basaltic ash-fall deposits, fluvial conglomerate dominated by basalt clasts, and wave-washed volcaniclastic sandstone.

Age: The age of the Strand Fiord Formation is provided by absolute age determinations and biostratigraphic constraints inferred from the age of bounding units and regional geological relationships. Absolute age determinations for Strand Fiord Formation were summarized by Villeneuve and Williamson (2006). An unpublished ^{40}Ar-^{39}Ar age of 100±62 Ma was provided by Muecke and Reynolds *in* Villeneuve and Williamson (2006), or late Albian to early Cenomanian. However, the geological relationships and analysis techniques are unknown. The 'upper lava flows' from a section north of Strand Fiord yield a whole-rock ^{40}Ar-^{39}Ar

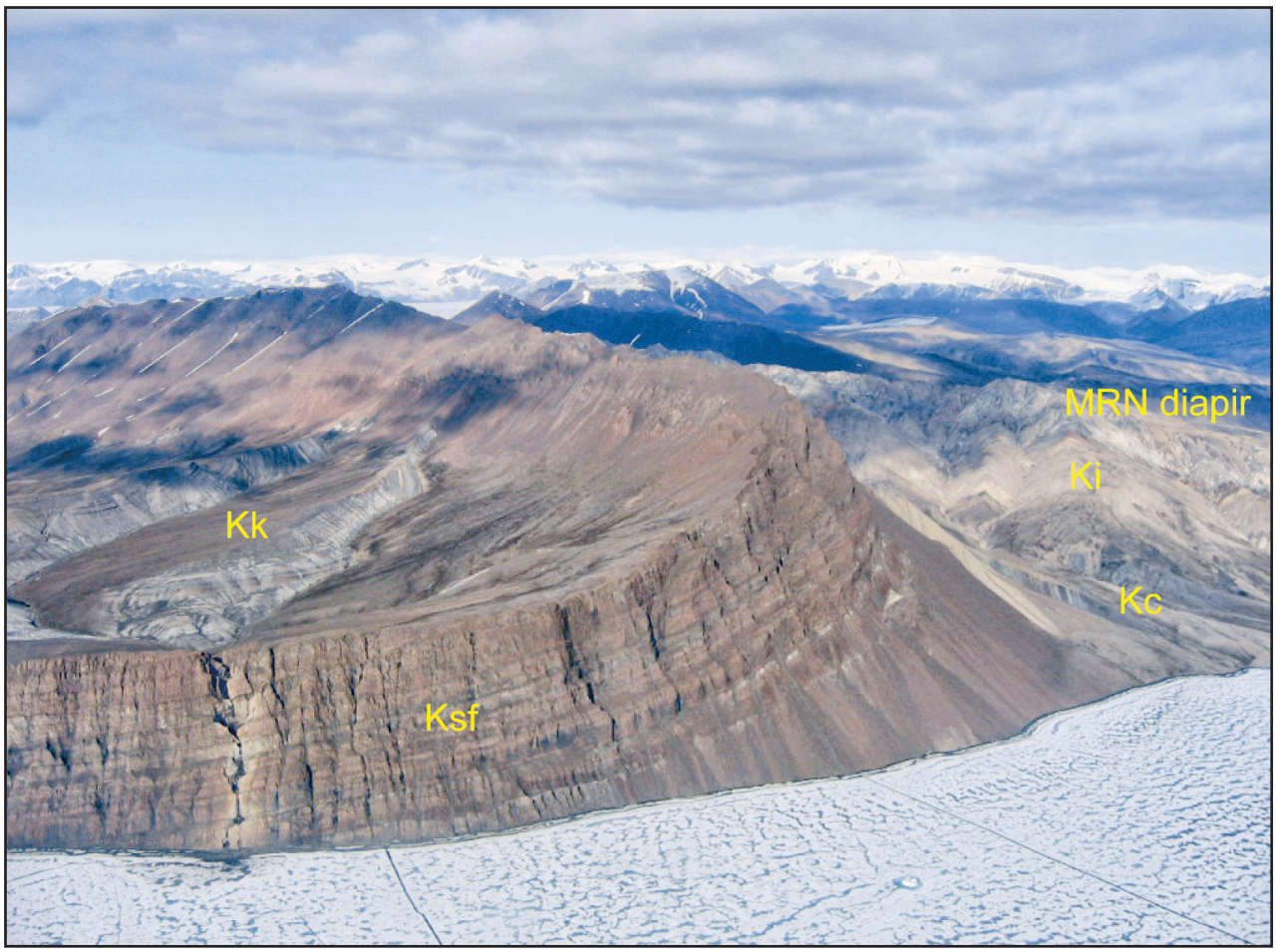

Figure 37. Prominent cliffs near Dragon Mountain feature Strand Fiord Formation (Ksf) with recessive grey Kanguk Formation (Kk) occupying the axis of the minibasin at upper left. Evaporites at right are part of Muskox Ridge North (MRN) diapir; also present against the diapir are Isachsen Formation (Ki) and, above this, Christopher Formation (Kc). View is to the northeast, with Expedition Fiord in the foreground. (GSC Photo No. 2014-093)

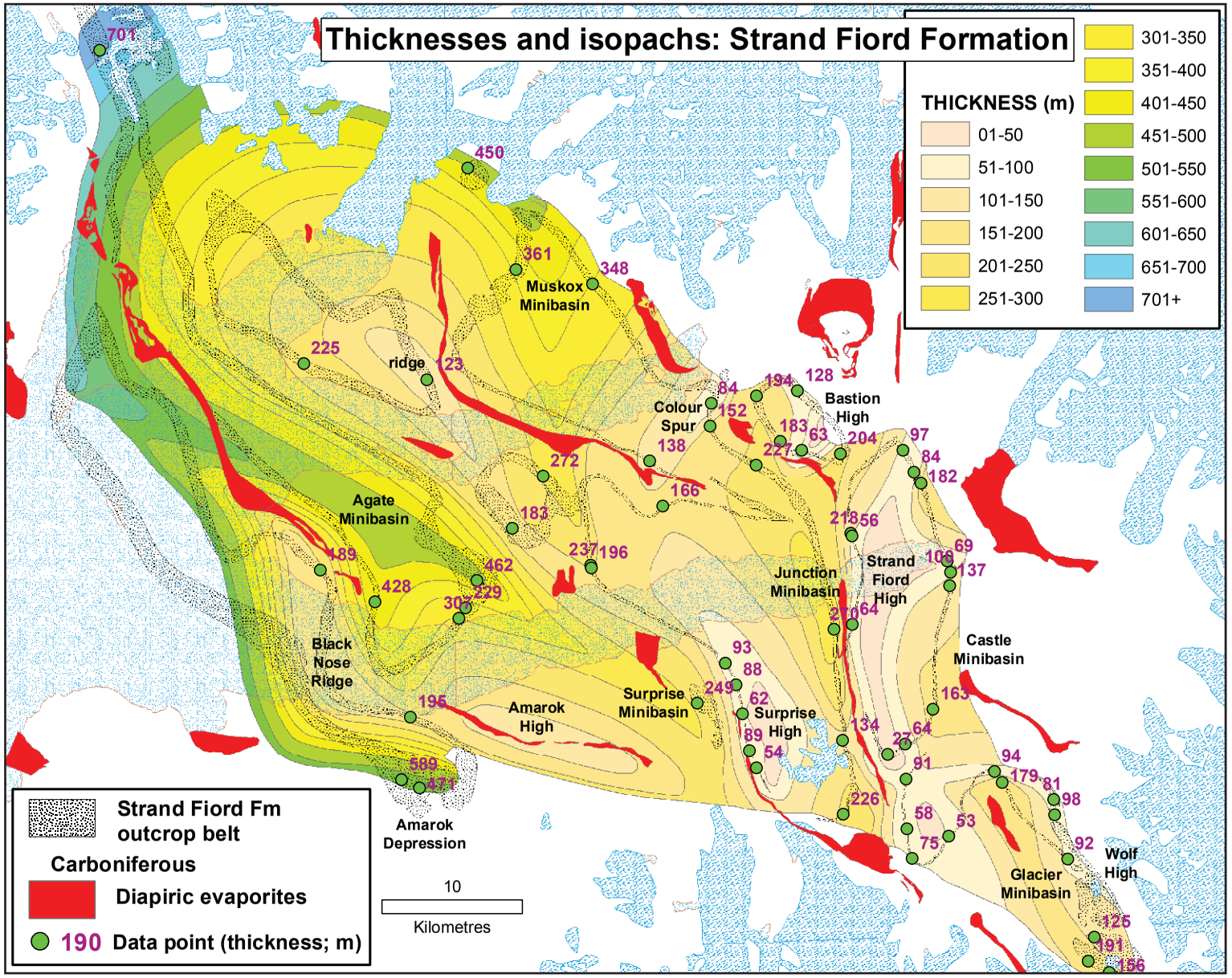

Figure 38. Isopachs and spot thicknesses for Strand Fiord Formation. Range of thickness is 53 to 701 m.

age of 95.3±60.2 Ma (Tarduno et al., 1997), a date that lies in the middle Cenomanian.

New whole-rock ^{40}Ar-^{39}Ar ages, reported by Villeneuve and Williamson (2006) from the Strand Fiord Formation, are controversial primarily because they imply extrusion during deposition of Kanguk Formation elsewhere. Dated samples from the Strand Fiord Formation at two locations on northwestern Axel Heiberg Island are inconsistent with other observations, not only because they have an anomalously young age (83.8±61.2 Ma; early Santonian to early Campanian) but also because a dated sample from the base of the formation (92.3±61.1 Ma; early to middle Turonian) is significantly younger than an age from the top (96.1±61.9 Ma; early to late Cenomanian). Especially controversial is a very young whole-rock ^{40}Ar-^{39}Ar age of 80.7±61.1 Ma (early to mid-Campanian) from the "central portion of a succession of ten lava flows" at Twisted Ridge, south of Expedition Fiord (Villeneuve and Williamson, 2006).

Volcanic flows of the Strand Fiord Formation within the report area interfinger with shales of the Bastion Ridge Formation, and to the east and southeast, Strand Fiord Formation feathers out in Bastion Ridge shale. The Bastion Ridge Formation contains a late Albian, or more likely a Cenomanian, dinoflagellate assemblage (MacRae, 1996), which suggests that the lower part of the Strand Fiord Formation is also this age. The biostratigraphic constraints on the upper age limit of the Strand Fiord Formation are provided by faunal assemblages in the overlying Kanguk Formation (*see below*). As far as is known, the Kanguk and Strand Fiord formations do not interfinger. The contact has been described, at least locally, as a disconformity (Tozer, 1963b; Tarduno et al., 1997). Similarly, dykes and sills related to the Strand Fiord Formation volcanism are not known to intrude the Kanguk Formation or any higher units. This, however, does not rule out the possibility that the Strand Fiord Formation somewhere on Axel Heiberg Island is age equivalent to some part of the Kanguk Formation in other areas of the Arctic where volcanic rocks are absent above the Hassel Formation. For this reason, biostratigraphic constraints on the upper age limit of the Strand Fiord Formation are only valid for fossil assemblages from the Strand Fiord Formation itself or from he Kanguk Formation where the latter unit actually lies on Strand Fiord volcanic flows. The stratigraphically lowest collections from the Kanguk Formation on south-central Strand Peninsula are foraminifera of Turonian to early Santonian age from 30.2 m above the base (J.H. Wall *in* Ricketts, 1991).

Considering the above data collectively, we think the Strand Fiord Formation is definitely upper Albian at the base and contains flows ranging from late Albian to middle Cenomanian, as implied by the whole-rock ages of Muecke and Reynolds (*in* Villeneuve and Williamson, 2006) and Tarduno et al. (1997). Also inferred before overstep by Kanguk shale within the report area are Strand Fiord Formation flows of late Cenomanian and Turonian ages—for example, the volcanic flows of northwestern Axel Heiberg Island, as indicated by the absolute ages reported by Villeneuve and Williamson (2006). However, this interpretation would require that the Strand Fiord Formation of northwestern Axel Heiberg Island be age-equivalent to the lower Kanguk Formation where it contains late Cenomanian to Turonian fauna elsewhere in the Arctic (i.e. western Ellesmere, Amund Ringnes, and Graham islands; Greiner, 1963; Thorsteinsson and Tozer, 1970; J.A. Jeletzky *in* Balkwill, 1983). The possibility of local volcanic activity within the report area continuing into the early Campanian is implied by the highly controversial ^{40}Ar-^{39}Ar age from Strand Fiord Formation at Twisted Ridge (*in* Villeneuve and Williamson, 2006). However, this date needs to be confirmed.

Intrusive igneous rocks

Composition: Mafic intrusions of the report area, variously described as diabase, porphyritic diabase, diabasic-gabbro, and gabbro, were first described by Blackadar (1963) and Fricker (1963). These rocks intruded as dykes and sills in Lower Cretaceous and older strata and are common as irregular masses within many of the diapirs. The mapped intrusions are weathering-resistant rocks that shed blocky talus and contain sufficient iron to weather to a dark brown limonitic rind. Predominant are labradoritic plagioclase and augitic clinopyroxene partly replaced by amphibole. Iron-rich opaque phases are ilmenite and magnetite. Small amounts of olivine are replaced by chlorite, and quartz occurs sparingly in some pegmatitic cumulates (Fricker, 1963). Geochemical studies by Williamson (1988) indicate these intrusions are iron-rich continental tholeiites.

Dyke swarms: Intrusive igneous rocks in the report area are associated with two mafic dyke swarms of the Canadian Arctic Islands (Buchan and Ernst, 2003). The larger of these is the Queen Elizabeth swarm, which strikes northerly on Axel Heiberg Island (N10°E to N10°W in the report area) but forms a radial pattern that extends outward from a focal area on the continental margin north of the island. Included in this swarm are northeasterly-striking dykes and related linear aeromagnetic anomalies of the western Arctic Islands (Balkwill and Foxe, 1983), and northwesterly-striking dykes of Ellesmere Island (Buchan and Ernst, 2003). The second dyke set, the Surprise swarm, strikes east-northeasterly and extends from Ellef Ringnes and King Christian islands eastward through the southern half of Axel Heiberg Island (Buchan and Ernst, 2003). Related to these swarms are sills and flows of the Strand Fiord and upper Isachsen formations and sills in all intervening and older rocks including the diapirs. Although volcanic activity is evident in the Kanguk Formation in the form of bentonite and tuff layers (*see below*), within the report area neither sills nor dykes appear in the Kanguk Formation; nor do any igneous rocks appear in the overlying Eureka Sound Group.

Dykes are generally more abundant on the periphery of the report area than within the central region. The reason for this is presumably the preponderance of post-dyke units at the surface in the centre of the map area and the greater occurrence of pre-dyke map units on the map margins. Dykes and sills may be more abundant in the east and north than along the southern and western margins of the map area. The greatest concentration of intrusions appears to be in a region from northwest of Colour diapir north of Expedition diapir. Mafic igneous sheets—whether these are of intrusive or extrusive origin is unknown—are especially abundant in the upper part of the Isachsen Formation of this region and much less common above this level.

Within the report area, there is no clear distinction between dyke trend and the age or stratigraphic level of emplacement. Northwest of Colour diapir, for example, are two large northerly-striking dykes that could be assigned to the Queen Elizabeth swarm. One of these is 350 m wide. These dykes cut the Awingak through lower Isachsen succession and appear to be conduits for sills and/or flows in the upper Isachsen Formation. Nearby to the southeast, as far as Expedition River, are east-northeast- and northeasterly-striking dykes (one as much as 500 m wide). All are arguably of the Surprise swarm and appear to feed igneous sheets in the upper Isachsen Formation but, in addition, cut strata as high as the Christopher Formation. Surprise swarm dykes are also common at Good Friday diapir and between Duck Bay and Peeawahto diapirs. Several of these dykes cut the Christopher Formation west of Duck Bay.

Dykes, which are also assignable to the two named swarms, have been mapped between Strand and Glacier diapirs. Although future targeted fieldwork, sampling, and geochemistry may help to resolve relative age and geochemical differences, field relationships as presently understood indicate that the lower Isachsen Formation is the youngest unit cut by these dykes and that igneous sheets are common at the surface in the youngest preserved Isachsen beds.

To summarize this local evidence, northerly-trending Queen Elizabeth dykes cut units as high as the lower Isachsen Formation and clearly feed igneous sheets in the upper Isachsen. It is not known, however, whether the Queen Elizabeth swarm actually served as feeders for Isachsen volcanic events. Equally possible is that this swarm feeds sills in the Isachsen Formation that are entirely of post-Isachsen age. East-northeasterly-trending Surprise swarm dykes cut units as high as the Christopher Formation. Surprise dykes also appear to represent feeders for igneous sheets in the Isachsen Formation, and the dykes may have been volcanic conduits in both late Isachsen and Strand Fiord times.

Age: Is it possible that the Surprise and Queen Elizabeth swarms are coeval? Villeneuve and Williamson (2006) provided new whole-rock ^{40}Ar-^{39}Ar ages for selected Cretaceous-Palaeocene igneous rocks of the Arctic Islands and a summary of all other available absolute ages. On the basis of two whole-rock and two single-mineral ^{40}Ar-^{39}Ar ages, dykes and sills of Axel Heiberg Island range from 129±2 Ma to 113±6 Ma. This age corresponds to the interval from the late Hauterivian to the middle Albian. There is no indication in the Villeneuve and Williamson (2006) paper as to which, if any, of these dykes is part of the Queen Elizabeth swarm. However, two K-Ar whole-rock ages from

Queen Elizabeth dykes of Grinnell Peninsula (112±5, 117±5 Ma; early Aptian to early Albian) and one of Melville Island (123±6 Ma; early Barremian to mid-Aptian) have a similar but narrower age range. The maximum late Hauterivian- to middle Albian-equivalent age range of these absolute ages coincides stratigraphically with deposition of the upper Paterson Island through Walker Island members of the Isachsen Formation and the bulk of the Christopher Formation. This age range matches that of known intrusive and extrusive igneous rocks in the report area. The lower age limit is especially noteworthy because evidence of volcanism does not appear in the Valanginian part of the Paterson Island Member. However, clasts of volcanic material first appear several hundred metres above the base of this unit in beds inferred to be of Hauterivian age.

None of the dated dykes and sills of Axel Heiberg Island are age-equivalent to Strand Fiord Formation (Villeneuve and Williamson, 2006). Neither do they overlap the maximum possible range of ^{40}Ar-^{39}Ar ages from lava flows of that unit (100±2–80.7±1.1 Ma; late Albian to mid-Campanian). In contrast, sills and other intrusions of northernmost Ellesmere Island do coincide with the age of Strand Fiord Formation. The implication of these observations is that the intrusive rocks of Axel Heiberg Island are coeval with volcanism recorded in the Isachsen and Christopher formations. In contrast, the Strand Fiord Formation, at least in the report area, comprised far-travelled low-viscosity flows for which intrusive feeders are yet to be discovered farther north. It follows then that the hot spot delivering these Cretaceous igneous rocks was located under Axel Heiberg Island in Hauterivian to mid-Albian time and then shifted northward for renewed volcanism starting in the late Albian.

Kanguk Formation

Definition: The Kanguk Formation was named by Souther (1963) for 190 m of recessive-weathering dark grey silty shale exposed above the Strand Fiord Formation volcanic rocks at the east end of Kanguk Peninsula (Fig. 39). Above the shale and also included in the formation was a 23 m interval of sandstone and another 38 m of shale. Subsequently, the Kanguk Formation included all shales of Late Cretaceous age exposed from Banks Island to northern Ellesmere Island (Embry, 1991). Typical rock types of the report area include dark grey silty shale with dusky-red-weathering calcareous concretions and, in the lower part of the formation, perhaps four beds of greyish-yellow tuff or bentonite (Souther, 1963). The basal contact was described as apparently conformable. A greywacke bed at the base on western Kanguk Peninsula, however, is considered an erosion product derived from the Strand Fiord Formation.

Composition: Fricker (1963) published two sections from Bastion Ridge in the Expedition River area and recognized a lower member (~200 m) of dark grey to black laminated soft shale, with minor siltstone and sandstone (in beds to 3 m), and an upper member of pale olive-grey laminated sandy micaceous siltstone with interbeds of sandstone and shale (130 m thick). Reddish clay-ironstone layers, tuff, and bivalve remains are noted in both members. The lower contact with Strand Fiord Formation is abrupt. Thickness range based on isopachs for Kanguk Formation across the report area is 31 to 847 m (Fig. 40).

The marked contrast in weathering between the Strand Fiord and Kanguk formations poses challenges to mapping. Although this contact is sharp, the upper surface of the resistant the Strand Fiord Formation commonly forms a long dip slope. In contrast, Kanguk shales are commonly covered by vegetation or colluvium. As a result the precise dip-slope location of the Kanguk lower contact is commonly uncertain. The upper contact with the Eureka Sound Group is also poorly defined owing to the highly gradational and interbedded nature of the shale, siltstone, and sandstone through this interval. In general, we follow Ricketts (1991), who emended the type Kanguk Formation and placed the siltstone-sandstone-dominated upper part in the lowest part of his Eureka Sound Group (the lower member of Expedition Formation). On this basis, measured sections of the emended Kanguk Formation range from 110 to approximately 350 m.

Age: The age of the Kanguk Formation within the report area is based on bivalve collections, foraminifera, dinoflagellates, and magnetostratigraphic studies. The oldest microfauna are foraminifera of the *Dorothia smokyensis* assemblage (Turonian to early Campanian) located 30.2 and 42.0 m above base of formation near the central south coast

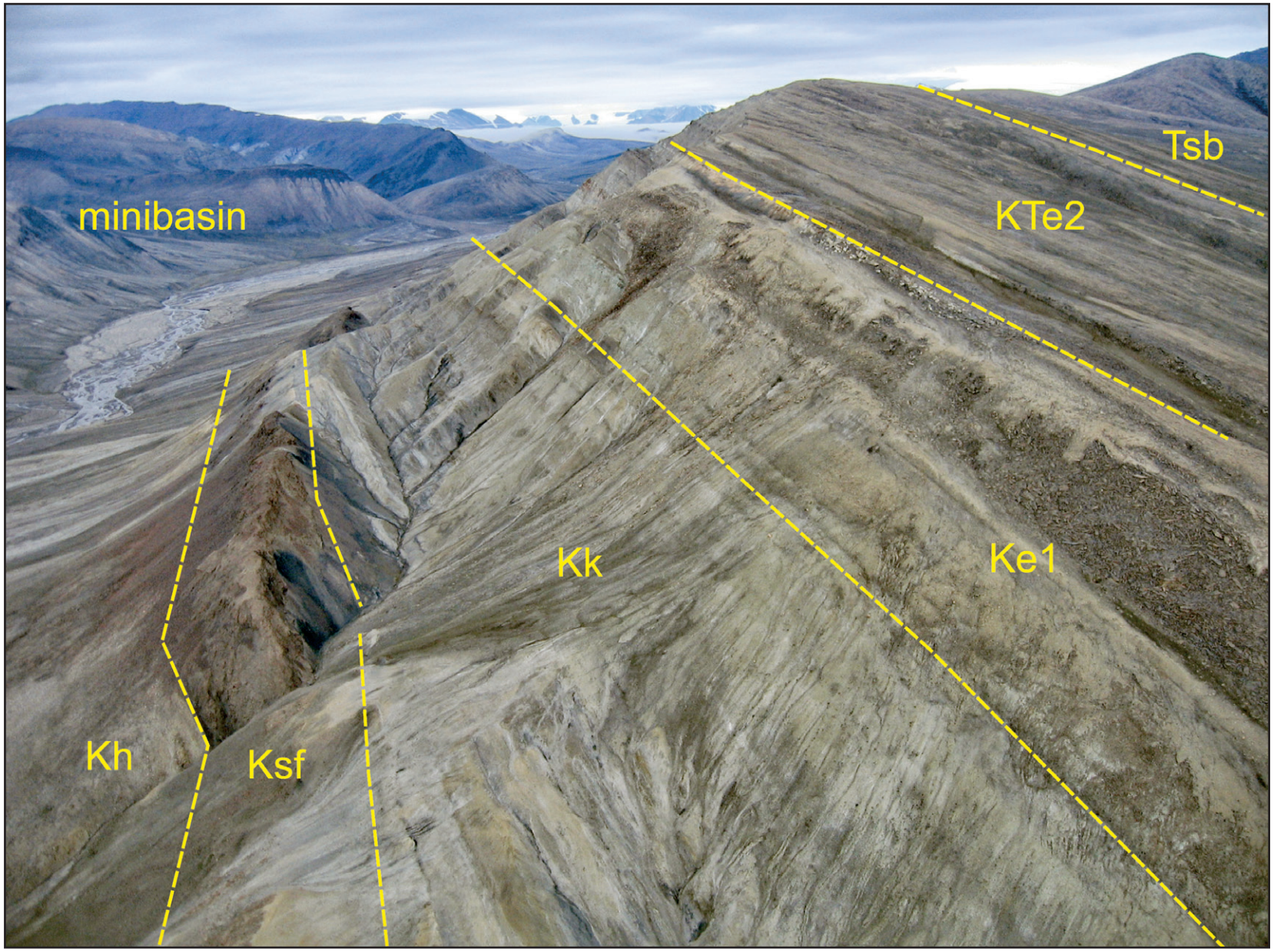

Figure 39. In this outcrop on the west limb of Kanguk River syncline is a cliff section of Hassel Formation (Kh), thin reddish-brown, ledge-forming Strand Fiord Formation (Ksf), greenish-grey-banded Kanguk Formation (Kk), which is recessive in the lower part, and yellow-banded Expedition Formation (Ke1, KTe2) underlying the hill top. Contact drawn at base of Strand Bay Formation (Tsb) is uncertain. View is to the north. (GSC Photo No. 2014-094)

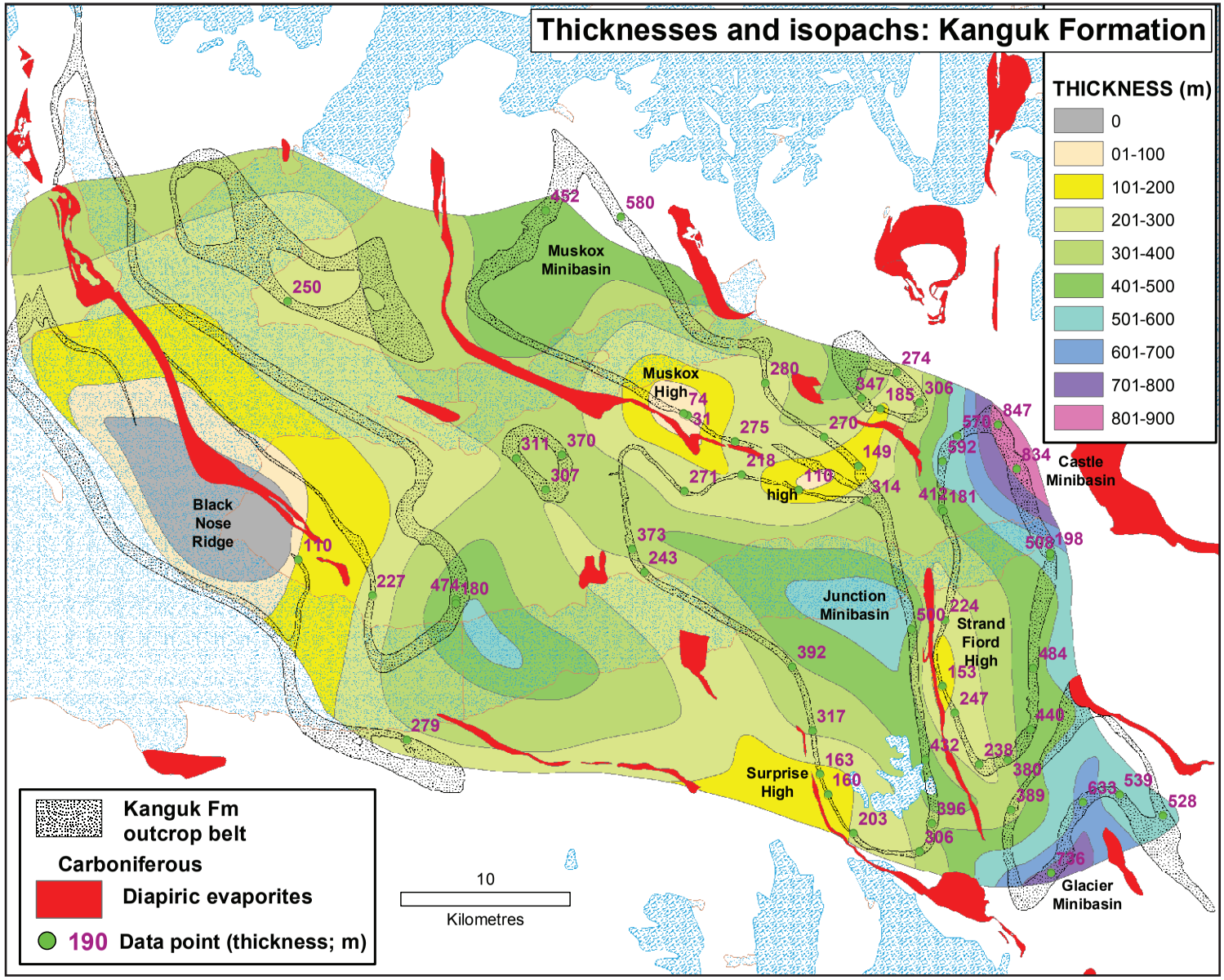

Figure 40. Isopachs and spot thicknesses for Kanguk Formation. Range of thickness is 31 to 847 m.

of Kanguk Peninsula (J.H. Wall *in* Ricketts, 1991). Dinoflagellates of Turonian to Santonian age occur between 30.2 and 107.8 m in this same section (D.J. McIntyre, *in* Ricketts, 1991). Magnetostratigraphic studies by Tarduno et al. (1997) indicate that the Kanguk Formation of central Kanguk Peninsula may include chrons 34n (early Aptian to Santonian) and 33r (early Campanian). Megafauna from the base of Kanguk Formation near Dragon Mountain include ectothermic reptiles (champosaurs and turtles) and lepisosteid, amiid, and teleost fish remains (Friedman et al., 2003). Apart from indicating warm mean annual temperatures (exceeding 14° C) for the Late Cretaceous of Axel Heiberg Island (Tarduno et al., 1997), these faunal assemblages alone do not constrain age. The oldest Kanguk Formation strata must be no older than the youngest volcanic flows of the Strand Fiord Formation in this area (^{40}Ar-^{39}Ar age of 95.3±0.2 Ma or middle Cenomanian; Tarduno et al., 1997).

The highest beds of the Kanguk Formation as defined by Ricketts (1991) contain elements of both Turonian to early Campanian *Dorothia smokyensis* and late Campanian *Verneuilinoides bearpawensis* assemblages (J.H. Wall *in* Ricketts, 1991), which probably indicates an age somewhere in the Campanian. The upper third of the Kanguk Formation on Kanguk Peninsula also contains gastropods, ammonites, and a Santonian to early Campanian inoceramid bivalve assemblage (F.H. McLean *in* Souther, 1963), including *Inoceramus lundbreckensis* (mid-late Santonian to early Campanian; J.A. Jeletzky, *in* Ricketts, 1991).

Age of the Kanguk Formation beyond western Axel Heiberg Island ranges from upper Cenomanian to end of the Campanian or even into early Maastrichtian (*see* description of the Strand Fiord Formation, *above,* and Harrison et al., 1999). However, this potentially diachronous upper age limit for the Strand Fiord Formation may cloud the timing of Kanguk deposition within the report area.

Eurekan Orogeny

Sverdrup Basin and its basement were both shortened during the Paleogene Eurekan Orogeny. Shortening resulted from motion of the ancestral Greenland plate during seafloor spreading in the Labrador Sea and the North Atlantic between approximately 62 and 33 Ma (chrons 27n to 13n, or base Selandian to end Eocene). The end of Eurekan deformation is marked by a profound regional angular unconformity that separates Paleogene and Neogene strata.

The Eurekan Orogeny is recorded by terrestrial coarse-clastic sediments of the Eureka Sound Group (Miall, 1991; Ricketts, 1991; Fig. 3). Biostratigraphic and chronostratigraphic data indicate that the first significant phase of the Eurekan Orogeny was extrusion (in chron 27n) of plume-related flood basalts in West Greenland and development of an unconformity between lower Maastrichtian and basal Selandian strata throughout the Arctic Islands (Harrison et al., 1999). This initial deformation led to accelerated seafloor spreading following Cretaceous to Danian slow rifting in the Labrador Sea. Greenland (and all of Eurasia) retreated northeastward from the Baffin margin of North America. Easterly to northeasterly striking thrusts formed during this first phase of the orogeny across North Greenland and on northern Ellesmere Island. Derived deltaic and terrestrial sediments accumulated rapidly (as much as 400 m/m.y.) in the medial parts of the Eureka Sound Group on central Ellesmere Island and throughout the eastern report area.

A second phase of the Eurekan Orogeny began with the main pulse (in chron 24r) of flood-basalt volcanism in East Greenland, seafloor spreading in the North Atlantic between Greenland and northwestern Europe, and a shift in the plate motion of Greenland with respect to North America. Simultaneous spreading in the Labrador Sea and the North Atlantic, starting near the base of the Eocene, realigned the motion of Greenland toward the northwest. This realignment rotated northern Ellesmere counterclockwise (~33±8°; Wynne et al., 1988), and northerly and northwesterly striking thrusts and folds propagated across central Ellesmere Island and Axel Heiberg Island (including the report area) and into the western Arctic Islands. The Eurekan Orogeny ended as seafloor spreading ceased in the Labrador Sea between chrons 22 and 13 (mid-Eocene to basal Oligocene). Thereafter Greenland no longer moved with respect to North America. The Eurekan Orogen was eroded to sea level along the Arctic continental margin from Meighen Island to Banks Island. Post-orogenic cover ranges from middle Miocene to Pliocene.

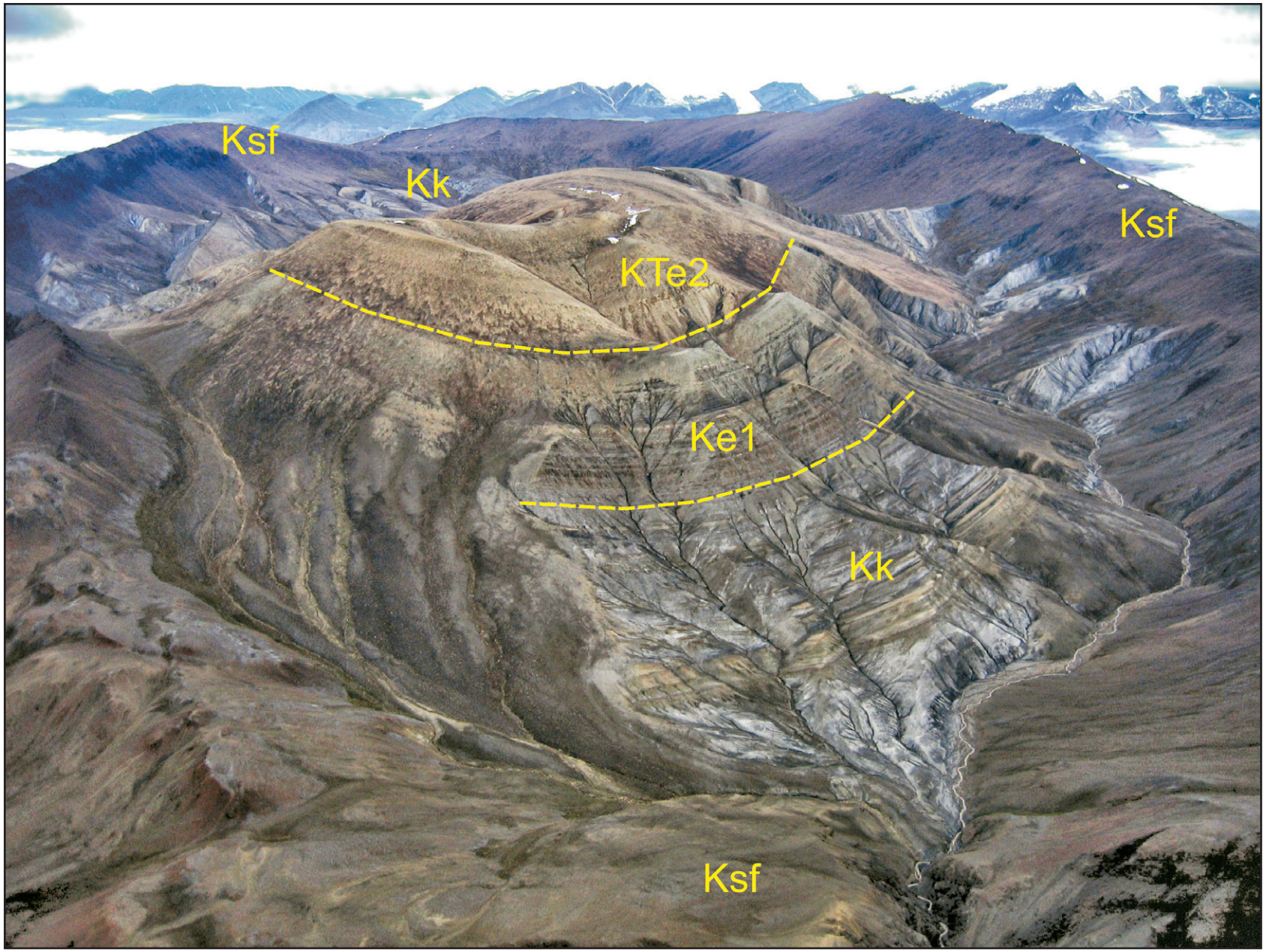

Figure 41. Bastion minibasin is exposed in Kanguk River syncline, just east of Bastion Ridge diapir. The minibasin contains Strand Fiord Formation (Ksf) on its perimeter, overlain by recessive grey Kanguk Formation (Kk), by the yellowish-brown Lower Member (Ke1) and Upper member (KTe2) of Expedition Formation. The upper Kanguk and Expedition formations appear to display four coarsening-upward grand cycles. View to the north. (GSC Photo No. 2014-095)

Stratigraphic units deposited during the Eurekan Orogeny in the report area include the Expedition, Strand Bay, and Iceberg Bay formations.

Expedition Formation - Lower Member

Definition: The Expedition Formation was named by Ricketts (1991) for a type section of interbedded sandstone and shale east of Kanguk River and above the Kanguk Formation, 2.5 km north of Strand Fiord (Fig. 41).

Composition: The proportion of shale (~60%) in the Lower Member, 160 to 320 m thick, exceeds that of sandstone (~40%) throughout all but the top several tens of metres. Sandstones were described by Ricketts (1991) as "dirty," presumably meaning argillaceous and mineralogically poorly sorted, intensely bioturbated, arranged in coarsening-upward cycles in the lower part and fining-upward cycles in the upper part. Bed thickness generally increases upsection to a maximum of 2 m at the top. However, a pair of massive cliff-forming sandstones, as much as 20 and 42 m thick, cap the member east of the type section. The Lower Member also includes planar-cross-stratification, ripples, inoceramid remains, plant fragments, and leaf impressions.

Depositional setting: The Lower Member is the upper part of a regressive systems tract that began subsequent to maximum marine flooding during Kanguk Formation deposition. The Expedition Lower Member was interpreted by Ricketts (1991) as having been deposited in marine prodelta and lower to upper shoreface settings in the lower part; foreshore deposits appear at the tops of cycles in the middle part of the member; and channelized distributary settings appear in the upper part. Facies change westward on Kanguk Peninsula to thinner and more distal sandstones. The overall thickness of the Lower Member (Fig. 42) reaches a maximum of 947 m in Glacier minibasin north of Wolf diapir.

Age: The age of the Lower Member of the Expedition Formation is based on probable Campanian foraminifera in the upper Kanguk Formation (J.H. Wall *in* Ricketts, 1991) and *Inoceramus (Sphenoceras) lundbreckensis* in the upper Kanguk Formation (late Santonian to early Campanian) and as fragments in the upper part of the Expedition Lower Member below the highest thick sandstone bed of the type section (J.A. Jeletzky *in* Ricketts, 1991). The unit is not younger than early Maastrichtian because terrestrial pollen assemblages of that age occur between the thick sandstones at the top of the Lower Member in the type section and in the lower part of the Upper Member (D J. McIntyre *in* Ricketts, 1991).

The section on south-central Kanguk Peninsula by Tarduno et al. (1997) contains a reverse-polarity interval between two intervals of normal magnetic polarity. The top of another reversely polarized section is recorded at the base and is continuous with a similar interval in the upper Kanguk Formation. In those authors' preferred model this is interpreted as chron 33r at the base (early Campanian), 33n through 32n for the lower normal-polarity interval (middle and late Campanian), 31r for the upper reverse-polarity interval (early Maastrichtian), and an amalgamation of chrons 31n through 27n (late Maastrichtian to end Danian) for the top of the section. However, this interpretation does not account for early Maastrichtian palynomorphs at the top of the member and a complete absence of late Maastrichtian and Palaeocene fossils. We interpret the base of the section as chron 33r and the top as mostly 32n and adjust the intervening section accordingly (see Fig. 12). Considering all available data we infer the Lower Member of the Expedition Formation to be lower Campanian to upper Campanian, and perhaps lower Maastrichtian.

Expedition Formation - Upper Member

Thickness and Composition: The Upper Member of the Expedition Formation (0 to 746 m thick; Fig. 43) consists of sandstone and shale in coarsening-upward cycles (Ricketts, 1991). Sandstone is commonly bioturbated but is more sorted and washed than are sandstones of the Lower Member. Sandstone is dominant in the eastern type section area and contains medium- to coarse-grained cross-bedded intervals with pebble lags. The unit grades westward to increasing shale and coaly shale, and the Upper Member is unrecognized on western Kanguk Peninsula where shale of the overlying Strand Bay Formation lies directly on Expedition Lower Member (Ricketts, 1991). The Upper Member is interpreted as the product of westward-directed shoreface and strandplain (Ricketts, 1991) progradation in a wave-dominated delta system containing ledge-forming distributary-channel sandstone bodies.

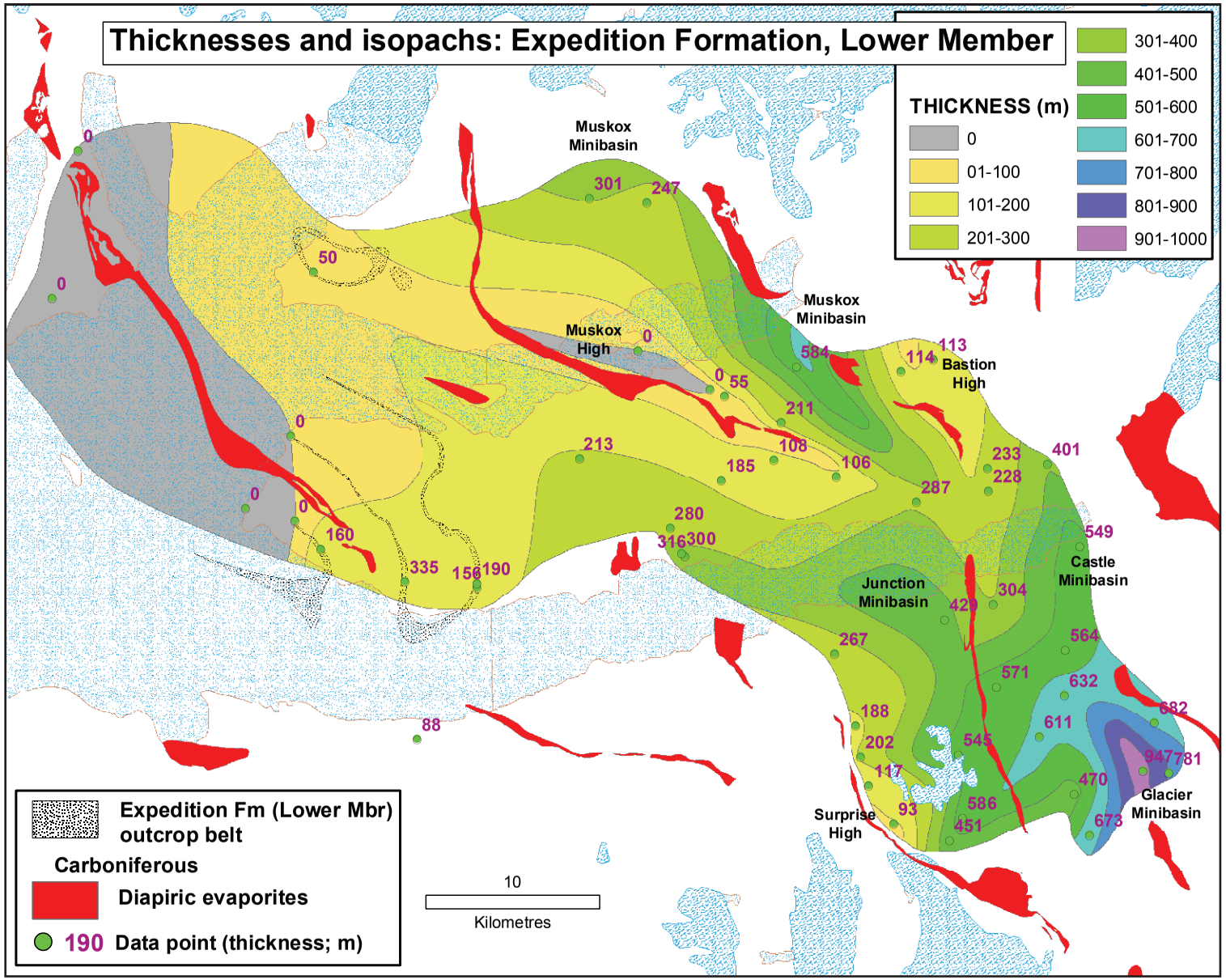

Figure 42. Isopachs and spot thicknesses for the Lower member of Expedition Formation. Range of thickness is up to 947 m.

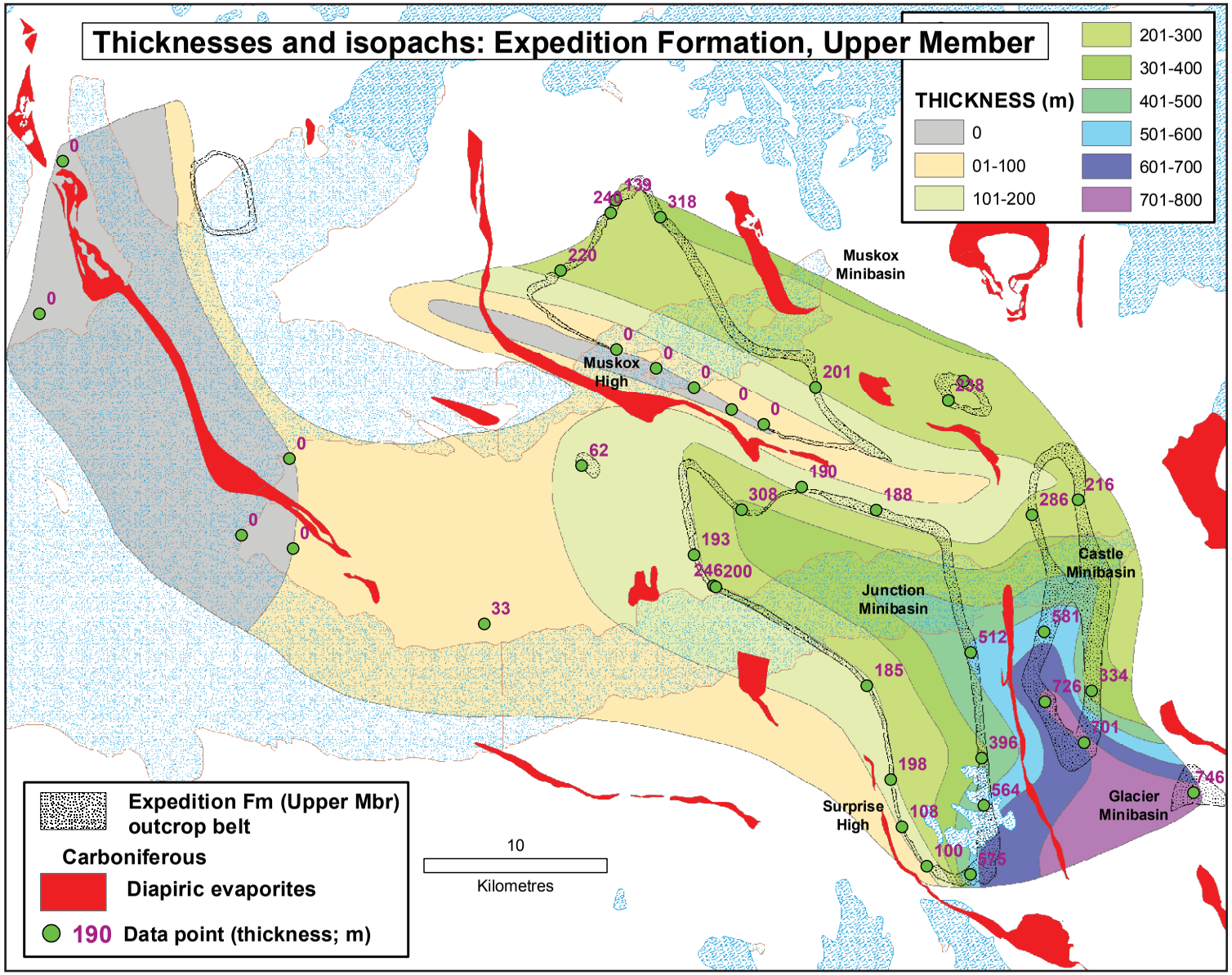

Figure 43. Isopachs and spot thicknesses for the Upper member of Expedition Formation. Range of thickness is up to 746 m.

Age: On central Kanguk Peninsula the Upper Member of the Expedition Formation contains early Maastrichtian terrestrial pollen assemblages in the lower 70 m and late Palaeocene palynomorphs in the highest beds below Strand Bay Formation, as indicated by *Momipites anellus* and *Insulapollenites rugulatus* (D.J. McIntyre *in* Ricketts, 1991). Contrary to the interpretation of Ricketts (1991), no proven upper Maastrichtian or lower Palaeocene (Danian) strata appear anywhere on western Axel Heiberg Island. In most parts of the Arctic Islands the base of the upper Palaeocene (Selandian) lies disconformably on lower Maastrichtian and older rocks. Indeed, the Selandian oversteps all older strata and in many areas of Ellesmere Island lies unconformably on rocks of Cambrian to Devonian age (*see* summary in Harrison et al., 1999). For the report area we suggest that a disconformity between Maastrichtian and Selandian strata lies within the Expedition Formation, Upper Member.

The entire Upper Member on south-central Kanguk Peninsula has reverse polarity and an age of what Tarduno et al. (1997) interpreted as chron 26r (Selandian). It is more likely, however, that the Maastrichtian part of the Upper Member is chron 31r and that it is overlain disconformably by chron 26r strata, also Upper Member. Chron 31r ranges through the early Maastrichtian. Our inference is consistent with the age of early Maastrichtian palynomorphs in the section. Because no positive-polarity strata have been found in the bulk of the Upper Member, strata equivalent to positive polarity chrons 30n through 27n (upper Maastrichtian through Danian) probably either are eroded or were not deposited.

Strand Bay Formation

Definition: The Strand Bay Formation is a shale-dominated upper Palaeocene unit (of the medial Eureka Sound Group) erected for a type section on western Kanguk Peninsula 3 km east of Twin diapirs (Ricketts, 1991). The unit is 287 m thick at the type section but is 141 m on the west end of Kanguk Peninsula (Ricketts, 1991) and perhaps as little as 75 m in the eastern part of the report area. The isopach map points to a thickness range of 53 to 783 m (Fig. 44).

Composition: Rock types were described by Ricketts (1991) as grey shale, in part silty, with a fine blocky fracture. A resistant 30 m thick interval in mid-formation comprises four beds of planar- and trough-cross-stratified, fine- to medium-grained, well-sorted quartz-sandstone containing pebbly sandstone lags and fossil wood remains as much as 4 m thick. These beds on western Kanguk Peninsula are interbedded with thin coals (as much as 5 cm thick) and overlain by a 1 m thick coal seam. Ricketts (1991) correlated these marker strata from central to western Kanguk Peninsula. These beds also have a distinct air photographic expression, which we used to distinguish lower and upper members in the synclines north and south of Expedition Fiord and westward to Iceberg Bay. An important stratigraphic relationship is expressed in the syncline north and east of the Muskox diapirs. The upper and lower members of the Strand Bay Formation together with the sandstone marker are traceable around the northeastern and northwestern limbs of the syncline on both sides of Expedition Fiord. However, the upper informal member of the Strand Bay Formation cuts out the lower member in the southeastern hinge of the syncline. To the west the upper member cuts out underlying map units, including both members of the Expedition Formation, and lies directly on the Kanguk Formation within 800 m of the hanging wall evaporites of Muskox South diapir.

Depositional setting: Ricketts (1991) interpreted the shale of the Strand Bay Formation as prodeltaic in origin. The medial sheet sandstones between our two informal members are interpreted as either remnant barrier sands or shelf-bar sands supplied by driftwood. We suggest that the disconformity in the medial Strand Bay Formation is a consequence of local salt tectonics on the ancestral Muskox South diapir. Sand reworking is linked to subaerial exposure and erosion of the Expedition Formation previously deposited over long-lived salt diapirs. These diapirs were emergent in the medial Strand Bay prodelta setting and formed forested diapiric islands, which were rimmed by strand and barrier-island sand bars containing driftwood from the local forests.

Age: Strand Bay Formation contains foraminifera of the *Saccammina-Trochammina* assemblage (late Palaeocene to early Eocene; J.H. Wall *in* Ricketts, 1991), a middle and late Palaeocene terrestrial palynomorph assemblage, and an abundance of reworked palynomorphs derived from the Kanguk Formation (Turonian to

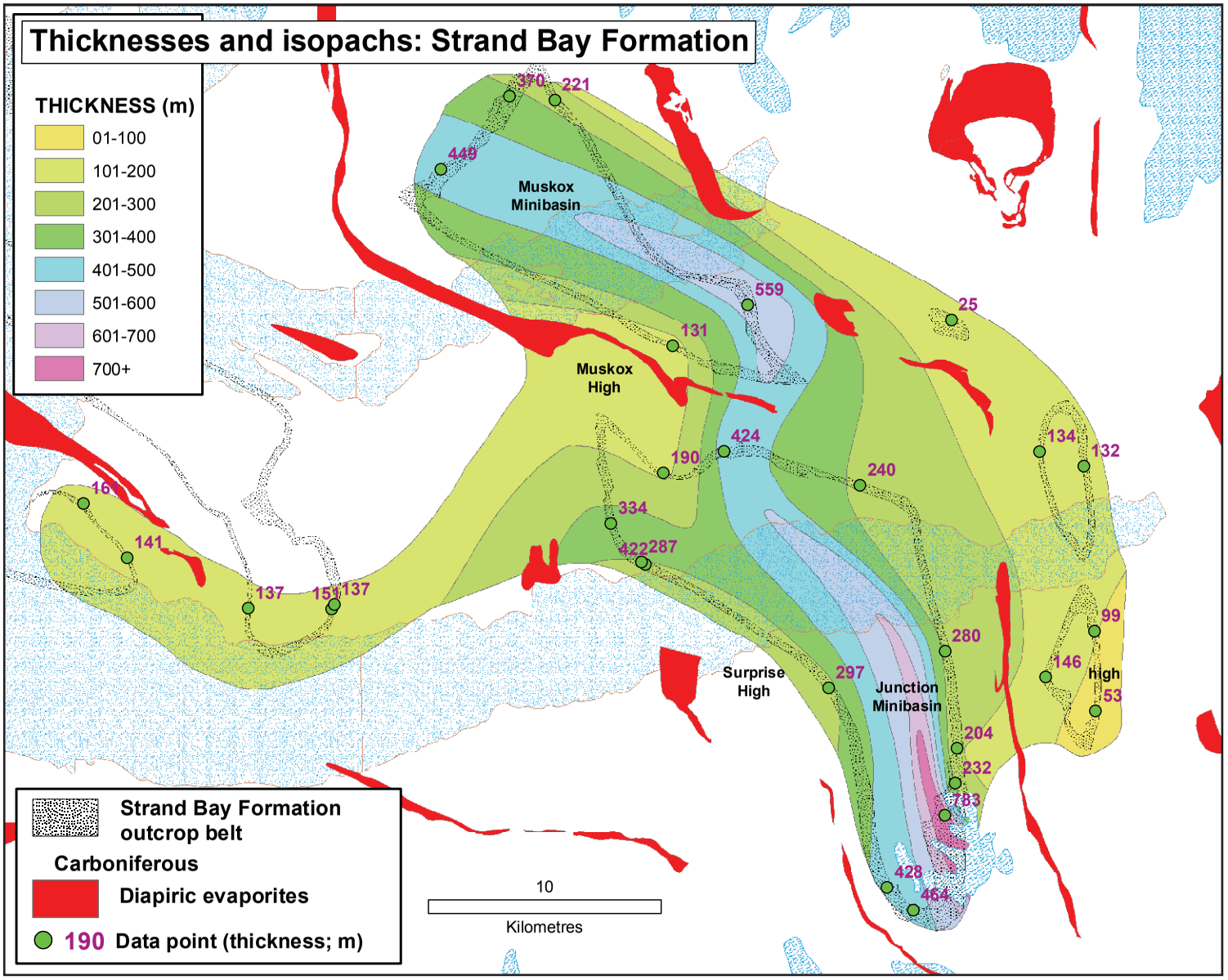

Figure 44. Isopachs and spot thicknesses for Strand Bay Formation. Thickness is 53 m ranging up to 783 m.

Santonian pollen) and the lower Maastrichtian part of the Expedition Formation (D.J. McIntyre *in* Ricketts, 1991). The entire formation has a reverse magnetic polarity that Tarduno et al. (1997) interpreted as chon 26r (Selandian).

Iceberg Bay Formation - Lower Member

Definition: The Lower Member of the Iceberg Bay Formation is mapped throughout the synclines of the report area from the head of Strand Fiord in the east to the tip of Kanguk Peninsula and the western shore of Agate Fiord in the west and northwest. Ricketts (1991) provided a full description and interpretation of the Iceberg Bay Formation and its members, which is summarized below.

Composition: The Lower Member is a unit of shale, sandstone (30–50%), and minor coal arranged in coarsening-upward cycles (as much as 1838 m in thickness within Junction minibasin). The lower contact with the Strand Bay Formation is conformable and gradational. The shales are medium to dark grey, fractured, and in part calcareous. The sandstones are planar and hummocky-cross-stratified and partly calcareous. They contain common plant debris fines and horizontal surface trace fossils. Cycles are 15 to 45 m thick in the lower part of the member and decrease to 5 to 15 m thick each in the upper part. Some cycles in the upper part of the member are capped by coal or shaly coal (Ricketts, 1991).

Depositional setting: The cycles in the Lower Member are interpreted to be part of a fluvial-dominated deltaic system in which individual cycles prograde upward from prodeltaic and lower shoreface to upper shoreface and foreshore. Thin coal seams are associated with crevasse splay sandstones and are perhaps part of a vegetated interdistributary bay-fill facies. The member as a whole is progradational, and a regional shallowing-upward trend is identified (Ricketts, 1991).

Age: Shale in the type section of the Lower Member contains a late Palaeocene palynomorph assemblage (D.J. McIntyre in Ricketts, 1991). The lower part of the member has reverse magnetic polarity, which Tarduno et al. (1997) interpreted as continuous from the Strand Bay Formation and, therefore, chron 26r (Selandian). The top 150 m has normal polarity and was interpreted as lying above the base of chron 26n (Tarduno et al., 1997) (early Thanetian and younger).

Iceberg Bay Formation - Coal Member

Composition: The Coal Member of the Iceberg Bay Formation is the highest preserved map unit below Quaternary cover in three synclines of central and western Kanguk Peninsula and in a fourth syncline that is also exposed on the north shore of Expedition Fiord. Maximum preserved thickness is 1060 m. According to Ricketts (1991), the Coal Member consists of variably indurated sandstone, coal, and grey shale in fining-upward cycles each 1 to 10 m thick. Sandstones are commonly capped by coal seams and interbedded lenses of nodular ironstone. Cycles near the base of the member have pebble lags. Mineralized wood fragments and fossil stumps, leaf impressions, basal lags of mud chips, and trough cross-stratification occur in sandstones throughout the member. Bioturbation is rare.

Depositional setting: Depositional facies of the Coal Member are interpreted as the product of a meandering fluvial system including distributary channels, overbanks, swamps, and floodplains. Brief marine incursions are inferred for some sandstone beds and for a coarsening-upward facies in some of the youngest beds. The ironstones are interpreted as paleosol horizons.

Age: The lower approximately 390 m of the Coal Member contains a palynomorph assemblage of late Palaeocene age similar to that found in the upper part of the Lower member (D.J. McIntyre *in* Ricketts, 1991). The following ~382 m of the Coal Member contains early Eocene (Ypresian) palynomorphs, and pollen from the highest 200 m have some middle Eocene (Lutetian- Bartonian) characteristics but are less diverse than the microflora of the fossil forest beds in the Buchanan Lake Formation on eastern Axel Heiberg Island (D.J. McIntyre *in* Ricketts, 1991). The magnetostratigraphic character of the Coal Member is complicated but appears to include chrons 26n through 23n (Tarduno et al., 1997) (Thanetian through mid-early Eocene).

Pleistocene and Holocene sediments

The geology map of the wall-and-basin region (published separately, Harrison and Jackson, 2011) does not attempt a full analysis of Pleistocene and Holocene sediments of the report area. The intention is to display these young sediments where the geological relationships between Paleogene and older rocks must be inferred through this

unconformable cover. The nine mapped units are mostly Holocene in age and consist of

1, 2: glacier-marginal deposits (lateral moraine and terminal push moraine) still being formed and modified by valley glaciers;

3: valley-bottom fluvial gravels, notably braid-plain deposits;

4: alluvial-fan deposits that commonly coalesce laterally and are building out into the major valley bottoms from the mouths of canyons and side streams; and

5: fan-delta deposits where fluvial gravels are prograding into existing lakes, bays, and fiords.

6-9. Somewhat older, but still presumably post-Pleistocene, units are raised delta deposits that form erosional remnants generally found on the margins of the still-active fan deltas. Raised deltas consist of a subhorizontal upper surface, or bench, bounded by steeply sloping, unconsolidated sediments. The bench upper surface is interpreted to be a former depositional surface near sea level built by fluvial deltaic deposits that prograded into an adjacent water body during a temporary marine highstand in postglacial times.

As many as four raised delta sequences are recognized on airphotos. These sequences are designated as units 'Qrd1' through 'Qrd4' on Geological Survey of Canada Map 2157A (Harrison and Jackson, 2011) with raised delta unit 'Qrd4' representing the highest and presumably oldest of these sequences.

Structure

Wall-and-basin region

The wall-and-basin region on west-central Axel Heiberg Island underlies a rhombic area approximately 72 km east-west by 54 km north-south (Fig. 2). Surrounding the wall-and-basin region area are long, subparallel fold trains and 26 sporadically exposed diapirs, which are mostly equant stocks (Fig. 2, 45). The large Paleogene (Eurekan) anticlines have a regular 20 km wavelength and unimodal trend north-northwest (Fig. 45). These Eurekan contractional folds probably detach on autochthonous Carboniferous Otto Fiord evaporites. The folds have sinusoidal or box-fold profiles; anticlines and synclines are equally wide. This combination of huge, parallel, linear buckle folds studded with salt stocks is common in salt-bearing foreland fold belts (as in the Zagros Ranges of Iran (Jahani et al., 2009).

In contrast to this outer region, the smaller wall-and-basin region has a distinctively different style unique on Axel Heiberg Island. Folds in the wall-and-basin region have an irregular wavelength of approximately 10 km, which is half that of the regional folds. The wall-and-basin trends are irregular but roughly bimodal north-northwest and west-northwest. Crooked walls of diapiric anhydrite crop out in cores of tight anticlines. Within the wall-and-basin region, 19 diapirs of various shapes are exposed, and another 12 diapirs are exposed on its margins. Wider synclinal minibasins separate the narrow diapiric walls and anticlines. The minibasins are found only within the wall-and-basin region. These 21 open minibasins, which contain mid-Cretaceous to Eocene strata, have circular, polygonal, kidney, oval, and arrowhead planforms.

Van Berkel et al. (1984) speculated that the bimodal trends of the diapirs were caused by either the rising of diapirs along two sets of vertical fractures or by the superposition of two buckling episodes. They also speculated that rising salt was trapped as a sheet below an igneous sill or competent sandstone. Their evidence of a salt sheet was solely the parallel style of buckle folds (van Berkel et al., 1984, p. 357). This logic is questionable, but our work supports the idea of a shallow detachment confined to the wall-and-basin region for other reasons (Fig. 46). We interpret exposed diapirs within the wall-and-basin region to detach on a shallow evaporite canopy formed by extrusive coalescence of allochthonous evaporite sheets that spread during the Early Cretaceous (Jackson and Harrison, 2006; Harrison and Jackson, 2008). We infer that the salt canopy was buried in the Cretaceous and Paleogene and acted as an allochthonous source layer for second-generation diapirs, now exhumed and exposed by the Paleogene Eurekan Orogeny. We envisage that all diapirs in the wall-and-basin region rose from the shallow canopy between minibasins subsiding into allochthonous salt. In contrast, diapirs along the margin of the wall-and-basin region and outside this area rose from autochthonous Carboniferous evaporites.

An alternative is that the allochthonous salt sheet formed an intrusive body of laccolith type. This interpretation is rejected because laccoliths are concordant along their basal contact whereas the salt sheet of the wall-and-basin region in many places forms a discordant basal surface. Additional evidence is that the wall-and-basin salt sheet was emergent at the surface, most notably in Awingak and Isachsen times.

All previous workers, such as Ricketts (1991), thought that the wall-and-basin diapirs rose entirely from a deep autochthonous level (Fig. 46a). Inferring a buried salt canopy is a radical reinterpretation of the wall-and-basin region (Fig. 46b). We make the case for this reinterpretation by reviewing evidence of the existence of a salt canopy and presenting criteria to define its limits.

Evidence of a canopy

Four features of the wall-and-basin region are unusual and support the existence of a salt canopy:

First, a halving of fold wavelength from 20 to 10 km points to a much shallower detachment in the wall-and-basin region than in the adjoining areas of the island. The thinner the overburden being buckled, the narrower is the fold wavelength (Ramsay and Huber, 1987). A Zagros analogue would be the narrow wavelength of folds detaching above the shallow Gachsaran evaporite, as compared with folds detaching on deeper décollements

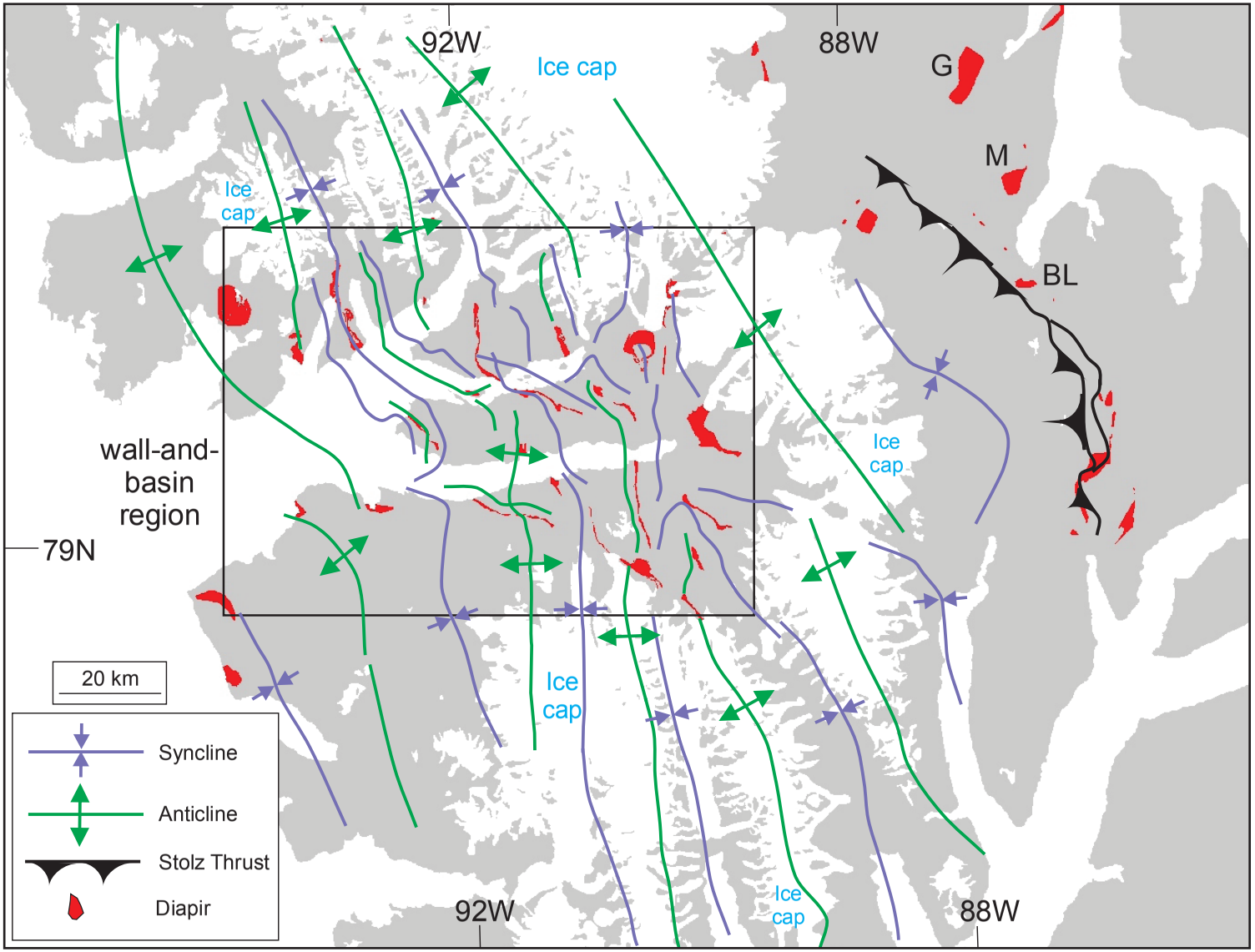

Figure 45. Simplified map of diapirs and folds and thrusts produced by the Eurekan Orogeny on west-central Axel Heiberg Island (after Thorsteinsson, 1971a, b, 1972a, b; Harrison and Jackson, 2008). Locations mentioned in the text beyond the wall-and-basin region include Buchanan Lake (BL), Gibs Fiord diapir (G), and Mokka Fiord diapir (M).

(Jahani et al., 2009). Increased Eurekan shortening would also decrease fold wavelength, but shortening magnitude inside and outside the wall-and-basin region appears too similar to account for the radically different wavelengths.

Second, the outcrop of anomalously young strata of Paleogene and Upper Cretaceous age is compatible with a regional depocentre that sank deep enough into a canopy to be preserved despite orogenic exhumation.

Third, unlike elongated linear synclines, the clustered equant minibasins are typical of subsidence over large salt canopies, such as those in the northern Gulf of Mexico (Diegel et al., 1995). Minibasins can also sink into autochthonous salt, as in the flanks of the Central Graben in the North Sea (Clausen et al., 2012), but their existence in the wall-and-basin area points to a relatively thin overburden, which is compatible with a shallowly buried canopy.

Fourth, and most important, the oldest roof strata exposed against a diapir provide valuable clues to its source layer. This technique, which was introduced by Jackson and Harrison (2006), exploits the tendency of allochthonous salt sheets to be flat-topped (Schultz-Ela and Jackson, 1996) and hence overlain by roof strata of uniform age. The age of emplacement of a salt canopy is inferred from the ages of strata immediately below and above the allochthonous evaporites (Fig. 47a). For diapirs outside the wall-and-basin region and thus beyond the inferred canopy, contact strata range from Carboniferous to Lower Cretaceous, with distinct peaks associated with the Heiberg Formation, Blaa Mountain Group, and the Isachsen Formation; other units are also present (Fig. 47b). For diapirs along the wall-and-basin boundary, contact strata range from Permian to Lower Cretaceous. A peak frequency coincides with the Heiberg Formation. In stark contrast, diapir contacts inside the wall-and-basin region are overwhelmingly against the Lower Cretaceous Isachsen Formation. This consistent diapir piercement level within the wall-and-basin region is 3 to 6 km above the autochthonous Otto Fiord evaporites. This uniform level of piercement suggests that the canopy acted as a stratiform allochthonous source layer that supplied evaporites to the diapirs exposed within the wall-and-basin region (Fig. 47).

The simplest interpretation of this stratigraphic uniformity for wall-and-basin diapirs is that allochthonous evaporites spread laterally and coalesced into a canopy during deposition of the Isachsen Formation. Whether the wall-and-basin area is underlain by a complete canopy or by several smaller ones can be reliably determined only from subsurface data that currently do not exist. However, the specific level of canopy emplacement can be deduced from the stratigraphic position of angular unconformities. If these diapir-centred angular unconformities are genetically linked to canopy emplacement, then emplacement was above the base of Paterson Island Member but below Rondon Member, approximately in Hauterivian time. Any mild shortening would have squeezed the diapirs and encouraged their extruded contents to coalesce as a canopy. Shortening could have been induced by uplift of the eastern Sverdrup Basin margin in the Hautervian, which is recorded by stratigraphic thinning and excision.

Inferred canopy limit

Although little of the canopy is revealed by exposure to be definitively allochthonous, canopy limits can be mapped by proxy features (Fig. 48). The first features to consider (but not delineated in Fig. 48) are the geometry and distribution of diapir sheets and walls. Some of these diapirs (Agate, Kanguk, Muskox Ridge, Surprise, and Bastion Ridge) appear to rise from a common source in the Lower Cretaceous level. However, other evaporite sheets have risen from stratigraphic levels as low as the Triassic (Good Friday, Junction, Lost Hammer, Hidden, and Expedition diapirs). Most of this variation could be explained by different positions within the wall-and-basin region (*see* following section Diapirs). The exposed geometry of diapirs is especially revealing along the south margin of the inferred canopy. Here north-trending regional Eurekan folds end abruptly in a crosscutting chain of diapirs: Junction, Good Friday East, Good Friday Central, Good Friday West, and Duck Bay. Curvature of folds against this sharp, west-northwest-trending boundary is compatible with sinistral strike-slip. This geometry does not by itself prove a salt canopy (the same feature could be controlled by shear along a crustal boundary). However, this cross trend refines the south boundary of a canopy suggested by other criteria outlined in the following paragraphs.

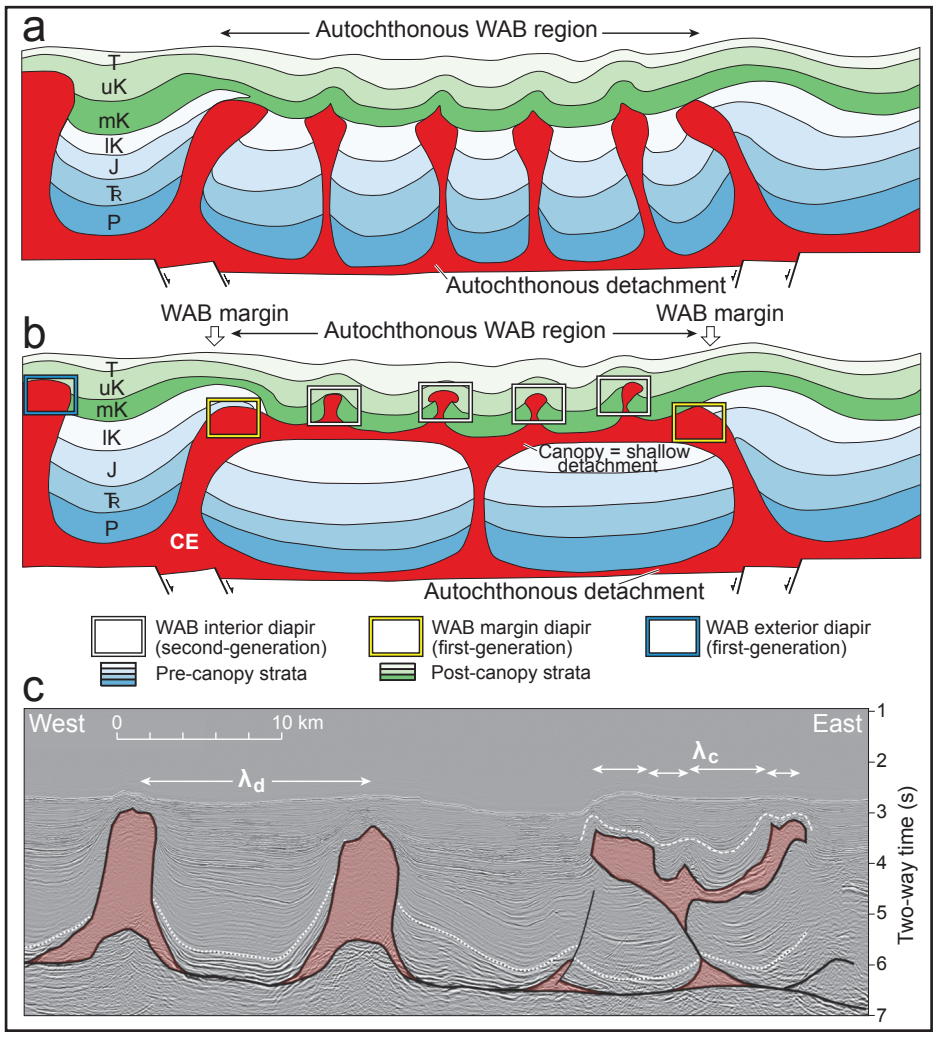

Figure 46. Conceptual sketches showing different ideas for the source of diapirs exposed in the wall-and-basin (WAB) region. a) Previous interpretation of diapirs sourced in autochthonous Carboniferous evaporites. b) New interpretation of diapirs sourced from a shallow allochthonous salt canopy and the distinction between diapirs rising from this canopy and diapirs at the margin of the canopy. Labels: CE: Carboniferous evaporites; P: Permian; TR: Triassic; J: Jurassic; lK: Lower Cretaceous; mK: mid-Cretaceous (Albian); uK: Upper Cretaceous; T: Tertiary (Paleocene, Eocene). c) Seismic example of the effects of a shallow detachment of allochthonous salt in reducing dominant fold wavelength (λd) (Espirito Santo Basin, offshore Brazil; after Rowan and Vendeville, 2006).

A second proxy to delineate the Axel Heiberg canopy is the limit of Albian to Eocene strata (Fig. 48). This anomalously young depocentre is a discrete entity surrounded by older strata and is unique in the western part of the island. The reasoning here is that young stratigraphic units would have subsided into the canopy, providing a local sink for accommodating these units and preserving them from erosion during Cenozoic uplift. As the depocentre sank, salt was expelled upward as supracanopy diapirs. For example, along the Muskox Ridge South diapir, second-order diapirs rose from culminations along the first-order wall during deposition and onlap of the Isachsen Formation (Valanginian to Aptian). One issue is that in the northwest and at several places in the south and southeast, Albian strata appear to extend beyond the central wall-and-basin region. In these areas, Albian preservation may simply result from synclinal folding or differential erosion.

A third means of delineating the canopy is the lateral extent of minibasins. The validity of this criterion is similar to that of the second criterion: the minibasins are likely to have originated by evaporite withdrawal from a thick cushion of shallow salt. Some minibasins may have begun subsiding before the canopy was emplaced. In particular, minibasin-like features are north and east of Expedition diapir, northeast of Glacier diapir, and on either side of Strand diapir. In all these areas, strata as old as Triassic record a long history of evaporite expulsion.

The fourth proxy to delineate the canopy limit is the extent of the Isachsen Formation directly overlying evaporites. This is the most common level of emplacement of diapiric salt in the wall-and-basin region and, as noted, is deemed to be the stratigraphic level of the canopy. Some uncertainty exists in the northwest and west as to the boundary between Isachsen strata and evaporites. South Fiord diapir is apparently surrounded by the Isachsen

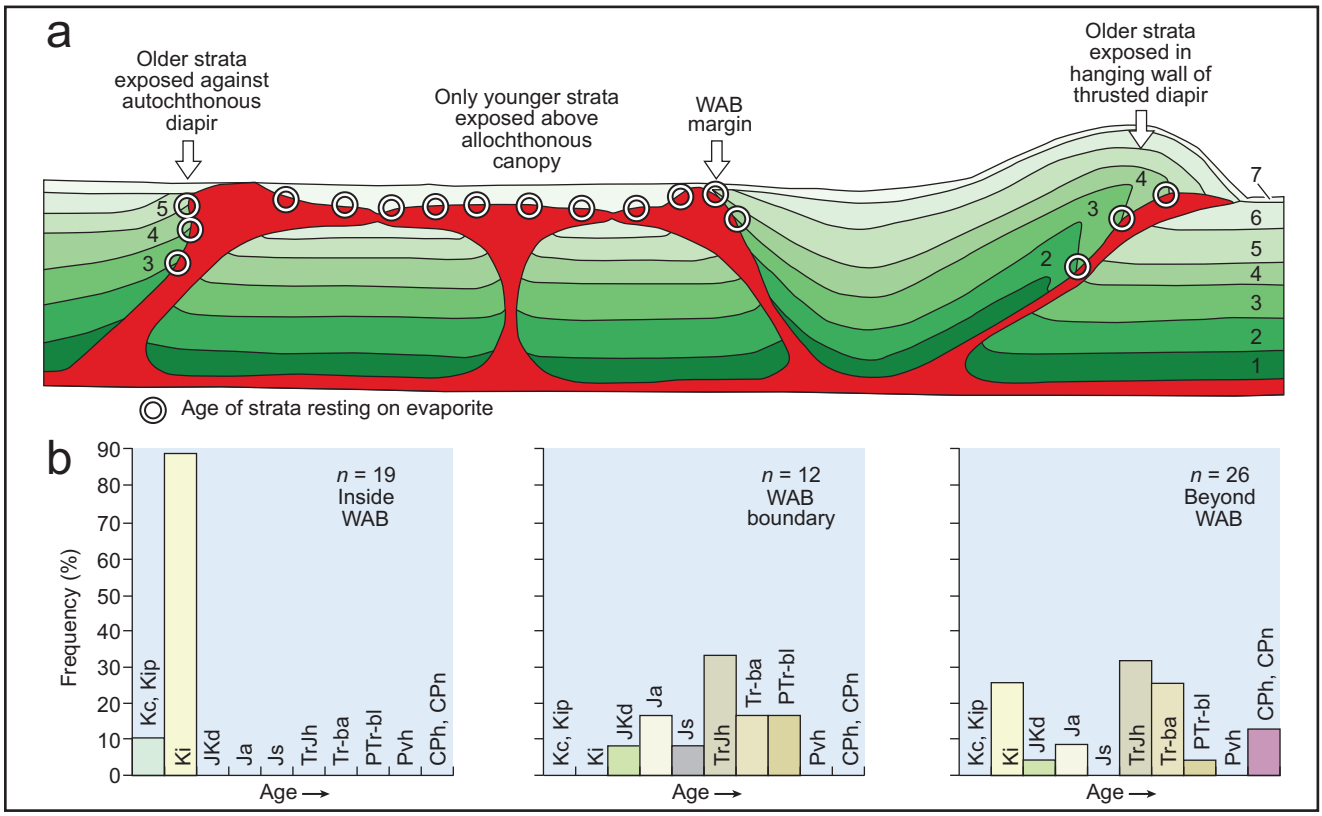

Figure 47. Distinction of autochthonous and allochthonous source layers. a) The principle: diapirs sourced by deep, autochthonous evaporites have contact strata widely varying in age; in contrast, diapirs sourced by shallow, allochthonous evaporites have consistently younger contact strata. b) The data: in contrast to other diapirs, diapirs within the wall-and-basin region are consistently overlain by the same relatively young unit, Isachsen Formation, indicating that this unit formed the roof of a Hauterivian shallow salt canopy. Age of strata resting on evaporites: Nansen Formation (CPn), Hare Fiord Formation (CPh), Van Hauen Formation (Pvh), Blind Fiord Formation (PTr-bl), Blaa Mountain Formation (Tr-ba), Heiberg Formation (TrJh), Savik beds (Js), Awingak Formation (Ja), Deer Bay Formation (JKd), Isachsen Formation (Ki), Christopher Formation and Invincible Point Member (Kc, Kip). WAB: wall-and-basin.

Formation (although it is masked by Quaternary deposits) but is excluded from the canopy region because it does not fit any other wall-and-basin criteria. In contrast, the Agate diapirs are inferred to be inside the canopy region because they are flanked by a major minibasin to the east.

The striking cluster of diapirs—and especially the presence of an inferred canopy—in the wall-and-basin region implies a source of locally thick evaporites in the axis of Sverdrup Basin. The salt depocentre is too deep to interpret meaningfully, but the irregular rhombic planform suggests to us that these thick evaporites might have accumulated in a Carboniferous pull-apart basin. This speculative basin would be bounded by sinistral wrench faulting on northerly striking strike-slip faults and pull-apart extension on west-northwest-striking normal faults. These two trends are especially strong in the wall-and-basin region and partly delineate its boundaries. Alternatively, the evaporite depocentre could be part of the east-west-trending belt of thick salt marked by diapirs, which runs through the axis of Sverdrup Basin.

Diapirs

All diapirs in the study area have similar lithology at the present level of erosion: anhydrite (superficially hydrated to gypsum), subordinate interbedded limestone, and sporadic mafic igneous inclusions. Schwerdtner and Osadetz (1983) envisaged that this anhydrite hood was underlain by a core of halite, as confirmed in the well in the Hoodoo diapir on south-central Ellef Ringnes Island

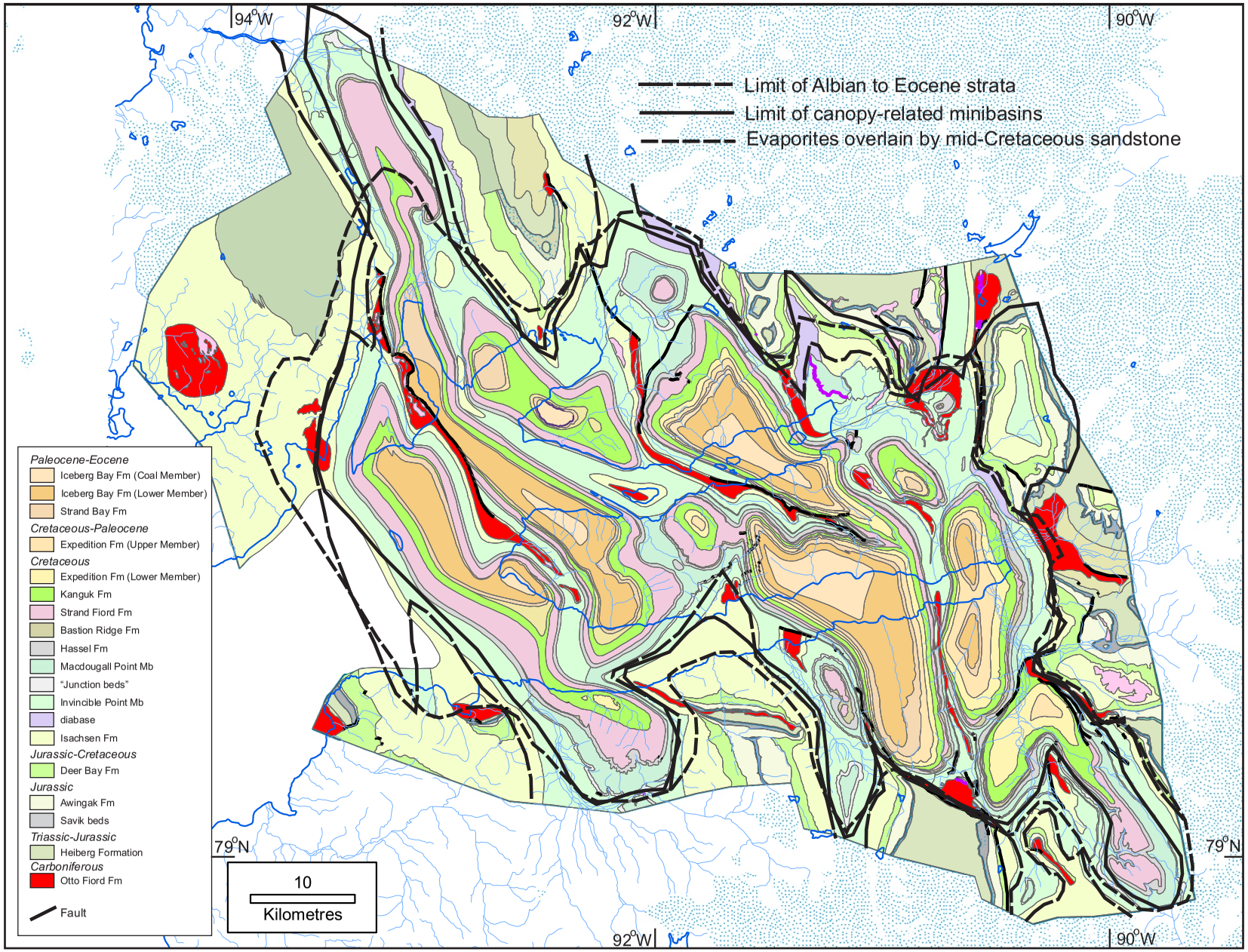

Figure 48. Three proxies to d elineate the limits of the inferred salt canopy in west-central Axel Heiberg Island. Each criterion delineates slightly different margins, but overall these are consistent. *See* Figure 2 for additional legend.

and in outcrop in Stolz diapir on Axel Heiberg Island (Hugon and Schwerdtner 1982). They envisaged that during diapirism, the normally dense anhydrite (>2900 kg/m^3) became a buoyant mush of anhydrite crystals and water released by conversion of the original gypsum to anhydrite. The anhydrite is today a compact rock composed of nodules, variably deformed into a foliated fabric with a distinct stretching lineation Strain analysis of the deformed nodules has yielded valuable information on the internal structure of diapirs and anticlines on Axel Heiberg Island (e.g. Schwerdtner and Clark, 1967; van Berkel, 1986).

Diapirs outside the wall-and-basin region

Diapirs beyond the wall-and-basin region are especially well represented on the east side of the island (Thorsteinsson, 1972a, b; Thorsteinsson and Trettin, 1972). They range in plan view from ovoid stocks to lenticular or teardrop-shaped walls, the latter being most common in the Stolz thrust zone. Oldest strata enclosing the diapirs range from the Hare Fiord to Van Hauen, Blaa Mountain, and Heiberg formations. Adjoining some diapirs are Quaternary deposits and the Paleogene Eureka Sound Group strata. Gibs Fiord and Mokka Fiord diapirs (Fig. 63), to name just two, rise several hundred metres above the surrounding plain, which is underlain by various Mesozoic and Paleogene strata (Fig. 1).

Also probably outside (but west of) the wall-and-basin region is South Fiord diapir. Like diapirs on eastern Axel Heiberg Island, this stock is roughly circular and has high relief of approximately 400 m. The diapir is emplaced at the mid-Cretaceous level, which is compatible with the wall-and-basin diapir family. However, its pluglike shape is notably different from a wall, and no minibasins flank it, which suggests that the stock is not linked to evacuation of evaporite at the canopy level.

Diapirs of the wall-and-basin boundary region

On or near the margin of the canopy are two types of diapir. The first kind is an asymmetric, thrusted diapir flanked by a hanging wall of Triassic to Lower Cretaceous strata and a footwall of mid-Cretaceous and post-canopy strata. Examples of such diapirs include Junction (Fig. 49), Glacier Fiord East, Glacier Fiord West, Hidden, Expedition, and, possibly, Duck Bay. We infer that each of these marginal diapirs is where a diapir sourced in autochthonous evaporites spread laterally at the stratigraphic level of the canopy. Also implied by several diapirs is that allochthonous evaporites continued to migrate upsection after canopy emplacement.

The second type of diapir along the canopy boundary is a wall or sheet in a tight antiform flanked by symmetrical limbs of precanopy Triassic to Cretaceous age, but along strike the same diapir is flanked by canopy-level strata. Examples include Good Friday East, Central, and West diapirs. These three diapirs appear to have originated as a single wall now segmented by salt welds. The eastern diapirs (Good Friday East and Good Friday Central) are flanked by Upper Triassic to Upper Jurassic strata.

Prominent next to the wall-and-basin boundary diapirs are angular unconformities at various stratigraphic levels. These diapirs are described sequentially counterclockwise from the southwest. On the margins of Duck Bay diapir, the Awingak Formation cuts out the Savik beds, and the Isachsen Formation cuts out the Deer Bay Formation (Fig. 50). Next to Good Friday West diapir, the Awingak Formation cuts out the Savik beds, and the Isachsen Formation cuts out all strata from the Heiberg to Deer Bay formations. At the opposite end of the anticline, beyond Good Friday East diapir, the Awingak Formation cuts out the Savik beds, the Deer Bay Formation cuts out the Awingak and Heiberg formations, and the Isachsen Formation cuts out the top of the Deer Bay Formation. The older units are relatively tightly folded through an east-plunging anticline that remains evident in the lower Isachsen Formation. Stacking of unconformities over the anticline indicates that folding—like diapirism—was long lived. Next to Glacier Fiord East and West diapirs, the Awingak Formation cuts out the Savik beds, the Deer Bay Formation cuts out the Awingak Formation, and the Isachsen Formation cuts out part of the Deer Bay Formation. On each side of Strand diapir, the Isachsen Formation cuts out all four units from the Heiberg to the Deer Bay formations. In the northeast, the Isachsen Formation on the east margin of Hidden diapir cuts out most of the Deer Bay Formation. All these angular unconformities record uplift and erosion centred on each actively

rising diapir. These unconformities extend for distances of as much as 2 km, which is probably too far to be purely halokinetic (Rowan et al., 2003; Giles and Rowan, 2012). Instead, these large unconformities probably record mild regional shortening in which diapiric roof strata were bulged up and flanking strata steepened.

Diapirs inside the wall-and-basin region

Diapirs within and between the minibasins are inferred to be sourced by the canopy and form part of the same allochthonous system. Two types of diapir are distinguished by their overall shapes. Circular or ovoid stocks include Index, Iceberg, Bastion Ridge Northwest, Wolf, and Twin diapirs. Exposed level of emplacement for all these diapirs is mid-Cretaceous (mostly the Isachsen Formation and, locally, the Christopher Formation).

The second type of diapir shape within the wall-and-basin region is sheets of evaporite pinched into walls and enclosed by strata that are steep, vertical, and even overturned. Along their length, the diapiric walls pinch and swell and are variably welded. Strata enclosing the walls range from mid-Cretaceous to Upper Cretaceous and Paleogene. Numerous examples include Bastion Ridge South, Bastion Ridge Central, Bastion Ridge North, Surprise South, Surprise Central, Muskox Ridge South (Fig. 30), Muskox Ridge North, Kanguk North, Agate Fiord South (Fig. 51), Agate Fiord North, and Colour diapirs.

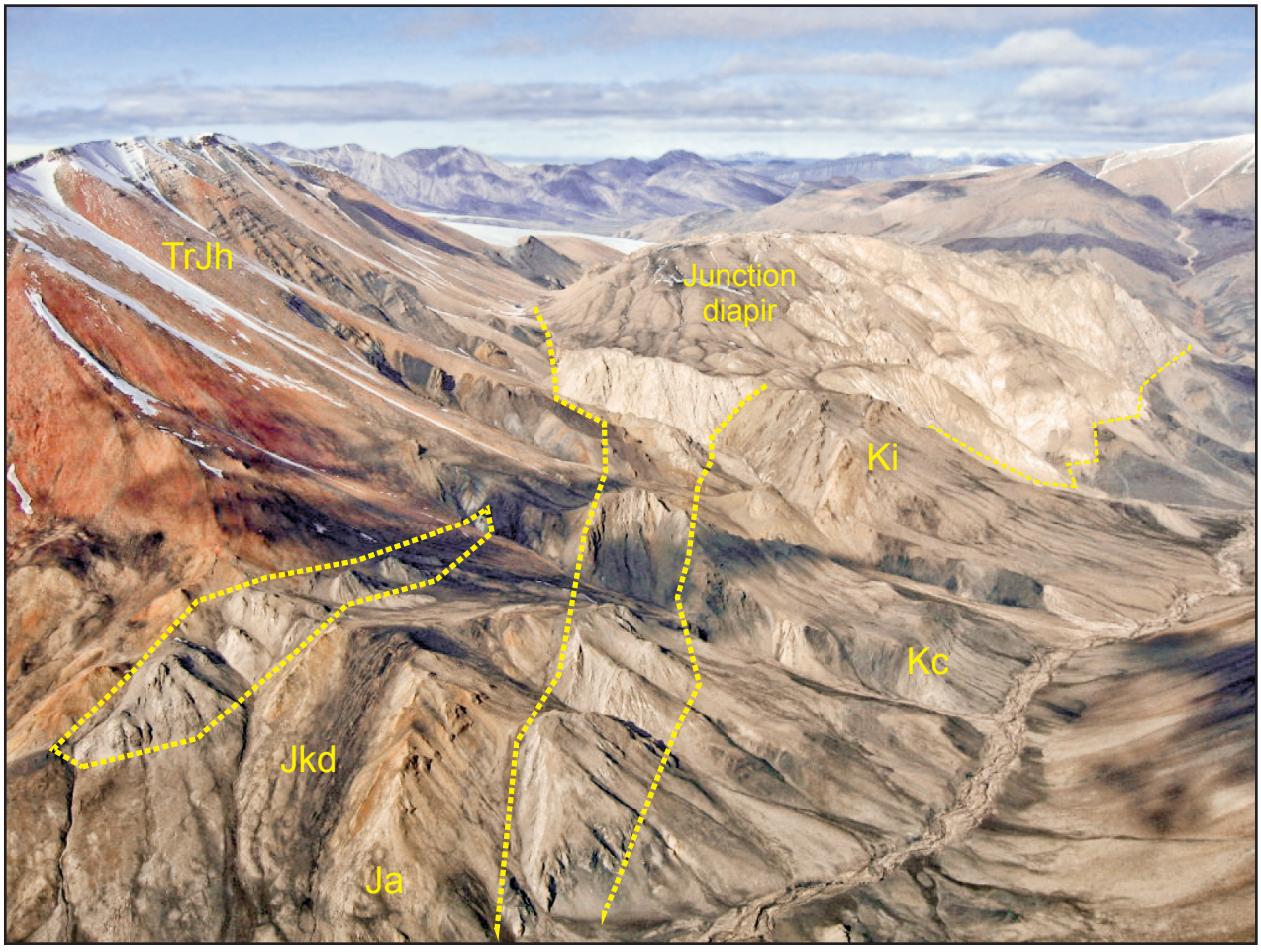

Figure 49. Junction diapir comprises a broad core of anhydrite-rich evaporites and a narrow margin of brecciated carbonates in anhydrite, all derived from the Carboniferous Otto Fiord Formation. The diapir is thrust over Isachsen Formation (Hauterivian to Aptian; Ki) along its northeast margin (at right). At left is downfaulted Heiberg Formation (TrJh). In the foreground are lenses of evaporite enclosed in Awingak Formation (Ja), Deer Bay Formation (JKd), and Christopher Formation (Kc). View is to the northwest.

Diapirs within the wall-and-basin region can also be classified by their structural relationships. Kanguk South diapir is a type example having a simple anticlinal roof. Other diapirs in this group are Bastion Ridge North, Bastion Ridge Northwest, East Fiord North, East Fiord South, Index, Kanguk North, and Twin. A second type of diapir has a faulted anticlinal roof, exemplified by Muskox Ridge South diapir. Other examples are Muskox Ridge North, Wolf, and Surprise Central diapirs. A third type of diapir has a welded stem, exemplified by Bastion Ridge South diapir. Similar diapirs include Bastion Ridge Central and Surprise South. The fourth type of diapir has a sagging, synclinal roof, such as Expedition (also a canopy-margin diapir), Surprise North, and Surprise Central diapirs.

Minibasins and diapir-related sedimentation

Introduction

Stratigraphy and sedimentation in the wall-and-basin region were analyzed by using 1) the existing suite of measured sections and 2) unit thicknesses calculated from bedding attitudes derived from georeferenced air photographs and satellite-derived DEMs. Results are presented as contour maps: one for each stratigraphic unit from the Heiberg Formation (Upper Triassic to Lower Jurassic) to the Strand Bay Formation (Thanetian to Lutetian). These maps illustrate the growth of minibasins and evaporite diapirs and the pattern of

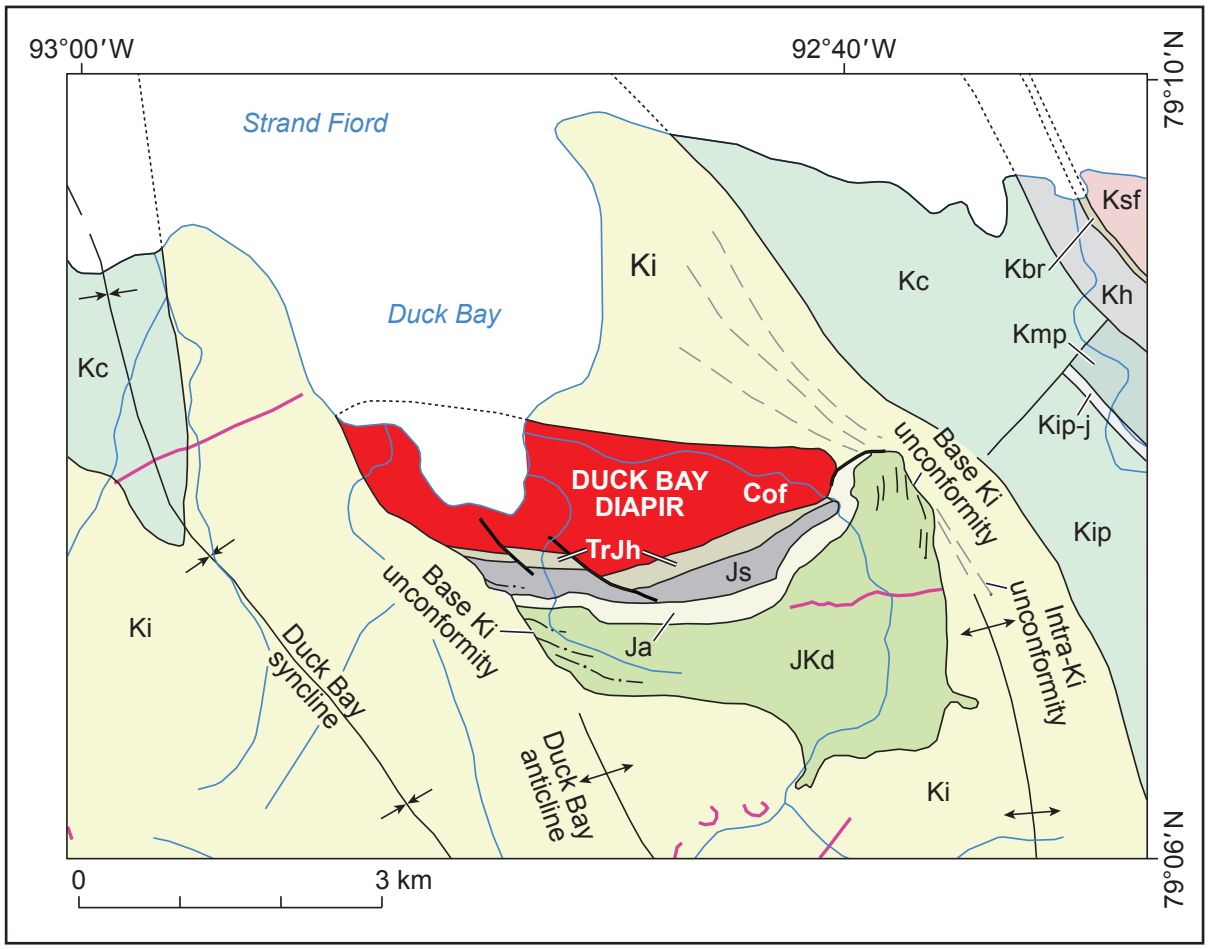

Figure 50. Unconformity low in Isachsen Formation near Duck Bay diapir. Unit labels: Cof: Otto Fiord Formation; TrJh: Heiberg Formation; Js: Savik beds; Ja: Awingak Formation; JKd: Deer Bay Formation; Ki: Isachsen Formation; Kc: Christopher Formation; Kip: Invincible Point Member; Kip-j: Junction beds; Kmp: Macdougall Point Member; Kh: Hassel Formation; Kbr: Bastion Ridge Formation; Ksf: Strand Fiord Formation.

Figure 51. Agate South diapir (AS) is thrust over the Lower member of Iceberg Bay Formation (Tib, lower right). Other units in view are Isachsen Formation (Ki), Cretaceous diabase (Kdi), and Strand Fiord Formation (Ksf). View is to the northeast toward Agate Fiord. (GSC Photo No. 2014-096)

canopy tectonics from approximately 216 to 59 Ma. Major features are summarized in Figure 52.

Classification

We divide minibasins in the wall-and-basin region into three types. The first type is the oldest. Within the wall-and-basin region, the earliest sedimentation and related diapiric structures originated in Triassic or Jurassic time and were subsiding before the canopy was emplaced. Some of these minibasins continued to subside during and after the canopy was emplaced. Included in the older minibasins are the Heiberg Formation, the Savik beds, and Awingak and Deer Bay formations. The interpretation placed on this evolution is that stratigraphic thickness variation may partly reflect lateral migration of autochthonous evaporites. Other explanations are possible, such as the lateral migration of clastic sediment sources, especially for deltaic units such as the Heiberg and Awingak formations.

Diapir-related sedimentation of the second type began or was rejuvenated in mid-Cretaceous time while the canopy was emplaced. This time interval is recorded by the Isachsen, Christopher, Hassel, and Bastion Ridge formations. The interpretation placed on this evolution is that units varied in thickness as a consequence of the lateral migration of evaporites within the canopy. As a result, accommodation space and sediment thickening increased above deflating parts of the canopy, whereas sediments thinned above inflating parts of the canopy.

Minibasins of the third type are initially associated with extrusion of flood basalts (Strand Fiord Formation) beginning in the Cenomanian. Shale and pyroclastic material were deposited during the rest of the Cretaceous, and fluvial-deltaic strata dominate the Palaeocene and Eocene.

Triassic and Jurassic diapirism and sedimentation

Thickness variations in the oldest map unit (Upper Triassic–Lower Jurassic Heiberg Formation; Fig. 15) are exposed next to diapirs located on what would eventually be the canopy margin. However, these thickness variations do not clearly delineate minibasins, partly because outcrops of strata this old are rare. Rather, isopach contours indicate marked thinning from 1250 m in Phantom depression southward to less than 500 m on the east flank of Hidden diapir. The Heiberg Formation thins by more than 50% westward toward Strand diapir, and a case can be made that respective thicknesses of 550 m and 213 m adjacent to Peeawahto and Duck Bay diapirs were reduced because of uplift near Triassic evaporite diapirs.

Significant thickness variations of the Savik beds (Toarcian to late Oxfordian) trend northwesterly and affect all of the diapirs of the (future) canopy margin (Fig. 17). Noteworthy are minibasins and depressions east and northwest of Strand diapir and north of Expedition and Colour diapirs. The largest thickness variation is between Duck Bay diapir (270 m) and Peeawahto diapir (819 m). In the north is White Peak depression, which trends westerly and is limited to the southwest by Colour diapir and to the southeast by Expedition diapir.

The northeasterly isopach trend is especially true for the Good Friday minibasin between Good Friday East and Good Friday Central diapirs. Bounding highs on this minibasin coincide with Junction diapir to the southeast and with Good Friday West diapir to the northwest. Clearly evident for the first time is the northwest-trending Glacier minibasin on the flank of Lost Hammer diapir. A longer-lived structure in this time slice is Strand diapir, which is bound by local depocentres both to the north (Monkhead minibasin) and to the south (Strand Pass minibasin). In the north, White Peak depression remains active between and north of Colour and Expedition diapirs. This depression is not proven to be a minibasin because the associated isopachs are undefined at the lateral limit of mapping.

Features first mapped in the Toarcian to Kimmeridgian intervals (Savik beds and Awingak Formation) continue to be represented on the isopach map of the Deer Bay Formation (late Kimmeridgian to middle Valanginian). Notable are 1) White Peak depression north of Colour and Expedition diapirs, 2) Monkhead and Strand Pass minibasins north and south of Strand diapir, 3) Glacier minibasin north of Lost Hammer diapir, and 4) Good Friday minibasin mostly south of Good Friday Central diapir.

Early Cretaceous and younger minibasins

Because the isopach interval represented by late Valanginian to late Aptian strata (Isachsen Formation) is the lowest above the evaporite canopy, it is commonly in contact with allochthonous evaporites (Fig. 26). As described previously

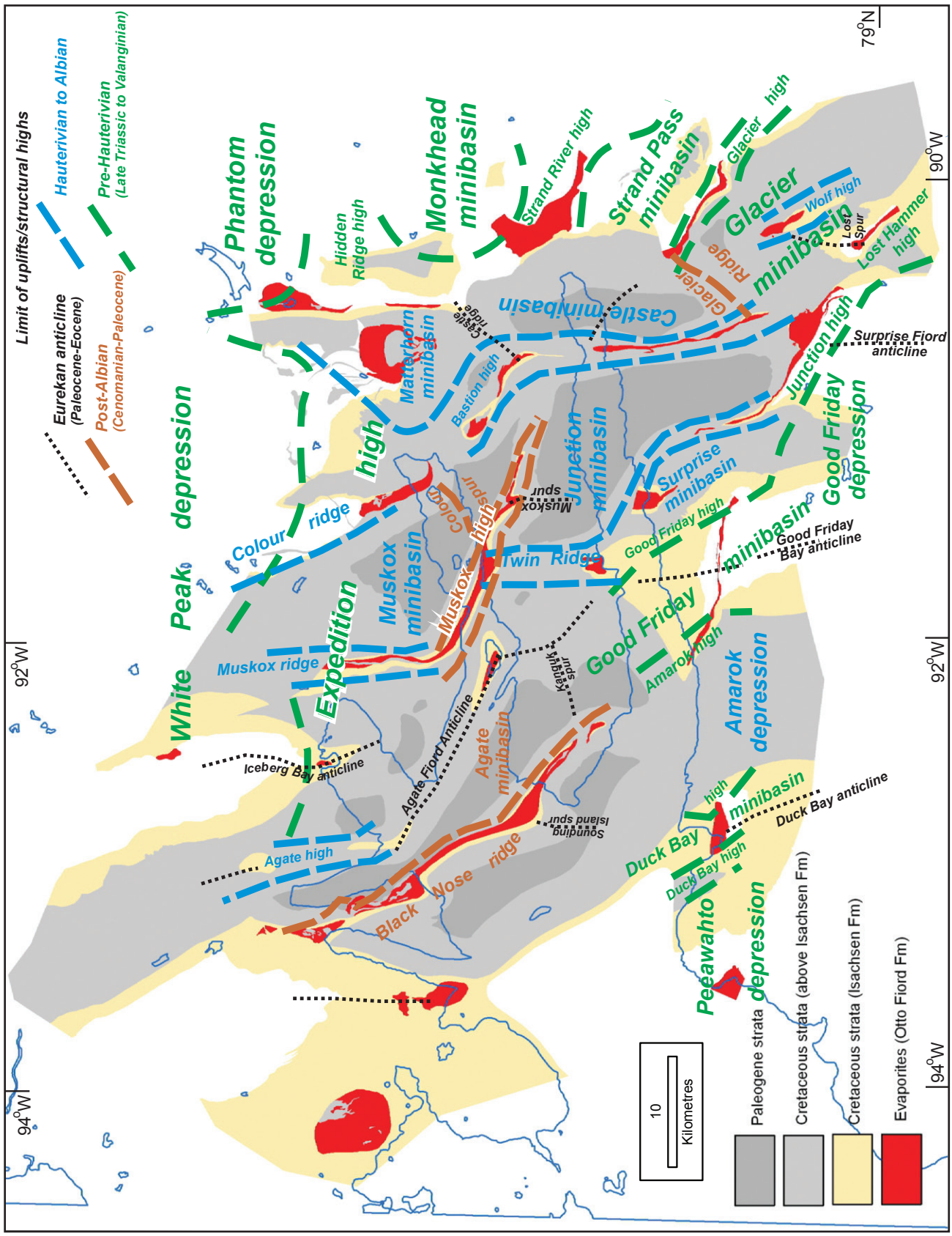

Figure 52. Summary of minibasins and structural highs of the wall-and-basin region organized by age range.

in this account, the Isachsen Formation carries convincing evidence of syndepositional diapirism and erosional unroofing of evaporites. For this reason, some, perhaps most, sections of the Isachsen Formation adjacent to evaporites were deposited directly on the evaporites.

Many of the minibasins and depressions evident on the Triassic and Jurassic isopach maps continue to evolve during late Valanginian to late Aptian time. Good Friday depression is still present, but the depocentre has migrated to the west. Glacier minibasin is still present north of Lost Hammer diapir, but it is now apparently linked in the north to Strand Pass minibasin. Monkhead minibasin has apparently migrated to the west. Behind it is a high where the Isachsen Formation has a local minimum of 92 m. Other highs newly featured on this time slice are Colour Ridge, which runs from Colour diapir to the east end of Muskox Ridge South diapir, and Twin Ridge, which lies between Twin diapirs and a more westerly portion of Muskox Ridge South diapir. Overall, this time slice presents a mix of both westerly and northerly trending isopachs.

Isopach maps are available for both the Invincible Point Member and overlying Macdougall Point Member. However, data are insufficient to discuss Macdougall Point Member in isolation. Instead, we examine the combined isopachs for these two units, which together represent the Christopher Formation (Fig. 33). The dominant features in this time slice include Glacier minibasin and Amarok depression in the southwest, where in both places the Christopher Formation is more than 2100 m thick. Another thickness maximum is along the southern edge of Expedition diapir, where the Christopher Formation exceeds 1600 m. At the other extreme is Strand Fiord high, linked in the north to Colour Ridge, where the preserved thickness of the Christopher Formation is apparently only a few hundred metres. Similar thinning of this formation is indicated on Bastion high (east of Bastion Ridge diapirs), where the preserved Christopher Formation is as little as 343 m thick.

Features on the time-slice map for the late Albian Hassel Formation are relatively subtle (Fig. 35). Named local depocentres with maximum measured thicknesses include Surprise minibasin (510 m), Junction minibasin (413 m), and Glacier minibasin (330 m). Depositional minima occur along Bastion high (126 m) and Twin ridge (134 m), which persisted from late Valanginian to late Albian time.

Trends are unclear on the higher unit of the late Albian Bastion Ridge Formation. The range in measured thickness is from 31 m or less to more than 230 m. All thickness estimates of the Bastion Ridge Formation are approximate, however, because contacts are covered by talus and this interval is commonly invaded by diabase sills.

Late Cretaceous and younger minibasins

The oldest unit in the Upper Cretaceous to Eocene interval is represented by the Strand Fiord Formation (Cenomanian to Turonian). Thickness (up to 701 m) varies greatly. In general, the Strand Fiord Formation is relatively thin throughout the wall-and-basin region (54–272 m) and uniformly thick beyond the wall-and-basin region in the west (Fig. 38). Named syndepositional highs, which trend to the north and include Strand Fiord high and Surprise high, appear to be genetically linked to Bastion Ridge South and Central diapirs and to Surprise South and Central diapirs. Another syndepositional high (Bastion high) is associated with Muskox Ridge North diapir.

On the next three time slices (Turonian to Campanian, Fig. 40; Campanian to early Maastrichtian, Fig. 42; and Selandian, Fig. 43), only throughgoing trends are mentioned here. These include one or more highs on the north side of Muskox Ridge South diapir (Muskox high), a persistent depocentre between Junction and Glacier diapirs (Glacier minibasin), and another depocentre bound by the Surprise diapirs in the south and by Bastion Ridge Central diapir in the east (Junction minibasin). Less clear are the trend and extent of Muskox minibasin, which is not fully resolved until Strand Bay Formation time (Selandian; Fig. 44). Another trend worth noting is the westward disappearance of the Expedition Formation on these maps. The absence of the the Expedition Formation needs to be confirmed but, if proven correct, could indicate that the Palaeocene Strand Bay Formation may lie directly on the Kanguk Formation, for example, east of Agate South and Agate North diapirs.

Structure sections

Three east-west structure sections (Fig. 53) cross the structural grain of the wall-and-basin region: Section A from South diapir to Monkhead Mountain syncline behind Hidden diapir, Section B from Good

Friday diapir to Strand diapir, and Section C from Black Nose syncline to Glacier Fiord East diapir. Although shallow structure is tightly constrained by excellent exposures, geology beneath the canopy is highly speculative without subsurface data. Thus, rather than commit to a single, potentially erroneous interpretation of deep structure, we illustrate different working hypotheses on each of the three cross sections. This range of possibilities is presented as factual in the descriptions but is largely conjectural.

Section A

This section provides the widest view of canopy structure underlying mid-Cretaceous sandstone between Triangle Peninsula syncline in the west to Castle Mountain syncline in the east. The section depicts deformation during rifting and inversion as diffuse rather than concentrated in discrete structures. Faults are illustrated arising from basement but are not considered a significant part of the evolving basin history. Likewise, local variations in subcanopy unit thickness, especially evident in the Heiberg Formation, are considered likely but speculative in detail. The presalt basement is deeper below the canopy, where thick Otto Fiord evaporites sourced the Axel Heiberg salt canopy. Deep anticlines are pierced by autochthonous diapirs and deep synclines generally underlie supracanopy synforms, such as Black Nose, Index Peninsula, and Erratics Island synclines. Other shallow synclines overlie diapirs rooted at the autochthonous (Carboniferous) level, such as below Agate Fiord syncline. Like similar minibasins in the northern Gulf of Mexico (Pilcher et al., 2011), underlying evaporites were most likely displaced laterally into the canopy and into second-generation diapirs rising from the canopy. An analogous picture is evident under Bastion Ridge syncline, where an underlying diapiric feeder of the canopy is depicted as out of the plane of section. Farther east, a sheet of evaporite emplaced unusually high in the Christopher Formation is part of Expedition diapir. Along the canopy margin, this diapir is most likely rooted to an autochthonous source north of the line of section. Other autochthonous diapirs near the wall-and-basin margin in Section A include South Fiord, East Fiord South, and Hidden diapirs. The latter two diapirs along the margin accommodate massive subsidence of the wall-and-basin fill. Kinematically they are similar to salt rollers formed by asymmetric extension.

Section B

Section B differs from Section A by emphasizing large, rift-age half grabens that could provide major relief in the basement. This deformation style fits with the present understanding of the origins of the Sverdrup Basin when Carboniferous evaporites accumulated during rifting. The hypothesis featured in Section B proposes that the faults remained active from the Permian to the Jurassic as salt was driven upsection in autochthonous diapirs. Nevertheless, this interpretation of subcanopy structure is highly speculative.

The section also depicts westward progradation during the Permian to Jurassic, which created expulsion rollovers. Shortening is suggested by 1) narrowing of diapirs or canopy feeders sourced in autochthonous evaporites, 2) steepening of diapir flanks below the canopy, and 3) tightening of synclinal minibasins above the canopy. In this tapering corner of the wall-and-basin region, the canopy is limited to diapirs between Surprise North diapir in the west and Bastion Ridge South diapir in the east. Diapirs at either end of the section, including Good Friday West and Strand, are sourced in the autochthonous level. Nevertheless, both of these outer diapirs are flanked by thinned stratigraphic units of Triassic to Early Cretaceous age. The two canopy-rooted diapirs are associated with marked thinning of mid-Cretaceous sandstone (Isachsen Formation) and two major synclines on either side of Bastion Ridge South diapir. These two synclinal minibasins subsided into the canopy from the mid-Cretaceous onward until the canopy welded below the minibasins. Diapirs at either end of the section, including Good Friday West and Strand, are sourced in the autochthonous level but are flanked by thinned stratigraphic units of Triassic to Early Cretaceous age.

Section C

Section C differs from the other two sections by showing rifted basement strongly inverted by later shortening. Inversion was concentrated as a major thrust zone offsetting the basement. This zone marks the crustal boundary of the wall-and-basin region, which may coincide with the margin

of the inferred Carboniferous pull-apart graben. The profile crosses the southern tip of the wall-and-basin region. It crosses two regional anticlines west of the wall-and-basin region and three named diapirs to the east. Outside the wall-and-basin region, Good Friday Bay and Surprise Fiord regional anticlines are drawn as simple thrust anticlines detached on autochthonous evaporites. The underlying thrust ramp and flat place Carboniferous evaporite over Middle Triassic strata. Farther east are Junction and Wolf diapirs. Junction diapir, on the canopy margin, is rooted at both the autochthonous level under the limb of Surprise Fiord anticline and at the canopy level below mid-Cretaceous sandstone. Westward-vergent parasitic thrust anticlines have formed in the overthrusted mid-Cretaceous section, presumably detached on shallow evaporites.

At the eastern end of the profile, Wolf diapir is probably sourced by the canopy because it is enclosed by the Isachsen Formation. In contrast, Glacier Fiord East diapir is unusual for being enclosed by Upper Jurassic strata. To explain this anomaly, the diapir is shown decoupled from its autochthonous root by a thrust weld.

Key diapirs in the wall-and-basin region

The structure of the wall-and-basin region is exemplified by six diverse and well-exposed diapirs. Each lies on one of our regional cross-sections, illustrating their structural context. Three diapirs are on the edge of the wall-and-basin region (Good Friday West, Junction, and Expedition), and three are inside the wall-and-basin region (Wolf, Muskox Ridge South, and Surprise North) (Fig. 2).

Good Friday West diapir

This diapir is a squeezed wall along the south edge of the wall-and-basin region (Fig. 54a). The diapir forms the core of a tight anticline (Fig. 54b, c) that abruptly crosses two north-trending regional Eurekan folds (Good Friday anticline and Black Nose syncline). Strata exposed against the diapir are as old as Triassic and Jurassic. The diapir is therefore rooted below the canopy in autochthonous salt. On the basis of criteria in Figure 48, we infer the canopy margin to be a few kilometres northeast of the diapir (Fig. 54b. However, this marginal position does not exclude the possibility that allochthonous salt might have extruded at a higher level across the Isachsen unconformity (now eroded off, Fig. 54b). Contacts of this and other diapirs in the wall-and-basin region indicate a strong probability that any such extrusion was in Hauterivian time. This allochthonous extrusion would have been aided by regional tectonic compression, which squeezed the diapir.

Good Friday West diapir is notable for its prominent angular unconformities resulting from arching, erosion, and excision of strata around the actively rising diapiric wall (Fig. 54).

Junction diapir

Junction diapir lies at the junction of three anticlines and three intervening minibasins. To the southeast, the diapir tapers into Jurassic and Lower Cretaceous strata containing slivers of diapiric anhydrite interleaved by thrusting (Fig. 34 and 55a). In this same area, debris flows were shed from the diapir in the Late Jurassic (Fig. 19 and 20). To the northwest, the tapered wall merges with Surprise South diapir. Junction diapir is bounded on the southwest side by uplifted Heiberg strata outside the wall-and-basin region (Fig. 55b). The middle of the diapir bulges strongly toward Glacier Fiord syncline in the northeast. The basal contact of this diapiric bulge climbs allochthonously in the same direction across overturned, imbricated strata of the Lower Cretaceous Isachsen and Christopher formations (Fig. 51 and 55a). The large difference in stratigraphic position of flanking strata in the southwest (Upper Triassic) and northeast (Lower Cretaceous) could be explained by a deep upthrust (Fig. 55b). This deep upthrust coincides with the margin of the inferred Carboniferous half graben, which controlled the location of the canopy and, hence, the wall-and-basin region.

Expedition diapir

Expedition diapir has the whimsical distinction of being the world's only known example of a salt glacier partly overridden by an ice glacier (Thompson Glacier). This diapir near the northeast margin of the wall-and-basin region is also notable for other reasons, despite having been partly obscured by gravels of Expedition River (Fig. 56a).

First, the diapir is adjoined to the north by a deep Jurassic minibasin, which is well exposed in

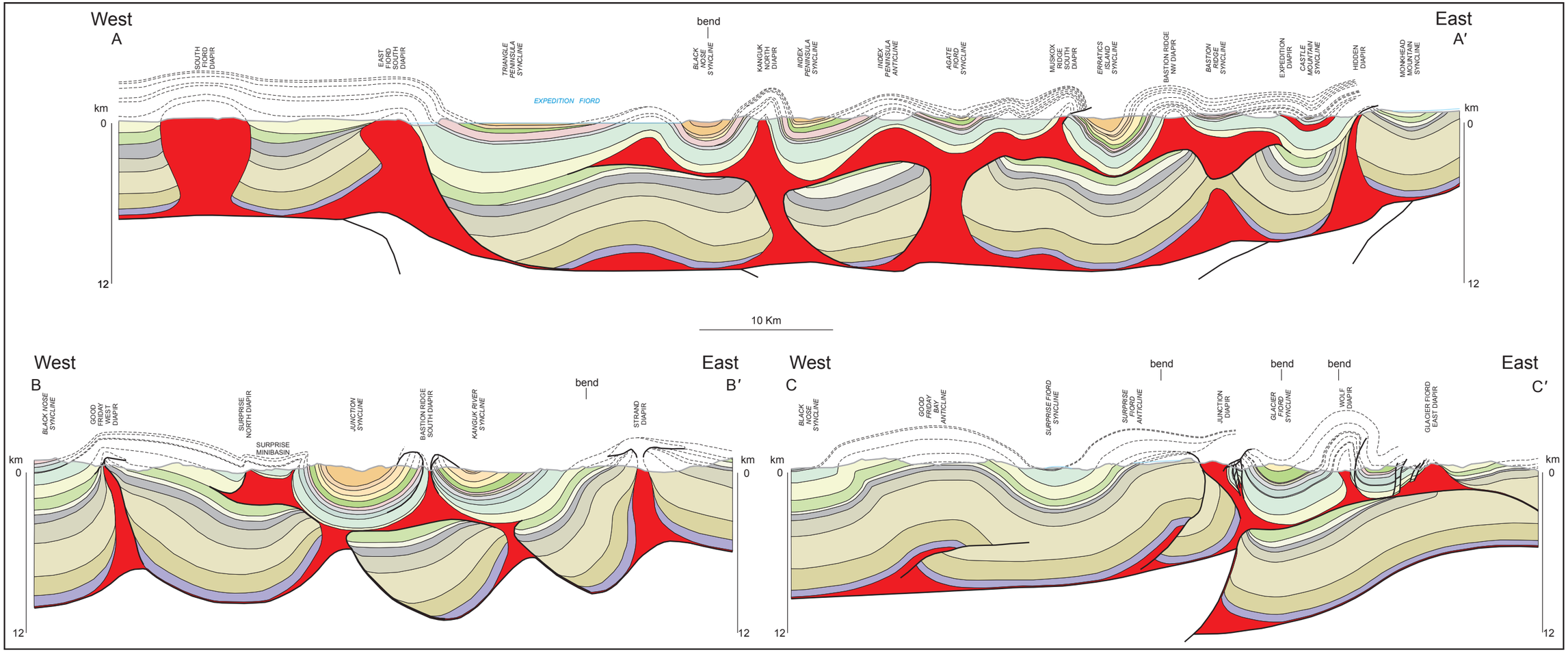

Figure 53. Three regional cross-sections across the wall-and-basin region and its nearby surroundings. Cross-sections are projected to depth from outcrop. Each illustrates different possible interpretations for the deep structure, which is poorly constrained. For location and stratigraphic key, *see* Figure 2.

oblique section (Fig. 56a). The minibasin is filled by the Savik beds and Awingak and Deer Bay formations. These strata thin toward the north margin of Expedition diapir, and some are truncated along unconformities that intensify toward the diapir. The minibasin records Jurassic expulsion of salt below it into the growing Expedition diapir.

Second, the diapir's contacts with the Christopher Formation indicate that the diapir was emplaced at a higher stratigraphic level (Fig. 56b) than other allochthonous salt sheets in the wall-and-basin region, which are typically enclosed by strata within or below the Isachsen Formation. Although the basal contacts of Expedition diapir are extremely well exposed in places (Fig. 56c), whether the evaporites have flowed over or have been thrust over their country rock is unclear. This ambiguity applies equally to allochthonous sheets in the Gulf of Mexico (Hudec and Jackson, 2009). Assuming that the thrusted wall of Hidden diapir, which is 2 km to the east, is a good proxy for the orientation of Eurekan shortening, Expedition diapir was probably shortened by west-directed compression. But this Paleogene compression acting on the underlying stem of the diapir would have caused allochthonous extrusion in all directions, as well as thrusting toward the east and west.

Third, Expedition diapir is unusual in occupying a major syncline. Downfolding in the Castle Mountain syncline has preserved an outlier of the diapir's roof.

Wolf diapir

This diapir in the southern part of the wall-and-basin region is a classic example of an active diapir overlain by an arched roof (Fig. 57a, b). The south end of this elliptical diapir is draped by an arched roof of Isachsen sandstone (Fig. 57c). At the north end of Wolf diapir, the roof has been erosionally breached to expose the anhydrite core of an unnamed anticline. This north-northeast-trending anticline of Eurekan age, cored by Wolf diapir, had a complex history. Minibasins record shifting patterns of halokinetic salt expulsion as various neighbouring diapirs competed for salt. The anticline then buckled upward during Eurekan shortening, which began in the Palaeocene. The formerly synclinal minibasins were forced to invert into an anticline, probably because a regional anticline to the south propagated northward into the wall-and-basin region (Fig. 45). Wolf diapir, on the trend of the regional anticline, also focused upward buckling because of its weakness.

The same Eurekan northward propagation refolded Glacier Bay syncline across its path, creating a crescentic interference pattern. Glacier Bay syncline had a multistage history as a minibasin but greatly deepened as an area of salt expulsion in Late Cretaceous to Palaeocene times (Expedition Formation).

Muskox Ridge South diapir

This diapir is part of one of the longest walls inside the wall-and-basin area, having a length of more than 30 km, including its unexposed part below Expedition Fiord. The diapiric wall acted as a detachment for crossfolding in the form of two lift-off anticlines, which plunge to the southwest (Fig. 58a). These anticlines form local swellings in the wall. The northern swelling is the core of Gap Ridge anticline. The narrower southern swelling is an unnamed anticline, which indents Junction syncline to the south. Anhydrite boulders shed from the diapir into the overlying basal Isachsen strata (Fig. 31 indicate that Muskox Ridge South diapir already formed a local ridge in Valanginian to late Aptian time. Moreover, onlap of Isachsen roof strata against the flanks of the Gap Ridge anticlinal swelling indicates that this swelling was also initiated by late Aptian time. Muskox Ridge South diapir was growing vigorously in Albian time, as evidenced by the isopachs of an enclosing minibasin (Fig. 33. Thereafter, isopach maps indicate a persistent Muskox high along the length of Muskox Ridge South diapir from Turonian to Selandian time (Fig. 40, 42, 43).

By Selandian (mid-Palaeocene) time, the Eureka Orogeny had begun. Muskox Ridge South diapir, along with its cover, was thrust northeastward over the Erratics Island syncline (Fig. 58a, b, c). Two lines of evidence suggest that during the same orogeny, the smaller of the two diapiric crossfolds tightened by regional compression. First, as noted by van Berkel (1986), the anticlinal crossfold arches a several-kilometre thickness of roof strata to Palaeocene levels, which is too thick for mere halokinesis to deform. Second, strain analysis of anhydrite nodules here by van Berkel (1986) indicates flattening parallel to the axial surface and extension parallel to the fold axis. He concluded that two sets of oblate fabrics formed: the first striking west-northwest parallel to the length of

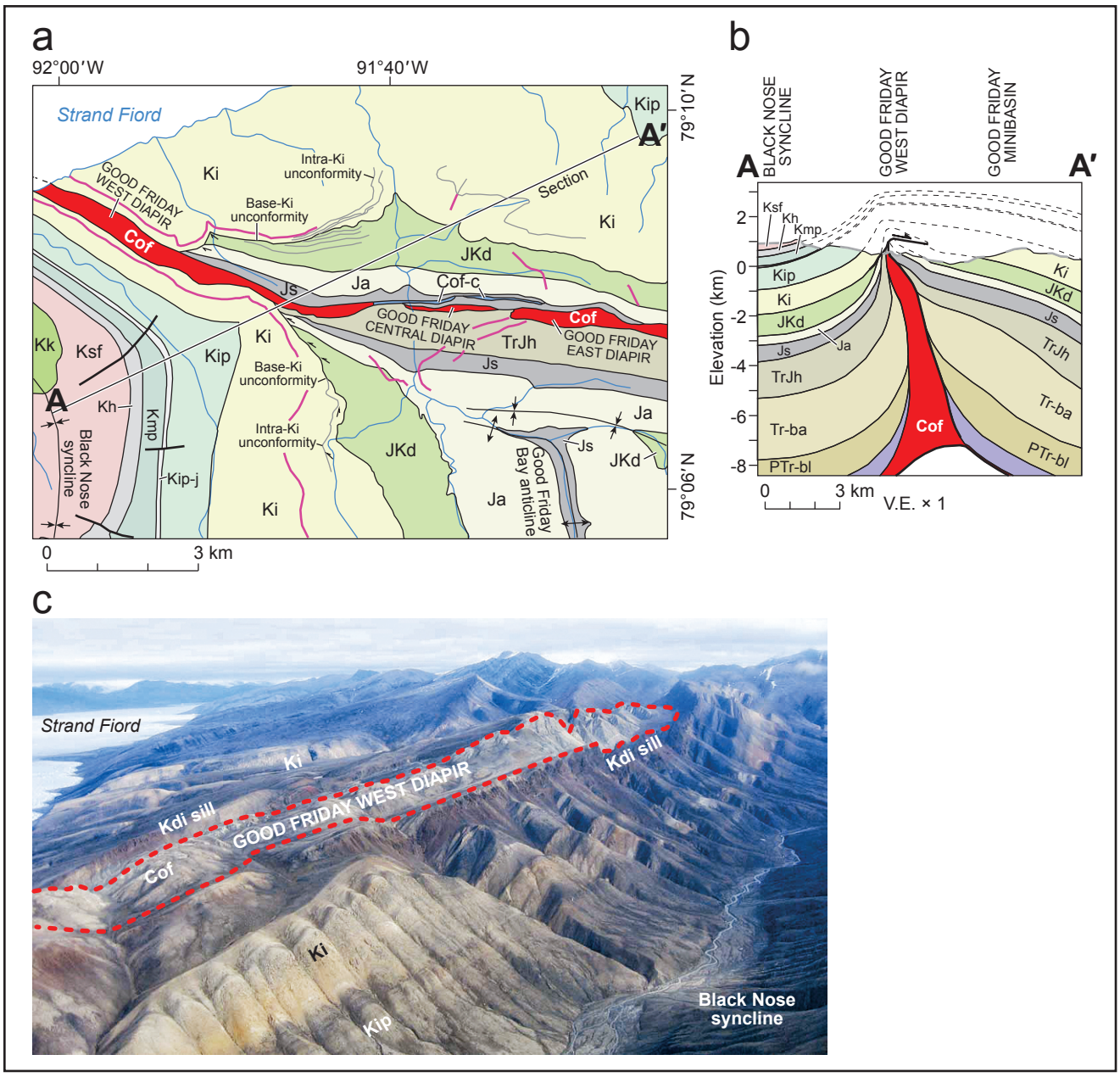

Figure 54. Geology of Good Friday West diapir and surroundings. a) Geological map, b) geological cross-section, c) aerial view to the east. Unit labels as in Figure 50; also Cof-c: carbonates in Otto Fiord evaporites; PTr-bl, Blind Fiord Formation; Tr-ba, Blaa Mountain Formation; Kmp: Macdougall Point Member; Kk, Kanguk Formation; Kdi: Cretaceous diabase.

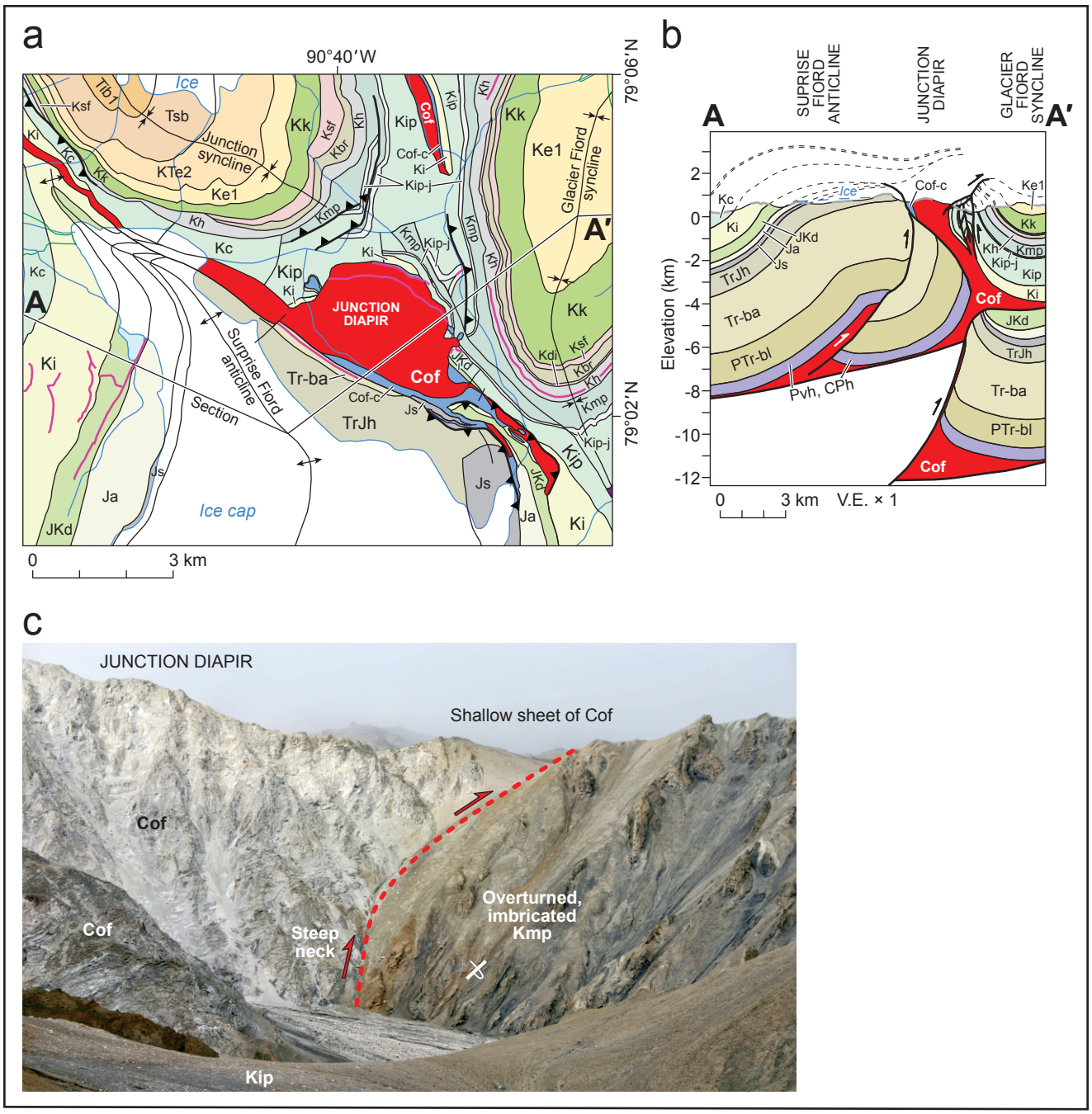

Figure 55. Geology of Junction diapir and surroundings. a) Geological map, b) geological cross-section, c) view to the northeast, showing the steep contact of the neck of this diapir flaring upward to form an allochthonous sheet overlying overturned, imbricated mid-Cretaceous country rock. Unit labels: Cof, Otto Fiord Formation; Cof-c, carbonate facies of Otto Fiord Formation; CPh, Hare Fiord and Trappers Cove formations; Pvh, Van Hauen Formation; PTr-bl, Blind Fiord Formation; Tr-ba, Blaa Mountain Formation; TrJh, Heiberg Formation; Js, Savik beds; Ja, Awingak Formation; JKd, Deer Bay Formation; Ki, Isachsen Formation; Kc, Christopher Formation; Kip, Invincible Point Member; Kip-j, Junction beds; Kmp, Macdougall Point Member; Kdi, Cretaceous diabase; Kh, Hassel Formation; Kbr, Bastion Ridge Formation; Ksf, Strand Fiord Formation; Kk, Kanguk Formation; Ke1, KTe2, Expedition Formation; Tsb, Strand Bay Formation; Tib1, Iceberg Bay Formation, Lower Member.

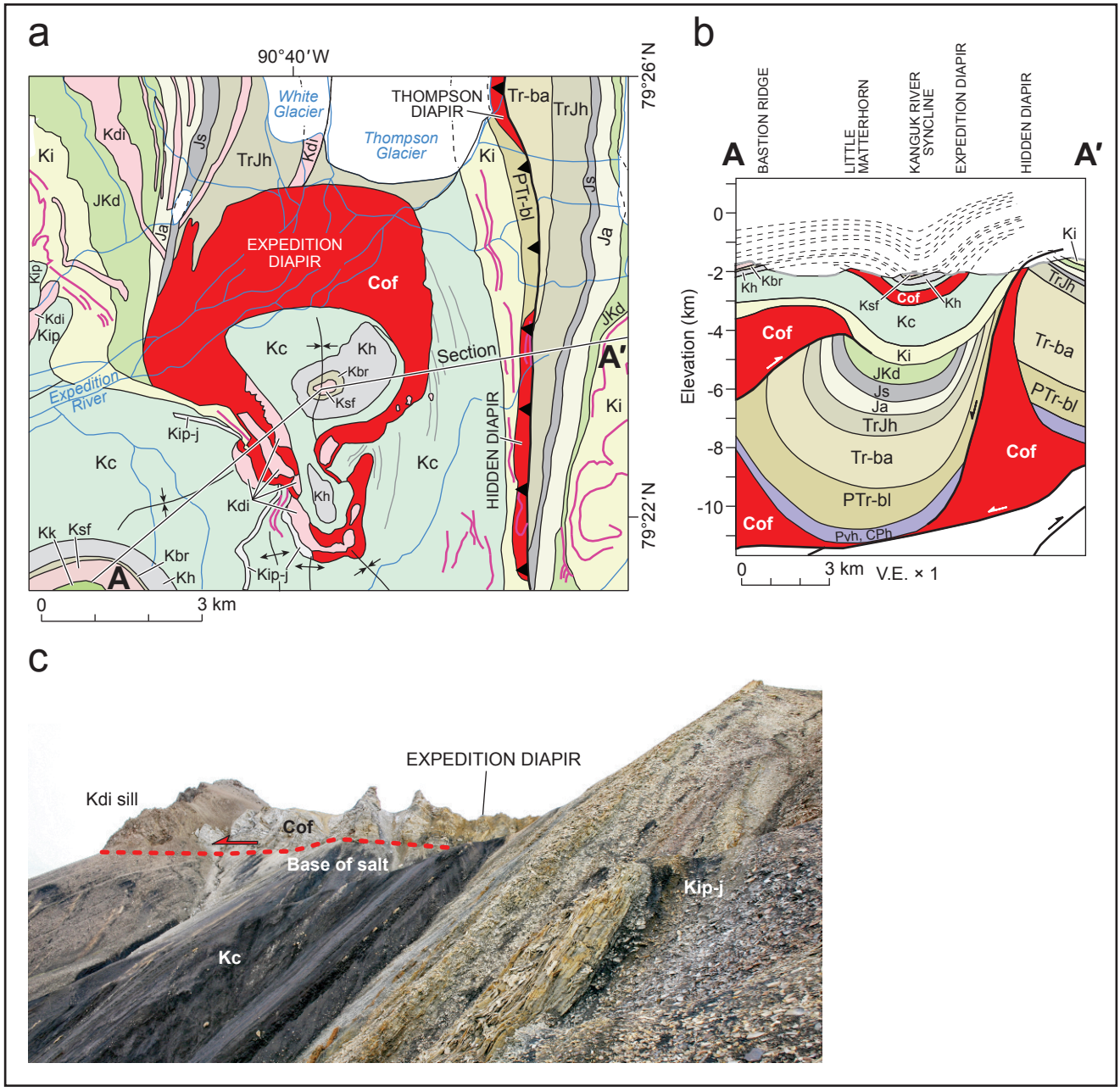

Figure 56. Geology of Expedition diapir and surroundings. a) Geological map, b) geological cross-section, c) view to the north of the southwest contact of the diapir, showing the subhorizontal basal contact of the diapir extruded or thrusted over steeper lower Albian strata. Unit labels as in Figure 55.

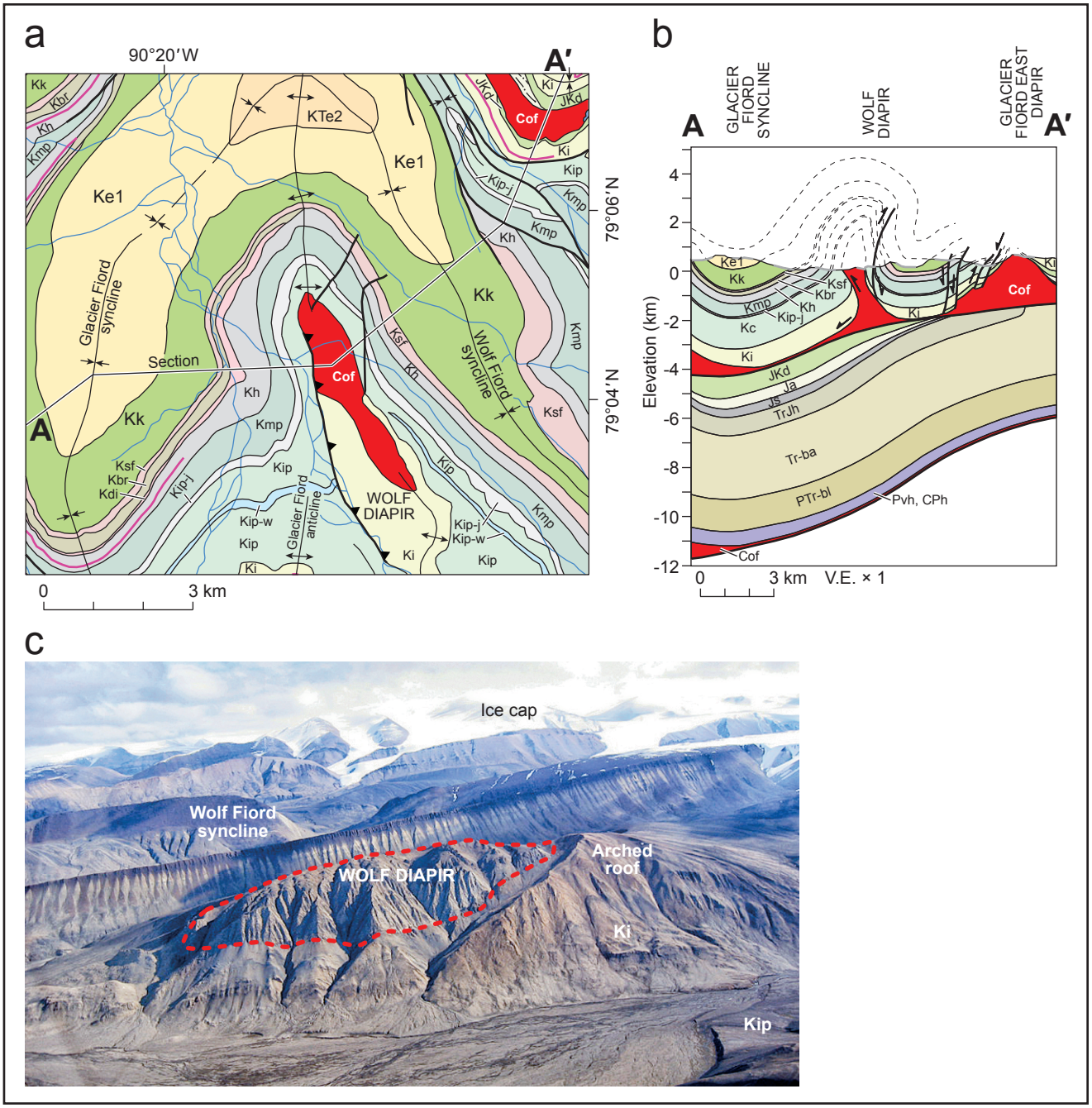

Figure 57. Geology of Wolf diapir and surroundings. a) Geological map, b) geological cross-section, c) view to the east, showing the diapiric core draped by an anticlinal roof of Isachsen Formation (Ki), flanked in the distance by Wolf Fiord syncline. Unit labels as in Figure 55; also Kip-w, Wolf Tongue.

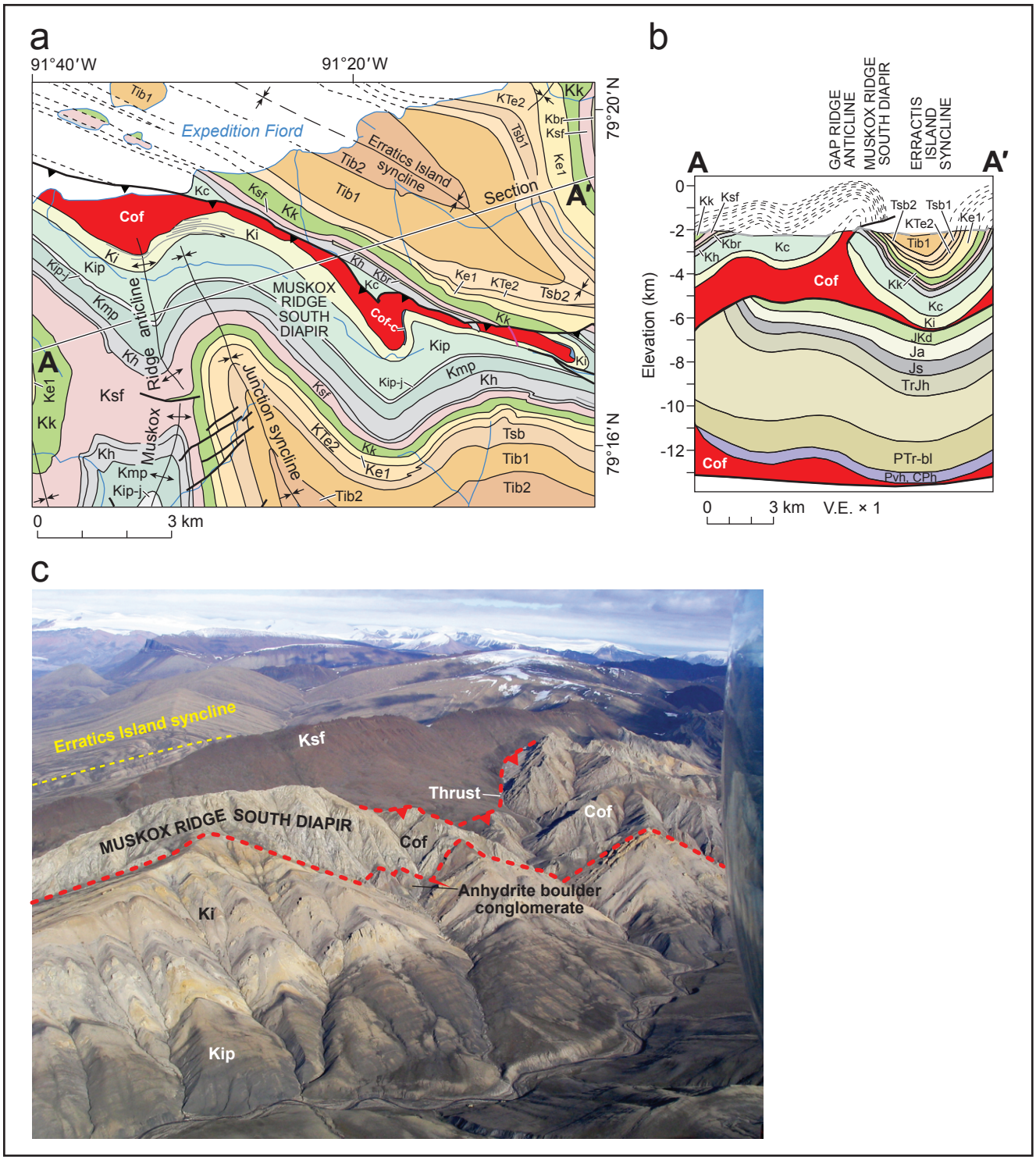

Figure 58. Geology of Muskox Ridge South diapir and surroundings. a) Geological map, b) geological cross-section, c) view to the east, showing the diapiric core overthrusting the Erratics Island syncline in a direction obliquely away from the viewer. On the other flank of the diapir are exposed Isachsen (Ki) and Invincible Point (Kip) roof strata, dipping obliquely toward the viewer. Unit labels as in Figure 55. Also: Strand Bay Formation, lower and upper members (Tsb1, Tsb2), Iceberg Bay Formation, Coal Member (Tib2).

the diapiric wall; the second striking north, parallel to the crossfold. Because of its orientation, this second fabric, at least, can be attributed to Eureka shortening. The two fabrics were superimposed at high angles, resulting in finite oblate strain, which is strongest in the core of the anticline.

Surprise North diapir

Along with Expedition diapir, the partly exposed Surprise North diapir is the only one still covered by a synclinal roof (Fig. 59). This short, unnamed syncline dies out to the south, where it steps over to the major Surprise Fiord syncline. The latter continues south of the wall-and-basin region and has the northward trend and broad wavelength typical of the Eurekan folding. This continuity suggests that the roof of Surprise North diapir was synclinally folded during the same orogeny. On either flank of the roof syncline, the diapir is exposed as sharp projections. The western projection widens northward into the main body of Surprise North diapir. The eastern projection is not exposed in the line of section but is overlain by a thrust slightly oblique to bedding (Fig. 59a). Farther south it surfaces in the form of an anhydrite thrust sliver called Surprise Central diapir.

Why was the roof of Surprise North diapir depressed as a synform during the Eurekan Orogeny? Two explanations are possible. The first is that this was a local minibasin. According to the isopach maps, the synclinal roof of Surprise North diapir began forming the Surprise minibasin in late Aptian to Albian time (Fig. 33). By Cenomanian time, local thickening here was much less and was not apparent by the Turonian (Fig. 38, 40).

A second explanation for the synformal roof is similar to that for Wolf diapir. The major Surprise Fiord syncline of Eurekan age may have propagated northward into the wall-and-basin region and downbuckled the roof of the diapir. To do this, the propagating syncline would have had to step to the right, perhaps exploiting the synformal shape of the Surprise minibasin.

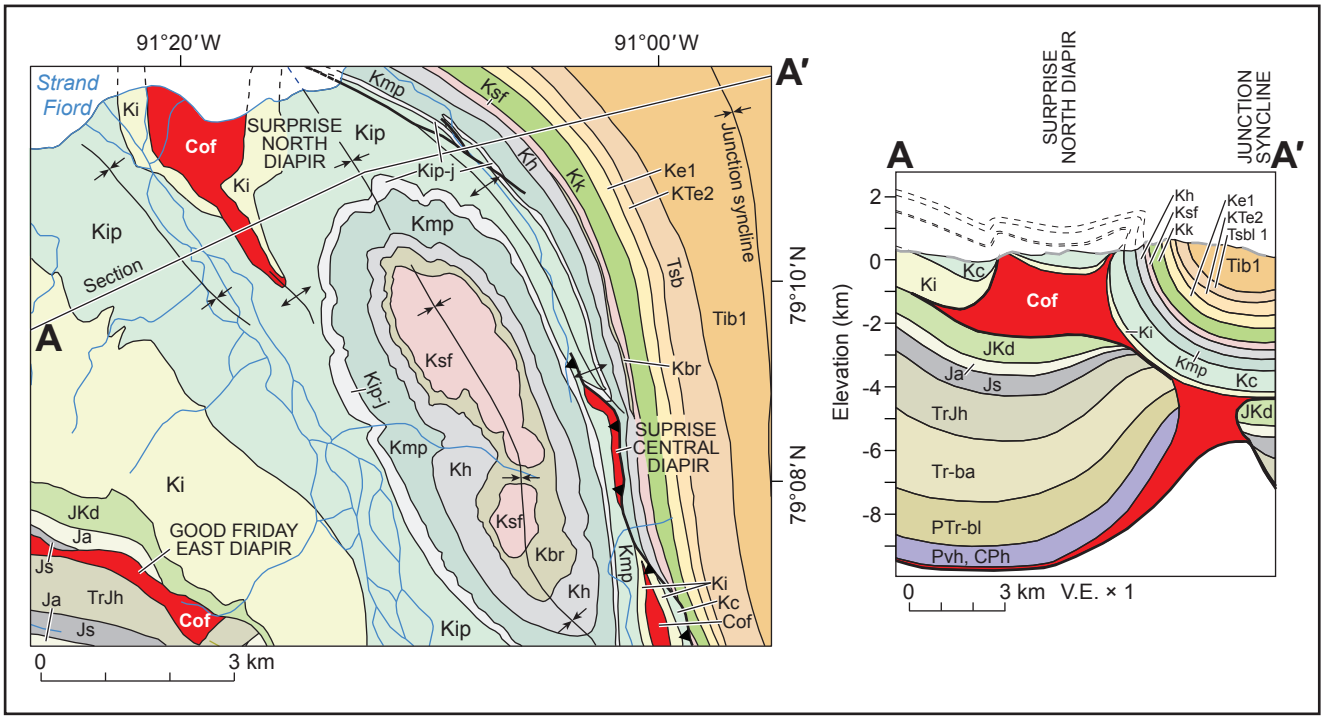

Figure 59. Geology of Surprise North diapir and surroundings. a) Geological map, b) geological cross-section. Unit labels as in Figure 55. Also, Strand Bay Formation, Lower Member (Tsb1).

Ellipsoidal synclines in wall-and-basin region

Synclines exposed inside the canopy limit are interpreted as minibasins accommodated by underlying salt expulsion. This inference is based on a long history of subsidence into salt, as evidenced by isopach variations, some of which are illustrated here, and all of which are included in an earlier report (Harrison and Jackson, 2008). Allochthonous salt emplaced within Hauterivian strata was expelled from beneath multiple depocentres during the Early Cretaceous through the Paleogene. Minibasins indicate that during this period, salt was expelled from deep parts of the canopy to feed second-generation diapirs rising from the canopy. As in minibasins elsewhere, this process had positive feedback: salt expulsion provided new accommodation space for sediments, and their additional load caused additional expulsion and diapiric rise.

All the minibasins were variably affected by the Paleogene Eurekan Orogeny. Tectonic shortening was directed westward, as evidenced by the orientation of regional buckle folds and thrusts outside the wall-and-basin region. Minibasins trending north are therefore likely to have been tightened by Eurekan compression. In contrast, minibasins trending at high angles to tectonic shortening would be less prone to shorten, but they could be refolded like the crescentic Glacier Fiord syncline, or even widened.

Influence of pre-existing structural anisotropy on salt tectonics

As noted, the dominant structural trend outside the wall-and-basin region is north-northwesterly (Fig. 16). This Eurekan fold-and-thrust trend affects units as deep as the Heiberg Formation in the south and as low as the Blind Fiord Formation in the north. As in the Zagros fold belt, this trend is likely to reflect the interplay of orogenic stress and older basement structures. Similar north-northwesterly trends inside and outside the wall-and-basin region suggest a similar origin. North-northwest is one of two peak orientations of wall-and-basin diapirs. An example is the regional-scale anticline connecting Good Friday Central diapir through Twin diapir to Muskox Ridge South diapir in the north. Others are Kanguk River syncline and the south end of Junction syncline.

The other equally dominant trend is west-northwesterly (van Berkel, 1986), which is rare outside the wall-and-basin region. A prominent example is Junction diapir on the southwest side. Other canopy-margin diapirs have the same trend, so they may also be influenced by a deep structure. These include Good Friday Bay, Lost Hammer, and Glacier Fiord diapirs. This west-northwesterly trend has to be explained by deformation restricted to the wall-and-basin region. Two possible tectonic phases have compatible strain orientations. Both are extensional. The first is the Carboniferous boundaries of the speculative sinistral transtensional pull-apart basin, which may have sourced the canopy. The second is mid-Permian to Early Jurassic extension as Sverdrup Basin subsided. Extension in the Late Cretaceous as the Eurasian basin rifted has a compatible orientation but is too late to have initiated the west-northwest-trending salt walls. These diapirs began rising in the mid-Early Cretaceous within the wall-and-basin region and in the Triassic or earlier on the borders of the wall-and-basin region.

Diapiric freeboard

A diapir's freeboard is its relief above the surrounding plain (Talbot, 1998). Most emergent diapirs around the world have freeboards less than 200 m (Davison et al., 1996, table 1). An exception to this global trend are the diapirs in the Zagros fold belt, which build unusually high freeboards because of regional shortening induced by collision of the Arabian and Iranian plates (Talbot, 2005). Another exception are the unusually high freeboards of some diapirs on Axel Heiberg Island, previously noted to be 400 m or more, which suggests they might be elevated by mild regional compression today. The Eurekan Orogeny ended prior to the Oligocene, and mid-Miocene is the age of the oldest postorogenic strata preserved in the region (Harrison et al., 1999). Any current compression would therefore be post-Eurekan. Theoretical diapiric freeboards can be calculated assuming static, thick salt in a horizontal source layer, and particular densities and thicknesses for salt and overburden. At static equilibrium, an emergent salt diapir is supported by the weight of the surrounding overburden on the source layer (Talbot, 2005),

so that

$$\rho_s g h_s = \rho_o g h_o$$

where ρ_s and h_s are density and height of a salt diapir above its base; ρ_o and h_o are density and thickness of its overburden; and g is acceleration due to gravity. The thickness of overburden above autochthonous salt is unknown, but we estimate roughly 10,000 m (Fig. 3). The overburden comprises mostly siliciclastic sediments and subordinate carbonates near the base and some igneous rocks near the top, so the bulk density of the overburden is likely to be about 2500 kg/m^3 (Jackson and Talbot, 1986). Where exposed on neighbouring Ellesmere Island, the Otto Fiord evaporites comprise about 400 m of anhydrite (density 2970 kg/m^3) and minor limestone (density 2300–2700 kg/m^3), so we assume an overall density of 2700 kg/m^3 for this composite cap of anhydrite and limestone. The subsurface thickness of the composite cap is unknown, but it is underlain by at least 4000 m of halite (Hoodoo L-41 well).

We can calculate what proportion of composite cap to halite is needed to support a 400 m freeboard by gravitational loading alone. These calculations suggest that an Axel Heiberg diapir rising from autochthonous salt is easily buoyant enough to support a 400 m high freeboard if the thickness ratio is 1:2 (composite cap to halite). The same diapir is almost buoyant enough to have the same high freeboard if the thickness ratio is 1:1. Under these conditions, little or no tectonic compression is necessary to maintain the unusually high freeboard of some Axel Heiberg diapirs. However, if our assumptions are adjusted in any of the following ways, then ongoing tectonic compression could be suspected: thickness ratio of 1:1 or more, thinner overburden, less-dense overburden, or greater proportions of limestone in the composite cap in the basin centre.

Diapiric freeboards also provide evidence of the existence of the salt canopy. The greatest freeboards (400 m) are in diapirs rooted in autochthonous salt either outside the wall-and-basin region (especially South Fiord to the west and Gibs Fiord and Mokka Fiord diapirs to the east) or bordering the wall-and-basin region (Junction diapir). Freeboards of diapirs inferred to rise from the canopy are much less: ranging from the Kanguk diapirs, which have less than 100 m of freeboard, to diapirs having almost no freeboard. Such diapirs could have risen from a much shallower source layer (pressurized by only thin overburden) or one that became depleted in salt because it was never thick—both qualities expected in a canopy.

Evolution of salt tectonics and origin of canopy

Figure 60 summarizes the tectonic evolution along cross-section A. These sections were restored using LithoTect software. Stratigraphic units were decompacted using lithology estimates derived from outcrop. Folds in extensional and halokinetic structures were restored using vertical simple shear. Contractional structures were restored using flexural slip. Salt cross-sectional area was constrained by a salt budget that maintained area when all salt structures were buried, and which lost area forward in time whenever salt structures emerged at the surface and began to dissolve. Evidence of shortening was provided by the narrowness of welded diapirs and their overthrust flanks. Some diapirs grew passively and were at the surface for much of their history, so no roof strata are preserved to record the paleowidths of the diapirs until late in their history. Thus the total shortening is mostly an educated guess. We estimated that the original widths of the diapirs were unlikely to be less than 2 km wide, which is roughly the lower size limit of unsqueezed salt diapirs around the world.

The sequence begins with rifting and salt deposition in the Carboniferous. The original thickness of salt is impossible to determine even approximately without present-day subsurface data. The area of salt in this restoration, however, is speculatively shown to increase substantially after rifting ended. This area increase conveys the possibility that salt entered the cross-section after being expelled from the east by prograding sedimentary loads in the Permo-Triassic. Alternatively the salt basin could have been thick from the start. Certainly this was the depocentre of Sverdrup Basin, presumably overlying the most highly thinned continental crust.

The first of three main episodes of inferred regional shortening occurred in the Jurassic and Early Cretaceous. This tectonic shortening would have encouraged active diapirism, which arched up the roofs of the diapirs. As noted previously, the 2 km width of the upturned strata preserved today suggests that mild shortening was needed for such

large-scale upturn of flanking strata. Active diapirism would also have been driven by the overburden load on the adjoining source layer. By the Early Cretaceous the actively arched roof strata were eroded off because they formed local topographic highs, possibly aided by widespread uplift, erosion, and exhumation associated with mild compression.

A second shortening episode, which may have been a continuation of the first, is inferred to have emplaced the Axel Heiberg canopy in Hauterivian time during Isachsen Formation deposition near the Sverdrup Basin centre. Evidence of this is presented in the section on 'Origin and significance of evaporite canopy.' Even mild tectonic squeezing of diapirs can cause them to extrude and coalesce into a canopy if the diapirs are wide enough to supply enough salt. Salt extruded from the squeezed diapirs and the extrusions of allochthonous salt coalesced to form a canopy. Only where autochthonous salt was thick enough to supply copious diapiric salt could the extrusive outflows merge into a canopy—hence, our inference that the canopy overlies the depocentre of the salt source layer in Sverdrup Basin.

In Hauterivian time the canopy began to be locally eroded and buried. Although minibasins began to sink into autochthonous salt as early as the Triassic, most of the isopach evidence of minibasins is in Hauterivian and younger strata, which sank into the canopy. To a large degree, this greater evidence is because the supracanopy minibasins are more exposed than deeper, older minibasins.

The canopy continued to be buried until the third and largest episode of regional shortening began as the Eurekan Orogeny in the Palaeogene. Eurekan shortening decreases westward across Sverdrup Basin, away from the orogenic hinterland on Ellesmere Island. Our restoration suggests 15 km of shortening along the cross-section. The Eurekan Orogeny reversed the process of burial as widespread uplift accompanied shortening and partly exhumed the allochthonous system of canopy and supracanopy diapirs and minibasins.

Bulk strains and relationship to plate tectonics

Inferred qualitative bulk strain ellipses for regional tectonic events are shown in Figure 61. The ellipse for the Triassic and Early Jurassic coincides with the subsidence phase of Sverdrup Basin and is based on the extensional trend of grabens in the Carboniferous and Early Permian. Graben trends defined by outcrop and seismic data in the southwestern Sverdrup Basin are aligned to the east-northeast (Harrison, 1995). Closer to the wall-and-basin region are structures on northern Axel Heiberg Island that strike to the west-northwest for likely normal faults and southerly for presumed sinistral faults (Mayr et al., 2002). These trends are consistent with the model that the wall-and-basin region was initially formed in a Carboniferous sinistral releasing bend (Fig. 8).

The ellipse for the Middle Jurassic through pre-Hauterivian Early Cretaceous is based on the strike of Jurassic normal faults in the Prince Patrick Island area in the western Arctic (Harrison and Brent, 2005) and the trend of the Cretaceous rifted Arctic continental margin northwest of the Arctic Islands. Onset of this new fault set also shows a dramatic shift in depositional limits for mapped units beginning in the Toarcian. West-northwesterly-trending structure active during this interval within the wall-and-basin region (Fig. 52) is consistent with regional tectonic shortening. Example structures forming at this time include Strand Pass, Glacier, and Good Friday minibasins and Expedition, Glacier, Junction, and Lost Hammer highs (Fig. 52).

The strain ellipse for the Hautervian and later Early Cretaceous is based on northerly-striking trends of the Queen Elizabeth mafic dyke swarm through Ellesmere and Axel Heiberg islands (Buchan and Ernst, 2003, 2006) Consistent with this direction is potential extension to form the northerly-trending Castle, Junction, and Muskox minibasins and the intervening Bastion, Colour, Muskox, and Agate highs (Fig. 52).

The Late Cretaceous ellipse is based on the assumption that the trailing margins of the Barents Shelf and the Lomonosov Ridge began as rifted margins at this time. Structures apparently forming in extension through this interval include the northwesterly-trending Muskox high and Black Nose ridge (Fig. 52).

Finally, Paleogene ellipses are derived from plate motions of Greenland with respect to the Arctic Islands, which produced northeasterly-striking thrusts in the earlier Palaeocene and more north-northwesterly-striking thrusts and folds

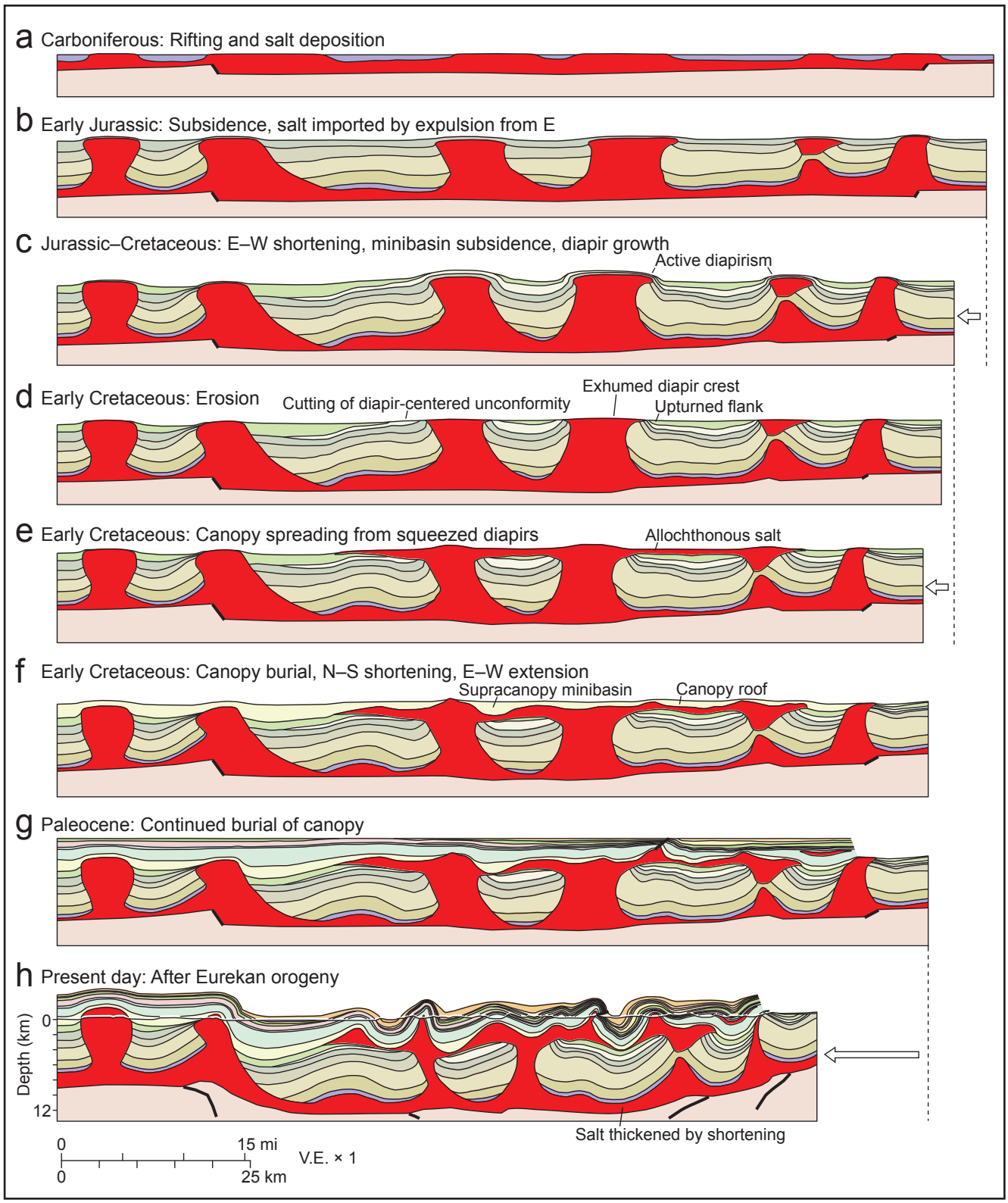

Figure 60. Restoration of cross-section A, showing tectonic evolution. *See* Figure 2 and 48 for stratigraphic colour key. Restored using LithoTect software: episodes of shortening were restored using flexural slip; other deformation restored using vertical shear.

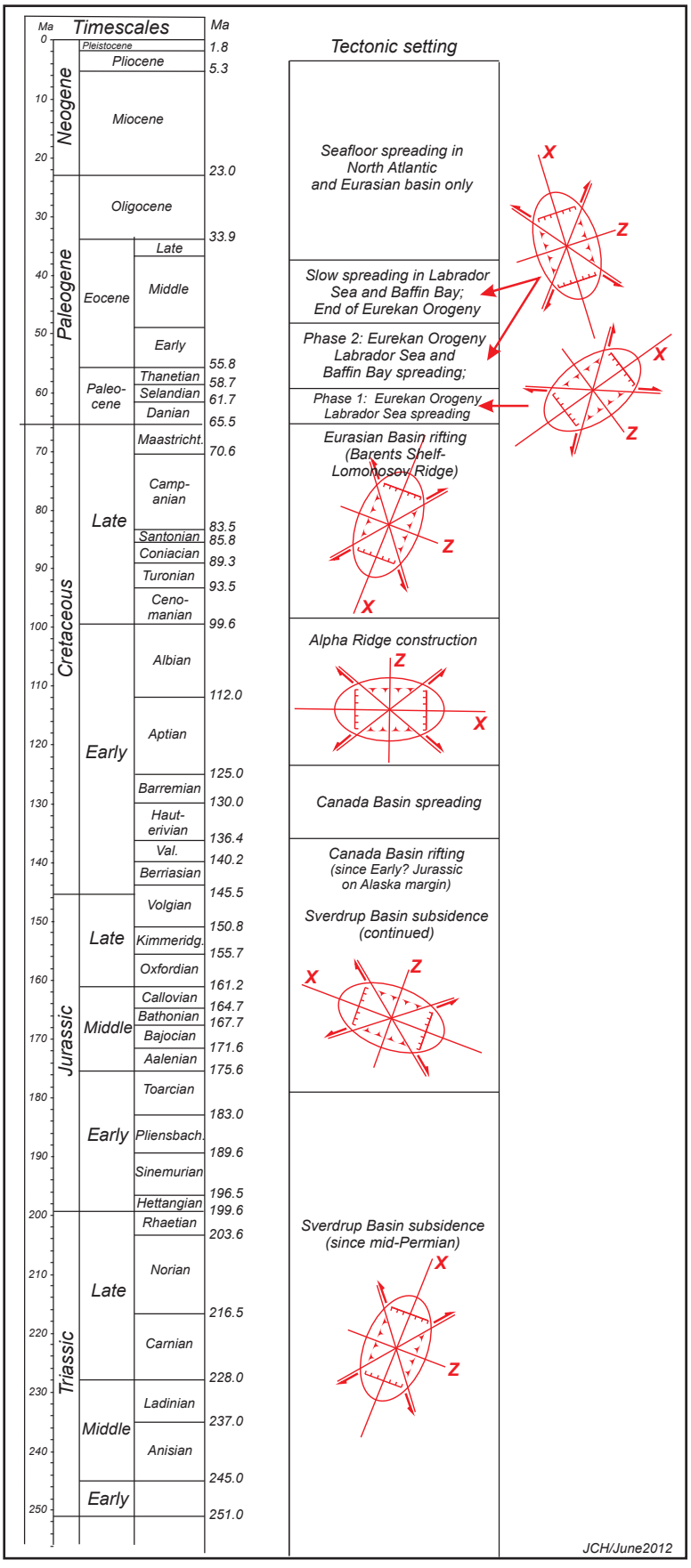

Figure 61. Tectonic history of the report area summarized by a bulk strain ellipse for each of six tectonic phases. The ellipses are purely diagrammatic and have no implication for the magnitude of strain, but they emphasize the wide range of contractional, shortening, and strike-slip structures successively overprinted on this area.

in the later Palaeocene and Eocene. The second phase of the Eurekan Orogeny presumably caused the shortening of various north-northwesterly trending evaporite walls and other north-northwesterly trending anticlines on Axel Heiberg Island beyond the wall-and-basin region (Fig. 45, 52). The implication of the proposed late Palaeocene–Eocene strain ellipse is that prominent northwesterly striking structure was the consequence of sinistral transpression.

Origin and significance of evaporite canopy

Evidence presented earlier in this report points to the Hauterivian as the time of breakout and spreading of the Axel Heiberg canopy. These events coincide with deposition of the Paterson Island Member of the Isachsen Formation. At this time, basaltic volcanism began, which was possibly related to the High Arctic Large Igneous Province (HALIP) (Buchan and Ernst, 2006). This produced for the first time in the Hauterivian an extensive dyke and sill swarm and basaltic volcanism. Dykes associated with HALIP trend northerly on northern Ellesmere Island and throughout Axel Heiberg Island as the Queen Elizabeth swarm. As noted in the previous section, this trend is strong evidence of east-west crustal extension. However, shortening is a more effective way of emplacing a canopy because squeezing diapirs helps to extrude their contents as allochthonous flows. Shortening to trigger canopy coalescence in the Early Cretaceous could have occurred in three different settings (Fig. 30, 60). First, shortening could have been directed toward the east-northeast if it had accompanied the end of perpendicular Canada Basin rifting. Second, shortening could have been directed toward the south as mafic volcanism began in the northern Sverdrup Basin and as seafloor spreading started in the Canada Basin and the Alpha Ridge was emplaced. Third, shortening may have been induced by gravity gliding from the east. What is the evidence for west-directed gravity sliding? The Isachsen Formation varies greatly in thickness within the wall-and-basin region (<100–>1500 m), but it is consistently thinner on eastern Axel Heiberg Island and on west-central Ellesmere Island. The eastern basin margin, located on eastern Axel Heiberg and western Ellesmere islands, is missing the upper Valanginian, Hauterivian, and lower Barremian parts of the Isachsen Formation (Trettin, 1991). A major disconformity separates the Upper Jurassic Deer Bay Formation from disconformable cover of the Barremian Isachsen Formation. The eastern belts of Isachsen Formation were therefore deposited on eroded uplands. This is compatible with thermal uplift of the basin margin during the HALIP event. Basin marginal tilting to the west would trigger thin-skinned gravity tectonics. The toe of such a system in the basin centre would favour local shortening in the wall-and-basin region.

Discovery of the evaporite canopy on Axel Heiberg Island is extremely significant for salt tectonics. Much larger salt canopies are known in several basins, most notably in the northern and southern Gulf of Mexico (Diegel et al., 1995), the Lower Congo Basin (Tari et al., 2003), and the Precaspian Basin (Volozh et al., 2003). However, none of these canopies is exposed at the surface, let alone subaerially, which allows outcrops to be mapped in far greater detail than is possible in the subsurface. Allochthonous salt, typically degraded by dissolution, is exposed on land in several fold-and-thrust belts, most notably in the Zagros (Kent, 1979; Talbot, 1998; Jahani et al., 2009; Callot et al., 2013), Qom (Talbot and Aftabi, 2004), Atlas (Vila, 1995), Tajik (Dooley et al., 2014), Sub-Alpine chain of France (Dardeau and de Graciansky, 1990; Graham et al., 2012), Katanga fold belt (François, 1994; Jackson et al., 2003), and Flinders fold belt (Dyson, 2005; Rowan and Vendeville, 2006). None of this allochthonous salt, however, is known to form canopies, although such a discovery is possible in the future.

Sverdrup Basin is one of only three regions in which a salt canopy and associated diapirs are well exposed. None of these outcrop examples is augmented by subsurface data, but all are well exposed and exhumed by orogenic shortening and uplift. Each is unique. In Great Kavir, the largest canopy comprises 12 coalesced stocks (Jackson et al., 1990) and about 40 other diapirs. The canopy consists of Eocene marine evaporites and Miocene lacustrine evaporites (Lower Red Formation), which rose through upper Miocene overburden (Upper Red Formation). The two photogeologically distinctive evaporite units form a cellular pattern inside the canopy, which outlines the 12 coalesced stocks. In the Neogene, the basin was mildly shortened in the foreland of the Alborz Orogen. The erosion surface

cuts precisely through the canopy, which is tilted gently to the west. The area has been mapped only by photogeology, which is unable to differentiate the monotonous Upper Red Formation into more than two units. The stratigraphy is therefore poorly known, and no minibasins have been identified.

The second example is the Axel Heiberg canopy (Jackson and Harrison, 2006; Harrison and Jackson, 2008), which is the type area for wall-and-basin structure. The Eurekan Orogeny has caused the basin to be more strongly shortened than the Great Kavir. Shortening is expressed as synformal deepening of minibasins and narrowing of salt walls. The level of exposure is largely above the canopy and intersects second-generation diapirs rising from the canopy and secondary minibasins sinking into the canopy. As documented in the present account, the stratigraphy is comprehensive and known in great detail. The presence of more than 20 distinctive stratigraphic units has allowed exhaustive geological mapping and isopach analysis.

The third example is in Sivas Basin in central Turkey (Callot et al., 2013; Ringenbach et al., 2013). This example resembles the Axel Heiberg pattern of wall-and-basin structure in several respects. Investigation of the salt tectonics in Sivas Basin is still in the early stages and mostly confined to a small central part of the evaporite basin. It remains to be seen which of the many exposed diapiric walls have risen from the allochthonous canopy or from the deeper autochthonous level. The general level of exposure, however, appears to be largely beneath the canopy and intersects primary minibasins and adjoining diapiric walls. The orogenic overprint is strong; until recently this basin was regarded as a simple fold-and-thrust belt. The degree of shortening is high enough to have tilted some minibasins into subvertical dips. Conventional stratigraphic subdivisions in this basin are fairly coarse but are being recorded in increasing detail (Callot et al., 2013; Ringenbach et al., 2013).

In summary, these three areas provide a complementary set of excellent exposures of salt canopies and primary and secondary minibasins (Fig. 62). The exposures form a diverse set, partly because they display a range of shortening intensity but chiefly because they are erosional slices through three different structural levels: above the inferred canopy (Axel Heiberg), through the canopy (Great Kavir), and beneath a possible canopy (Sivas).

Evidence of neotectonic diapirism

Several topographic, tectonic, and depositional elements point to a neotectonic, probably postglacial, history for some diapirs, and perhaps others, too, on Axel Heiberg Island. Our examples cover a range from apparently still-rising diapirs to apparently dormant diapirs.

Most diapirs on Axel Heiberg Island stand well above the surrounding countryside. Classic high-standing freeboards include Gibs Fiord and Mokka Fiord (Fig. 63) diapirs, to name just two on eastern Axel Heiberg Island, which rise several hundred metres above the surrounding plain, and South Fiord diapir in the west, which has relief of 400 m (Fig. 64). Other examples include Kanguk North and Kanguk South diapirs (Fig. 65). These diapirs are located along the thalweg of a U-shaped valley. Related features are anhydrite cliffs of Expedition diapir that appear to have pushed through the wall of another U-shaped valley (Fig. 66). Because anhydrite would be readily removed by a valley

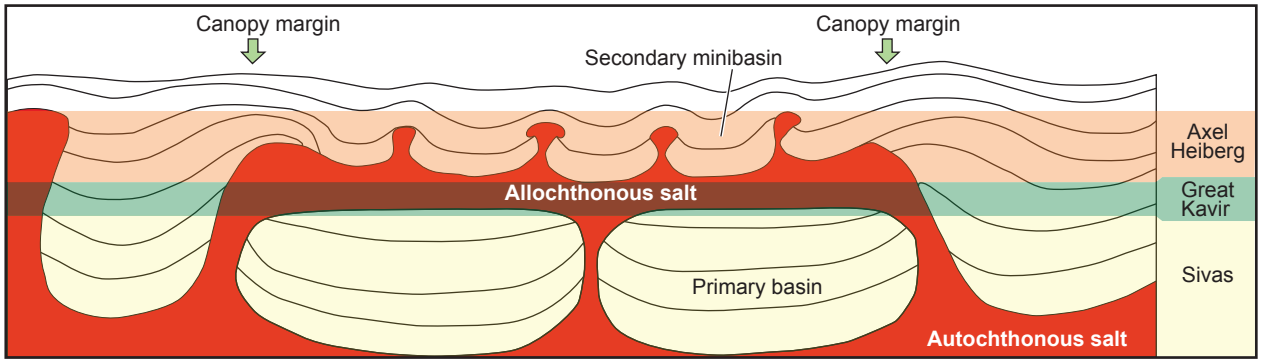

Figure 62. Schematic cross-section illustrating the three different and complementary levels of exposure inferred for Axel Heiberg Island, the Great Kavir (central Iran), and the Sivas Basin (central Turkey).

glacier, all this relief may have been produced since the latest glaciation; conceivably a viscous response to removal of the glacial ice cap load. Other neotectonic features of Expedition diapir include shoestring flows that appear to place anhydrite over Recent colluvium (Fig. 67) and gravity block slides of anhydrite (Fig. 68).

Another spectacular example is Junction diapir. Small subaerial debris flows occur along the collapsed northeast flank of the diapir. Another much larger subaerial debris flow lies at the base of the steep northwestern diapir margin (Fig. 69, 70). On all sides of the mountain, steep gullies drain gravel-sized clasts of anhydrite and limestone into talus cones having a steep angle of repose (Fig. 71). Despite the high volume of clasts mechanically weathering off the diapir and the solubility of anhydrite, the relief of Junction diapir is 400 m above the surrounding valleys. The combination of rapid mass wasting and high relief point to continued diapiric uplift today.

An exception to the relief of most of the diapirs on Axel Heiberg Island is Strand diapir (Fig. 72). Strand diapir had a typical salt-tectonic history from the Triassic to the mid-Cretaceous but appears to have been more-or-less dormant since the Isachsen Formation was deposited. Most of the diapir is currently buried by braidplain gravels. Another dormant diapir is Three Lakes diapir (*see* Fig. 1 for location), which cores an anticline in eastern Axel Heiberg Island. Hills here are underlain by the Middle Triassic Blaa Mountain Formation, which is intruded by Cretaceous sills. The diapir itself is tiny and seen only in streambanks that have eroded selectively such that evaporitic rocks now lie well below the level of the surrounding shales and gabbro (Fig. 73). This pattern suggests that diapiric activity has finished. Nevertheless, Cretaceous or younger hydrothermal activity here has produced tufa-related carbonate breccias and layered carbonate-celestite deposits in a collar around the southern diapir margin (Fig. 74, 75). This deposition suggests that even after these diapirs have stopped rising, they continue to provide conduits for rising hydrothermal fluids.

Figure 63. Mokka Fiord diapir rising above the coastal plain on east central Axel Heiberg Island (*see* Fig. 1 for location). (GSC Photo No. 2014-097)

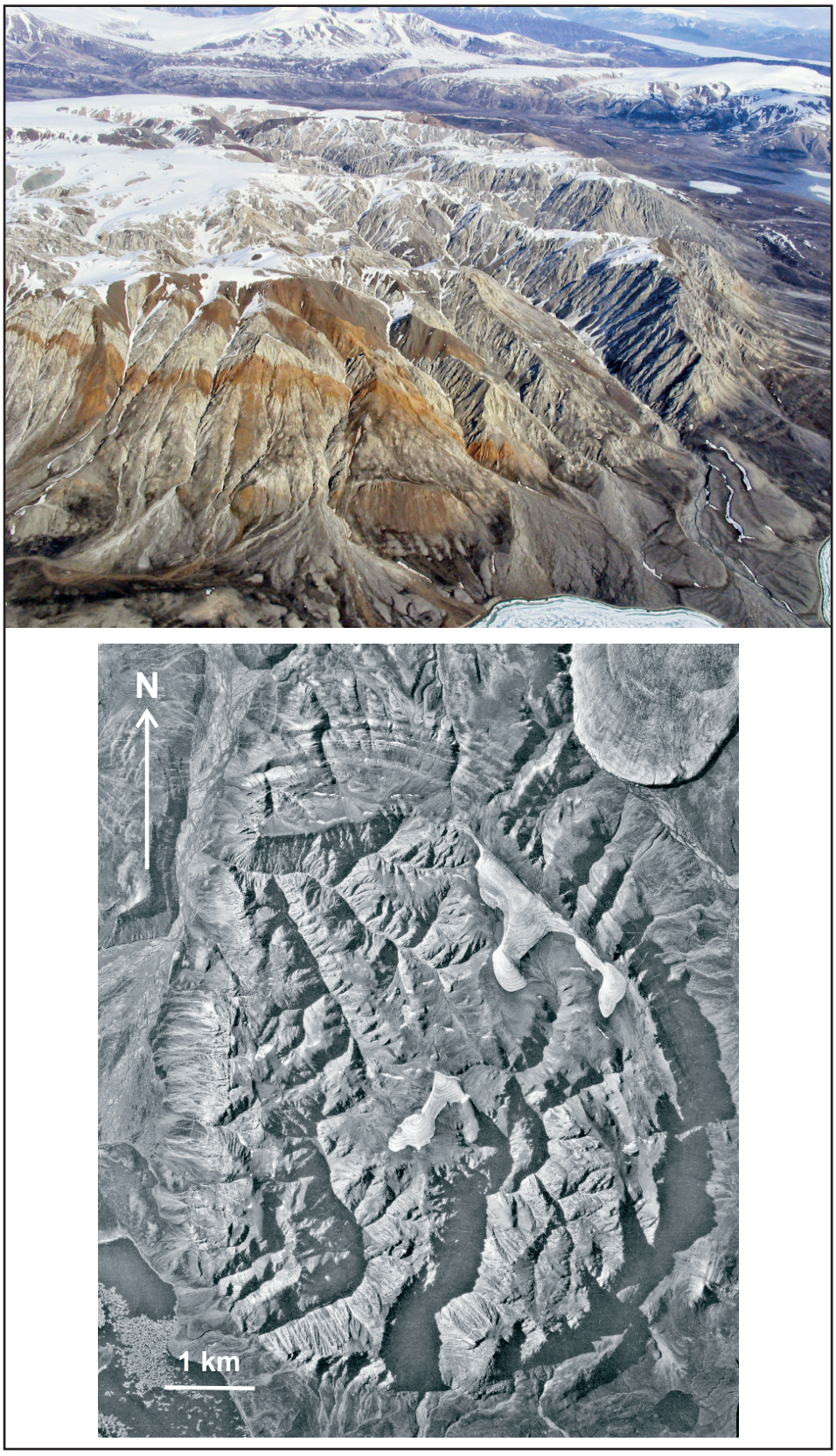

Figure 64. Aerial views of the 400 m high South Fiord diapir on western Axel Heiberg Island: Field photograph (top). The diapir is heavily intruded by mafic sills (dark brown). View is to the northeast. Portion of National Air Photo Library (NAPL) photo A16183-073 (bottom).

Economic geology

The eastern and central parts of Sverdrup Basin, including Axel Heiberg Island, have attracted little exploration interest compared with adjacent areas to the west. Reasons include presumed higher degree of deformation and metamorphism, pervasive intrusion by diabase, and deeper level of erosion. These arguments do not universally apply to the wall-and-basin region.

Potential reservoir strata include (from top down) the Hassel, Isachsen, and Awingak formations and possibly parts of the Heiberg Formation. Although compositionally favourable, the Hassel and Isachsen formations can largely be excluded from this list because they are widely exposed and any contained hydrocarbons have probably been driven off or degraded. According to Embry et al. (1991), Awingak Formation is a minor reservoir where it has been encountered by drilling in western Sverdrup Basin. Nevertheless, it has not been tested in the wall-and-basin region or throughout most of Axel Heiberg Island. This leaves Heiberg Formation, which Embry et al. (1991) cited as a key reservoir on Ellef Ringnes Island.

Potential source rocks, including the Kanguk, Deer Bay, and Savik formations and Blaa Mountain Group, are described by Powell (1978), Embry et al. (1991), and Nunez-Betelu (1994). Compositionally most favourable are shales of the 'bituminous member' of the (Cenomanian-Turonian) Kanguk Formation, which have been analyzed by Nunez-Betelu (1994). On eastern and southern Axel Heiberg Island these shales contain Type II (and Type III) kerogen with total organic carbon (TOC) ranging to more than 7.3%. Potential to generate oil is described as moderate. The Kanguk Formation is immature to marginally mature, however, and its position high in the stratigraphy indicates a negligible potential for migration and entrapment.

Continuing downsection, the next potential source rock is the Deer Bay Formation. This formation is described by Powell (1978) as having poor source rock characteristics except locally on Ellef Ringnes Island, where heating attributed to intrusive activity has generated locally favourable hydrocarbon yields. In general, the Deer Bay Formation is considered a poor oil source rock, but it is capable of yielding considerable gas. Next downsection, the Savik beds are thermally overmature throughout the central Sverdrup Basin. However, data for Axel Heiberg Island are entirely lacking. The Savik beds, especially the Jameson Bay Formation, are generally described as favourable for gas but poor for oil. Most favourable of the Mesozoic units is the Middle Triassic Murray Harbour Formation in the lower part of Blaa Mountain Group. Embry et al. (1991) described this unit as a Type II source rock containing as much as 10% TOC. Key unanswered questions remain: Do these favourable source rocks occur in the Blaa Mountain Group of Axel Heiberg Island, and have they produced migrated oil?

A key feature of the wall-and-basin region likely to generate exploration interest is the possibility of an evaporite seal provided by the canopy. Features of the canopy margin indicate that units of the Triassic and Jurassic as high as the Awingak and Deer Bay formations form common angular unconformities beneath Isachsen Formation and may be sealed by the Otto Fiord Formation where it forms a canopy at the level of the lower (not lowermost) Isachsen Formation. Favourable conditions for potential hydrocarbon entrapment are indicated on our cross-sections (Fig. 53, although subcanopy structure has to be interpreted with extreme caution without subsurface data. Example features include the Awingak and Heiberg formations potentially sealed by evaporite canopy under Black Nose syncline, Index Peninsula anticline, and Agate Fiord syncline (Fig. 53 Cross-section A); similarly canopy seals under Junction and Glacier Fiord East diapirs (Cross-section C).

Turning to mineral potential, it is clear that hydrothermal activity affected some diapirs. Most notable are the tufa deposits located over and adjacent to Three Lakes diapir on eastern Axel Heiberg Island (Fig. 73–75). Disseminated pyrite is also present in the immediate contact zone of several diapirs (Junction, Bastion Ridge South, and Muskox Ridge South). Massive pyrite is associated with gossans in the Deer Bay Formation near Junction diapir (Fig. 76). Gossans are common around diapirs along the north range of the wall-and-basin region in association with diabase intrusions and may account for the colour in Colour diapir. Although these gossans are presumed to have developed over disseminated and massive pyrite, some potential remains for metal sulphides of commercial interest.

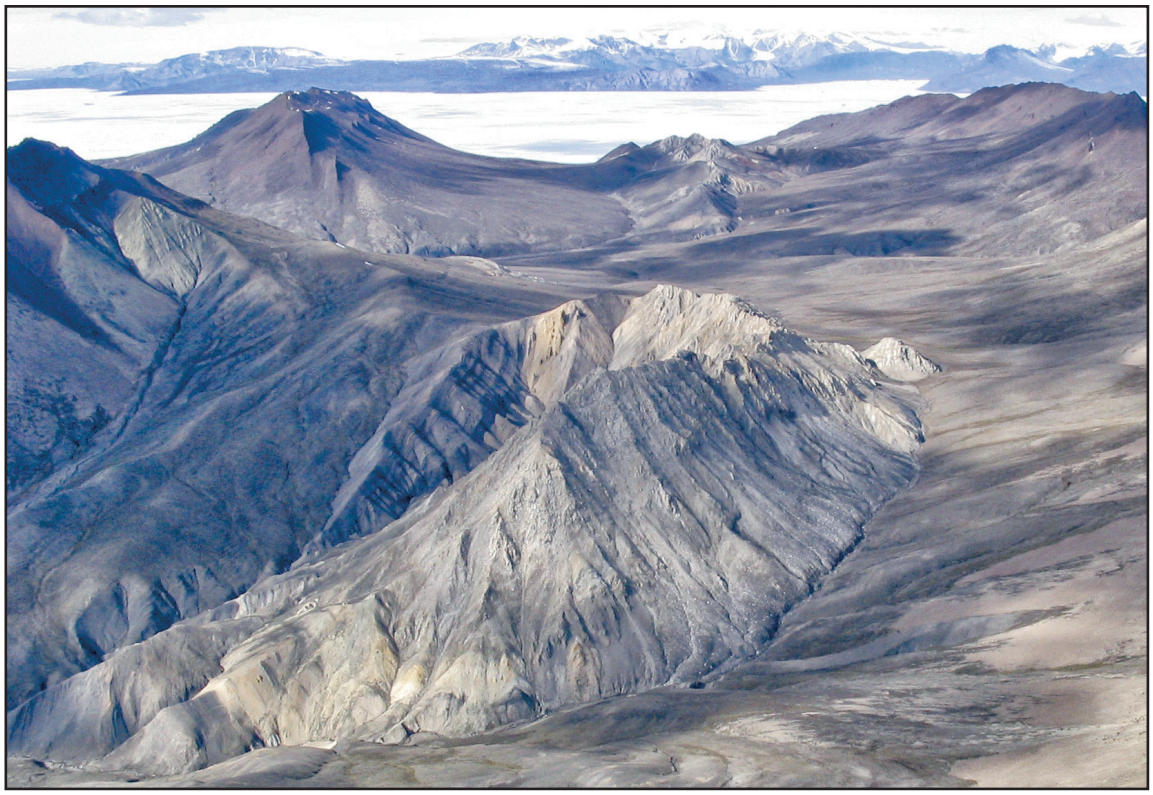

Figure 65. The resistant Kanguk North (foreground) and Kanguk South (background) diapirs are situated along the axis of a U-shaped glacial valley. This pattern suggests that diapiric relief is younger than the glacier that shaped the valley. (GSC Photo No. 2014-098)

Figure 66. Evaporites of Expedition diapir have been pressed through the valley wall to form bulging cliffs that appear to be younger than valley-forming glacial events. (GSC Photo No. 2014-099)

Figure 67. Recent shoestring debris flows of evaporites emplaced over colluvium of Expedition diapir. (GSC Photo No. 2014-100)

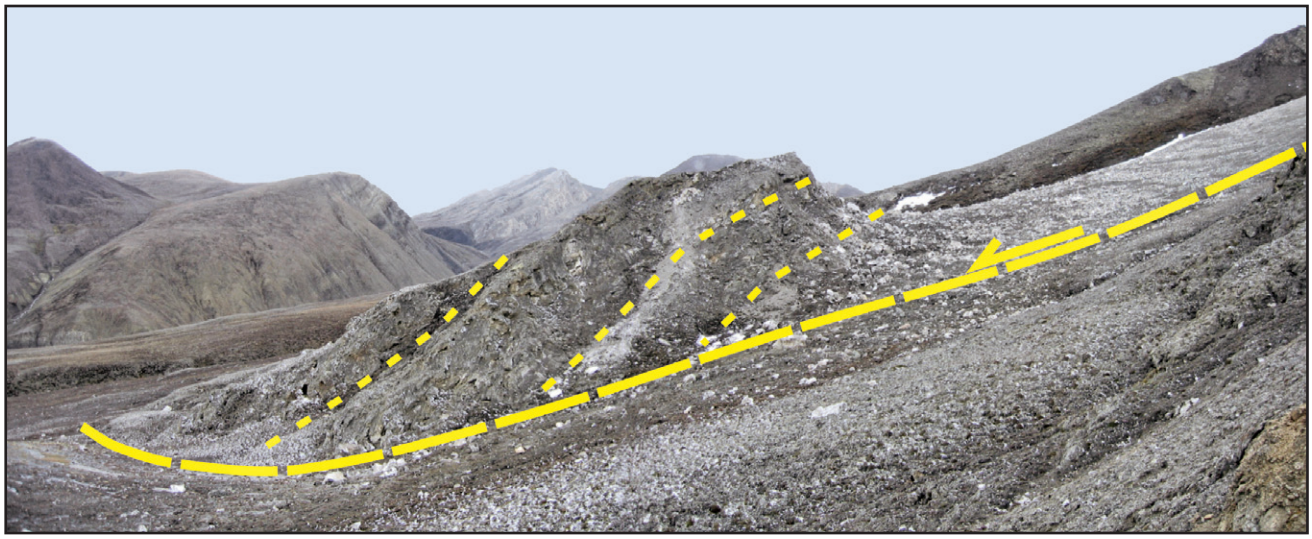

Figure 68. Slide block of anhydrite (~20 m high) located on the north-facing slope of Expedition diapir. (GSC Photo No. 2014-101)

Figure 69. Subaerial debris flow on the northwest-facing lower slopes of Junction diapir. The debris flow has shed from the mountainous diapir and spread out over recessive Christopher Formation (Kc) in the valley bottom. The debris flow is about 300 m wide at its widest point. View is to the east. (GSC Photo No. 2014-102)

Figure 70. Convolute bedding exposed in the toe area of the debris flow on the northwest-facing lower slope of Junction diapir, illustrated in Figure 69. (GSC Photo No. 2014-103)

Figure 71. Steep talus cone of anhydrite and limestone clasts shed from the northern flank of Junction diapir. This mass wasting, combined with the 400 m of diapiric relief, points to continued diapiric uplift today.

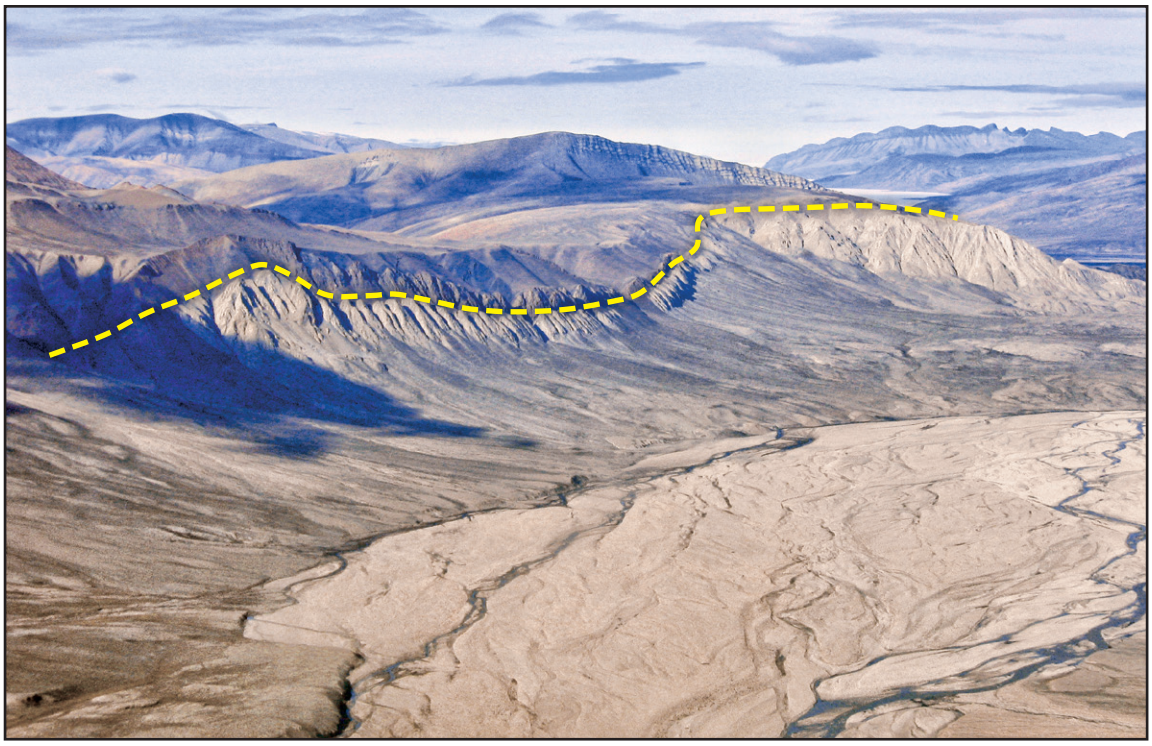

Figure 72. Strand diapir. Exposed margin of the diapir is marked with a yellow dashed line. Most of the diapiric evaporite is overlain by colluvium and braided channel deposits in the foreground, which suggests that the diapir is tectonically dormant. View is to the west. (GSC Photo No. 2014-104)

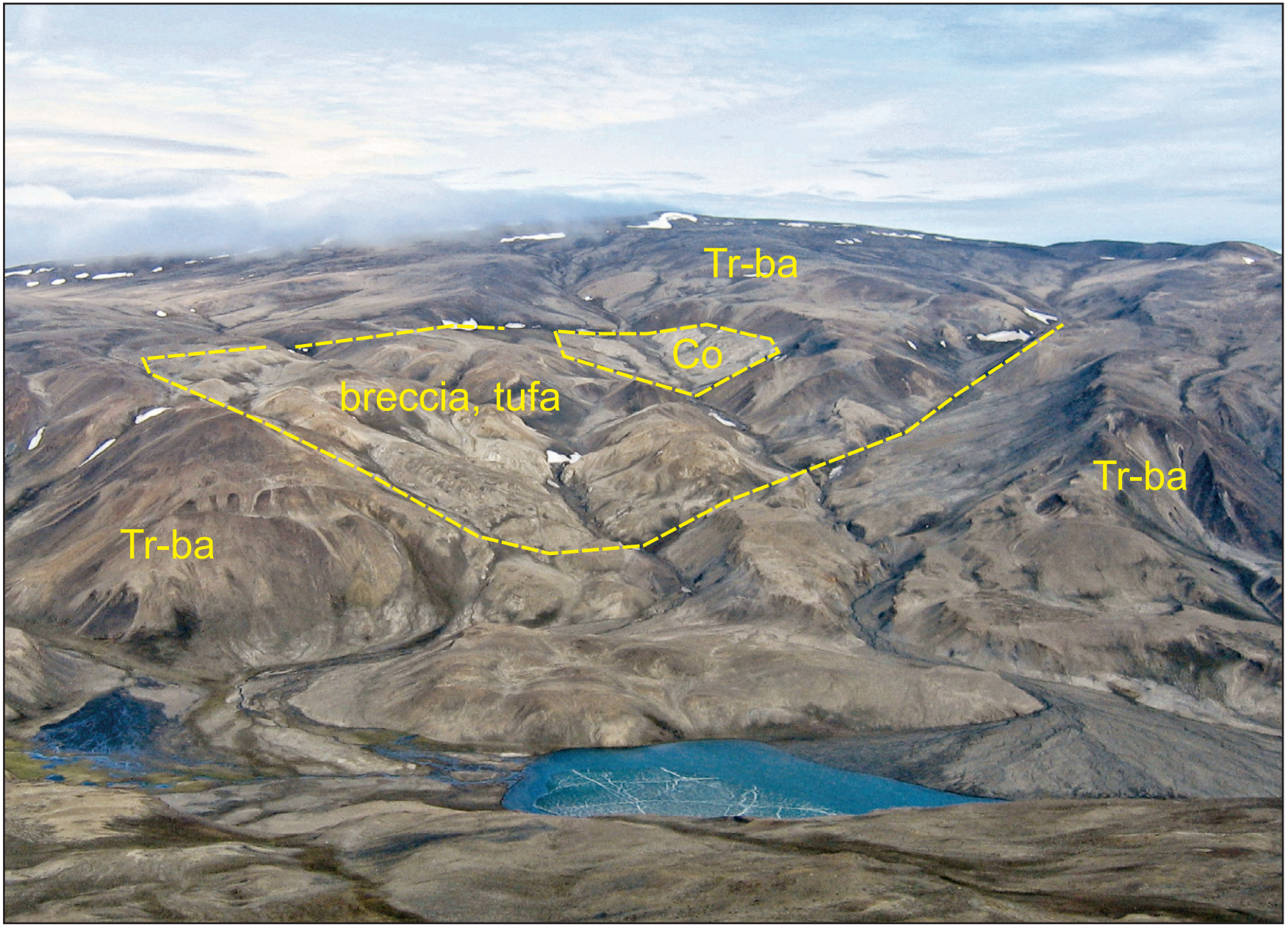

Figure 73. Three Lakes diapir of east-central Axel Heiberg Island. View is to the north. Evaporites (Co) here are recessive weathering, suggesting that the diapir is dormant. Intruded strata are Blaa Mountain Formation (Tr-ba). (GSC Photo No. 2014-105)

Figure 74. Carbonate breccia of hydrothermal origin on the flanks of Three Lakes diapir. (GSC Photo No. 2014-106)

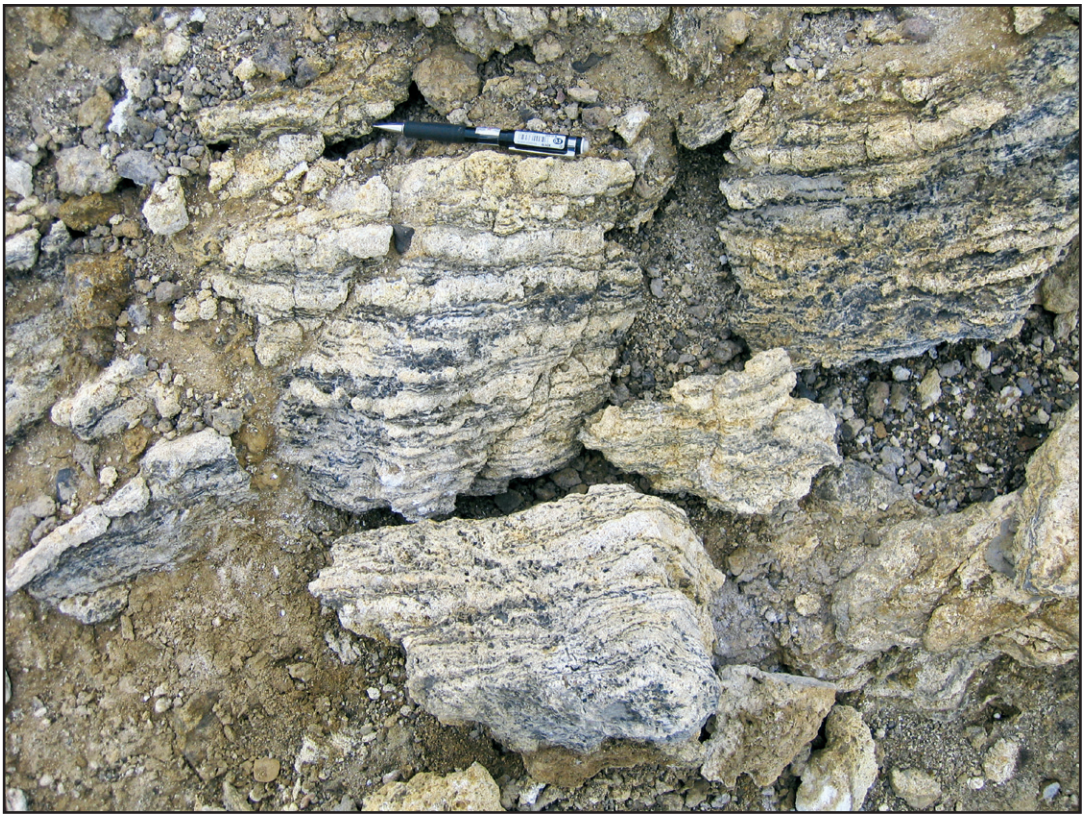

Figure 75. Stratified carbonate-celestite tufa from the flank of Three Lakes diapir. (GSC Photo No. 2014-107)

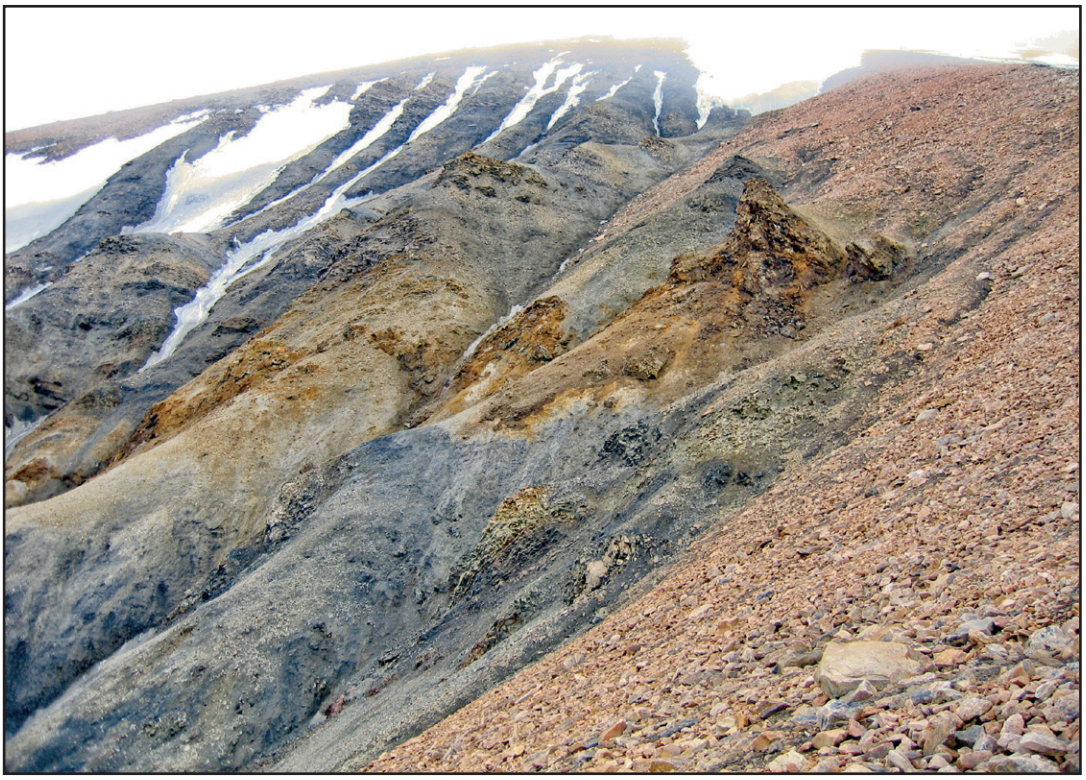

Figure 76. Massive pyrite gossan (~30 m high) in Deer Bay Formation adjacent to Junction diapir. (GSC Photo No. 2014-108)

Conclusions

The wall-and-basin region of west-central Axel Heiberg Island presents a unique area of salt tectonics. Here, near the centre of Sverdrup Basin, a salt-tectonic history is recorded by stratigraphic thickness variations spanning the Late Triassic (Norian) through the Paleogene. Also recording phases of Mesozoic salt tectonics are angular unconformities under the Awingak Formation, Deer Bay Formation, Isachsen Formation (most important), and the Palaeocene upper member of the Strand Bay Formation. These unconformities are centred on several diapirs and extend for distances of as much as 2 km, which is probably too far to be purely halokinetic. Instead, these large unconformities indicate an origin by mild regional shortening in which diapiric roof strata were bulged up and flanking strata steepened. Depositional evidence of salt tectonics is also recorded and includes submarine debris flows in the basal Awingak Formation of Junction diapir, carbonate-bearing gravels in the Isachsen Formation of Bastion Ridge South diapir, and boulder conglomerates containing anh-ydrite clasts also in the Isachsen Formation of Muskox Ridge South diapir.

Major exposed structures of the wall-and-basin region include diapiric stocks, walls, and welds and intervening minibasins. These minibasins and all the diapirs inside the wall-and-basin region are interpreted to overlie a salt canopy. A salt canopy needs an especially thick autochthonous source layer and may have been localized by originally thicker evaporites ponded in a sinistral pull-apart basin of Carboniferous age. The canopy is interpreted to have coalesced during mild shortening, possibly induced by uplift of the eastern Sverdrup Basin margin in the Hauterivian, which is recorded by stratigraphic thinning and excision. The wall-and-basin minibasins formed and evolved as salt was expelled from the canopy beneath them in post-Hauterivian time. The expelled salt rose between the minibasins as second-generation diapirs sourced by allochthonous salt in the canopy. Diapirs along the margins of the wall-and-basin region are sourced in autochthonous salt as first-generation diapirs. Extreme local relief, tectonic slide blocks, vigorous mass wasting, and subaerial debris flows indicate that many and perhaps most wall-and-basin diapirs have continued to rise until the present.

The Axel Heiberg canopy is one of only three known exposed evaporite canopies, each revealed at a different structural level: above the canopy (Axel Heiberg), through the canopy (Great Kavir), and beneath the canopy (Sivas).

Acknowledgments

Research was funded by the Applied Geodynamics Laboratory consortium and the Jackson School of Geosciences Foundation and Kosmos Energy (Jackson) and by the Climate Change Technology Innovation and Investment—Unconventional Gas Supply, Northern Resources Development and Geo-mapping for Energy and Minerals programs of Natural Resources Canada (Harrison). The venture was part of an expedition led by Benoit Beauchamp (Arctic Institute of North America). Fieldwork would have been impossible without logistical and air support by the Polar Continental Shelf Program, Canada, and the hospitality of the Base Commander of Eureka Weather Station. We thank Geo-Logic Systems and Halliburton for the use of LithoTectTM software. Paul Budkewitsch and colleagues with the Canada Centre for Remote Sensing are thanked for developing and providing digital elevation models from satellite imagery covering the eastern and central parts of the report area. These models were critical for our analysis of unit thickness variations in the mapped strata. We would also like to thank the Canadian Geo-mapping for Energy and Minerals (GEM) program for support in bringing this paper to publication. We are especially indebted to the reviewers Ashton Embry, Peter Eichhubl, Carol Evenchick, Chris Talbot, Kirk Osadetz, Jean-Paul Callot, and Chris Jackson for suggestions that improved the final manuscript and to Susie Doenges for editing the text. Publication authorized by the Director, Bureau of Economic Geology and by Natural Resources Canada, Earth Science Sector.

References

Balkwill, H.R., 1983. Geology of Amund Ringnes, Cornwall and Haig-Thomas islands, District of Franklin, Geological Survey of Canada, Memoir 390, 76 p.

Balkwill, H.R. and Foxe, F.G., 1983. Incipient rift zone, western Sverdrup Basin, Arctic Canada; *in* Arctic Geology and Geophysics, (ed.) A.F. Embry and H.R. Balkwill; Canadian Society of Petroleum Geologists, Memoir 8, p. 171–187.

Balkwill, H.R., Hopkins, W.S., and Wall, J.H., 1977. Ringnes Formation (Upper Jurassic), Sverdrup Basin, Canadian Arctic Archipelago; Bulletin of Canadian Petroleum Geology, v. 25, p. 1115–1144.

Beauchamp, B. and Henderson, C.M., 1994. The Lower Permian (Artinskian) Raanes, Great Bear Cape and Trappers Cove formations, Sverdrup Basin, Canadian Arctic: stratigraphy and conodont zonation; Bulletin of Canadian Petroleum Geology, v. 42, p. 565–600.

Beauchamp, B., Harrison, J.C., Utting, J., Brent, T.A., and Pinard, S., 2001. Carboniferous and Permian subsurface stratigraphy, Prince Patrick Island, Northwest Territories, Canadian Arctic; Geological Survey of Canada, Bulletin 565, 93 p.

Beauchamp, B., Henderson, C.M., Grasby, S.E., Gates, L.T., Beatty, T.W., Utting, J., and James, N.P., 2009. Late Permian sedimentation in Sverdrup Basin, Canadian Arctic: the Lindstrom and Black Stripe formations; Bulletin of Canadian Petroleum Geology, v. 57, p. 167–191.

Beauchamp, B., Sherry, C.T., Mayr, U., Harrison, J.C., and Desrochers, A., 1995. Moscovian (Upper Carboniferous) to Sakmarian (Lower Permian) stratigraphy (Nansen and Hare Fiord formations; Unit C2), Hvitland Peninsula, northwestern Ellesmere Island, Arctic Canada; Geological Survey of Canada, Current Research 1995-B, p. 37–46.

Blackadar, R.G., 1963. Basic dykes and sills, in Geology of the North-Central Part of the Arctic Archipelago, Northwest Territories (Operation Franklin); Geological Survey of Canada, Memoir 320, p. 95–100.

Bruvoli, V., Kristoffersen, Y., Coakley, B. J., Hopper, J.R., Planke, S., and Kandilarov, A., 2012. The nature of the acoustic basement on Mendeleev and northwestern Alpha ridges, Arctic Ocean; Tectonophysics, 514–517, 123–145.

Buchan, K.L. and Ernst, R.E., 2003. Diabase dyke swarms and related units in Canada and adjacent regions; Geological Survey of Canada, Map 2022A.

Buchan, K.L. and Ernst, R.E., 2006. Giant dyke swarms and the reconstruction of the Canadian Arctic islands, Greenland, Svalbard and Franz Josef Land; *in* Dyke Swarms—Time Markers of Crustal Evolution, (ed.) E. Hanski, S. Mertanen, T. Tamo, and J. Vuollo; Taylor and Francis/ Balkema, London, U.K., p. 27–48.

Callot, J.-P., Bonnel, C., Ribes, C., Kergaravat, C., Poisson, A., Vrielynick, B., Temiz, H., Salel, J.-F., and Ringenbach, J-C., 2014. The Sivas Basin (Turkey): walking across salt walls and minibasins; Terra Nova (in press).

Callot, J.-P., Trochme, V., Letouzey, J., Albouy, E., Jahani, S., and Sherkati, S., 2012. Pre-existing salt structures and the folding of the Zagros Mountains; Geological Society, London, Special Publications, v. 363, p. 545–561.

Chen, Z., Osadetz, K.G., Embry, A.F., Gao, H., and Hannigan, P.K. 2000. Petroleum potential in western Sverdrup Basin, Canadian Arctic Archipelago; Bulletin of Canadian Petroleum Geology, v. 48, p. 323–338.

Clausen, O.R., Nielsen, S.B., Egholm, D.L., and Goledowski, B., Cenozoic structures in the eastern North sea basin – A case for salt tectonics; Tectonophysics, v. 514-517, p. 156-167.

Dardeau, G. and De Graciansky, P.C., 1990. Halocinèse et rifting te ´thysien dans les Alpes-maritimes (France); Bulletin Centres Recherche Exploration-Production Elf-Aquitaine, 14, p. 443–464.

Davies, E.H., 1984. The dinoflagellate Oppel-zonation of the Jurassic-Cretaceous sequence in Sverdrup Basin; Geological Survey of Canada, Bulletin 359, 59 p.

Davies, G.R. and Nassichuk, W.W., 1991. Chapter 13, Carboniferous and Permian history of the Sverdrup Basin, Arctic Islands; *in* Geology of the Innuitian Orogen and Arctic Platform of Canada and Greenland, (ed.) H.P. Trettin; Geological Survey of Canada, Geology of Canada Series 3, p. 345–367.

Davison, I., Bosence, D.W., Alsop, G.I., and Al-Aawah, M., 1996. Deformation and sedimentation around active Miocene salt diapirs on the Tihama Plain, northwest Yemen, *in* Salt Tectonics, (ed.) G.I. Alsop, D.J. Blundell, and I. Davison; Geological Society, Special Publication, 100, p. 23–39.

Diegel, F.A., Karlo, J.K., Schuster, D.C., Shoup, R.C., and Tauvers, P.R., 1995. Cenozoic structural evolution and tectonostratigraphic framework of the northern Gulf Coast continental margin, *in* Salt Tectonics: A Global Perspective, (ed.) M.P.A. Jackson, D.G. Roberts, and S. Snelson; AAPG Memoir 65, p. 109–151.

Dooley, T.P., Jackson, M.P.A., and Hudec, M.H., 2014, Breakout of squeezed stocks: source of salt, dispersal of roof fragments, and interaction with regional thrust faults; Basin Research, DOI: 10.1111/bre.12056.

Dyson, I.A., 2005. Evolution of allochthonous salt systems during development of a divergent margin: the Adelaide Geosyncline of South Australia; GCSSEPM 25th Bob F. Perkins Research Conference, p. 541–573.

Embry, A.F., 1983: Stratigraphic subdivision of the Heiberg Formation, eastern and central Sverdrup Basin, Arctic Islands; *in* Current Research, Part B Geological Survey of Canada, Paper 83-1B, p. 205-213.

Embry, A.F., 1984. The Wilkie Point Group (Lower-Upper Jurassic), Sverdrup Basin, Arctic Islands; Geological Survey of Canada, Paper 84-1B, p. 299–308.

Embry, A.F., 1985. Stratigraphic subdivision of Isachsen and Christopher formations (Lower Cretaceous), Arctic Islands; Geological Survey of Canada, Paper 85-1B, p. 239–246.

Embry, A.F., 1991. Chapter 14, Mesozoic history of the Arctic Islands, *in* Geology of the Innuitian Orogen and Arctic Platform of Canada and Greenland, (ed.) H.P. Trettin; Geological Survey of Canada, Geology of Canada Series no. 3, p. 371–433.

Embry, A.F. and Osadetz, K.G., 1988. Stratigraphy and tectonic significance of Cretaceous volcanism in the Queen Elizabeth Islands, Canadian Arctic Archipelago; Canadian Journal of Earth Sciences, v. 25, p. 1209–1219.

Embry, A.F., Powell, T.G., and Mayr, U., 1991. Chapter 20, A. Petroleum Resources, Arctic Islands, *in* Geology of the Innuitian Orogen and Arctic Platform of Canada and Greenland, (ed.) H.P. Trettin; Geological Survey of Canada, Geology of Canada Series no. 3, p. 517–525.

Fortier, Y.O., Blackadar, R.G., Glenister, B.F., Greiner, H.R., McLaren, D.J., McMillan, N.J., Norris, A.W., Roots, E.F., Souther, J.G., Thorsteinsson, R., and Tozer, E.T., 1963. Geology of the North-Central part of the Arctic Archipelago, Northwest Territories (Operation Franklin); Geological Survey of Canada, Memoir 320, 671 p.

François, A., 1994. La structure tectonique du Katanguien dans la region de Kolwezi (Shaba, Rép. du Zaire); Annales de la Société géologique de Belgique, v. 116, p. 87–104.

Frebold, H., 1961. The Jurassic faunas of the Canadian Arctic; Middle and Upper Jurassic ammonites; Geological Survey of Canada, Bulletin 74, 43 p.

Frebold, H., 1964. The Jurassic faunas of the Canadian Arctic: Cadoceratinae; Geological Survey of Canada, Bulletin 119.

Fricker, P.E., 1963. Geology of Expedition area, western central Axel Heiberg Island, Canadian Arctic Archipelago; Jacobsen-McGill Arctic Research Expedition 1959–1962; McGill University, Montreal; Axel Heiberg Island Research Report, Geology, no.1, 156 p.

Friedman, M., Tarduno, J.A., and Brinkman, D.B., 2003. Fossil fishes from the high Canadian Arctic: further paleobiological evidence for extreme climatic warmth during the Late Cretaceous (Turonian-Coniacian); Cretaceous Research, v. 24, p. 615–632.

Geological Survey of Canada, 1959. Axel Heiberg and Stor Islands, District of Franklin, Northwest Territories; Geological Survey of Canada, Preliminary Map 36-1959.

Giles, K.A. and Rowan, M.G., 2012. Concepts in halokinetic-sequence deformation and stratigraphy; Geological Society, London, Special Publications, v. 363, no. 1, p. 7–31, doi: 10.1144/SP363.2.

Glenister, H.R., 1963. Graham Island; *in* Geology of the North-Central Part of the Arctic Archipelago, Northwest Territories (Operation Franklin); Geological Survey of Canada, Memoir 320, p. 407–412.

Gradstein, F.M., Ogg, J.G., Schmitz, M. and Ogg, G. 2012. The geologic time scale 2012, Elsevier, 1144 p.

Graham, R., Jackson, M., Pilcher, R., and Kilsdonk, B., 2012. Allochthonous salt in the sub-Alpine fold-and-thrust belt of Haute Provence, France, *in* Salt Tectonics, Sediments and Prospectivity, (ed.) G.I. Alsop, S.G. Archer, A.J. Hartley, N.T. Grant, and R. Hodgkinson; Geological Society, London, Special Publications, v. 363, p. 595–615. http://dx.doi.org/10.1144/SP363.30.

Grantz, A., Hart, P.E., and Childers, V.A., 2011. Geology and tectonic development of the Amerasia and Canada basins, Arctic Ocean, *in* Arctic Petroleum Geology, (ed.) A.M. Spencer, A.F. Embry, D.L. Gautier, A.V. Stoupakova, and K. Sorensen; Geological Society, London, Chapter 50, v. 35, p. 771–799.

Greiner, H.R.1963. Graham Island *in* Geology of the North-Central Part of the Arctic Archipelago, Northwest Territories (Operation Franklin); Geological Survey of Canada, Memoir 320, p. 407-412.

Greinert, J. and Derkachev, A., 2004. Glendonites and methane-derived Mg-calcites in the Sea of Okhotsk, eastern Siberia: implications of a venting-related ikaite/glendonite formation; Marine Geology, v. 204, p. 129–144.

Groves, J.R., Nassichuk, W.W., Lin, R., and Pinard, S., 1994. Middle Carboniferous Fusulinacean biostratigraphy, northern Ellesmere Island (Sverdrup Basin), Canadian Arctic Archipelago; Geological Survey of Canada, Bulletin 469, 55 p.

Hall, R.L., MacRae, R.A., and Hills, L.V., 2005. Middle Albian (Lower Cretaceous) Gastroplitinid ammonites and dinoflagellates from the Christopher Formation (Dragon Mountain, Axel Heiberg Island, Canadian Arctic Islands) and a revision of the genus *Pseudogastroplites* Jeletzky, 1980; Journal of Paleontology, v. 79, p. 219–241.

Harrison, J.C., 1995. Melville Island's salt-based fold belt, Arctic Canada; Geological Survey of Canada, Bulletin 472, 344 p. (13 sheets).

Harrison, J.C. and Brent, T.A., 2005. Basins and fold belts of Prince Patrick Island and adjacent area, Canadian Arctic Islands; Geological Survey of Canada, Bulletin 560, 208 p., 1 CD-ROM.

Harrison, J.C. and Jackson, M.P., 2008. Bedrock geology, Strand Fiord–Expedition Fiord area, western Axel Heiberg Island, northern Nunavut (parts of NTS 59E, F, G, and H); Geological Survey of Canada, Open File 5590, scale 1:125 000.

Harrison, J.C. and Jackson, M.P., 2011. Bedrock geology, Strand Fiord–Expedition Fiord area, western Axel Heiberg Island, northern Nunavut (parts of NTS 59E, F, G, and H); Geological Survey of Canada, Map 2157A, scale 1:125 000.

Harrison, J.C., Mayr, U., McNeil, D.H., Sweet, A.R., McIntyre, D.J., Eberle, J.J., Harington, C.R., Chalmers, J.A., Dam, G., and Nøhr-Hansen, H., 1999. Correlation of Cenozoic sequences of the Canadian Arctic region and Greenland; implications for the tectonic history of northern North America; Bulletin of Canadian Petroleum Geology, v. 47, no. 3, p. 223–254.

Heywood, W.W., 1955. Arctic piercement domes; Transactions of the Canadian Institute of Mining and Metallurgy, v. 58, p. 27–32.

Heywood, W.W., 1957. Isachsen area, Ellef Ringnes Island, District of Franklin, Northwest Territories; Geological Survey of Canada, Paper 56-8, 36 p.

Heywood, W.W., 1959. Ellef Ringnes, Amund Ringnes, Cornwall and Lougheed islands, District of Franklin, Northwest Territories; Geological Survey of Canada, Preliminary Map 14-1959.

Hoen, E.W., 1964. The anhydrite diapirs of central western Axel Heiberg island; Jacobsen-McGill Arctic Research Expedition 1959–1962, McGill University, Montreal; Axel Heiberg Island Research Report, Geology, No. 2, 44 p.

Hudec, M.R. and Jackson, M.P.A., 2009. Interaction between spreading salt canopies and their peripheral thrust systems; Journal of Structural Geology, v. 31, p. 1114–1129.

Hugon, H. and Schwerdtner, W.M., 1982. Discovery of halite in a small evaporite diapir on southeastern Axel Heiberg Island, Canadian Arctic Archipelago; Bulletin of Canadian Petroleum Geology, v. 30, p. 303–305.

Jackson, M.P.A. and Harrison, J.C., 2006. An allochthonous salt canopy on Axel Heiberg Island, Sverdrup Basin, Arctic Canada; Geology, v. 34, p. 1045–1048.

Jackson, M.P.A. and Talbot, C.J., 1986. External shapes, strain rates, and dynamics of salt structures; Geological Society of America Bulletin, v. 97, p. 305–323.

Jackson, M.P.A., Cornelius, R.R., Craig, C.H., Gansser, A., Stöcklin, J., and Talbot, C.J., 1990. Salt diapirs of the Great Kavir, central Iran; Geological Society of America, Memoir 177, 139 p.

Jackson, M.P.A., Warin, O.N., Woad, G.M., and Hudec, M.R., 2003. Neoproterozoic allochthonous salt tectonics during the Lufilian Orogeny in the Katangan Copperbelt, central Africa; Geological Society of America Bulletin, v. 115, no. 3, p. 314–330.

Jahani, S., Callot, J.-P., Letouzey, J., and Frizon de La Motte, D., 2009. The eastern termination of the Zagros fold-and-thrust belt, Iran: Structures, evolution, and relationships between salt plugs, folding, and faulting; Tectonics, v. 28, p. TC6004.

Jeletzky, J.A., 1966. Upper Volgian (latest Jurassic) ammonites and Buchias of Arctic Canada; Geological Survey of Canada, Bulletin 128, 51 p.

Jeletzky, J.A., 1970. Cretaceous macrofaunas; *in* Geology and Economic Minerals of Canada, (ed.) R.J.W. Douglas; Geological Survey of Canada, Economic Geology Report No. 1, p. 649–662.

Jeletzky, J.A., 1973. Biochronology of the marine boreal latest Jurassic, Berriasian and Valanginian in Canada; Geological Journal, Special Issue No. 5; The Boreal Lower Cretaceous, p. 41–80.

Jeletzky, J.A., 1980. New or formerly poorly known, biochronologically and paleobiogeographically important gastroplitinid and cleoniceratinid (Ammonitida) taxa from middle Albian rocks of mid-Western and Arctic Canada; Geological Survey of Canada, Paper 79-22, 63 p.

Jeletzky, J.A., 1983. Report on Jurassic and Cretaceous fossils collected by Dr. A. Embry on Axel Heiberg Island, N.W.T., District of Franklin (NTS 59E,59H); Geological Survey of Canada (Calgary), Paleontology Report Km-19-1983-JAJ, 6 p.

Kemper, E., 1975. Upper Deer Bay Formation (Berriasian-Valanginian) of Sverdrup Basin and biostratigraphy of the Arctic Valanginian; Geological Survey of Canada, Report of Activities 75-1B, p. 245–254.

Kemper, E., 1977. Biostratigraphy of the Valanginian in Sverdrup Basin, District of Franklin; Geological Survey of Canada, Paper 76-32, 6 p.

Kemper E. and Jeletzky, J.A. 1979. New stratigraphically and phylogenetically important olcostephanid (Ammonitida) taxa from the uppermost lower and upper Valanginian of Sverdrup Basin, NWT; Geological Survey of Canada, Paper 79-19, 25 p.

Kemper, E. and Schmitz, H.H., 1975. Stellate nodules from the upper Deer Bay Formation (Valanginian) of Arctic Canada; Geological Survey of Canada, Paper 75-1C, p. 109–119.

Kent, P.E., 1979. The emergent Hormuz salt plugs of southern Iran; Journal of Petroleum Geology, v. 2, p. 117–144.

MacRae, R.A., 1996. Late Albian palynology and sequence stratigraphy, central Sverdrup Basin, Axel Heiberg Island, N.W.T.; Ph.D. thesis, University of Calgary, 442 p.

MacRae, R.A., Hills, L.V., and McIntyre, D.J., 1997 The paleoecological significance of new species of *Limbicysta* (Acritarcha) from the upper Albian of the Canadian Arctic Islands; Canadian Journal of Earth Sciences, v. 33, p. 1475–1486.

Mayr, U., Beauchamp, B., Embry, A.F., and Harrison, J.C., 2002. Geology of upper Paleozoic and Mesozoic formations of northern Axel Heiberg Island, Nunavut; Geological Survey of Canada, Open File 3513, scale 1:125 000.

Miall, A.D., 1991. Chapter 15: Late Cretaceous and Tertiary Basin Development and Sedimentation, Arctic Islands; *in* Geology of the Innuitian Orogen and Arctic Platform of Canada and Greenland, (ed.) H.P. Trettin; Geological Survey of Canada, Geology of Canada Series no. 3, p. 437–458.

Muller, F., 1963. Preliminary report, 1961–1962; Jacobsen-McGill Arctic Research Expedition, 1959–1962, Axel Heiberg Island Research Reports, McGill University, Montreal, 241 p.

Nassichuk, W.W., 1975. Carboniferous ammonoids and stratigraphy in the Canadian Arctic Archipelago; Geological Survey of Canada, Bulletin 237, 240 p.

Nassichuk, W.W. and Davies, G.R., 1980. Stratigraphy and sedimentation of Otto Fiord Formation; Geological Survey of Canada, Bulletin 286, 87 p.

Nohr-Hansen, H. and McIntyre, D.J., 1998. Upper Barremian to upper Albian (Lower Cretaceous) dinoflagellate cyst assemblages, Canadian Arctic Archipelago; Palynology, v. 22, p. 143–166.

Nunez-Betelu, L.M., 1994. Sequence stratigraphy of a coastal to offshore transition, Upper Cretaceous Kanguk Formation: a palynological, sedimentological, and Rock-Eval characterization of a depositional sequence, northeastern Sverdrup Basin, Canadian Arctic; Ph.D. thesis, University of Calgary, 569 p.

Pilcher, R.S., Kilsdonk, B., and Trude, J., 2011. Primary basins and their boundaries in the deep-water northern Gulf of Mexico: Origin, trap types, and petroleum system implications; AAPG Bulletin, v. 95, 219–240.

Pollard, W., Omelon, C., Andersen, D., and McKay, C., 1999. Perennial spring occurrence in Expedition Fiord area of western Axel Heiberg Island, Canadian High Arctic; Canadian Journal of Earth Sciences, v. 36, p. 105–120.

Poulton, T.P., 1984. Report on 15 collections of Jurassic fossils collected in 1983 by A. F. Embry, on western Axel Heiberg Island (NTS 59G); Geological Survey of Canada (Calgary), Paleontology Report 2-TPP-1984, 4 p.

Powell, T.G., 1978. An assessment of hydrocarbon source rock potential of the Canadian Arctic Islands; Geological Survey of Canada, Paper 78-12, 82 p.

Price, G.D., 1999. The evidence and implications of polar ice during the Mesozoic; Earth Science Reviews, v. 48, p. 183–210.

Ramsay, J.G. and Huber, M.I., 1987. The techniques of modern structural geology; Academic Press, London, 700 p.

Ricketts, B.D., 1991. Delta evolution in the Eureka Sound Group, western Axel Heiberg Island: the transition from wave-dominated to fluvial-dominated deltas; Geological Survey of Canada, Bulletin 402, 72 p.

Ricketts, B.D., Osadetz, K.G., and Embry, A.F., 1985. Volcanic style in Strand Fiord Formation (Upper Cretaceous), Axel Heiberg Island, Canadian Arctic Archipelago; Polar Research, v. 3, no. 1, p.107–122.

Ringenbach, J.-C., Salel, J.-F., Kergaravat, C., Ribes, C., Bonnel, C., and Callot, J.-P., 2013. Salt tectonics in the Sivas Basin, Turkey: outstanding seismic analogues from outcrops; First Break, v. 31, p. 93–101.

Rowan, M.G. and Vendeville, B.C., 2006. Foldbelts with early salt withdrawal and diapirism: physical model and examples from the northern Gulf of Mexico and the Flinders Ranges, Australia; Marine and Petroleum Geology, v. 23, p. 871–891.

Rowan, M.G., Lawton, T.F., Giles, K.A., Ratliff, R.A., 2003. Near-salt deformation in La Popa Basin, Mexico, and the northern Gulf of Mexico: a general model for passive diapirism; AAPG Bulletin, v. 87, p. 733–756.

Rysgaard, S., Glud, R.N., Lennert, K., Cooper, M., Halden, N., Leakey, R.J.G., Hawthorne, F.C. Barber, D., 2012. Ikaite crystals in melting sea ice – implications for pCO2 and pH levels in Arctic surface waters; Cryosphere, v. 6, p. 901-908.

Schwerdtner, W.M. and Clark, A.R., 1967. Structural analysis of Mokka Fiord and South Fiord domes, Axel Heiberg Island, Canadian Arctic; Canadian Journal of Earth Sciences, v. 4, p. 1229–1245.

Schwerdtner, W.M. and Osadetz, K., 1983. Evaporite diapirism in Sverdrup Basin: new insights and unsolved problems; Bulletin of Canadian Petroleum Geology, v. 31, p. 27–36.

Schwerdtner, W.M. and van Kranendonk, M., 1984. Structure of Stolz diapir—a well-exposed salt dome on Axel Heiberg Island, Canadian Arctic Archipelago; Bulletin of Canadian Petroleum Geology, v. 32, p. 237–241.

Sliter, W.V. 1981. Albian foraminifers from the Lower Cretaceous Christopher Formation of the Canadian Arctic Islands; *in* Contributions to Canadian Paleontology, (ed.) M. Kennedy; Geological Survey of Canada Bulletin 300, p. 41–70.

Souther, J.G., 1963. Geological traverse across Axel Heiberg Island from Buchanan Lake to Strand Fiord; *in* Geology of the North-Central Part of the Arctic Archipelago, Northwest Territories (Operation Franklin); Geological Survey of Canada, Memoir 320, p. 426–448.

Swainson, I.P. and Hammond, R.P., 2001. Ikaite, $CaCO_3$ $6H_2O$: cold comfort for glendonites as paleothermometers; American Mineralogist, v. 86, p. 1530–1533.

Talbot, C.J., 1998. Extrusions of Hormuz salt in Iran, *in* Lyell: The Past Is the Key to the Present, (ed.) D.J. Blundell and A.C. Scott; Geological Society, London, Special Publications, v. 143, p. 315–334.

Talbot, C.J., 2005. Discussion of "Evidence for Triassic salt domes in the Tunisian Atlas from gravity and geological data"; Tectonophysics, v. 406, p. 249–254.

Talbot, C.J. and Aftabi, P., 2004. Geology and models of salt extrusion at Qum Kuh, central Iran; Journal of the Geological Society, London, v. 161, p. 321–334.

Tarduno, J.A., Cottrell, R.D., and Wilkinson, S.L., 1997. Magnetostratigraphy of the Late Cretaceous to Eocene Sverdrup Basin: implications for heterochroneity, deformation and rotations in the Canadian Arctic archipelago; Journal of Geophysical Research, v. 102, no. B1, p. 723–746.

Tari, G., Molnar, J. and Ashton, P., 2003. Examples of salt tectonics from West Africa: a comparative approach; Geological Society Special Publication, v. 207, p. 85-104.

Thériault, P., Beauchamp, B., Harrison, J.C., Mayr, U., and Steel, R., 1995. Serpukhovian and Bashkirian(Carboniferous) stratigraphy (Borup Fiord and Otto Fiord formations; Unit C1), Hvitland Peninsula and adjacent areas, northwestern Ellesmere Island, Arctic Canada; *in* Interior Plains and Arctic Canada; Geological Survey of Canada, Current Research no. 1995-B, p. 29–36.

Thériault, P., Beauchamp, B., and Steel, R., 1993. Syntectonic deposition of the Carboniferous Borup Fiord Formation, northwestern Ellesmere Island, Northwest Territories; Geological Survey of Canada, Paper 93-1E, p. 105–112.

Thorsteinsson, R., 1971a. Geology, Middle Fiord, District of Franklin; Geological Survey of Canada, Map 1299A, scale 1:250 000.

Thorsteinsson, R., 1971b. Geology, Strand Fiord, District of Franklin; Geological Survey of Canada, Map 1301A, scale 1:250 000.

Thorsteinsson, R., 1972a. Geology, Glacier Fiord, District of Franklin; Geological Survey of Canada, Map 1304A, scale 1:250 000.

Thorsteinsson, R., 1972b. Geology, Eureka Sound South, District of Franklin; Geological Survey of Canada, Map 1300A, scale 1:250 000.

Thorsteinsson, R., 1974. Carboniferous and Permian stratigraphy of Axel Heiberg Island and western Ellesmere Island, Canadian Arctic Archipelago; Geological Survey of Canada, Bulletin 224, 115 p.

Thorsteinsson, R. and Tozer, E.T., 1970. Geology of the Arctic Archipelago; *in* Geology and Economic Minerals of Canada, (ed.) R.J.W. Douglas; Geological Survey of Canada, Economic Geology Report No. 1, p. 547–674.

Thorsteinsson, R. and Trettin, H.P., 1972. Geology, Otto Fiord, District of Franklin; Geological Survey of Canada, Map 1309A, scale 1:250 000.

Tozer, E.T., 1960. Summary account of Mesozoic and Tertiary stratigraphy, Canadian Arctic Archipelago; Geological Survey of Canada, Paper 60-5, 24 p.

Tozer, E.T., 1963a. South side of Strand Fiord; *in* Geology of the North-Central Part of the Arctic Archipelago, Northwest Territories (Operation Franklin); Geological Survey of Canada, Memoir 320, p. 448–456.

Tozer, E.T., 1963b. Mesozoic and Tertiary stratigraphy, western Ellesmere Island and Axel Heiberg Island, District of Franklin; Geological Survey of Canada, Paper 63-30, 38 p.

Trettin, H.P., 1991. Geotectonic correlation chart; Figure 4, Sheet 2 in Innuitian Orogen and Arctic Platform: Canada and Greenland, (ed.) H.P. Trettin; Geological Survey of Canada, Geology of Canada, no. 3.

Trettin, H.P., 1998. Pre-Carboniferous geology of the northern part of the Arctic Islands; Geological Survey of Canada, Bulletin 425, 401 p.

Troelsen, J.C., 1950. Contributions to the geology of northwest Greenland, Ellesmere Island and Axel Heiberg Island; Meddelelser on Groenland, v. 149, no. 7, 85 p.

van Berkel, J.T., 1986. A structural study of evaporite diapirs, folds and faults, Axel Heiberg Island, Canadian Arctic Islands; GUA Papers of Geology, Series 1, No. 26-1986, University of Amsterdam, The Netherlands, 149 p.

van Berkel, J.T., Hugon, H., Schwerdtner, W.M., and Bouchez, J.-L., 1983. Study of anticlines, faults and diapirs in the central Eureka Sound fold belt, Canadian Arctic Islands: Preliminary results; Bulletin of Canadian Petroleum Geology, v. 32, p. 109–116.

van Berkel, J.T., Hugon, H., Schwerdtner, W.M., and Torrance, J.G., 1984. Wall-and-basin structure: an intriguing tectonic prototype in the central Sverdrup Basin; Bulletin of Canadian Petroleum Geology, v. 32, p. 343–358.

Vila, J.M., 1995. First terrestrial study of a large submarine salt glacier—The eastern part of the Ouenza-Ladjebel-Meridef structure (Algerian Tunisian confines): Proposal for an emplacement scenario and comparisons; Bulletin de la Societé Géologique de France, v. 166, p. 149–167.

Villeneuve, M. and Williamson, M.-C., 2006. 40Ar/39Ar dating of mafic magmatism from Sverdrup Basin Magmatic Province; *in* Proceedings of the Fourth International Conference on Arctic Margins (Dartmouth, Nova Scotia, 2003), OCS study MMS 2006-003, U.S. Department of the Interior. p. 206-215.

Volozh, Y., Talbot, C., and Ismail-Zadeh, A.,2003. Salt structures and hydrocarbons in the Pricaspian basin; AAPG Bulletin, v. 87, p. 313-334.

Wall, J.H., 1983. Jurassic and Cretaceous foraminiferal biostratigraphy in the eastern Sverdrup Basin, Canadian Arctic Archipelago (Axel Heiberg Island, Ellesmere Island); Bulletin of Canadian Petroleum Geology, v. 31, p. 246–281.

Wall, J.H., 1988 Micropaleontology report on 12 outcrop samples from the Cretaceous of Strand Fiord map-area, central Axel Heiberg Island, District of Franklin, Geological Survey of Canada (Calgary), Paleontology Report 9-JHW-1988, 4 p.

Williamson, M.-C., 1988. The Cretaceous igneous province of Sverdrup Basin, Canadian Arctic: field relations and petrochemical studies; Ph.D. thesis, Dalhousie University, Halifax, Nova Scotia, 417 p.

Wynne, P. J., Irving, E., and Osadetz, K.G., 1988. Paleomagnetism of Cretaceous volcanic rocks of Sverdrup Basin—magnetostratigraphy, paleolatitudes and rotations; Canadian Journal of Earth Sciences, v. 25, p. 1220–1239.